8TH INTERNATIONAL CONFERENCE ON

ENERGY - MATERIALS - NANOTECHNOLOGY

22 - 25 November 2014: Orlando - Florida

Orlando Skyline. Source: Vikipedia

PROGRAM AND ABSTRACTS

OMICS Group Open-Access House of Science and Technology

UESTC 1956

sensors an open access journal by MDPI

UNIVERSITY OF ARKANSAS

APS physics

Springer

EMN FALL 2014

November 22nd – November 25th

Orlando, FL

MEETING PROGRAM

Contents

DOUBLETREE BY HILTON ORLANDO AT SEAWORLD
TOWER CONFERENCE CENTER

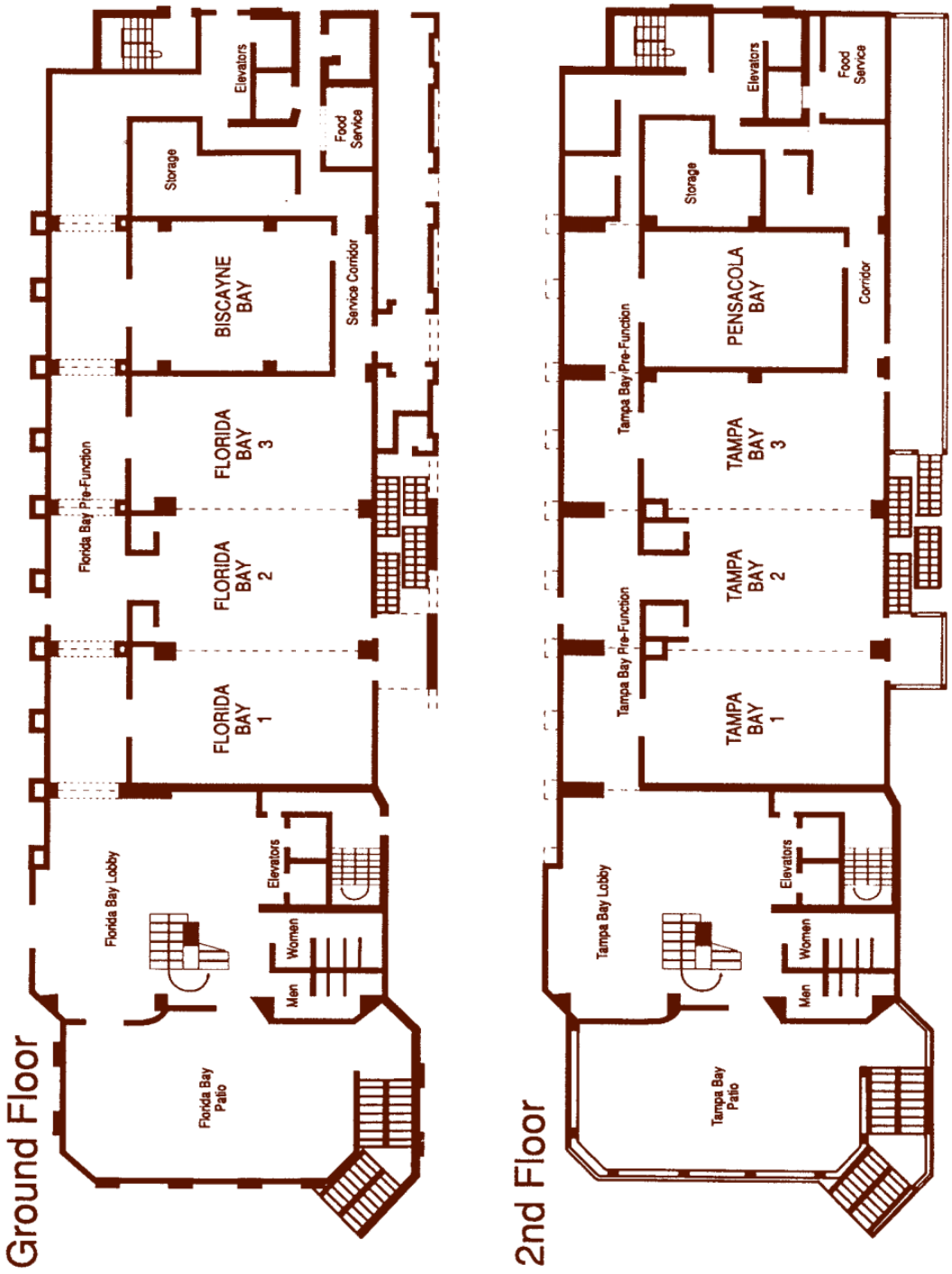

General Information

The 8th Energy, Materials, and Nanotechnology (EMN) Meeting will be held at the DoubleTree Orlando @ SeaWorld Hotel in Orlando, Florida. The conference begins on Saturday November 22 and ends at noon on Tuesday November 25, 2014.

Workshops on selected focus topics in materials science will include invited and contributed oral presentations. The Meeting will also feature Keynote Sessions on Saturday and Sunday, and poster presentations on Monday evening.

REGISTRATION DESK HOURS

The EMN registration desk, located in the Florida Bay Lobby, will be open during the following hours:

Friday, November 21st .....3:00pm – 7:00pm
Saturday, November 22nd .....7:15am – 7:00pm
Sunday, November 23rd .....7:15am – 6:30pm
Monday, November 24th.....7:15am – 6:30pm
Tuesday, November 25th.....8:00am – 1pm

BREAKFAST AND SESSION BREAKS

Complimentary continental breakfast will be available starting from 7:30am in the Florida Bay pre-function area. Coffee and refreshments will be provided during morning and afternoon session breaks.

Sessions will break for lunch from 12:30pm – 2:00pm. For dining options in and around the DoubleTree, please consult the hotel concierge.

SPONSORS

The EMN Fall 2014 Meeting is operated by Open Access Host and sponsored by Springer, APS Physics, *Sensors*, The University of Electronic Science and Technology of China, and The University of Arkansas.

COMMITTEES

The 2014 meeting is co-chaired by Zhiming Wang, *University of Electronic Science and Technology of China*, and Manh-Huong Phan, *University of South Florida* and organized by the following committees:

Advisory Committee

Orlando Auciello, *University of Texas, USA*
Tamio Endo, *Mie University, Japan*
Luis Liz-Marzan, *CIC biomaGUNE, Spain*
Rodrigo Martins, *New University of Lisbon, Portugal*
Chaker Mohamed, *INRS-EMT, Canada*
Ninoslav Stojadinovic, *University of Nis, Serbia*
Ashok Vijh, *Institut de Recherche d'Hydro-Québec, Canada*
Masahiro Yoshimura, *National Cheng Kung University, Taiwan*

Program Committee

Balakumar Subramanian, *University of Madras, India*
Gennadiy Burlak, *CIICAp, UAEM, México*
Tamio Endo, *Mie University, Japan*
Gregory K. L. Goh, *Institute of Materials Research and Engineering, Singapore*
Xingyi Ling, *Nanyang Technological University, Singapore*
Federico Rosei, *National Institute for Scientific Research, Canada*
Felix Jaetae Seo, *Hampton University, USA*
Hari Srikanth, *University of South Florida, USA*
Qing Zhang, *Nanyang Technological University, Singapore*
Arcady Zhukov, *University of the Basque Country, Spain*

Organizing Committee

Dany Carlier, *ICMCB-CNRS, France*
Peng Chen, *Nanyang Technological University, Singapore*
Yoshitake Masuda, *National Institute of Advanced Industrial Science and Technology, Japan*
Rao Tatavarti, *MicroLink Devices, Inc., USA*
Tetyana V. Torchynska, *ESFM-National Polytechnic Institute, Mexico*
Suresh Valiyaveetil, *National University of Singapore, Singapore*
Ning Wang, *University of Electronic Science and Technology of China, China*
Wei David Wei, *University of Florida, USA*
Hui Ying Yang, *Singapore University of Technology and Design, Singapore*
Masahiro Yoshimura, *National Cheng Kung University, Taiwan*

PUBLICATION INFORMATION

Nanoscale Research Letters

Selected papers from the EMN Meeting will be published as a special issue of *Nanoscale Research Letters*. Manuscripts based on invited and contributed abstracts (oral or poster) presented at the EMN Fall 2014 Meeting will be considered for publication in this issue. Electronic manuscript submission is now open through the NRL website and closes January 1, 2015. Authors should select SI: EMN for the article type when submitting.

Open access publishing is not without costs. For EMN submissions, Springer will provide a 50% discount for each article accepted for publication. Fee to be paid by the author if the article is accepted for publication.

Sensors

Selected papers from the EMN Meeting will be published as a special issue on Functional Nanomaterials and Devices for Biomedical Engineering and Sensing Applications in the journal *Sensors*. Manuscripts based on invited and contributed abstracts (oral or poster) presented at the EMN Fall 2014 Meeting will be considered for publication in this issue. Electronic manuscript submission is now open through the Sensors website and closes January 15, 2015. Authors should make the following selections when submitting their manuscript:

- Journal: Sensors
- Section: All
- Special Issue: Functional Nanomaterials and Devices for Biomedical Engineering and Sensing Applications' Papers Selected from the Energy Materials Nanotechnology (EMN) Fall Meeting, November 22–25, 2014, Orlando, USA
- Collection: All

Open access publishing is not without costs. For EMN submissions, a 20% discount will be provided for each article accepted for publication. Fee to be paid by the author if the article is accepted for publication.

Additional titles

An expedited review process will be carried out on EMN submissions to the following publications:

- NRL Advances (Springer; 50% discount on open access publication fee)
- Nano-Micro Letters (OAHOST)
- Journal of Semiconductors (IOP)
- Lecture Notes in Nanoscale Science and Technology (Springer)
- Springer Series in Materials Science (Springer)

Authors should indicate their affiliation with the EMN Meeting in the cover letter upon regular submission.

BEST POSTER AWARD

An award for best poster will be made based on an evaluation of the scientific merit of the displayed work and the quality of the presentation of the work by the author. The winning author will be presented with a certificate and a $100 cash prize sponsored by the American Physical Society. All participants in the poster sessions are eligible to receive the award, however the author(s) must be present during their specified poster session time to be considered.

Special Events

Evening activities are free of charge to registered EMN attendees. Advance notice of participation in off-site activities (Treasure Tavern, SeaWorld) is kindly requested for ticketing and transportation purposes.

Saturday, November 22nd - Welcome dinner

Dinner buffet and brief welcoming remarks by Manh-Huong Phan, EMN Fall 2014 Meeting co-Chair.

7:00 pm, Ontario Room, DoubleTree Orlando@SeaWorld

Sunday, November 23rd - Treasure Tavern

Dinner theater and variety show: treasuretavern.com

Transportation to the restaurant will be arranged by bus, departing from the main hotel lobby at 6:30 pm. Please register in advance at the EMN desk.

Monday, November 24th - EMN Poster Session

Refreshments, beer, and wine will be provided during the poster session.

6:00 pm – 7:30 pm, Tampa Bay 1-3, DoubleTree Orlando@SeaWorld

Tuesday, November 25th - SeaWorld Excursion

Tickets to the SeaWorld Orlando Theme Park (seaworldparks.com) can be picked up from the EMN desk starting at 12 pm. Tickets are valid until the Park closes at 9 pm. SeaWorld is within walking distance of the DoubleTree hotel. Please register in advance at the EMN desk to receive a ticket.

KEYNOTE SESSIONS

Keynote Session I
Saturday, November 22nd
Tampa Bay 1-2

5:45pm
The Next Big Thing in the Energy Field: Photovoltaics-Generated DC Electricity

Rajendra Singh
D. Houser Banks Professor & Director Center for Silicon Nanoelectronics
Holcombe Department of Electrical and Computer Engineering, Clemson University

With the advent of low-cost solar panels and our ability to generate, store and use electrical energy locally without the need for long-range transmission, the electricity industry in developed economies is on the cusp of a dramatic transformation. This transformation is being driven by a series of changes that includes the emergence of rooftop solar and battery storage as the dominant distributed generation source, real time grid monitoring, emergence of microgrid and nanogrid in place of integrated electric grid, improved energy efficiency, advantages of direct current in place of alternating current, and the growing demands of technologies such as cyber and grid security, climate control and weather tolerant electric infrastructures.

The use of photovoltaics (PV) as source of direct current (DC) power reduces the cost and improves the reliability of PV systems. The continuous decrease in the cost of PV-generated electricity is now making it possible to eradicate global energy poverty through DC microgrid and nanogrid technologies. For example, DC nanogrid powered by photovoltaics and battery storage is providing electricity in villages of north India located at 14,200 feet above sea level. The objective of this keynote talk is to highlight the specific research areas in materials, processing and manufacturing of photovoltaic devices and systems that have further transformational capabilities.

6:20pm
Element Strategies for New Nanomaterials

Hiroshi Kitagawa
Division of Chemistry, Graduate School of Science, Kyoto University, Kyoto 606-8502, JAPAN
Email:kitagawa@kuchem.kyoto-u.ac.jp, web site: http://www.kuchem.kyoto-u.ac.jp/ossc/index.html

There are currently 118 known elements represented on the periodic table. Out of these 118 elements, only about 80 elements are stable, nonradioactive, and widely available for our society. We need to fully utilize these elements from the viewpoint of “elements strategy”, i.e. by replacing or reducing rare or toxic metal elements while retaining their properties. Through the combination of the properties of more abundant elements, there is a potential to enhance the properties of these rare or toxic existing materials or to create new functional materials with novel properties.

Atomic-level (solid-solution) alloying has the advantage of being able to continuously control chemical and physical properties of elements by changing compositions and/or combinations of constituent elements. However, solid-solution phases in alloys are limited to specific combinations of elements. In this talk I discuss the establishment of inter-element-fusion science to create innovative functional materials

where the immiscible metallic elements in the bulk state are mixing at the atomic level using nanotechnology. I report an example of a Ag-Rh solid-solution alloy exhibiting a hydrogen-storage property. Other combinations are also presented and discussed.

Keynote Session II
Sunday, November 23rd
Tampa Bay 1-2

8:00am
Prospects for Single-Layer Ferromagnetic Semiconductors

David Mandrus

Department of Materials Science and Engineering, University of Tennessee, Knoxville, TN 37996 USA
Materials Science and Technology Division, Oak Ridge National Laboratory, Oak Ridge, TN 37831 USA

In recent years there has been an explosion of research on two-dimensional materials beyond graphene. One of the frontiers of this research involves the creation of new spintronic materials. In this talk I will summarize current progress on two-dimensional ferromagnetic semiconductors.

Keynote Session III
Sunday, November 23rd
Tampa Bay 1-2

5:40pm
Translating Nanomaterials and Technologies to Biomedical Applications: What's on the Horizon?

Shyam S. Mohapatra

Internal Medicine Department, Morsani College of Medicine and Graduate Programs of College of Pharmacy, University of South Florida, Tampa, FL, USA

The last decade has seen spectacular advances in fundamental science and an explosion in nanotechnology applications in the biomedical arena. One such area is nanomedicine, which has helped medical science grow in leaps and bounds in the areas of treatment, diagnosis and drug safety. These welcome advances have brought hope to the treatment of many incurable diseases. While nanomedicine has displayed extensive potential, a major focus of nanomedicine has been in the treatment of cancer and is slowly moving towards insurmountable diseases. Polymeric and lipid nanoparticles, micellar systems, liposomes and other carriers are widely explored as nanotechnology platforms to enable targeted delivery to sites hitherto considered unreachable. Nevertheless, a number of obstacles need to be surpassed to enable maximum exploitation of the nanotechnology platforms successfully in nanomedicine. Cost-effective biomaterials and scalable technologies prove a major constraint, limiting impacts due to affordability. This keynote talk will provide a historical perspective of nanomedicine with snapshots of contemporary advances and a discussion of the major challenges in innovations that could fructify into nanomedicinal technologies for the benefit of mankind.

Program at-a-glance

Saturday Morning, November 22	
MM: Novel Magnetic Materials and Phenomena I	8:25am – 12:00pm *Florida Bay 1*
GE: EMN General Workshop on Energy I	8:10am – 12:25pm *Florida Bay 2*
FM: Functional Materials I	8:30am – 12:25pm *Florida Bay 3*
SS: Smart Sensor Materials and Technologies	8:25am – 12:20pm *Pensacola Bay*

Saturday Afternoon, November 22	
MM: Novel Magnetic Materials and Phenomena I	2:00pm – 4:30pm *Florida Bay 1*
GN: EMN General Workshop on Nanotechnology I	2:00pm – 5:25pm *Florida Bay 2*
MT: Metamaterials and Transformation Optics	2:00pm – 3:40pm *Florida Bay 3*
AB: Advanced Nanomaterials and Nanotechnologies for Biomedical Applications I	3:50pm – 5:30pm *Florida Bay 3*

Saturday Evening, November 22	
K1: Keynote Session I	5:45pm – 6:55pm *Tampa Bay 1-2*
Welcome Dinner	7:00pm *Ontario Room*

Sunday Morning, November 23	
K2: Keynote Session II	8:00am – 8:35am *Tampa Bay 1-2*
GE: EMN General Workshop on Energy II	8:45am – 12:20pm *Florida Bay 1*
GM: EMN General Workshop on Materials I	8:45am – 11:55am *Florida Bay 2*
GE: EMN General Workshop on Nanotechnology II	8:45am – 12:35pm *Florida Bay 3*
MM: Novel Magnetic Materials and Phenomena II	8:45am – 12:20pm *Pensacola Bay*
AP: Advanced Photonics and Plasmonics for Nano-bio Application	8:45am – 12:35pm *Tampa Bay 3*

Sunday Afternoon, November 23	
GE: EMN General Workshop on Energy II	2:00pm – 3:40pm *Florida Bay 1*
GN: EMN General Workshop on Nanotechnology II	3:50pm – 5:25pm *Florida Bay 1*
GM: EMN General Workshop on Materials I	2:00pm – 4:40pm *Florida Bay 2*
SC: Nanomaterials for Photochemical Solar Cells	2:00pm – 5:00pm *Florida Bay 3*
CG: CNT's, Graphene, and 2D Materials I	2:00pm – 5:30pm *Tampa Bay 3*

Sunday Evening, November 23

K3: Keynote Session III	5:40pm – 6:15pm *Tampa Bay 1-2*
Off-site dinner theater: Treasure Tavern	6:30pm *Main Lobby*

Monday Morning, November 24

FM: Functional Materials II	8:00am – 12:15pm *Florida Bay 1*
NP: Nanophotonics and Plasmonics	8:25am – 12:20pm *Florida Bay 2*
NS: Nanocarbon Based Supercapacitors	8:25am – 12:05pm *Florida Bay 3*
RS: Resistive Switchings of Oxides and Related Nanocompostes/Heterostructures	8:00am – 12:05pm *Tampa Bay 3*
AB: Advanced Nanomaterials and Nanotechnologies for Biomedical Applications II	10:20am – 12:20pm *Pensacola Bay*

Monday Afternoon, November 24

FM: Functional Materials II	2:00pm – 5:20pm *Florida Bay 1*
NP: Nanophotonics and Plasmonics	2:00pm – 5:30pm *Florida Bay 2*
GM: EMN General Workshop on Materials II	2:00pm – 5:10pm *Florida Bay 3*
AB: Advanced Nanomaterials and Nanotechnologies for Biomedical Applications II	2:00pm – 4:40pm *Pensacola Bay*

Monday Evening, November 24

Poster Session 6:00pm – 7:30pm
Beer, wine, refreshments *Tampa Bay 1-3*

Tuesday Morning, November 25

NO: Nanoscale Optics and Photonics 8:30am – 12:00pm
Florida Bay 1

CG: CNT's, Graphene, and 2D Materials II 8:55am – 10:30am
Florida Bay 2

AB: Advanced Nanomaterials and Nanotechnologies for Biomedical Applications III 10:45am – 12:00pm
Florida Bay 2

Tuesday Afternoon, November 25

SeaWorld Excursion **Ticket pick-up 12:00pm**
Registration Desk

Novel Magnetic Materials and Phenomena I

Saturday Morning, November 22nd
Florida Bay 1
Xavier Moya, *Chair*

MM-01
8:25a-8:50a: Spin-torque nano-oscillators for wireless communication
Byoung-Chul Min, Korea Institute of Science and Technology, South Korea

MM-02
8:50a-9:15a: Theory and simulation of magnetic materials: Surface effects and spin transport
Hung T. Diep, Université de Cergy-Pontoise, France

MM-03
9:15a-9:40a: Spin caloritronics in ordered alloy systems
Koki Takanashi, Tohoku University, Japan

MM-04
9:40a-10:05a: Tunneling magneto-Seebeck effect
Andy Thomas, Bielefeld University, Germany

Coffee Break

MM-05
10:20a-10:45a: Half-metallic Co_2MnSi/diamond Schottky junctions for spintronics applications
Kenji Ueda, Nagoya University, Japan

MM-06
10:45a-11:10a: Kondo physics in nanoscopic metallic non-local spin transport devices
Chris Leighton, University of Minnesota, USA

MM-07
11:10a-11:35a: Magneto-transport phenomena in amorphous ferrimagnets
Jiwei Lu, University of Virginia, USA

MM-08
11:35a-12:00p: Novel magnetoresistance in semiconductors
Xiaozhong Zhang, Tsinghua University, China

EMN General Workshop on Energy I

Saturday Morning, November 22nd
Florida Bay 2
Khang Hoang, *Chair*

GE-01
8:10a-8:25a: Hierarchical nanoporous carbons for energy storage applications
Michael Fröba, Institute of Inorganic and Applied Chemistry, University of Hamburg, Germany

GE-02
8:25a-8:50a: Novel flux coating technique of hierarchically-structured crystal layers for all-solid-state LIB
Katsuya Teshima, Shinshu University, Japan

GE-03
8:50a-9:15a: Multiscale simulations for battery materials
Ryoji Asahi, Toyota Central Research and Development Labs, Japan

GE-04
9:15a-9:40a: Nanostructure composite anode materials for Lithium ion batteries
Meicheng Li, North China Electric Power University, China

GE-05
9:40a-10:05a: In-situ (S)TEM observations of energy storage materials and batteries
Nigel D. Browning, Pacific Northwest National Laboratory, USA

Coffee Break

GE-06
10:20a-10:45a: Thin films for Li and Li-ion all-solid-state batteries
Brigitte Pecquenard, ICMCB- Groupe Energie Matériaux pour Batteries, France

GE-07
10:45a-11:10a: High energy density positive electrode materials for Lithium-ion batteries

Laurence Croguennec, ICMCB-CNRS, France

GE-08
11:10a-11:35a: On the insertion mechanism of A_xFePO_4 (A=Li, Na) through the combination of experiments and DFT calculations, the importance of the $A_{2/3}FePO_4$ composition
Florent Boucher, CNRS-IMN, France

GE-09
11:35a-12:00p: PVD processes for energy applications
Alain Billard, Université de Technologie de Belfort-Montbéliard, France

GE-10
12:00p-12:25p: Oxide thin films for thermoelectricity
Hanns-Ulrich Habermeier, Max-Planck-Institut für Festkörperforschung

---

Functional Materials I

Saturday Morning, November 22nd
Florida Bay 3
Hariharan Srikanth, *Co-Chair*
Federico Rosei, *Co-Chair*

FM-01
8:30a-8:45a: In Situ TEM analysis of low-yemperature creep of Si nanowires grown with Sn-catalysts
Shengyi Qian, Nanjing University, China

FM-02
8:45a-9:00a: Tuning the work function of polyaniline via camphorsulfonic acid; an XPS study
Omar Abdulrazzaq, University of Arkansas at Little Rock, USA

FM-03
9:00a-9:15a: A novel growth process for the deposition of $CH_3NH_3PbI_{3-x}Cl_x$ perovskite films
Chaminda Hettiarachchi, University of South Florida, USA

FM-04
9:15a-9:40a: Studies of polymer-like behaviour in ultrathin nanowires
Ludovico Cademartiri, Iowa State University, USA

FM-05
9:40a-10:05a: Advanced laser ablation techniques for ferroelectric and multiferroic heterostructures of perovskite-oxides
Devajyoti Mukherjee, University of South Florida, USA

Coffee Break

FM-06
10:20a-10:45a: Recent progress in studies of magnetic microwires
Arkady Pavlovich Zhukov, University of Basque Country, Spain

FM-07
10:45a-11:10a: The nano revolution and its impact in materials for energy applications
Victor Castaño, Centro de Física Aplicada y Tecnología Avanzada, Mexico

FM-08
11:10a-11:35a: Tandem photovoltaics using transparent conducting photonic crystal contacts
Nazir P. Kherani, University of Toronto, Canada

FM-09
11:35a-12:00p: Piezoelectric MEMS energy harvesters
Susan Trolier-McKinstry, The Pennsylvania State University, USA

Smart Sensor Materials and Technologies

Saturday Morning, November 22nd
Pensacola Bay
Arkady Zhukov, *Co-Chair*
Dennis K. Killinger, *Co-Chair*

SS-01
8:25a-8:50a: About processes and performance of integrated gas sensor components

Siegfried Selberherr, Technische Universität Wien, Austria

SS-02
8:50a-9:15a: Effect of magnetic field in organic semiconductor devices
Tho Nguyen, University of Georgia, USA

SS-03
9:15a-9:40a: Design and fabrication of magnetic tips for high resolution magnetic force microscopy
Masaaki Futamoto Chuo University, Japan

SS-04
9:40a-10:05a: Laser spectroscopic techniques for remote probing of trace species
Dennis K. Killinger, University of South Florida, USA

Coffee Break

SS-05
10:20a-10:45a: Sensing RF and microwave energy with fiber Bragg grating heating via soft ferromagnetic glass-coated microwires
Philip Colosimo, University of Washington, USA

SS-06
10:45a-11:10a: Rapidly quenched amorphous and nanocrystalline bilayer ribbons for energy and sensor applications
Ivan Skorvanek, Institute of Experimental Physics, Slovakia

SS-07
11:10a-11:35a: Triboluminescent materials: uses in smart sensors and technology
Andy Hollerman, University of Louisiana at Lafayette, USA

SS-08
11:35a-11:50a: Development of highly sensitive magneto-impedance sensor and its application to P300 brainwaves measurement
Tsuyoshi Uchiyama, Nagoya University, Japan

SS-09
11:50a-12:05p: Design and synthesis of hierarchical nanostructured materials for gas sensing applications
Sunkara V. Manorama, CSIR-Indian Institute of Chemical Technology, India

SS-10
12:30p-12:45p: Study of zinc sulphide (ZnS) nanocrystaline thin films prepared by varying complexing agent for biosensing application
Sachin V. Mukhamale, Savitribai Phule Pune University, India

Novel Magnetic Materials and Phenomena I

Saturday Afternoon, November 22nd
Florida Bay 1
Oscar Iglesias, *Chair*

MM-09
2:00p-2:25p: Engineering materials and devices for all optical magnetic recording
Stephane Mangin, Université de Lorraine, France

MM-10
2:25p-2:50p: Irreversibility of magnetic domain evolution of Co/Pt multilayers during magnetization reversal
Dong-Hyun Kim, Chungbuk National University, South Korea

MM-11
2:50p-3:15p: Imaging of magnetoelectric heterostructures by photoemission electron microscopy
Xavier Moya, University of Cambridge, UK

MM-12
3:15p-3:40p: Nanocrystalline glass-coated microwires – magnetization process and applications
Rastislav Varga, Institute of Physics, Slovakia

Coffee Break

MM-13
3:50p-4:15p: Spontaneous superlattice formation via magnetic field induced phase separation
Naoki Wakiya, Shizuoka University, Japan

MM-14
4:15p-4:30p: Giant magnetoresistance in double organic-spacer-layers spin valves (DOSVs)
Shiheng Liang, University of Georgia, USA

EMN General Workshop on Nanotechnology I

Saturday Afternoon, November 22nd
Florida Bay 2
Tho Nguyen, Chair

GN-01
2:00p-2:25p: Green synthesis and characterization of gold nanoparticles and their sensing for antioxidant activity based on rapid colorimetric measurement
Ju Chou, Florida Gulf Coast University, USA

GN-02
2:25p-2:50p: Nanoparticles and nanowires using polyol/alcohol-based synthesis techniques
Balachandran Jeyadevan, The University of Shiga Prefecture, Japan

GN-03
2:50p-3:15p: Facile fabrication of tungsten bronze nanoparticles for heat-ray shielding via solvothermal reaction
Tsugio Sato, Institute of Multidisciplinary Research for Advanced Materials,Tohoku University, Japan

GN-04
3:15p-3:40p: Detonation nanodiamond as attractive building block for nanotechnology
Alexander Vul, Ioffe Physical-Technical Institute, Russia

Coffee Break

GN-05
3:50p-4:15p: Probing structure and dynamics of nanoparticles for energy applications
Thomas E. Ashton, University of Glasgow, UK

GN-06
4:15p-4:40p: Plasma nanocoatings for preventing/inhibiting biofilms
Qingsong Yu, University of Missouri, USA

GN-07
4:40p-4:55p: Nanomaterials: A key tool for improvising waste water technologies
Shivani Bhardwaj, Mishra. University of Johannesburg, South Africa

GN-08
4:55p-5:10p: Enzymatic grafting: A novel approach to develop multifunctional materials of interest
Hafiz M.N. Iqbal, University of Westminster, UK

Metamaterials and Transformation Optics

Saturday Afternoon, November 22nd
Florida Bay 3
Binh Duong, *Chair*

MT-01
2:00p-2:25p: Metamaterials for terahertz photonics
Marco Rahm, University of Kaiserslautern, Germany

MT-02
2:25p-2:50p: Storage and manipulation of electromagnetic waves in metamaterials
Toshihiro Nakanishi, Kyoto University, Japan

MT-03
2:50p-3:15p: Bistability in nonlinear metamaterials
Jiangfeng Zhou, University of South Florida, USA

Advanced Nanomaterials and Nanotechnologies for Biomedical Applications I

Saturday Afternoon, November 22nd
Florida Bay 3
Jon Dobson, *Co-Chair*
Gil Lee, *Co-Chair*

AB-01
3:50p-4:15p: Potential of graphene as nanomaterial for biomedical applications
Subhra Mohapatra, University of South Florida, USA

AB-02
4:15p-4:40p: Multifunctional nanoparticles for lung cancer therapy
Nguyen Kytai Truong, The University of Texas at Arlington, USA

AB-03
4:40p-5:05p: Study of the interaction of superparamagnetic nanoparticles with cells: Targeting and mechanochemical response
Gil Lee, Conway Institute of Biomolecular & Biomedical Research, Ireland

AB-04
5:05p-5:30p: Graphene-based biosensors and graphene synthesis
Kenzo Maehashi, Osaka University, Japan

Keynote Session I

Saturday Evening, November 22nd
Tampa Bay 1-2
Dennis K. Killinger, *Chair*

K-1
5:45p-6:20p: The next big thing in the energy field: Photovoltaics-generated DC electricity
Rajendra Singh
Clemson University, USA

K-2
6:20p-6:55p: Elemental strategy for new nano-materials
Hiroshi Kitagawa
Kyoto University, Japan

Keynote Session II

Sunday Morning, November 23rd
Tampa Bay 1-2
Manh-Huong Phan, *Chair*

K-3
8:00p-8:35p: Prospects for single-layer ferromagnetic semiconductors
David Mandrus
University of Tennessee, USA

EMN General Workshop on Energy II

Sunday Morning, November 23rd
Florida Bay 1
Khang Hoang, Chair

GE-11
8:45a-9:10a: Strategies for the synthesis of new nanoscale materials used as electrode materials for Li or Na ion batteries
Valerie Pralong, CNRS, France

GE-12
9:10a-9:25a: All-solid-state lithium-ion microbatteries using a silicon negative electrode for microelectronic systems
Frédéric Le Cras, Minatec Campus, France

GE-13
9:25a-9:40a: GeO_2/Multiplates graphene composite based cathode electrodes for magnesium-ion battery
Eslam Sheha, Benha University, Egypt

GE-14
9:40a-10:05a: Triple-phase boundary and power density enhancement in thin solid oxide fuel cells by controlled etching of the nickel anode
Rabi Ebrahim, University of Houston, USA

GE-15
10:05a-10:30a: Metal-organic frameworks for hydrogen storage applications
Myunghyun Paik Suh, Hanyang University & Seoul National University, Republic of Korea

Coffee Break

GE-16
10:40a-11:05a: Theory and modeling of advanced materials for energy storage and conversion applications
Khang Hoang, North Dakota State University, USA

GE-17
11:05a-11:30a: Efficient solar water-splitting using a nanocrystalline CoO photocatalyst
Jiming Bao, University of Houston, USA

GE-18
11:30a-11:55a: Advanced photovoltaic approaches to increase efficiency and reduce cost
Gavin Conibeer, University of New South Wales, Australia

EMN General Workshop on Materials I

Sunday Morning, November 23rd
Florida Bay 2
Serge Nakhmanson, *Chair*

GM-01
8:45a-9:10a: High pressure-induced polymorphic transformation of maleic hydrazide
Kai Wang, Jilin University, China

GM-02
9:10a-9:25a: Effects of flexible spacing coating on macroscopic supramolecular assembly
Mengjiao Cheng, Beijing University of Chemical Technology, China

GM-03
9:25a-9:50a: High pressure supramolecular chemistry: pressure induced assemblies and their functions
Bo Zou, Jilin University, China

GM-04
9:50a-10:15a: Heavy metal fluoride glasses and fibers
Mohammed Saad, Thorlabs, USA

GM-05
10:15a-10:30a: Properties of zigzag silicene nanoribbons
Nam B. Le, University of South Florida, USA

Coffee Break

GM-06
10:40a-11:05a: A band alignment of tunnel-FET heterojunction by internal photoemission
Nhan V. Nguyen, National Institute of Standards and Technology, USA

GM-07
11:05a-11:30a: Silicon nanoparticles as potential light emitters: Synthesis, Separation by Color, and Applications
Naoto Shirahata, National Institute for Materials Science, Japan

GM-08
11:30a-11:55a: On the nature of organic semiconductors: Improving the mobility and stability of organic devices
Nobuo Ueno, Chiba University, Japan

GM-09
11:55p-12:20p: Nanomaterials for excitonic solar cells
Alberto Vomiero, National Institute for Scientific Research, Canada

EMN General Workshop on Nanotechnology II

Sunday Morning, November 23rd
Florida Bay 3
Ju Chou, Chair

GN-09
8:45a-9:10a: Controlled synthesis and property of Cu- and Bi-based functional semiconductor nanomaterials
Guanjun Xiao, Jilin University, China

GN-10
9:10a-9:35a: Ultrahigh density arrays of semiconducting nanotubes for high performance logic electronics
Qing Cao IBM T.J. Watson Research Center, USA

GN-11
9:35a-10:00a: Metal-semiconductor hybrid nanostructures with plasmon-enhanced photocatalytic activities
Can Xue, Nanyang Technological University, Singapore

GN-12
10:00a-10:25a: Lattice dynamics of bismuth nanoislands and nanoparticles studied by ultrafast electron diffraction
Hani E. Elsayed-Ali, Old Dominion University, USA

Coffee Break

GN-13
10:40a-11:05a: In situ synchrotron studies of reactivity at model complex oxide surfaces
Dillon D. Fong, Argonne National Laboratory, USA

GN-14
11:05a-11:30a: Functional thin films using nanotechnology: epitaxy anywhere
Gertjan Koster, University of Twente, The Netherlands

GN-15
11:30a-11:55a: Fatigue crack growth and retardation in nanostructured materials
Ming Dao, Massachusetts Institute of Technology, USA

Novel Magnetic Materials and Phenomena II

Sunday Morning, November 23rd
Pensacola Bay
Xavier Moya, *Chair*

MM-15
8:45a-9:10a: Interactions in magnetic nanoparticles: phenomenology and atomistic modeling
Òscar Iglesias, Universitat de Barcelona, Spain

MM-16
9:10a-9:35a: Neutron scattering studies of molecule based magnets
Javier Campo, Universidad de Zaragoza C, Spain

MM-17
9:35a-10:00a: Magnetization dynamics and collective phenomena in magnetic nanostructures
Javier Alonso Masa, Basque Center for Materials, Spain

MM-18
10:00a-10:15a: Ordered arrays of magnetic nanostructures in thin films: synthesis and modeling
Paola Tiberto, INRIM, Italy

MM-19
10:15a-10:30a: Tunable ferromagnetism in diluted amorphous $Ge_{1-x}Mn_x$
Giampiero Amato, INRIM, Italy

Coffee Break

MM-20
10:40a-11:05a: Caloric effects near tricritical points
Karl G. Sandeman, CUNY, USA; Imperial College London, UK

MM-21
11:05a-11:30a: Revisiting magneto-volume anomalies and magneto-caloric effect in R_2Fe_{17} intermetallics
Pedro Gorria, University of Oviedo, Spain

MM-22
11:30a-11:55a: $FeMnP_{1-x}Si_x$ – Phase Diagram, structure and magnetocaloric potential
Per Nordblad, Uppsala University, Sweden

MM-23
11:55a-12:20p: Ferromagnetic shape memory effect: underlying physics and practical importance
Volodymyr A. Chernenko, Universidad del Pais Vasco UPV/EHU, Spain

Advanced Photonics and Plasmonics for Nano-bio Application

Sunday Morning, November 23rd
Tampa Bay 3
Kaoru Tamada, *Co-Chair*
Koichi Okamoto, *Co-Chair*
Kotaro Kajikawa, *Co-Chair*

AP-01
8:45a-9:10a: Tuning of the surface plasmon resonance in the UV-IR range for biological applications
Koichi Okamoto, Kyushu University, Japan

AP-02
9:10a-9:35a: Quantum dots and upconverting nanoparticles: using solid-phase platforms for multiplexed optical sensing by resonance energy transfer
Ulrich Krull, University of Toronto, Mississauga, Canada

AP-03
9:35a-10:00a: Label-free multichannel biochip based on anomalous reflection of gold
Kotaro Kajikawa, Tokyo Institute of Technology, Japan

AP-04
10:00a-10:25a: Control of exciton dynamics in a single colloidal quantum dot by localized surface plasmon
Sadahiro Masuo, Kwansei Gakuin University, Japan

Coffee Break

AP-05
10:40a-11:05a: Assay on a tip – plasmonic fiber tip probe for intracellular protein detection

Qimin Quan, Harvard University, USA

AP-06
11:05a-11:30a: Highly confined, enhanced surface fluorescence imaging with 2D silver nanoparticle sheets
Kaoru Tamada, Kyushu University, Japan

AP-07
11:30a-11:55a: Short-range ordered plasmonic nanoholes and nanopores for sensing
Takumi Sannomiya, Tokyo Institute of Technology, Japan

EMN General Workshop on Energy II

Sunday Afternoon A, November 23rd
Florida Bay 1
Dev Mukherjee, *Chair*

GE-19
2:00p-2:25p: Molecular design of novel D-pi-A type organic dyes for efficient dye-Sensitized solar cells
Vinich Promarak, Suranaree University of Technology, Thailand

GE-20
2:25p-2:40p: Interfacial effect of charge carriers on stabilizing zinc oxide in poly(vinylidene fluoride) and study their enhanced dielectric properties for electro-mechanical applications
Radhamanohar Aepuru, Defence Institute of Advanced Technology, India

GE-21
2:40p-2:55p: Study of CZTS nanocrystaline thin films by using electrodeposition for solar cell application
Vilas A. Tabhane, Savitribai Phule Pune University, India

GE-22
2:55p-3:10p: Study of the effect of silicon substrate on the performance of organic-inorganic hybrid solar cells
Viney Saini, University of Arkansas at Little Rock, USA

GE-23
3:10p-3:25p: Hybrid nanomaterials and new designs for energy storage applications
Leela Mohana Reddy Arava Wayne State University, USA

EMN General Workshop on Nanotechnology II

Sunday Afternoon B, November 23rd
Florida Bay 1
Tho Nguyen, Chair

GN-16
3:50p-4:15p: Size, shape, stability and plamonic properties of metal nanoparticles
Cecilia Noguez, Universidad Nacional Autonoma de Mexico, Mexico

GN-17
4:15p-4:40p: Revisiting aluminum for Li-ion battery anodes: core-shell $NiSi_x$-Al nanowire structures
Didier Pribat, Sungkyunkwan University, Korea

GN-18
4:40p-4:55p: Toward roll-to-roll production of nanomaterials using microwave
Xinyu Zhang, Auburn University, USA

GN-19
4:55p-5:10p: Composites and nanocomposites: An application towards wastewater treatment
Ajay Kumar, Mishra University of Johannesburg, South Africa

GN-20
5:10p-5:25p: Characterization of functionalized multiwalled - carbon nanotubes / Kevlar fiber hybrid reinforced epoxy composites using vacuum resin infusion process
Mohamed Bassyouni, King Abdulaziz University, Saudi Arabia

EMN General Workshop on Materials I

Sunday Afternoon, November 23rd
Florida Bay 2
Hafsa Khurshid, *Chair*

GM-10
2:00p-2:25p: From point defects to defect superstructures in complex oxides
Peter Sushko, Pacific Northwest National Laboratory, USA

GM-11
2:25p-2:50p: Applications of density-functional and tight-binding theory in complex materials
Dimitrios A. Papaconstantopoulos, George Mason University, USA

GM-12
2:50p-3:15p: Multiscale modeling of layered electroactive materials
Serge M. Nakhmanson, University of Connecticut, USA

GM-13
3:15p-3:40p: All oxide piezo-MEMS devices: the role of clamping on piezo electric properties
Guus Rijnders, University of Twente, The Netherlands

Coffee Break

GM-14
3:50p-4:15p: Phase change of Ba-substituted sodium bismuth titanate ferroelectrics with Bi deficiency
Hirotaka Fujimori, Yamaguchi University, Japan

GM-15
4:15p-4:40p: Magneto-optical material and its application to silicon photonics
Tetsuya Mizumoto, Tokyo Institute of Technology, Japan

Nanomaterials for Photochemical Solar Cells

Sunday Afternoon, November 23rd
Florida Bay 3
Ngoc Diep Lai, *Chair*

SC-01
2:00p-2:25p: Radial tandem junction thin film solar cells design for optimal light harvesting and balanced photo-current generation
Linwei Yu, Ecole Polytechnique, France

SC-02
2:25p-2:50p: Conducting polymer-dye composites for photoelectrochemical solar cells and energy storage
Arash Takshi, University of South Florida, USA

SC-03
2:50p-3:15p: The Solar Thermal Electrochemical Process (STEP) for the high solar efficiency production of ammonia, fuels, iron, cement and the removal of carbon dioxide from the atmosphere
Stuart Licht, George Washington University, USA

SC-04
3:15p-3:40p: Synthesis of nanostructured titanium dioxide for solar energy conversion
Eray Aydil, University of Minnesota, USA

Coffee Break

SC-05
3:50p-4:15p: Intra- to inter-molecular singlet fission in oligoenes
Minh Tuan Trinh, Columbia University, USA

SC-06
4:15p-4:30p: On the solar hydrogen production of α-Fe_2O_3 nanorings
Heberton Wender, Universidade Federal do Mato Grosso do Sul, Brasil

SC-07
4:30p-4:45p: Discernment of possible organic magnetic field effect mechanisms using polymer light-emitting electrochemical cells
Rugang Geng, University of Georgia, USA

SC-08
4:45p-5:00p: Thin flexible dye-sensitized solar cell with SWCNT cathode
Vladimir Saik, International Scientific Centre for Thermophysics and Energetics, Russia

CNTs, Graphene and 2D Materials I

Sunday Afternoon, November 23rd
Tampa Bay 3
Didier Pribat, *Chair*

CG-01
2:00p-2:25p: One-step fabrication of functionalized graphene materials via submerged liquid plasma [SLP] in solvent under ambient conditions
Masahiro Yoshimura, National Cheng Kung University, Taiwan

CG-02
2:25p-2:50p: Interfaces between transferred, CVD-grown graphene and MoS_2 probed with STM and ARPES
Matthias Batzill, University of South Florida, USA

CG-03
2:50p-3:15p: Silicene, germanene and stanene: Novel 2D honeycomb crystals from first principles
Friedhelm Bechstedt, Institut für Festkörpertheorie und –optic, Germany

CG-04
3:15p-3:40p: Bandgap control in graphene-molybdenum disulfide bilayer structures
Cristian V. Ciobanu, Colorado School of Mines, USA

Coffee Break

CG-05
3:50p-4:15p: Chemistry and electronic structure at graphene edges
Shintaro Fujii, Tokyo Institute of Technology, Japan

CG-06
4:15p-4:40p: Tailoring the properties of two dimensional molybdenum disulfide
Saiful I. Khondaker, University of Central Florida, USA

CG-07
4:40p-5:05p: Band-to-band tunnel FETs in one and two-dimensional materials
Joachim Knoch, RWTH Aachen University, Germany

CG-08
5:05p-5:30p: In situ TEM analysis of catalyst-assisted growth of multiwall carbon nanotubes and nanofibers
Jean-Luc Maurice, CNRS, France

Keynote Session III

Sunday Evening, November 23rd
Tampa Bay 1-2
Ioanna Giouroudi, *Chair*

K-4
Translating Nanomaterials and Technologies to Biomedical Applications: What's in the Horizon?
Shyam Mohapatra
University of South Florida, USA

Functional Materials II

Monday Morning, November 24th
Florida Bay 1
Hariharan Srikanth, *Co-Chair*
Federico Rosei, *Co-Chair*

FM-10
8:00a-8:15a: Surface wrinkling of shape memory polymers
Jianliang Xiao, University of Colorado, USA

FM-11
8:15a-8:30a: Influence of crystal defects on the martensitic transformation in Ni-Mn-Ga alloy
Anna Kosogor, National University of Science and Technology "MISiS", Russia

FM-12
8:30a-8:55a: Magnetic shape memory thin films and nano-disks: effects of size reduction on magnetism, structure and microstructure
Franca Albertini, Institute of materials for electronics and magnetism, Italy

FM-13
8:55a-9:20a: Voltage-controlled exchange bias and exchange bias training
Christian Binek, University of Nebraska, USA

FM-14
9:20a-9:45a: Organic spintronic devices
Luis Hueso, CIC nanoGUNE, Spain

FM-15
9:45a-10:10a: Evolution of a Disordered Nanoparticle Network into Boolean Logic
Wilfred van der Wiel, University of Twente, The Netherlands

Coffee Break

FM-16
10:20a-10:45a: Transition metal based magneto caloric materials
Ekkes Brück, Delft University of Technology, The Netherlands

FM-17
10:45a-11:10a: Caloric effects in ferroic materials
Lluis Manosa, Universitat de Barcelona, Spain

FM-18
11:10a-11:35a: Emerging functional properties in Cobalt-based oxides
Chandrima Mitra, Oak Ridge National Laboratory, USA

FM-19
11:35a-12:00p: Near-infrared emitting nanoparticles for applications in biology
Fiorenzo Vetrone, National Institute for Scientific Research, Canada

FM-20
12:00p-12:15p: Internal friction and impact toughness of superelastic FeMnAlNi alloys
Vladimir V. Khovaylo, National University of Science and Technology "MISiS", Russia

Nanophotonics and Plasmonics I

Monday Morning, November 24th
Florida Bay 2
W. David Wei, *Chair*

NP-01
8:25a-8:50a: Nonlinear optical imaging of plasmonic nanostructures at the limits of temporal resolution and spatial precision
Ken Knappenberger, Florida State University, USA

NP-02
8:50a-9:15a: Optically launched acoustic phonon modes reveal adhesion strength to substrate supported gold nanodisks
Wei-Shun Chang, Rice University, USA

NP-03
9:15a-9:40a: Investigation of optical nonlinearities in graphene and layered semiconductors by multiphoton imaging
Lasse Karvonen, Aalto University, Finland

NP-04
9:40a-10:05a: Optical response of a single deposited metal nano-object
Fabrice Vallee, CNRS - Universite Lyon 1, France

Coffee Break

NP-05
10:20a-10:45a: Taming the blackbody: thermal radiation spectrum engineering with plasmonic semiconductor nanowires
Michael A. Filler, Georgia Institute of Technology, USA

NP-06
10:45a-11:05a: Glass nanowires for nonlinear optics and sensing: a top-down approach
Rand Ismaeel, University of Southampton, UK

NP-07
11:05a-11:30a: Light emission from group-IV nanostructures in silicon
Brian Julsgaard, Aarhus University, Denmark

NP-08
11:30a-11:55a: Bridging the particle size gap for nanoplasmonics and nanocatalysis
Hui Wang, University of South Carolina, USA

NP-09
11:55a-12:20p: Spatiotemporal near-field excitation dynamics in nanostructures
Katsuyuki Nobusada, Institute for Molecular Science, Japan

Nanocarbon Based Supercapacitors

Monday Morning, November 24th
Florida Bay 3
Peng Chen, *Chair*

NS-01
8:25a-8:50a: Facile preparation of hierarchical porous carbon/graphene for energy storage
Yufeng Zhao, Yanshan University, China

NS-02
8:50a-9:15a: Printed highly ordered carbon nanostructures for enhanced supercapacitor performance
Binh Duong, Worcester Polytechnic Institute, USA

NS-03
9:15a-9:40a: Electrochemically synthesized polymer-graphene oxide composite films as supercapacitor materials
Pia Damlin, University of Turku, Finland

NS-04
9:40a-10:05a: Application of graphene oxide ionic liquid gels for supercapacitor electrodes
Hiroshi Hyodo, Tohoku University, Japan

Coffee Break

NS-05
10:20a-10:45a: Graphene materials based supercapacitors
Peng Chen, Nanyang Technological University, Singapore

NS-06
11:35a-11:50a: Hybrid composites of porous carbon and iron oxide for supercapacitors - morphological and electrochemical studies
Thanyalak Chaisuwan, Chulalongkorn University, Thailand

Advanced Nanomaterials and Nanotechnologies for Biomedical Applications II

Monday Morning, November 24th
Pensacola Bay
Jon Dobson, *Co-Chair*
Gil Lee, *Co-Chair*

AB-05
10:20a-10:45a: Fundamentals and applications of zinc oxide nanorods in enhanced optical bioassays
Jong-in Hahm, Georgetown University, USA

AB-06
10:45a-11:10a: Protein hydrogel photonic crystal sensors for chemical and biological analytes
Sanford A. Asher, University of Pittsburgh, USA

AB-07
11:10a-11:35a: Lipid nanotechnologies for drug screening and biosensor microarrays
Steven Lenhert, Florida State University, USA

AB-08
11:35a-11:50a: CdS nanocrystals prepared by colloidal solution method for biosensing application
Archana A. Meshram, Dr. Ambedkar College, India

AB-09
11:50a-12:05p: Erbium-doped $Y_3Ga_5O_{12}$ nano-garnet as optical nanothermometer in bioassays
Víctor Lavín, Universidad de La Laguna, Spain

AB-10
12:05p-12:20p: Optical labels based on depolarized light scattering from plasmonic nanoparticles
George Chumanov, Clemson University, USA

Resistive Switchings of Oxides and Related Nanocompostes/Heterostructures

Monday Morning, November 24th
Tampa Bay 3
Tamio Endo, *Co-Chair*
Jayan Thomas, *Co-Chair*
Hiroaki Nishikawa, *Co-Chair*
Seisuke Nakashima, *Co-Chair*

RS-01
8:00a-8:40a: p-n characteristics and switchings of LBMO/ZnO hetero-junctions
Tamio Endo, Mie University, Japan

RS-02
8:40a-9:05a: Ag/a-Si/c-Si crossbar switch: From discovery to commercialization
Yajie Dong, University of Central Florida, USA

RS-03
9:05a-9:30a: Electrical coupling of isolated cardiomyocyte clusters grown on aligned conductive nanofibrous meshes using electrospinning technique
Meng-Yi Bai, National Taiwan University of Science and Technology, Taiwan

RS-04
9:30a-9:55a: Making oxide nanocrystals via green chemistry: A story of cuprous oxide
Chun-Hong, Kuo Academia Sinica, Taiwan

Coffee Break

RS-05
10:10a-10:50a: Nonlinear optical absorption properties of LBMO/ZnO/LAO thin films
Reji Philip, Raman Research Institute, India

RS-06
10:50a-11:15a: Improving memory performance of Cu/HfO_2/Pt conducting-bridge RAM by solvent substitution
Kentaro Kinoshita, Tottori University, Japan

RS-07
11:15a-11:40a: The effect of changing electrode materials for the same resistive random access memory filament
Sang-Gyu Koh, Tottori University, Japan

RS-08
11:40a-12:05p: Advancing high resolution characterization for 2D materials
Laurene Tetard, University of Central Florida, USA

Functional Materials II

Monday Afternoon, November 24th
Florida Bay 1
Hariharan Srikanth, *Co-Chair*
Federico Rosei, *Co-Chair*

FM-21
2:00p-2:25p: Perovskite materials for energy related applications
Riad Nechache, Institut Nationale de la Recherche Scientifique, Canada

FM-22
2:25p-2:50p: An STM-guided search for 2D organic ferroelectrics and Co-crystals
Axel Enders, University of Nebraska, USA

FM-23
2:50p-3:15p: The role of surfaces and interfaces in multifunctional materials
Federico Rosei, National Institute for Scientific Research, Canada

FM-24
3:15p-3:40p: Using micro-origami techniques to create functional materials with complex architectures
Leszek Malkinski, University of New Orleans, USA

Coffee Break

FM-25
3:50p-4:15p: Controlling electrons through a single atom one at a time
Giuseppe C. Tettamanzi, The University of New South Wales, Australia

FM-26
4:15p-4:40p: From "smart" Material to "smart" Devices: Novel Applications based on the Insulator-to-Metal Transition in VO_2
Ali Hendaoui, LMN/INRS-EMT, Canada

FM-27
4:40p-5:05p: Nanostructured magnetoplasmonic metamaterials: a promising route for label-free molecular sensing applications
Paolo Vavassori, CIC nanoGUNE, Spain

FM-28
5:05p-5:20p: Europium tetrakis dibenzoylmethide triethylammonium: A bright functional material for smart sensors
Ross Fontenot, University of Louisiana at Lafayette, USA

Nanophotonics and Plasmonics II

Monday Afternoon, November 24th
Florida Bay 2
W. David Wei, *Chair*

NP-10
2:00p-2:25p: Enhanced light-matter interaction in graphene
Sanshui Xiao, Technical University of Denmark, Denmark

NP-11
2:25p-2:50p: Extreme light absorption architectures for solar-to-fuel conversion
Isabell Thomann, Rice University, USA

NP-12
2:50p-3:15p: Surface-enhanced solar energy harvesting and conversion using plasmon active nanostructures
Shanlin Pan, The University of Alabama, USA

NP-13
3:15p-3:40p: Plasmonic nanostructures for sensing and energy applications
Kevin L. Shuford, Baylor University, USA

Coffee Break

NP-14
3:50p-4:15p: Resonance energy transfer and hot electron transfer from plasmonic metal to semiconductor: applications in solar energy harvesting
Nianqiang Wu, West Virginia University, USA

NP-15
4:15p-4:40p: Boosting the photocatalytic efficiency of semiconductors via design of charge-transfer hybrid structures
Yujie Xiong,
University of Science and Technology of China, China

NP-16
4:40p-5:05p: From nanojets to threading plasmonic nanoparticle strings with light
Ventsislav K. Valev, University of Cambridge, UK

NP-17
5:05p-5:30p: Surface plasmon sensors with high sensitivity and resolution to study electric-field induced changes in the refractive index of liquid crystals and modifications in the Kretschmann configuration system for SPR measurements on not-easily-accessible samples

Suresh C. Sharma, The University of Texas at Arlington, USA

EMN General Workshop on Materials II

Monday Afternoon, November 24th

Florida Bay 3

Javier Alonso, *Chair*

GM-16

2:00p-2:25p: Nanocomposite materials for energy applications

Jackie Ying, Institute of Bioengineering and Nanotechnology, Singapore

GM-17

2:25p-2:50p: Small scale energy harvesting by magnetic shape memory alloys

Manfred Kohl, Karlsruhe Institute of Technology, Germany

GM-18

2:50p-3:05p: A study of the photovoltaic properties of AZO:N/p-Si with an inserted ZnO or AZO layer

Zoulikha Mouffak, California State University, Fresno, USA

GM-19

3:05p-3:30p: Synthesis of clathrate single crystals by spark plasma sintering

Yongkwon Dong, University of South Florida, USA

Coffee Break

GM-20

3:45p-4:10p: Synthesis of ZnO, In_2S_3, P_3HT, ZnS and In_2O_3 nanomaterials

Najoua Kamoun, Tunis University, Tunisia

GM-21

4:10p-4:25p: Synthesis and characterization of manganese oxide particles and investigation of their catalytic activities for oxidation of benzyl alcohol in liquid phase

Muhammed Saeed, Government College University Faisalabad, Pakistan

GM-22

4:25p-4:40p: New physical mechanism of diamond growth in low pressure linear microwave plasma

Štěpán Potocký, Institute of Physics of the ASCR,v.v.i. Czech Republic

GM-23

4:40p-4:55p: Synthesis of silica nanoparticles with controlled size for biological applications

Huseyin Kizil Istanbul Technical University, Turkey

GM-24

4:55p-5:10p: Structural, electronic and optical properties of semiconductor nanostructures

Ariadna Sanchez-Castillo, Universidad Autonoma del Estado de Hidalgo, Mexico

GM-25

5:10p-5:35p: Spin dynamics of skyrmionic magnetic bubbles and domain walls

Robert Reeve, Johannes Gutenberg-University Mainz, Germany

Advanced Nanomaterials and Nanotechnologies for Biomedical Applications II

Monday Afternoon, November 24th

Pensacola Bay

Jon Dobson, *Co-Chair*

Gil Lee, *Co-Chair*

AB-11

2:00p-2:25p: Nanomagnetic remote control of cell signaling and gene expression

Jon Dobson, University of Florida, USA

AB-12

2:25p-250p: Magnetic nanoparticles and the influence of their magnetic properties for biomedical applications

Cindi Dennis, The National Institute of Standards and Technology, USA

AB-13
2:50p-3:15p: Microfluidic biosensors using magnetic nanoparticles
Ioanna Giouroudi, Vienna University of Technology, Austria

AB-14
3:15p-3:40p: Magnetically barcoded microcarriers detection with TMR and asymmetric giant magneto-impedance sensors
Pratap Kollu, University of Cambridge, UK

Coffee Break

AB-15
3:50p-4:15p: The next generation of multifunctional magnetic nanoparticles for biomedical engineering applications
Hafsa Khurshid, University of South Florida, USA

AB-16
4:15p-4:40p: New class of magnetic bioceramics for biomedical applications
Aleksandr S. Kamzin, Ioffe Physical-Technical Institute of RAS, Russia

Poster Session – Group I
Carbon-based materials and technologies, Catalytic materials, Polymer composites

Monday Evening, 6p – 7:30p, November 24th
Tampa Bay 1-3
Dong-Hyun Kim, *Chair*

PC-01
Microstructure and surface properties of carbon nanostructured materials obtained by chlorination reaction of $Zr(C_5H_5)_2Cl_2$
D.J. Araujo-Pérez, Universidad Veracruzana, México

PC-02
Nanoporous carbon for applications in supercapacitors and batteries
Areeya Ninlerd
Chulalongkorn University, Thailand

PC-03
Facile synthesis of morphologically controlled nanoporous carbon using a soft-templating method for supercapacitors
Pornpichaya Thawepornpuriphong, Chulalongkorn University, Thailand

PC-04
Novel CO_2 storage by using hierarchical N-rich nanoporous carbon via facile templates synthesis as an adsorbent
Nanthawut Chokaksornsan, Chulalongkorn University, Thailand

PC-05
Theoretical study of hydrogen adsorption and diffusion in spillover process on microporous carbon
Masanori Tachikawa, Yokohama-city University, Japan

PC-06
Applications of Fe_3O_4@Ag nanoparticles above graphite
Anh D. Phan, University of Illinois, USA

PC-07
Electronic effects in nanoparticle silver catalysts
Nigora Turaeva, Webster University, USA

PC-08
Unexpected catalytic performance of Ni/SiO_2 nanoparticles prepared by magnetron sputtering deposition for reverse water gas shift reaction
Renato V. Gonçalves, University of São Paulo, Brazil

PC-09
Preparation of dewetting surface showing low contact angle hysteresis toward control of water droplet behavior
Takahiro Ishizaki, Shibaura Institute of Technology, Japan

Poster Session – Group II
Smart sensor materials, Soft magnetic materials, Optical properties

Monday Evening, 6p – 7:30p, November 24th
Tampa Bay 1-3
Khanh Kieu, *Chair*

PS-01
High frequency giant magnetoimpedance effect of amorphous microwires
Arkady Zhukov, University of Basque Country, Spain

PS-02
Radiation hardness of candidate luminescent sensor materials
Stephen Williams, University of Louisiana at Lafayette, USA

PS-03
Using luminescent materials to detect space radiation
Jacque Meche, University of Louisiana at Lafayette, USA

PS-04
High frequency magneto-resistance effects of Co-rich soft ferromagnetic ribbons and microwires
Dao Son Lam, University of South Florida, USA

PS-05
Excellent magnetocaloric properties of Gd-based amorphous microwires for active magnetic refrigeration in the liquid nitrogen temperature range
Hongxian Shen, Harbin Institute of Technology, China

PS-06
A novel biosensor based on magneto-impedance technology and functionalized magnetic nanoparticles for sensitive detection of cancer cells and biomolecules
Jagannath Devkota, University of South Florida, USA

PS-07
Tunable magnetocaloric response in high-speed melt-spun La-Ce-Fe-Si ribbons
XueLing Hou, Shanghai University, China

PS-08
Design and fabrication of interdigital nanocapacitors coated with Hafnium for biological sensing
Gabriel Gonzalez Contreras, Universidad Autonoma de San Luis Potosi, Mexico

PS-09
Modified solvothermal synthesis of cobalt ferrites ($CoFe_2O_4$) nanoparticles and their optical studies
Abdullah G. Al-Sehemi, King Khalid University, KSA

PS-10
Structural, optical and electrical studies on Eu-doped ZnO thin films for optoelectronic devices
Olfa Kamoun, Université de Tunis El-Manar, Tunisia

PS-11
First principles simulation of phonon confinement effects in Ge [111] nanowires
Alejandro Trejo Baños, Instituto Politécnico Nacional, México

PS-12
Magnetic deposition of aligned silver nanowire transparent electrodes
Oleksandr Trotsenko, University of Georgia, USA

Poster Session – Group III
Energy-related materials and applications
Biomedical materials and applications

Monday Evening, 6p – 7:30p, November 24th
Tampa Bay 1-3
Cindi Dennis, *Chair*

PE-01
Development of graphene based materials for energy conversion
Nanda Gopal Sahoo, Kumaun University, India

PE-02
Anisotropic thermoelectric generator made from semimetal microwire
L.A. Konopko, D.Ghitu Institute of Electronic Engineering and Nanotechnologies, Moldova

PE-03
Electrochemical behaviour of a new transparent conductive oxide(TCO) layer-less cell structure
Ho-Gyeong Yun, Electronics and Telecommunications Research Institute, Republic of Korea

PE-04
Fabrication and evaluation of Al paste with Bi_2O_3-B_2O_3-ZnO glass frit for screen-printed energy devices

Bit-Na Kim, Electronics and Telecommunications Research Institute, Republic of Korea

PE-05
Initial studies on silver sulfide sensitized metal oxide electrodes for solar cells
Pooja P. Magar, University of Pune, India

PE-06
Development of bioprocess technology for jet fuel production from photosynthetic cells
Ganapathy Sivakumar, Arkansas State University, USA

PE-07
Iron oxide nanoparticles with controlled morphology for advanced hyperthermia
Zohreh Nemati Porshokouh, University of South Florida, USA

PE-08
Mechanical properties of nanocomposite polymers for tissue regeneration
Bailey Barnes, University of Arkansas at Little Rock, USA

PE-09
Ceramic-metal bionanocomposites for improved performance of medical implants
José F. Bartolomé, Consejo Superior de Investigaciones Científicas, Spain

PE-10
Stability and instability of lipid multilayer drug screening microarrays
Nicholas Vafai, Florida State University, USA

PE-11
Impedance Analysis of Solvent Substitution Effect on Resistive Switching Property of HfO_2-CB-RAM
Masato Yoshihara, Tottori University, Japan

PE-12
Particle size and morphology dependent magnetic properties of o-$EuMnO_3$ and h-$YbMnO_3$ nanoparticles
Raja Das, University of South Florida, USA

Nanoscale Optics and Photonics

Tuesday Morning, November 25th

Florida Bay 1

Zhimin Shi, *Chair*

NO-01

8:30a-8:55a: Ultrafast fiber lasers enabled by carbon nanotubes and their applications

Khanh Kieu, University of Arizona, USA

NO-02

8:55a-9:20a: Controlled coupling of nanoparticles to polymer-based photonic structures

Ngoc Diep Lai, Institut D'Alembert, France

NO-03

9:20a-9:45a: Manipulating light with all-dielectric metasurfaces

Jason Valentine, Vanderbilt University, USA

NO-04

9:45a-10:10a: Quantum states of light in metamaterials require a new effective-medium theory

Martijn Wubs, Technical University of Denmark, Denmark

NO-05

10:10a-10:35a: Structured light-matter interactions at the nanoscale

Xiaobo Yin, University of Colorado at Boulder, USA

NO-06

10:45a-11:10a: Rainbow trapping effect: Broadband light trapping and splitting in hyperbolic metafilm patterns

Qiaoqiang Gan, The State University of New York at Buffalo, USA

NO-07

11:10a-11:35a: Superradiant thermal emission and light absorption

Zongfu Yu, University of Wisconsin Madison, USA

NO-08

11:35a-12:00p: Slow-light spectroscopic devices on chips

Zhimin Shi, University of South Florida, USA

CNTs, Graphene and 2D Materials II

Tuesday Morning A, November 25th

Florida Bay 2

Didier Pribat, *Chair*

CG-09

8:55a-9:20a: Atomically thin vertical heterojunction devices

Jing Guo, University of Florida, USA

CG-10

9:20a-9:45a: Applications of photon-electron interactions for advanced optoelectronics in 2D materials

Swastik Kar, Northeastern University, USA

CG-11

9:45a-10:00a: Effective thermal properties and interfacial thermal resistances of multiphase nanocomposites containing carbon nanotubes and inorganic nanoparticles

Feng Gong, National University of Singapore, Singapore

CG-12

10:00a-10:15a: Graphene oxide: bacterial stimulant or antimicrobial agent

Wen-Shuo Kuo, National Cheng Kung University, Taiwan

CG-13

10:15a-10:30a: Carbon nanospheres synthesis using palm oil and activated carbons

Arenst Andreas Arie, Parahyangan Catholic University, Indonesia

Advanced Nanomaterials and Nanotechnologies for Biomedical Applications III

Tuesday Morning B, November 25th

Florida Bay 2

Jon Dobson, *Co-Chair*

Gil Lee, *Co-Chair*

AB-17
10:45a-11:10a: Glucose-driven “Organic Engine” with enzyme membrane for autonomous drug release system as self-sustainable artificial pancreases for diabetes
Kohji Mitsubayashi, Tokyo Medical and Dental University, Spain

AB-18
11:10a-11:35a: New insights into the picosecond dynamics of water and solvated proteins
Vinh Q. Nguyen, Virginia Tech, USA

AB-19
11:35a-12:00p: Single cell endoscopy
Anna Pyayt, University of South Florida, USA

Session MM
NOVEL MAGNETIC MATERIALS AND PHENOMENA

MM-01 (Invited Talk)
Spin-torque nano-oscillators for wireless communication

Byoung-Chul Min[1], Chaun Jang[1], Jae-Hyun Park [1], Jung-Hwan Moon[2], Seung-Young Park[3], Kyung-Jin Lee[2], and Kyung-Ho Shin[1]

[1]Korea Institute of Science and Technology, Seoul 136-791, Korea
Email:min@kist.re.kr
[2]Korea University, Seoul 136-701, Korea
[3]Korea Basic Science Institute (KBSI), Daejeon 305-764, Korea

Spin-polarized current can excite magnetization precession in magnetic nanostructures by spin-transfer torque, leading to spin-torque nano-oscillators (STNOs). The STNOs raise prospects for the application in RF transceivers, but should overcome critical drawbacks such as weak output power and broad spectral line width. Previously, the STNOs have been realized with nano-magnetic elements, for instance, nano-pillars and nano-contacts having single magnetic domain or vortex structure. Here we employ a novel magnetic entity in STNOs, which can provide unique properties resolving major challenges. It is shown that, in a properly-tailored magnetic nano structure, the perpendicular spin current gives rise to microwave oscillation with a strong spectral intensity and narrow line width; and, more importantly, the microwave oscillation is observed even without applying external magnetic fields. This nano-tailoring of magnetic elements opens a new venue to engineer the properties of STNOs, and thereby sheds light on their real applications.

MM-02 (Invited Talk)
Theory and simulation of magnetic materials: Surface effects and spin transport

H. T. Diep

Laboratoire de Physique Théorique, UMR 8089 CNRS Université de Cergy-Pontoise, France

Email:diep@u-cergy.fr, web site: http://diep.u-cergy.fr/indexnfl_en.html

Magnetic materials have always been a subject of fascinating research due to their numerous applications. Today, technological advances allow for creating artificial materials both in composition and in shape which provide desired effects for applications. Many theoretically-known properties of materials are still under-exploited. Yet, theorists and experimentalists continue to work on new materials.

In this talk I will review some known results on surface effects in frustrated magnetic thin films obtained from both theories and Monte Carlo simulations. Frustrated spin systems [1] possess numerous spectacular bulk properties which have been discovered during the last 30 years. In thin films, the frustration enhances surface effects [2] which exist already in standard non frustrated magnetic thin films and are known a long-time ago [3]. I will also consider the spin transport phenomenon which depends intimately on the crystal magnetic structure and spin fluctuations [4]. I show that many experimental observations of spin resistivity can be explained by simple models which take into account interaction between itinerant spins and lattice spins. I will focus the discussion on phenomena which occur near the boundaries separating phases of different symmetries.

1. *Frustrated Spin Systems,* Ed. H. T. Diep (World Scientific, 2013).
2. V. Thanh Ngo and H. T. Diep, *Phys. Rev. B* 75, 035412 (2007) and references therein.
3. Diep-The-Hung, J. C. S. Levy and O. Nagai, *Phys. Stat. Solidi (b)* 93, 351 (1979).
4. Y. Magnin and H. T. Diep, *Phys. Rev. B* 85, 184413 (2012) and references therein.

MM-03 (Invited Talk)
Spin caloritronics in ordered alloy systems

Koki Takanashi

Institute for Materials Research, Tohoku University, Sendai 980-8577, Japan
Email: koki@imr.tohoku.ac.jp, web site: http://magmatelab.imr.tohoku.ac.jp/

Some of ordered alloys where different types of atoms show a regular arrangement are attracting materials for spintronics. Our group has been working on half-metallic Heusler alloys with high spin polarization, [1, 2] and $L1_0$-ordered ordered alloys with high magnetic anisotropy. [3, 4] Recently we are also interested in *spin caloritronics* in ordered alloys; particularly, anomalous Nernst effect in perpendicularly magnetized $L1_0$-oredered alloy films, and Peltier cooling effect in nano-pillars with half-metallic Heusler alloys.

Spin caloritronics is a newly established field, which concerns the correlation between heat current, spin current, and charge current. The recent discovery of the spin Seebeck effect, *i.e*., the generation of spin current from a temperature gradient, has explosively expanded this field.[5] The anomalous Nernst effect (ANE) is a phenomenon that an electric field is induced along the vector product direction of temperature gradient and magnetization. Although ANE has been well known since a long time ago, the systematic investigation including material dependence has not been made and the mechanism has neither fully elucidated. The discovery of the spin Seebeck effect has given a new insight into ANE and also stimulated interest in ANE again. In this study, the ANE in perpendicularly magnetized $L1_0$-FePt(001) thin films epitaxially grown on MgO(001) substrates by sputtering has been investigated[6]. The relationship between ANE and anomalous Hall effect (AHE) depending on the measurement temperature has also been examined. Uniaxial magnetic anisotropy energy (K_u) was changed in the range from 3.0×10^6 to 2.7×10^7 erg/cc, depending on the degree of $L1_0$ order, which was controlled by the deposition temperature from 300 to 500˚C. The ANE conductivity has been found to decrease with K_u, in contrast to the AHE conductivity showing an increase with K_u. This result suggests a contribution of magnon spin current to ANE.

Furthermore, we proposed a new-type of thermopile consisting of two ferromagnetic materials with ANE signals of opposite signs.[7] We have really demonstrated the enhancement of the thermoelectric voltage, using the combination of $L1_0$-FePt and $L1_0$-MnGa films, which is promising for thermoelectric applications.

Peltier cooling effect (PCE) will be one of promising methods to overcome heating problems in highly integrated electronics devices. Fukushima *et al.* [8] first reported enhanced PCE in Co/Au nano-pillars. Furthermore, the possibility of high thermoelectric cooling by adiabatic spin-entropy expansion was theoretically proposed when electrons flow from a highly spin-polarized ferromagnet to a paramagnet in nano-superstructure[8]. In this study, PCE has been studied in various ferromagnet/nonmagnet nano-pillars with different pillar diameters from 40 to 400 nm, using half-metallic Heusler alloy Co_2MnSi, non-half-metallic Heusler alloy Co_2FeSi, and conventional ferromagnets such as Fe and Co. Peltier coefficient, Π was evaluated from the shift of a parabolic resistance-current (R-I) curve. The enhancement of Π was clearly observed with decreasing the pillar diameter in all the cases. However, the result could not be explained by adiabatic spin-entropy expansion,[9] because the current direction for cooling is opposite to that predicted by the model.

1. T. Iwase *et al.*, Appl. Phys. Exp., **2**, 063003 (2009).
2. R. Okura *et al.*, Appl. Phys. Lett., **99**, 052510 (2011).
3. T. Seki *et al.*, Nature Mater., **7**, 125 (2008).
4. T. Seki *et al.*, Nature Commun., **4**:1726 doi:10.1038/ncomm2737 (2013).
5. K. Uchida *et al*., Nature, **455**, 778 (2008).
6. M. Mizuguchi *et al*., Appl. Phys. Exp., **5**, 093002 (2012).
7. Y. Sakuraba *et al*., Appl. Phys. Exp., **6**, 033003 (2013).
8. A. Fukushima *et al*., Jpn. J. Appl. Phys., **44**, L12 (2005).
9. H. Katayama-Yoshida *et al*., Jpn. J. Appl. Phys.,

46, L777 (2007).

MM-04 (Invited Talk)
Tunneling magneto-Seebeck effect

Andy Thomas
Bielefeld University
D2/ Thin films and physics of nanostructures
Universitaetsstrasse 25, 33615 Bielefeld
Germany

Email: andy.thomas@uni-bielefeld.de

We prepared Co-Fe-B/MgO/Co-Fe-B magnetic tunnel junctions (MTJ) by magnetron sputtering and observed the tunnel magnetoresistance (TMR) effect. The maximum TMR ratio was 330% and 530% at room temperature and 13K, respectively. If we heat our junctions with short laser pulses of a laser diode or a Ti:sapphire laser to induce a temperature gradient between the two electrodes, we observe the tunneling magneto Seebeck (TMS) effect. The TMS effect is similar to the TMR effect, but in this case the Seebeck coefficient of the junction changes if the magnetic configuration is altered. The Seebeck coefficients in parallel and antiparallel configurations are similar to the voltages known from the charge Seebeck effect. The tunneling magneto Seebeck effect was investigated in dependence of the base temperature and temperature gradient across the tunnel barrier. Recently, we also studied the effect of an applied bias voltage to the TMS effect leading to more than 3000% TMS ratio. This is supported by TEM studies of the microstructure, numeric simulations of the temperature profile in the junction and possible devices utilizing the tunneling magneto Seebeck effect.

MM-05 (Invited Talk)
Half-metallic Co_2MnSi/diamond Schottky junctions for spintronic applications

Kenji Ueda, Hidefumi Asano

Graduate School of Engineering, Nagoya University, Furo-cho, Chikusa-ku, Nagoya, Japan
Email: k-ueda@numse.nagoya-u.ac.jp

Semiconductor spintronics is expected as future basic technology for structuring advanced telecommunications and information society. In order to fabricate novel spintronic devices such as spin transistors, which are key components for unvolatile and low power electronic devices, efficient spin injection from ferromagnetic electrodes to semiconductors are necessary. However, best combination of ferromagnets and semiconductors for spin injection is not well established at present. It is considered one of the effective methods for efficient spin injection is to use half-metallic ferromagnets, which generate fully spin-polarized carriers, as spin sources.

Diamond semiconductors are promising for high-power and high-frequency devices because of its excellent physical properties such as its wide band gap, high breakdown voltage, high thermal conductivity, etc. [1]. We consider diamond is also an ideal host for spin transport [2]. This is mainly because diamond has long spin diffusion length because of its low spin-orbit interactions. However, there are no reports on spin injection to diamond. In this study, Schottky junctions using half-metallic Co_2MnSi (CMS)/diamond heterostructures were fabricated and their physical properties were investigated as a first step for spin injection to diamond.

Boron-doped homoepitaxial diamond films were grown on commercial (100) diamond substrates by microwave plasma CVD. Typical acceptor concentration and room temperature mobility were ~10^{17} cm^{-3} and ~1000 cm^2/Vs, respectively [3]. CMS films (50-100 nm) were deposited on diamond films by Ar ion-beam sputtering (IBS) or dual Ar ion-beam assisted sputtering (IBAS) [4]. Ferromagnetic Schottky junctions using CMS as Schottky contacts were fabricated on the B-doped diamond films by using usual photolithographic process.

Low temperature growth of CMS films below ~400°C was found to be important for obtaining abrupt CMS/diamond interfaces. The growth of the CMS films was performed by using ion-beam sputtering with Ar ion-beam assistance

(IBAS). For IBAS, ion-beam irradiation was performed during the film growth to give additional energy for film formation, reducing growth temperature (T_S). XRD measurements revealed that (110) oriented CMS films were obtained on diamond at 300-500°C by IBAS. The saturation magnetization (M_S) and coercive fields (H_C) of the CMS films were ~1060 emu/cc and ~70 Oe, respectively, which were comparable to those of bulk CMS (M_S: ~1100 emu/cc, H_C: ~5 Oe). The CMS films formed at 300-400°C showed a negative AMR of ~0.3% at 4 K, suggesting half-metallic characters of the CMS films. Schottky junctions using the CMS (T_S= 300-400°C)/diamond heterostructures showed clear rectification properties with a rectification ratio of >10^6 (Fig. 1). The Schottky barrier heights of the CMS/diamond interfaces were estimated to be ~1.0 eV with reasonable ideality factor (n= ~1.2) by using thermionic emission (TE) model. These results suggest that high quality CMS/diamond Schottky junctions for efficient spin injection can be obtained by the method.

1. K. Ueda et al., *IEEE Electron Dev. Lett.* **27**, 570 (2006).
2. K. Ueda, T. Soumiya and H. Asano, *Diamond Relat. Mater* **25**, 159 (2012).
3. K. Ueda, K. Kawamoto, T. Soumiya, and H. Asano, *Diamond Relat. Mater* **38**, 41 (2013).
4. K. Ueda, T. Soumiya, M. Nishiwaki, and H. Asano, *Appl. Phys. Lett.* **103**, 052408 (2013).

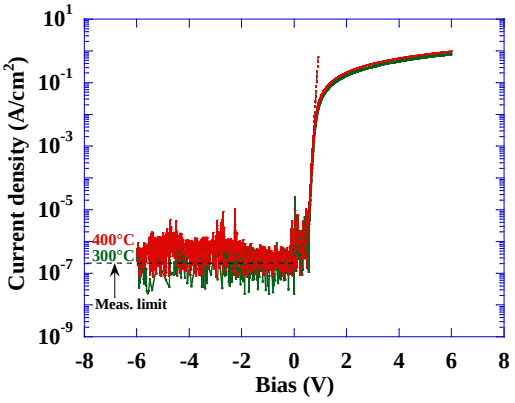

Fig. 1. Current-voltage characteristics for CMS (T_S= 300-400°C)/diamond Schottky junctions. The dotted line shows the fitting results using the equation for TE model.

MM-06 (Invited Talk)

Kondo physics in nanoscopic metallic non-local spin transport devices

Chris Leighton[1], L. O'Brien[1,2], D. Spivak[3], H. Ambaye[4], R.J. Goyette[4], V. Lauter[4], P.A. Crowell[3]

[1]*Department of Chemical Engineering and Materials Science, University of Minnesota, Minneapolis, MN, USA*
Email: leighton@umn.edu, web site: http://research.umn.edu/leighton/

[2]*Thin Film Magnetism, Cavendish Laboratory, University of Cambridge, UK*

[3]*School of Physics and Astronomy, University of Minnesota, Minneapolis, MN, USA*

[4]*Neutron Science Directorate, Oak Ridge National Laboratory, Oak Ridge, TN, USA*

Despite the maturity of metallic spintronics there remain large gaps in our understanding of spin transport in metals, particularly with injection of spins across ferromagnetic/non-magnetic (FM/NM) interfaces, and their subsequent diffusion and relaxation. Unresolved issues include the limits of applicability of the Elliott-Yafet spin relaxation mechanism, the influence of defects, surfaces, and interfaces on spin relaxation at nanoscopic dimensions, and the importance of magnetic and spin-orbit scattering. The non-local spin-valve is an enabling device in the study of such problems as, in addition to offering potentially disruptive applications, it allows for the separation of charge and spin currents. One particularly perplexing issue in metallic non-local spin valve devices is the often observed non-monotonicity in the temperature-dependent spin accumulation, where the spin signal actually *decreases* at low temperatures, in contrast to expectations. In this work, by studying an expanded range of FM/NM combinations (encompassing $Ni_{80}Fe_{20}$, Ni, Fe, Co, Cu, and Al), we demonstrate that this effect is not a property of a given FM or NM, but rather of the FM/NM *pair*. The non-monotonicity is in fact strongly correlated with the ability of the FM to form a

dilute local magnetic moment in the NM. We show that local moments, formed by FM/NM interdiffusion, suppress the injected spin polarization and diffusion length *via* a novel manifestation of the Kondo effect, thus explaining all observations associated with the low temperature downturn in spin accumulation. We further show: (a) that this effect can be promoted by thermal annealing, at which point the conventional charge transport Kondo effect can be simultaneously detected in the NM, and (b) that this suppression in spin accumulation can be quenched, even at interfaces that are highly susceptible to the effect, by insertion of a thin non-moment-supporting interlayer. Important implications, potentially even for room temperature devices, will be discussed.

Work at UMN supported by the NSF MRSEC (DMR-0819885), Seagate, and a Marie Curie International Outgoing Fellowship, 7th European Coomunity Framework Programme (No. 299376). Work at the SNS, ORNL, supported by US DOE.

1. L. O'Brien, M. Erickson, D. Spivak, H. Ambaye, R. Goyette, V. Lauter, P. Crowell and C. Leighton, *Nature Communications* **5**, 3927 (2014).

MM-07 (Invited Talk)

Magneto-transport phenomena in amorphous ferrimagnets

Jiwei Lu

Department of Materials Science and Engineering, University of Virginia, Charlottesville, USA
Email:jl5tk@viriginia.edu,
http://www.virginia.edu/ms/people/faculty/lu.html

Amorphous rare earth-transition metal alloy films have been studied as magneto-optical recording devices due to their large perpendicular magnetic anisotropy (PMA). There is renewed interest in these materials as spintronic and heat-assisted magnetic recording materials. In the theory of amorphous ferrimagnets, the coupling between RE and TM ions is antiferromagnetic. TM ions have a small magnetic anisotropy and RE ions, except Gd, have large anisotropy. The large TM-TM ferromagnetic coupling align the TM moments, while the large RE anisotropy causes the RE moments to form a 'cone'. The origins of PMA in amorphous films remain elusive. Current results are beginning to shed light in understanding these materials. Nevertheless, global anisotropic short-range order could still arise in amorphous films, perhaps associated with inevitable growth stresses initiated at the film-substrate interface. Previous studies attributed the PMA of RE-TM films to structural features ranging from columnar textures to crystallinity.

One attractive feature of the RE-TM films is that the saturation magnetization (M_s) can be tuned to very low values, which is desirable for low power spintronic devices. Due to the different temperature dependences of the sublattice magnetizations, by changing the RE and TM compositions, M_s can be made to vanish theoretically at the magnetic compensation temperature (T_{comp}). In *a*-GdFeCo and TbFeCo, the compensation temperature can be tuned by simply varying the composition. Magnetization reversal occurs near T_{comp}, where coupling between the RE and TM ions allows them to exchange angular momentum in ~10 femto-seconds, enabling ultrafast magnetic switching.

Amorphous TbFeCo and GdFeCo films with 30 at. % Tb or Gd and strong PMA were deposited at ambient temperature. High-resolution TEM study showed amorphous features on the nanometer scale, confirming the amorphous nature of the films. *a*-TbFeCo films show a low M_s~100 emu/cc and a high PMA coercivity comparable to or larger than those reported for $TbFe_2$ Laves-phase films. The out-of-plane magnetic coercive field (H_C) was ~0.66 T and anisotropy field (H_K) was ~1.6 T. An anisotropy energy (K_U) of ~10^6 erg/cc was

estimated from the hysteresis loops. A strong size dependence of coercivity in ferromagnetic *a*-TbFeCo films was observed. The anomalous Hall resistance exhibits the same compensation temperature as magnetic moment for both systems. An asymmetric magneto-resistance (MR) was observed in both TbFeCo and GdFeCo near their compensation temperatures. Such asymmetric MR reverses polarity at temperature below the compensation point indicating the different scattering mechanism than the anomalous Hall effect. The bi-stable magneto-resistance can be obtained with the absence of external H fields. The origin of such anomaly in the MR behaviors will be discussed. The bi-stable magneto-resistance may open new applications for these amorphous ferrimagnets.

MM-08 (Invited Talk)
Novel magnetoresistance in semiconductor

Xiaozhong Zhang[1], Zhaochu Luo [1]

[1]*School of Materials Science and Engineering, Tsinghua University, Beijing 100084, China*

Email: xzzhang@tsinghua.edu.cn

Magnetoresistance (MR) reported in some non-magnetic semiconductors particularly silicon has triggered considerable interest owing to the large magnitude of the effect. Here we showed that MR in lightly doped n-Si can be significantly enhanced by introducing two diodes and proper design of the carrier path [Figure 1]. We designed a geometrical enhanced magnetoresistance (GEMR) device whose room-temperature MR ratio reaching 30% at 0.065 T and 20000% at 1.2T, respectively, approaching the performance of commercial MR devices. The mechanism of this GEMR is: the diodes help to define a high resistive state (HRS) and a low resistive state (LRS) in device by their openness and closeness, respectively. The ratio of apparent resistance between HRS and LRS is determined by geometry of silicon wafer and electrodes. Magnetic field could induce a transition from LRS to HRS by reshaping potential and current distribution among silicon wafer, resulting in a giant enhancement of intrinsic MR [1,2].

We also demonstrate that this GEMR can be realized in GaAs and Ge. We expect that this GEMR could be also realized in other semiconductors. The combination of high sensitivity to low magnetic fields and large high-field response should make this device concept attractive to the magnetic field sensing industry. Moreover, because this MR device is based on a conventional silicon/semiconductor platform, it should be possible to integrate it with existing silicon/semiconductor devices and so aid the development of silicon/semiconductor-based magnetoelectronics. Also combining MR devices and semiconducting devices in a single Si/semiconductor chip may lead to some novel devices with hybrid function, such as electric-magnetic-photonic properties. Our work demonstrates that the charge property of semiconductor can be used in the magnetic sensing industry where the spin properties of magnetic materials play a role traditionally.

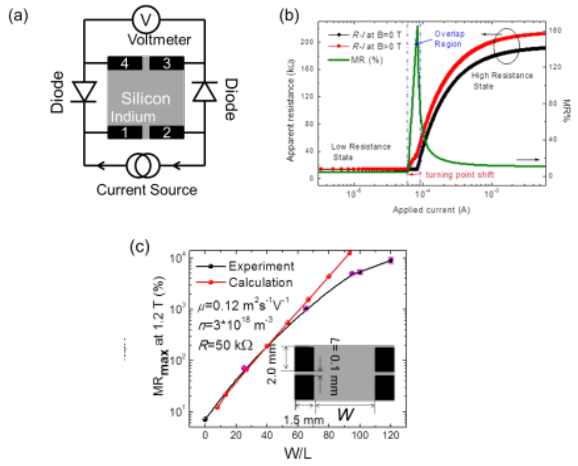

Fig.1 (a) asymmetrical geometry of electrodes placed on material and measurement circuit. (b) The MR approached the maximum at magnetic field-dependence transition from LRS to HRS. (c) MR_{max} changed with geometry factor *W*/*L* exponentially at 1.2 T.

1. C.H. Wan, X. Z. Zhang, X. L. Gao, J. M. Wang & X. Y. Tan, *Nature* **477**, 304 (2011).

2. X. Z. Zhang, C.H. Wan, X.L. Gao, J.M. Wang & X.Y. Tan, *Nature* **501,** E1-E2 (2013).

MM-09 (Invited Talk)
Engineering materials and devices for all optical magnetic recording

C.-H. Lambert[1,2,*], M. Gottwald, B.S. Varaprasad[3], Y.K. Takahashi[3], M. Hehn[1], M. Cinchetti[4], G. Malinowski[1], K. Hono[3], Y. Fainman[5], M. Aeschlimann[4] et E.E. Fullerton[2,5]. S. Mangin[1,2]

[1]*Institut Jean Lamour, UMR CNRS 7198 – Université de Lorraine, Nancy, France.*
[2]*Center for Magnetic Recording Research, University of California San Diego, La Jolla, USA.*
[3]*Magnetic Materials Unit, National Institute for Materials Science, Tsukuba, Japan.*
[4]*Department of Physics and Research Center Optimas, University of Kaiserslautern, Kaiserslautern, Germany.*
[5]*Department of Electrical and Computer Engineering, University of California San Diego, La Jolla, USA.*

** charles-henri.lambert@univ-lorraine.fr*

Often presented as a breaking point with the conventional magnetic recording methods the possibility to reverse the magnetization without any external magnetic field opens new horizons for the storage industry. Particularly the use of femtosecond laser pulses for magnetization switching is interesting since it enables a low power control of magnetization and that this pulses are 1000 to 10 000 times shorter than the shortest magnetic fields pulses or spin-polarized current pulses needed to induce magnetic reversal.

If most of the past 15 years were limited to the manipulation of the magnetization in a few GdFeCo alloy composition [1], we explore and broaden the possibilities for the observation of All-Optical Helicity Dependent Switching (AO-HDS) phenomenon. We will present a review of the materials that can be switched using circularly polarized pulses and the consequences for the understanding of the underlying mechanisms. The careful study of a wide range of Rare-Earth Transition Metal (RE-TM) combinations along with the development of specific alloys, multilayers, heterostructures and RE-free Co-Ir-based synthetic ferrimagnets (SFI) offer a novel approach to probe the phenomena. In addition the optical behavior observed for ferromagnets (highlighted in Fig1) such as Co/Pt, Co/Pd multilayers, CoNi alloys and more importantly FePt-$L1_0$ granular media open new possibilities for application in the recording media industry. These observations are compatible with mechanisms based on a combination of heat and angular momentum transfer from the laser pulses to the magnetic system.

Our finding shows that optical control of magnetic materials is a much more general phenomenon than previously assumed and may have a major impact on data memory and storage industries through the integration of optical control of ferromagnetic bits.

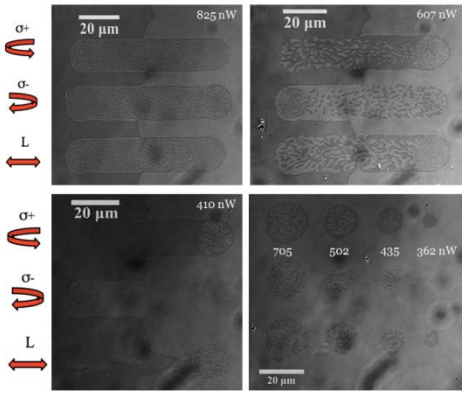

Fig. 1. Magneto-optical response in zero applied magnetic field of $[Co(0.4\ nm)/Pt(0.7\ nm)]_N$ multilayer samples to various laser polarizations. (A) N = 8 repeats. (B) N = 5 repeats. (C and D) N = 3 repeats. Both right and left circularity and linear polarization are represented. In (D), the laser was fixed at individual spots over a region of the sample with uniform magnetization. The average laser intensity at different spots is indicated in the image.

1. C. D. Stanciu, F. Hansteen, A. V. Kimel, A. Kirilyuk, A. Tsukamoto, *Physical Review Letter*, **99**, 4, 047601 (2007).
2. S. Mangin, M. Gottwald, C.-H. Lambert, D. Steil, V. Uhlir, L. Pang, M. Hehn, S. Alebrand, M. Cinchetti, G. Malinowsky, Y. Fainman, M. Aeschlimann, E. E. Fullerton, *Nature Materials*, **13**, 3 286-296 (2014).
3. C.-H. Lambert, S. Mangin, B.S. Varaprasad, T. Takahashi, M. Hehn, M. Cinchetti, G. Malinowski, K. Hono, Y. Fainman, M. Aeschlimann, E.E. Fullerton, Accepted in *Science*, http://arxiv.org/abs/1403.0784.

MM-10 (Invited Talk)
Irreversibility of Magnetic Domain Evolution of Co/Pt multilayers during Magnetization Reversal

Dong-Hyun Kim[1], Duy Truong Quach[1]

[1] *Department of Physics, Chungbuk National University, Cheongju 361-763, Chungbuk, South Korea*
Email:donghyun@cbnu.ac.kr, web site: http://spintronics.cbnu.ac.kr

Magnetization reversal phenomenon has attracted great attention due to its relevance with technological applications such as magnetic recording and spintronic devices. One of fundamental issues of magnetization reversal is a reversibility/irreversibility of magnetization reversal, particularly mediated by magnetic domain dynamics occurring on a microscopic scale. Magnetic return point memory, which measures the reproducibility of magnetization ensemble average observed along a ferromagnetic hysteresis loop has been intensively investigated mostly by scattering techniques[1,2]. Here, we report our detailed investigation on the reversibility/irreversibility of magnetic domain patterns, directly observed by magneto-optical Kerr microscopy for Co/Pt multilayers with perpendicular magnetic anisotropy. By systematic control of saturating and holding field, number of nucleations initiated in an early phase of magetization reversal is engineered, where a contrasting reversibility characteristics are observed between wall expansion and nucleation phenomena. For instance, an asymmetric nucleation (Fig. 1) provides a distinctive magnetization relaxation curve, quantitatively explained based on microscopic magnetic domain evolution patterns.

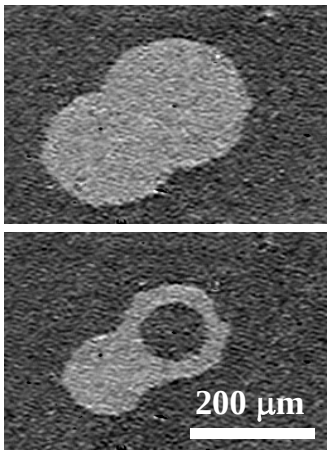

Fig. 1. Magnetic domain asymmetry originated from irreversible nucleation.

1. M. S. Pierce et al., *Phys. Rev. Lett.* **90**, 175502 (2003).
2. K. A. Seu et al., *New J. Phys.* **12**, 035009 (2010).

MM-11 (Invited Talk)
Imaging of magnetoelectric heterostructures by photoemission electron microscopy

X. Moya[1], F. Maccherozzi[2], A. I. Tovstolytkin[3], D. I. Podyalovskii[3], L. C. Phillips[1], W. Yan[1], M. Ghidini[1], M. E. Vickers[1], S. S. Dhesi[2] and N. D. Mathur[1]

[1]*Department of Materials Science, University of Cambridge, Cambridge, CB3 0FS, United Kingdom*

Email: xm212@cam.ac.uk

[2]*Diamond Light Source, Chilton, Didcot, Oxfordshire, OX11 0DE, United Kingdom*

[3]*Institute of Magnetism, 36b Vernadsky Blvd., Kyiv 03142, Ukraine*

The magnetic properties of epitaxial thin films can be electrically controlled via piezoelectric strain from ferroelectric substrates, and are typically monitored using bulk magnetometry [1,2]. Imaging techniques enable the microscopic study of magnetoelectric effects and provide insight into the strain-mediated coupling that is responsible. I will present photoemission electron microscopy (PEEM) images with contrast from x-ray magnetic circular dichroism (XMCD) in order to reveal the microscopic nature of the magnetoelectric coupling in epitaxial manganite films of $La_{0.67}Sr_{0.33}MnO_3$ grown on substrates of ferroelectric $BaTiO_3$ and the relaxor $Pb(Mg_{1/3}Nb_{2/3})_{0.72}Ti_{0.28}O_3$.

[1] W. Eerenstein, M. Wiora, J. L. Prieto, J. F. Scott and N. D. Mathur, *Nat. Mater.* **6**, 348 (2007).

[2] C. Thiele, K. Dörr, O. Bilani, J. Rödel and L. Schultz, *Phys. Rev. B* **75**, 054408 (2007).

MM-12 (Invited Talk)
Nanocrystalline glass-coated microwires – magnetization process and applications

R. Varga[1], P. Klein[1], R. El Kammouni[2] and M. Vazquez[2]

[1]*Faculty of Science, Institute of Physics, UPJS, Park Angelinum 9, 041 54 Košice, Slovakia, Email: rvarga@upjs.sk*

[2]*Instituto de Ciencia de Materiales de Madrid, CSIC, Sor Juana Inés de la Cruz 3, 28049 Cantoblanco, Madrid, Spain*

Amorphous glass-coated microwires are composite materials that consist of metallic nucleus (1-50 μm in diameter) covered by glass-coating (thickness 2-20 μm). Having positive magnetostriction, they are characterized by monodomain structure, within which the magnetization process runs through the single Barkhausen jump of single closure domain along entire wire [1]. This domain wall is characterized by extremely high domain wall velocities [2] sometimes higher than sound speed [3]. On the other hand, amorphous microwires have very poor time and thermal stability, which can be solved by application of nanocrystalline structure. Nanocrystalline materials are composite materials that consist of crystalline grains (with diameter cca. 10 nm) embedded in amorphous matrix. Hence, they combine excellent magnetic properties of amorphous alloys with high stability of crystalline materials [4,5].

In the first part of contribution, the fast domain wall dynamics in magnetic nanocrystalline microwires will be introduced. Different effects responsible for high velocity in microwires will be described (different anisotropies [6], various domain structures, etc.). Moreover, the effect of annealing on the domain wall dynamics stability will be shown.

In the second part, the application of the fast domain wall dynamics for construction of different miniaturized sensors of magnetic field, temperature [7], mechanical stress [8], etc.. will be discussed.

1. R. Varga, K.L. Garcia, M. Vazquez, P. Vojtanik, *Phys. Rev. Lett.* **94** 017201 (2005).
2. R. Varga, A. Zhukov, J. M. Blanco, M. Ipatov, V. Zhukova, J. Gonzalez, P. Vojtaník, *Phys. Rev B* **74** 212405 (2006).
3. R. Varga, A. Zhukov, J. M. Blanco, M. Ipatov, V. Zhukova, J. Gonzalez, P. Vojtaník, *Phys. Rev. B* **76** 132406 (2007).
4. E. Komova, M. Varga, **R. Varga**, P. Vojtanik, J. Bednarcik, J. Kovac, M. Provencio, M. Vazquez, *Appl Phys Lett* **93** 062502 (2008).
5. P. Klein, **R. Varga**, P. Vojtanik, J. Kovac, J. Ziman, G. A. Badini-Confalonieri, and M. Vazquez, *J. Phys.D:Appl.Phys.* **43** 045002 (2010).
6. K. Richter, R. Varga, G. A. Badini-Confalonieri and M. Vázquez, *Appl. Phys. Lett.* **96** 182507 (2010).
7. R. Hudák, R. Varga, J. Živčák, J. Hudák, J. Blažek and D. Praslička, *"Application of Magnetic Microwires in Titanium Implants – Conception of Intelligent Sensoric Implant"*,in *Aspects of Computational Intelligence: Theory and Applications Topics in Intelligent Engineering and Informatics*, Volume 2, Part 5, 413-434 (2013).

8. D. Praslička, J. Blažek, M. Šmelko, J. Hudák, A. Čverha, I. Mikita, R. Varga, A. Zhukov, *IEEE Trans. Magn.* **49** 128 (2013).

MM-13 (Invited Talk)
Spontaneous superlattice formation via magnetic field induced phase separation

Naoki Wakiya[1,2,3], Naonori Sakamoto[1,3], Toshimasa Sakakibara[3], Daiki Suzuki[3], Takanori Kiguchi[4], Kazuo Shinozaki[5], Hisao Suzuki[1,2,3]

[1]*Research Institute of Electronics, Shizuoka University, 3-5-1 Johoku Naka-ku, Hamamatsu 432-8561, Japan, E-mail: tnwakiy@ipc.shizuoka.ac.jp, web site: http://www.ipc.shizuoka.ac.jp/~tnsakam/*

[2]*Graduate School of Science and Technology, Shizuoka University, 3-5-1 Johoku Naka-ku, Hamamatsu 432-8561, Japan*

[3]*Department of Electronics and Materials Science, Shizuoka University, 3-5-1 Johoku Naka-ku, Hamamatsu 432-8561, Japan*

[4]*Institute for Materials Research, Tohoku University, 2-1-1 Katahira, Aoba-ku, Sendai 980-8577, Japan*

[5]*Department of Metallurgy and Ceramics Science, Tokyo Institute of Technology, 2-12-1 O-okayama, Meguro-ku, Tokyo 152-8550, Japan*

Pulsed laser deposition (PLD) is widely used to prepare thin films containing artificial superlattice. The artificial superlattice is prepared typically by alternative deposition using two targets with different chemical compositions. We have developed a specially designed PLD in which an electromagnet is installed in the vacuum chamber (Dynamic Aurora PLD) [1]. This equipment enables to deposited thin film at 800°C under 2 kG of a magnetic field. Using this equipment, we found that spontaneous superlattice formation is observed using a single target. We have succeeded to prepare thin films with spontaneous superlattice for epitaxially grown perovskite type compounds with A-site excess composition such as $SrTiO_3$, Nb- or La-doped $SrTiO_3$ and $(La,Sr)MnO_3$ thin films (an example for Nb-doped $SrTiO_3$ is shown in Fig. 1). TEM-EDS line scan measurements revealed that the film had a periodical compositional modulation. These facts suggest that the spontaneous superlattice formation is brought about by the spinodal decomposition. In general, spinodal decomposition occurs after annealing (aging) of a uniform phase. However, Tersoff predicted theoretically that the spinodal decomposition could also occur during epitaxial growth to form spontaneous superlattice [2]. The observation of emission spectra revealed that ionization of metal atoms are significantly increased by applying a magnetic field, suggesting ion impingement into the substrate occurs during thin film deposition. Chen *et al.* deposited TiC thin film by pulse-dc sputtering, and reported that ion-impingement lowers an activation energy for diffusion [3]. Therefore, we consider that applying magnetic field during PLD enhances automatic ion-impingement that lowers the activation energy for up-hill diffusion of spinodal decomposition. It should be noted that nucleation and growth is another possible mechanism for the spontaneous superlattice formation [4]. To determine which mechanism is plausible, we examined the relationship between the period and annealing time, and concluded that the mechanism is spinodal decomposition. This method is applicable for other compounds. Therefore this method could be a novel method to prepare superlattice using a single target.

1. N. Wakiya, K. Muraoka, T. Kadowaki, T. Kiguchi, N. Mizutani, H. Suzuki, K. Shinozaki, *J. Magn. Magn. Mater.* **310**, 2546 (2007).
2. I. Daruka I, J. Tersoff, *Phys. Rev. Lett.* **95**, 076102 (2005).
3. C. Q. Chen, Y. T. Pei, K. P. Shaha, and J. Th. M. De Hosson, *Appl. Phys. Lett.* **96**, 073103 (2010).
4. J. L. MacManus-Driscoll, *Adv. Func. Mater.* **20**, 2035-2045 (2010).

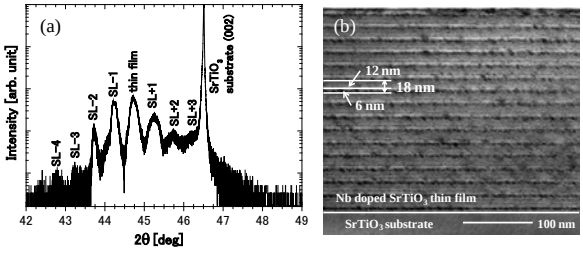

Figure 1. (a) XRD and (b) cross sectional TEM photograph of spontaneously formed superlattice for Nb-doped $SrTiO_3$ thin film.

MM-14 (Contributed Talk)

Giant Magnetoresistance in Double Organic-spacer-layers Spin Valves (DOSVs)

S. H. Liang[1], Q. T. Zhang[2,3], L. You[2], R. Geng[1], R. C. Subedi[1], J. L. Wang[2], X. F. Han[3] and T. D. Nguyen[1]*

1. Department of Physics & Astronomy, University of Georgia, Athens, GA 30602, USA
2.School of Materials Science and Engineering, Nanyang Technological University, Singapore 639798, Singapore
3.Beijing National Laboratory of Condensed Matter Physics, Institute of Physics, Chinese Academy of Sciences,
Beijing 100190, China
Email: ngtho@uga.edu, web site: https://www.physast.uga.edu/research/nguyen/

Organic semiconductors have been considered as promising and fascinating materials for various device applications due to their mechanical flexibility, chemically tunable electronic property, and their relatively low-cost manufacturing process. In addition, the materials possess long-spin lifetime due to the weak spin-orbit coupling and hyperfine interaction, making them excellent candidates for organic spin valves[1-3] (OSVs, see Fig. 1a), where spin injection, transport and detection have been demonstrated. Recently, there have been interested in bipolar OSVs, dubbed spin organic LEDs[4-5] where both spin aligned electrons and holes are injected into the organic spacer. In an ideal condition, the emission from the device can be turned on and off by a relative weak magnetic field. However, this condition is hard to achieve mainly because the spin injection capability from ferromagnetic electrodes is greatly diminished at an applied voltage above 1 volt while the emission normally happens at above 2.5 volts.

To overcome the degradation of the injected spin polarization at high applied voltages, we studied the magnetoresistance (MR) in the double-layer OSV (DOSV) structure (Fig. 1b). We observed the MR under an operation voltage as large as 6V in the Alq_3 DOSVs while MR in conventional Alq_3 OSV with the same spacer thickness disappears at above 1 volt (Fig. 1c, d). This implies that the injected spin polarization is enhanced in the DOSVs over the OSVs. Interestingly, we found that the spin diffusion length of Alq_3 does not depend on applied voltages and temperature, in contrast to what were reported in the literature. In addition, the injection capability reduces when the applied voltage and device temperature increases (Fig.2). Our studies suggest that the DOSVs might be a great device to study spin physics in organic semiconductors especially for spin organic LEDs.

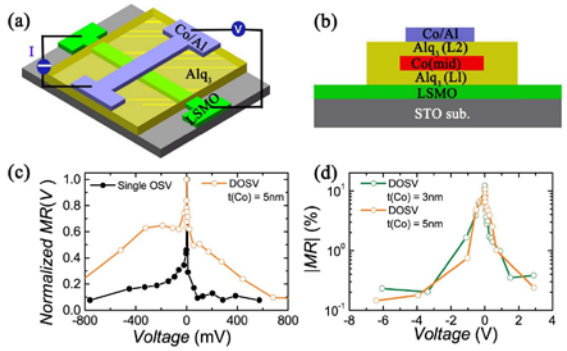

Fig. 1. (a) A scheme of a regular OSV device with the four probe measurement technique; (b) Schematic side views of a DOSV; (c) The MR bias voltage dependence properties at 10k, for the MR of regular OSV(black) and DOSVs(organce); (d) The |*MR*| valve versus bias voltage for DOSVs of LSMO(50)/Alq_3(25)/Co(*t*)/Alq_3(25)/Co(15nm) with *t*=5 nm(orange) and 3nm(olive).

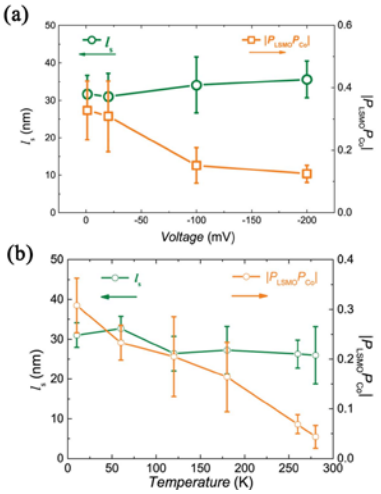

Fig. 2. Spin diffusion length l_s and the spin polarization, $|P_{LSMO}\cdot P_{Co}|$, *versus* bias (a) voltage and (b) temperature.

Reference
1. Z. H. Xiong, D. Wu, Z. V. Vardeny, and J. Shi, *Nature* **427**, 821 (2004).
2. F. J. Wang, C. G. Yang, Z. V. Vardeny, and X. G. Li, *Phys. Rev. B* **75**, 245324 (2007).
3. D. Sun, L.Yin, C. Sun, H. Guo, Z. Gai, X.-G. Zhang, T. Z. Ward, Z. Cheng, and J. Shen, *Phys. Rev. Lett.* **104**, 236602 (2010).
4. V. A. Dediu, L. E. Hueso, I. Bergenti, C. Taliani, *Nat. Mater.* **8**, 707 (2009).
5. T. D. Nguyen, E. Ehrenfreund, Z. Valy Vardeny, *Science* **337**, 204 (2012).

MM-15 (Invited Talk)
Interactions in magnetic nanoparticles: phenomenology and atomistic modeling

Òscar Iglesias

Dept. de Física Fonamental and Institut de Nanociència and Nanotecnologia de la UB (IN2UB),Universitat de Barcelona, Av. Diagonal 647, 08028 Spain. Email:oscar@ffn.ub.es, web site: http://www.ffn.ub.es/oscar

The properties of magnetic particles show interesting peculiar behavior when going to the nanometric and low temperature regimes. Nanoparticles (NP) with non-homogeneous compositions or peculiar morphologies, which can be tuned by proper control of the conditions of the synthesis method, have been shown to be useful for technological and biomedical applications. Over the last decades, it has been shown that finite-size and surface effects, together with collective effects, are crucial to understand the magnetic phenomenology of NP assemblies. In this contribution, we will start by reviewing the present theoretical frameworks used to explain the influence of intrinsic (surface and interfacial effects) [1] and collective [2] (dipolar and exchange interparticle interactions) features on the magnetic properties of NPs. We will also present a theoretical framework [3] that allows to study the interplay of the increased surface anisotropy due to the above mentioned surface effects and dipolar interpaticle interactions. The obtained analytical expressions for the magnetization curves (that agree well with MC simulations in the macrospin approximation) show that, depending on the overall sign of the parameters that govern both effects, intrinsic and collective terms may have competing or synergistic effects. Finally, we will exemplify the applicability of the previously introduced macrospin models by presenting simulation results that allow a better understanding of the improved hyperthermia properties in cubic NP chain assemblies [4] and the explanation of the different relaxation behaviors of Fe oxide NP coated by Silica and oleic acid [5] in terms of the change of dipolar field distributions induced by the alignment of the magnetic moments by the application of a magnetic field.

1. Ò. Iglesias, A. Labarta and X. Batlle, J. Nanoscience and Nanotecnology 8, 2761 (2008).
2. Ò. Iglesias, A. Labarta., Phys. Rev. B 70, 144401 (2004).
3. Z. Sabsabi, F. Vernay, Ò. Iglesias, H. Kachkachi, Phys. Rev. B 88, 104424 (2013).
4. C. Martínez-Boubeta et al., Scientific Reports 3, 1652 (2013).
5. C. Moya, Ò. Iglesias, X. Batlle, A. Labarta, in preparation (2014).

MM-16 (Invited Talk)
Neutron scattering studies of molecule based magnets

Javier Campo

Aragón Materials Science Institute, (CSIC-University of Zaragoza), C/ Pedro Cerbuna 12, 50009 Zaragoza, Spain.
Email: javier.campo@csic.es web site: http://icma.unizar-csic.es

Neutron scattering techniques can provide fundamental insight into the different magnetic behaviors shown by molecule based magnets. In a short introduction the properties of the neutron–matter interactions (strong and magnetic dipolar) and the fundamentals of neutron scattering will be presented in order to facilitate an understanding of the peculiarities of this probe in molecule based magnets. Selected examples will be presented of the use of different neutron scattering techniques on very different molecular

magnetic materials. *S-based organic magnets*. The sulphur based free-radical family p-X-$C_6F_4CNSSN\cdot$ (X = Br, NO_2, CN) represents an alternative to the classical nitrogen-oxygen construct for the design of purely organic magnets. This example shows how to explore and understand the magnetic interaction mechanisms, via spin density determination using polarized neutron diffraction [1] *Single molecule magnets*. Single crystal neutron diffraction at very low temperatures and high magnetic field shows how the Mn12-acetate SMM can order via the magnetic dipolar interaction. However, for magnetic fields larger than 5 T it undergoes a quantum phase transition into a zero magnetization phase [2]. The effect of crystal disorder on quantum tunneling in the single-molecule magnet Mn12-benzoate will also be illustrated through measurements of the energy levels using inelastic neutron scattering [3]. *Chiral magnets*. The control of magnetic chirality in a material could be employed in spintronic devices in order to create or manipulate a spin-current. This example will show how neutron Laue diffraction can help to determine magnetic structures (and therefore the magnetic chirality) in very small crystals of $[Cr(CN)_6][Mn(S)\text{-}pnH(H_2O)](H_2O)$ [4]. *Spin-crossover magnets*. It has proved possible to determine the correlation between the motion of the pyrazine rings and the high-low spin transition in the spin crossover compound {Fe(pz)[Pt(CN)4]} by measuring quasi-elastic neutron scattering [5]. *Spin-waves in Heisenberg Antiferromagnets*. It is shown how it is possible to determine the magnetic interaction constants in molecular magnets by measuring the spin-wave dispersion curves with neutron triple axis spectroscopy [6].

1. J. Luzón, et al. *Phys Rev B*. 81(2010)
2. F Luis, J Campo et al. *Phys Rev Let* 95, 227202 (2005)
3. Ch. Carbonera et al. *Phys Rev B* 81, 014427 (2010)
4. J Campo et al. submitted (2014)
5. J. A. Rodríguez-Velamazán et al. *J. Amer. Chem. Soc*. (2012)
6. J. Campo et al, *Phys Rev B*. 78, 054415 (2008).

MM-17 (Invited Talk)
Magnetization dynamics and collective phenomena in magnetic nanostructures

Javier Alonso[1,2], Luis Fernández Barquín[3], Diego Alba Venero[3,4], Mª Luisa Fdez-Gubieda[1,5], José Manuel Barandiarán[1,5], Andrey Svalov[5], Manh-Huong Phan[2], Hariharan Srikanth[2]

Email:jalonsomasa@gmail.com
[1]BCMaterials Edificio No. 500, Parque Tecnológico de Vizcaya, Derio 48160, Spain
[2]Department of Physics, University of South Florida, Tampa, FL 33620, USA
[3]CITIMAC Unidad Asociada CSIC, Universidad de Cantabria, 39005 Santander, Spain
[4]ISIS, STFC Rutherford Appleton Laboratory, Chilton Didcot, OX11 0QX, United Kingdom
[5]Depto. Electricidad y Electrónica, Universidad del País Vasco, Leioa 48940, Spain

Nanostructured magnetic materials have attracted enormous research attention because of their unique magnetic properties, such as exchange bias or giant magnetoresistance, and their promising applications, spreading from nano-scale electronic devices, sensors and high-density data storage media to controlled drug delivery and cancer theragnosis systems. Magnetic nanoparticles are a good example of such multi-functional materials. The magnetic properties of these nanoparticles depend strongly on different factors including their shape, size, spatial arrangement, and concentration. At very low concentrations, when the nanoparticles are well separated, each of them behaves like an individual nanomagnet characterized by the instability of the magnetization due to thermal disorder, and this results in the phenomenon of superparamagnetism. With increasing concentration of nanoparticles, magnetic interactions become relevant. First, long range interactions, such as dipolar, become noticeable and they tend modify the anisotropy barrier of each nanoparticle. This can result in a frustrated collective state that has many similarities with spin-glasses. However, with increasing nanoparticle density, long–range order

correlations tend to appear and a ferromagnetic-like state may be obtained [1,2].

We have focused on the study of the magnetization dynamics and collective phenomena of nanoparticle assemblies at different concentrations [3]. For this we have prepared Fe_xAg_{100-x} granular thin films, composed of Fe nanoparticles inside a Ag matrix by sputtering deposition technique, with Fe-concentrations $15 \leq x \leq 50$. Their structure was characterized by Transmission Electron Microscopy (TEM), X-ray Diffraction (XRD), and X-Ray Absorption Spectroscopy (XAS) measurements, showing that we have managed to obtain ensembles with a varying number of Fe nanoparticles, whose size (~3 nm) remains practically constant. This has allowed us to perform a thorough study of the collective magnetic behaviors as a function of the density of nanoparticles. Their magnetic behavior has been characterized by dc and ac magnetometry, together with transverse susceptibility, and has revealed that at intermediate concentrations, around 30-35 at. %, a magnetic percolation process takes place, characterized by, among other things, a sudden increase in the correlation length and a clear change in the magnetization dynamics. This gives rise to a crossover from a superspin glass (15-30 %) to a superferromagnetic behavior (> 40 %).

1. S. Bedanta and W. Kleemann, *J. Phys. D: Appl. Phys.*, **42**, 013001, (2009).
2. S. Mørup, M.F. Hansen, and C. Frandsen. *Beilstein J. Nanotechnol*. **1**, 182-190, (2010).
3. M.L. Fdez-Gubieda, J. Alonso Masa, and L. Fernández Barquín, "Collective magnetic behaviors in interacting magnetic nanoparticle" in *Nanoparticles Featuring Electromagnetic Properties: From Science to Engineering* (Kerala: Research Signpost) 167 (2012).

MM-18 (Invited Talk)
Ordered arrays of magnetic nanostructures in thin films: synthesis and modeling

Paola Tiberto[1], Gabriele Barrera[1], Federica Celegato[1], Marco Coisson[1], Alessandra Manzin[1], Franco Vinai[1]

[1]*Electromagnetics Division, INRIM,Torino, Italy*
Email:tiberto@inrim.it

Progress in nanomagnetism has been achieved by the simultaneous advances in nanotechnology that allows the fabrication of novel magnetic nanostructures, as arrays in magnetic thin films. This is primarily motivated by applications such as spintronics, magnetic sensing, and ultrahigh-density magnetic recording. In this context, fabrication process based either on high-resolution planar lithography (i.e. sequential optical, electron-beam and focused ion beam lithography) or large area self-assembly approaches (polystyrene nanospheres or nanotemplates) have played a major role and has been intensively worldwide investigated in the last decade. Alternative bottom-up techniques have been explored for its low cost and are becoming particularly appealing for spintronics, magnetic sensing, and ultrahigh-density magnetic recording [1].

In this work, conventional lithographical techniques (EBL and FIB) together with multi-step processes exploiting self-assembling of polystyrene nanospheres and block-copolymers to create arrays of nanostructures in magnetic thin films will be highlighted. Such arrays have been transferred to a wide variety of thin films (i.e. Co, Ni, $Ni_{80}Fe_{20}$, $Fe_{50}Pd_{50}$, $Fe_{50}Pt_{50}$ and Ni-Mn-Ga alloys) having functional magnetic properties [2]. As examples, Co dots embedded in a $Ni_{80}Fe_{20}$ matrix obtained by self-assembling are shown in Fig. 1 together with room-temperature magnetization properties acquired at every synthesis step. Magnetisation reversal and magnetotransport response will be discussed in the light of microstructural configuration.

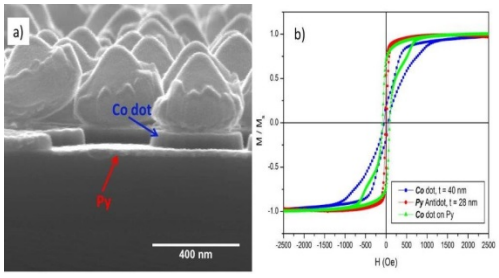

Fig. 1. (a) SEM image of patterned bicomponent array of nanostructures; (b) room-temperature hysteresis loops of Co MM array (blue curve), $Ni_{80}Fe_{20}$ hole array (red curve) and combination of the two nanostructures (green curve).

1. G.P. Wiederrecht, *Handbook for nanofabrication* (Elsevier, 2010)

2. P. Tiberto, G. Barrera, L. Boarino, F. Celegato, M. Coïsson, N. De Leo, F. Albertini, F. Casoli and P. Ranzieri, *J. Appl. Phys.* **113** , 17B516 (2013)

MM-19 (Contributed Talk)
Tunable ferromagnetism in diluted amorphous $Ge_{1-x}Mn_x$

Giampiero Amato[1], Gianluca Conta[2], Marco Coisson[1], Paola Tiberto[1]

[1]Electromagnetics Division, INRIM,Torino, Italy
[2]Chemistry Department, University of Torino, Torino, Italy
Email:g.amato@inrim.it

The introduction of spin degree of freedom into the semiconductor technology envisages the possibility of integrating both information processing and storage in a single device: one way to get this result is to introducetransition metal impurities in a semiconductor host, making a dilute magnetic semiconductor (DMS). Among various DMS alloys, $Ge_{1-x}Mn_x$ *inter alia* has gained considerable attention thanks to its compatibility with mainstream Si technology. One of the major research effort, together with increasing the critical temperature, is to overcome the Mn tendency to cluster and form precipitates like Ge_3Mn_5 and Ge_8Mn_{11} exhibiting large ferromagnetic interactions (T_c 270° C and 296° C respectively) and typically occurring in epitaxial films grown by Molecular Beam Epitaxy [1]. To avoid such a precipitation two main strategies are available, the first being to carefully tune the growth parameters as rate of deposition (R_d), temperature of the substrate (T_s) and Mn concentration of the epitaxial film. Another way is to grow the semiconductor on thermal SiO_2 avoiding the occurrence of epitaxial growth. In this work, $Ge_{1-x}Mn_x$ thin films with different Mn concentration (ranging in the interval 0.3-36 at%) were grown by low temperature (T_s = 150° C) UHV e-gun evaporation on SiO_2 substrate (300 nm thermal oxide) with R_d =12 Å/min, a condition which should promote the formation of the Ge_3Mn_5 and Ge_8Mn_{11} in a epitaxial films but not in amorphous ones [2].

Compositional analysis by XPS has been carried out in order to verify the Mn concentration and alloy homogeneity. The dependence of electrical resistivity on temperature has been studied indicating a metallic behavior at high Mn concentration (36%). Conversely, semiconductor-like behavior in specimens with low Mn% has been observed together with an increase of the film's resistivity.

Temperature evolution of magnetization has been measured by VSM-SQUID together with magnetization hysteresis loops as a function of temperature. All the films are characterized by a Tc lower than 200 K also for high Mn concentration excluding the formation of Ge_3Mn_5 and Ge_8Mn_{11} ferromagnetic precipitates. The ferromagnetic behavior of $Ge_{1-x}Mn_x$ films degrades after annealing that has been carried out with Rapid Thermal Annealing (RTA) for 1 min at 400°C. As evidenced by Raman spectroscopy, re-crystallization occurs in all samples depending on the content of Mn and influences their ferromagnetic role. Explanations for such an effect will be given.

1. M. Jamet, A. Barski, T. Devillers, V. Poydenot R. Dujardin, P. Bayle-Guillemaud and S. Tatarenko, *Nat. Mater.* **5**, 653 (2006)
2. S. Yada, R. Okazaki, S. Ohya and M. Tanaka *Applied Physics Express* **3** (2010) 123002.

MM-20 (Invited Talk)
Caloric Effects Near Tricritical Points

Karl G. Sandeman[1,2,3], J. Zemen[3], Z. Gercsi[3,4], J.B. Staunton[5]

[1]Department of Physics, Brooklyn College of the City University of New York, Brooklyn, NY 11210, USA
[2]The Graduate Center, City University of New York, 365 Fifth Avenue, New York, NY 10016, USA
[3]Department of Physics, Imperial College London, London SW7 2AZ, UK
[4]CRANN and School of Physics, Trinity College Dublin, Dublin 2, Ireland
[5]Department of Physics, University of Warwick, Coventry CV4 7AL, UK

Email:karlsandeman@brooklyn.cuny.edu, web site: http://www.brooklyn.cuny.edu/web/academics/faculty/faculty_profile.jsp?faculty=1199

Ferroic refrigerants are solids that possess a composition- and field-dependent phase transition with a large isothermal entropy change. [1] The manipulation of such a phase transition by a suitable driving field, for example strain, pressure, an electric field or a magnetic field yields a temperature change under adiabatic conditions that is the basis for gas-free cooling. The search for optimally performing ferroic refrigerants has led to a survey of novel critical and tricritical material systems [2] and the development of characterisation tools to study first order phase transitions. [3] The focus on tricritical materials in particular enables a balance to be struck between the benefits of large entropy changes at a first order transition and the disadvantages associated with thermal hysteresis.

In this presentation I will highlight the use of high resolution neutron diffraction data to accelerate materials design in the case of metamagnetic refrigerants and to test *ab initio* theories of finite temperature magnetism [4,5,6]. I will mention two examples of synergistic discovery: how an Ashby plot analysis [2] can be used to examine spin crossover as a potential new source of strain/pressure-driven caloric effects and how large piezomagnetic effects may be predicted from *ab initio* studies of noncollinear antiferromagnets.

The research leading to these results has received funding from the European Community's 7th Framework Programme under grant agreement Nos. 214864 (SSEEC) and 310748 (DRREAM).

1. S. Fähler et al., *Adv. Eng. Mater.* **14,** 10 (2012).
2. K.G. Sandeman, *Scr. Mater.* **67,** 566 (2012).
3. K.G. Sandeman, *Magn. Tech. Int.* **4,** 72 (2014).
4. Z. Gercsi et al., *Phys. Rev. B* **83,** 174403 (2011).
5. Z. Gercsi et al., *Phys. Rev. B* **88,** 024417 (2013).
6. J. B. Staunton et al., *Phys. Rev. B* **87,** 060404 (2013).

MM-21 (Invited Talk)

Revisiting magneto-volume anomalies and magneto-caloric effect in R_2Fe_{17} intermetallics

Pedro Gorria[1], Pablo Alvarez-Alonso[2], José L. Sánchez Llamzares[3], Jesús A. Blanco[4]

[1] Department of Physics & IUTA, EPI, University of Oviedo, 33203 Gijón, Spain
Email:pgorria@uniovi.es

[2]Departamento de Electricidad y Electrónica, Universidad del Pais Vasco, 48940 Leioa, Spain

[3]División de Materiales Avanzados, IPICYT, San Luis Potosí 78216, Mexico

[4]Department of Physics, Faculty of Sciences, University of Oviedo, 33007 Oviedo, Spain

The 'INVAR effect' was discovered by Guillaume in a ferromagnetic fcc $Fe_{65}Ni_{35}$ binary alloy at the end of XIX century. This effect consists of an almost constant -'invariant'- lattice parameter or unit cell volume of the alloy (nearly zero or low thermal expansion, LTE) in a wide temperature range below the Curie temperature [1]. Nowadays, an intense research activity is being developed in this topic, which is at the crossover between Solid State and Materials Physics. INVAR alloys are very attractive as functional materials for technological applications requiring temperature-independent geometry (i.e. precision sensors for aerospace technology or high-resolution screens). Therefore, the search for new INVAR materials and/or new processing methods in order to enlarge the temperature range for LTE above room temperature is a current challenging issue [2]. Moreover, ferromagnetic INVAR materials display other anomalies in their physical properties, such as the negative pressure dependence of the Curie temperature and the hyperfine field distribution, the elastic moduli or the heat capacity among others, which are commonly referred to as *magneto-volume anomalies* [1,3].

R_2Fe_{17} compounds (R = rare earth) exhibit a rich variety of magnetic behaviors (ferro-, antiferro-, or ferri-magnetic and more complex magnetic orderings such as helimagnetism or fan magnetic structures) depending on the rare earth element [4]. Moreover, all of them display large

magneto-volume anomalies induced by the strong dependence of the magnetic exchange interaction on the Fe-Fe interatomic distances [5,6]. In addition, these binary intermetallics show a moderate magneto-caloric effect, MCE, with values of the magnetic entropy change, ~ 6 $Jkg^{-1}K^{-1}$ (for $\mu_0\Delta H$ = 5 T) at room temperature (for R = Nd, Pr) [7-9].

In this talk we will show our recent and more interesting investigations on the magneto-volume anomalies and the magneto-caloric effect of R_2Fe_{17} alloys in polycrystalline, nanostructured and rapid quenched samples. The combination of magnetometry-based experimental techniques together with neutron and x-ray diffraction under extreme conditions (temperature and hydrostatic pressure) enables to pursue a detailed characterization of the alloys. Therefore, a deeper insight into the strong magneto-volume coupling, governed by the Fe-Fe interatomic distances, can be attained.

We acknowledge the financial support from MINECO, Spain (MAT2011-27573-C04) and CONACyT, Mexico (CB 2010-01-156932; 00232624).

1. E. F. Wassermann, *J. Magn. Magn. Mater.* **100**, 346 (1991).
2. P. Gorria *et al., Phys Rev. B* **69**, 214421 (2004); *ibid* **80**, 064421 (2009).
3. M. L. Winterrose *et al., Phys Rev. Lett.* **102**, 237202 (2009).
4. K.H.J. Buschow, *Rep. Prog. Phys.* **40**, 1179 (1977).
5. P. Gorria *et al., Acta Mater.* **57**, 1724 (2009).
6. P. Alvarez-Alonso, P. Gorria *et al., Phys Rev. B* **86**, 184411 (2012); *Acta Mater.* **61**, 7931 (2013).
7. P. Gorria *et al., J. Phys. D: Appl. Phys.* **41**, 192003 (2008).
8. P. Alvarez, P. Gorria *et al., J. Phys.: Condens. Matter* **22**, 216005 (2010).
9. C. F. Sánchez-Valdes *et al., Appl. Phys. Lett.*, **104**, (2014), (in press).

MM-22 (Invited Talk)

$FeMnP_{1-x}Si_x$ – Phase Diagram, structure and magnetocaloric potential

Per Nordblad[1], Mikael S Andersson[1], Tapati Sarkar[1], Matthias Hudl[1], Viktor Höglin[2], Johan Cedervall[2], Yvonne Andersson[2], Martin Sahlberg[2]

[1]*Department of Engineering Sciences, Uppsala University, Uppsala, Sweden*
Email:per.nordblad@angstrom.uu.se,

[2]*Department of Chemistry - The Angstrom laboratory, Uppsala University, Uppsala, Sweden*

Fe_2P exhibits a first order paramagnetic to ferromagnetic transition at 217 K. [1] The transition temperature, remaining first order, is tunable to room temperature and higher by substitution of Mn for Fe and/or Si for P. This, combined with a giant magnetocaloric effect, makes the system $FeMnP_{1-x}Si_x$ an attractive compound for magnetocaloric refrigeration applications. [2]

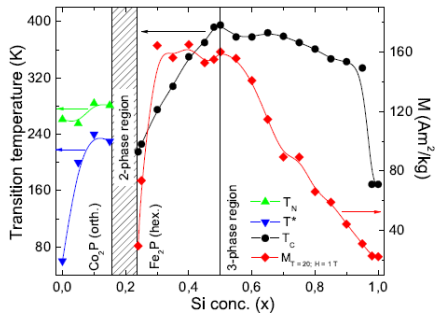

Fig. 1. Phase diagram of $FeMnP_{1-x}Si_x$ (from [3]). Magnetic transition temperatures; T_C and T_N, and magnetisation (at 20 K and 1T) are indicated.

Figure 1 shows the phase diagram of $FeMnP_{1-x}Si_x$, including transition temperatures and saturation moment. [3] The transition temperature in the single phase, Fe_2P, region $0.25<x<0.5$, increases rapidly from 200 K at x=0.25 to about 400 K at x=0.5. In addition, the Fe/Mn ratio and cation deficiency drastically affects the Curie temperature and also modifies the hysteresis behavior; making it possible to optimize the magnetocaloric performance of hexagonal (Fe_2P) samples within the FeMnPSi

system. Of certain interest is that the virgin effect (the transition temperature of an as quenched sample is lower at the first cooling below T_c than in subsequent cooling heating events) has been found to be associated with a minute structural modification. [3]

1. H. Fuji, T. Kamigaichi, T. Okamoto, *J. Phys. Soc. Jpn.* **43**, 41 (1977).
2. N. H. Dung et al., *Adv. Energy Mater.* **1**, 1215 (2011).
3. V. Höglin et al., unpublished (2014).

MM-23 (Invited Talk)

Ferromagnetic shape memory effect: underlying physics and practical importance

V.A. Chernenko[1,2]

[1]BCMaterials & Universidad del País Vasco(UPV/EHU), P.O. Box 644, E-48080 Bilbao, Spain
Email:volodymyr.chernenko@ehu.es

[2]IKERBASQUE, Basque Foundation for Science, 48011, Bilbao, Spain

The ferromagnetic shape memory effect (FSME) appears as a magnetic field-induced twinning/detwinning in the martensitic phase, resulting in the recoverable strain of the order of martensitic spontaneous distortion. The FSME is typical for thermoelastic martensites formed as a result of martensitic transformation in ferromagnetic matrix of Ni-Mn-Ga alloys which represent novel multifunctional materials with extreme mechanical, magneto-mechanical and mechano-magnetic properties as well as with peculiar type of magnetic behavior.

The concept of the equivalence of mechanical and magnetoelastic stress is deduced from the magnetoelastic model based on the Landau theory. The main consequences of this model are briefly discussed. Particularly, emphasis will be given on the origin of the magnetostress and magnetic anisotropy in martensite.

The magnetomechanics of ferromagnetic martensites in quasielastic and anelastic regimes at different schemes of loading will be considered.

The superelastic behavior of Ni-Mn-Ga ferromagnetic martensites at orthogonal magnetic field and giant magnetostrain response in the rotating magnetic field are described. The proper theoretical treatment combining a phenomenological magnetoelastic model and statistical approach was elaborated.

As far as applied aspect is concerned, some results of ongoing research on magnetic shape memory thin films will be presented. Emphasis will be given to the transformation behavior and magnetism of submicron Ni-Mn-Ga martensitic films deposited on different substrates. The results are discussed in terms of thickness dependent residual strains as well as microstructural and crystallographic features.

Session GE

EMN GENERAL WORKSHOP ON ENERGY

GE-01 (Invited Talk)
Hierarchical nanoporous carbons for energy storage applications

Michael Fröba[1], Ruben Heimböckel[1], Sebastian Kraas[1], Anika Juhl[1], Matthias Rogaczewski [1]

[1]Institute of Inorganic and Applied Chemistry, University of Hamburg, Hamburg, Germany Email:froeba@chemie.uni-hamburg.de, web site: http://www.chemie.uni-hamburg.de/ac/froeba/index.html

Carbons of different type play an important role in various electrochemical storage devices. While in lithium based batteries they will be used as anode, as conducting additives for cathodes (lithium ion batteries) or as porous matrices for lithium/sulfur or lithium/air batteries to host the active cathode material. In addition high surface area carbons with micropores are applied in supercapacitors to provide a high capacity accompanied with fast charging/discharging cycles. All these carbons have in common that they have to possess a good electrical conductivity which can be a problem if additional nanoporosity is introduced. In this oral contribution we present various hard- and soft-templating procedures to synthesize different nanoporous and even hierarchical structured carbons with appropriate surface areas and pore volumes which can be used in lithium based batteries or supercapacitors without having a low electrical conductivity. To provide sufficient amounts of carbon these synthesis procedures have to be upscalable. Different ways to run these syntheses on a larger scale will be explained too.

Figure 1 shows a hierarchical nanoporous carbon with macropores which possess a high pore volume and mesopores within the pore walls to provide the necessary high surface areas. This type of carbon is for example well suited for the usage in lithium/air batteries.

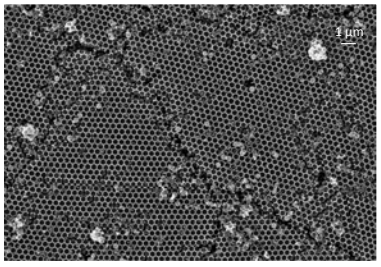

Fig. 1. REM image of a hierarchical structured nanoporous carbon.

Figure 2 exhibits hollow carbon spheres which possess a mesoporous shell of nanometer thickness. By tuning the synthesis conditions it is possible to vary the particle size, the shell thickness as well as the pore diameter. This type of carbon has a high potential for the application in lithium/sulfur batteries which are suffering from the polysulfide shuttle and which has to be suppressed to provide a long cycle stability.

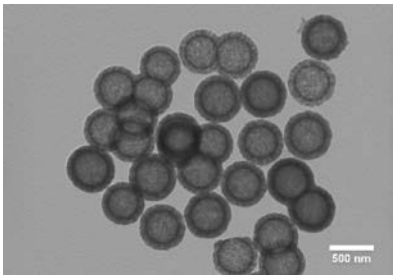

Fig. 2. TEM image of hollow carbon nanoparticles with a nanoporous shell.

GE-02 (Invited Talk)
Novel flux coating technique of hierarchically-structured crystal layers for all-solid-state LIB

Katsuya Teshima[1,2], Nobuyuki Zettsu[1,2], Shuji Oishi[2]

[1] Center for Energy and Environmental Science, Shinshu University, Nagano, Japan
[2] Department of Environmental Science and Technology, Faculty of Engineering, Shinshu University, Nagano, Japan
Email:teshima@shinshu-u.ac.jp, web site: http://www.kankyo.shinshu-u.ac.jp/~oishilab/

There have been growing interests in all-solid-state lithium-ion rechargeable batteries (LIBs) consisting of solid electrolyte materials because no use of organic liquid electrolyte increases packaging density and intrinsic safety of LIBs, which contribute the development on efficent utilization of electric energy for sustainable society. Among various solid electrolytes, inorganic electrolyte materials have achieved relatively slow Li-ion conductivity and better stability at an ambient atmosphere. Nevertheless, there is a drawback that is relatively high internal resistance owing to slow Li-ion movement caused by low crystallinity of materials, scattering at interfaces such as current collector / electrode active materials and electrode active materials / electrolyte materials. To overcome these difficulties, it is required to decrease the interface resistance by fabricating high-quality materials and designing its micro/nanostructures.

Our group has researched fabrication of hierarchically-structured crystal layers by “flux coating method”. Flux method is a liquid phase method in which highly crystallline materials can be obtained under the melting point of the target ones. The advantages of flux method are based on the fact that crystals can grow in an unconstrained fashion; that is, they can grow free from mechanical or thermal constraints into solution and therefore develop facets [1,2]. In addition, it provides simple, low-cost, and environmetally-benign pathway compared to conventional solid-state-reaction method. Recently, our group has developed a new flux method named “flux coating method”, in which high-quality crystal layers (= thin films) can be fabricated on various substrates [3-5]. In the flux coating method, raw material pastes (or solutions) are coated onto substrates via various coating techniques, such as bar-coating, dip-coating, inkjet printing, gravure printing and screen printing. The coated substrates are then heated to adequate temperatures and a large number of crystals can be directly grown onto the substrate surfaces. By heating the substrates, flux components melt, and then dissolve the solutes. As a result, crystals layers with each crystal having idiomorphic shapes can be formed on various substrates via the concept of flux crystal growth. In addition, if we used 3D designed raw materials on substrate, it is easy to convert it to target crystal layers with maintaining the special structure. Note that the flux coating process is applicable to mass-production, *i.e.* large-scale crystal layers on various substrates.

Figure 1 shows electrode active materials and electrolytes crystal layers fabricated by flux coating method. $LiCoO_2$ (LCO), and $LiNi_{0.5}Mn_{1.5}O_4$(LNMO) as a positive active material layers, $Li_4Ti_5O_{12}$ (LTO) as a negative active material layers, and, $Li_5La_3Nb_2O_{12}$(LLNO), as a solid-electrolyte layers were successfully fabricated by flux-coating method. The layered products consisting of the above materials were prepared on various substrates, i.e., LCO / current collector, LTO / current collector, and LLNO / LCO. The detail fabrication techniques and their electrochemical properties will be presented in EMN meeting.

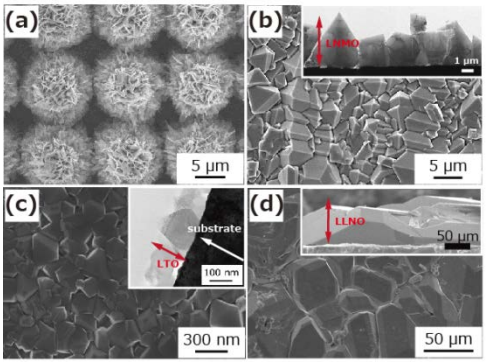

Fig. 1. Crystal layers fabricated by flux coating method; (a) $LiCoO_2$, (b) $LiNi_{0.5}Mn_{1.5}O_4$, (c) $Li_4Ti_5O_{12}$, and (d) $Li_5La_3Nb_2O_{12}$.

1. S. Suzuki, K. Teshima, S. Oishi *et.al.*, *Journal of Materials Chemistry* **21**, 13847 (2011).
2. F. Zhang, K. Teshima, S. Oishi, K. Domen *et.al.*, *Journal of the American Chemical Society* **134**, 8348 (2012).
3. Y. Mizuno, N. Zettsu, H. Wagata, S. Oishi, K. Teshima *et al.*, *Crystal Growth & Design* **14**,1882-1887 (2014)
4. H. Wagata, S. Oishi, K. Teshima *et al.*, *Crystal Growth & Design* **13**, 1187 (2013).

5. S. Suzuki, K. Teshima, K. Domen, S. Oishi *et.al*., *CrystEngComm* **14**, 7178 (2012).

GE-03 (Invited Talk)
Multiscale simulations for battery materials

Ryoji Asahi, Nobuko Ohba, Shunsuke Yamakawa

Sustainable Energy and Environment Department I, Toyota Central R&D Labs., Inc., Nagakute, Aichi, Japan
Email: rasahi@mosk.tytlabs.co.jp

Performance of the Li-ion battery, such as energy density, power, and durability, resides in complex materials system on the atomic-micrometer length scale, and dynamical behavior along with the Li-ion diffusion. It is therefore quite challenging for conventional atomistic simulations to handle realistic modelling for understanding and improving properties of the battery. Here we present two approaches to simulate Li-ion dynamics: one is the hybrid quantum-classical (QM-CL) simulation [1,2] for atomistic-nanometer scale, and another is the phase-field (PF) models [3,4] for nanometer-micrometer scale.

In the hybrid QM-CL simulation, Li and the surrounding atoms are set as the QM-region where the quantum mechanical calculation is adapted while they are embedded in the whole system described in classical interaction model. In this way, the both quantum effects such as charge transfer and dynamical behavior of the Li ion are considered for a reasonably large atomistic model (~10 nm). We demonstrate an insertion process of the Li ion at the interface between graphite (as a negative electrode) and ethylene carbonate (as an electrolyte).

The PF models are applied to understand the relation between the realistic polycrystalline microstructure of the active materials and the apparent Li-ion diffusion. The results show that the apparent Li diffusivity is affected by diffusivity of the grain boundaries, the spatial distribution of the crystal orientation for each grain, and the grain size. Such information is useful to optimize microstructures in the active materials and processing to realize them.

1. S. Ogata, *Phys. Rev.* **72**, 045348 (2005).
2. N. Ohba *et al.*, *J. Phys. Soc. Jpn.* **81**, 023601 (2012).
3. S. Yamakawa *et al., J. Power Sources* **223**, 199 (2013).
4. S. Yamakawa *et al., Solid State Ionics* **262**, 56 (2014).

GE-04 (Invited Talk)
Nanostructure composite anode materials for Lithium ion batteries

Meicheng Li[1], Xiaodan Li[1,2], Peng Cui[1], Lihua Chu[1], Dandan Song[1], Mwenya Trevor Chonto[1], Anthony Frank Hollenkamp[2], Guangsheng Song[2]

[1] State Key Laboratory of Alternate Electrical Power System with Renewable Energy Sources, School of Renewable Energy, North China Electric Power University, Beijing 102206, China
Email:mcli@ncepu.edu.cn, web site: http://nemd.ncepu.edu.cn

[2] CSIRO Energy Technology，Process Science and Engineering，Clayton VIC 3168, Australia

Lithium ion batteries (LIBs) have attracted worldwide concern and increasing research interest due to the fact that they can provide the power for portable electronics and be considered as the most promising energy-storage devices for electric vehicles and renewable energy. The current commercial Li-ion batteries (LIBs), using graphite anode with a relatively low theoretical capacity (372 mA h g^{-1}) and a lower operating voltage, cannot meet the ever-growing market demand for high energy density, high power density, and long cycle life batteries. Over the past decades, Si (Sn)-based materials, metal oxide (sulfide), various carbon nanomaterials have been explored for high performance LIBs application. Among these materials, Si-metal composite anode exhibits outstanding cycle stability and excellent rate capacity compare to Si anode, owing to the fine buffering and high conductivity of metal. Meanwhile, the two-dimensional structure (2D) metal sulfides

represented by molybdenum sulfide have been considered as potential anode materials as well due to their relatively small volume change (~103%) during lithiation and high capacity (669~1675 mA h g^{-1}).

In the study of Si-based anode, we prepared Si-Mg eutectic nanostructure in large-scale by melt-spinning method. This Si-Mg eutectic material was fabricated under Ar protection environment, which avoids the oxidation of Mg. Furthermore, the Si-Mg eutectic was fabricated by melt-spinning method to guarantee the formation nano-layered eutectic structure, reducing the strain produced during intercalation and deintercalation of Li ion. Thus, this anode material show impressive electrochemical performance compare to commercial Mg_2Si. Meanwhile, A porous Si nanostructure was also successfully obtained with silica gel as source using industrialized metallurgical approach followed by acid treated process. The excellence porous Si nanoparticle is a promising industrialized anode material for LIBs with high special capacity.

In order to improve electrochemical performance of MoS_2, we have designed TiO_2 nanobelt @ MoS_2 nanosheets core-shell hierarchical structure by facile hydrothermal method for LIBs application. The 2D MoS_2 nanosheets serve as large surface area active sites to provide an extremely short diffusion length for Li^+ ions, whereas the strainless TiO_2 nanobelt acts as backbone to guarantee the structure stability and electronic conductivity. Benefitting from these structual features, the TiO_2 @ MoS_2 core–shell hetrostructure can retain a high capacity of 534 mA h g^{-1} at the end of the 100th cycle compare to both pure TiO_2 and MoS_2 anodes. The excellent cycle stability, fine rate capability and high retention of TiO_2 @ MoS_2 core–shell hetrostructure indicating the promising use as high performance anode materials for lithium-ion batteries.

Acknowledgement:

This work was supported partially by the National Natural Science Foundation of China (Grant nos. 91333122, 51372082, 51172069, 50972032, 61204064 and 51202067), Ph.D. Programs Foundation of Ministry of Education of China (Grant nos. 20110036110006, 20120036120006, 20130036110012), Science and Technology Program Foundation of Suzhou City (SYG201215) and the Fundamental Research Funds for the Central Universities.

GE-05 (Invited Talk)
In-situ (S)TEM Observations of Energy Storage Materials and Batteries

Nigel D. Browning[1], Patricia Abellan[1], James Evans[2], Meng Gu[2], B. Layla Mehdi[1], Lucas R. Parent[1], Chong-Min Wang[2], Wu Xu[3], Ji-Guang Zhang[3]

[1]Fundamental and Computational Science Directorate, Pacific Northwest National Laboratory, Richland, WA 99352, USA.
Nigel.browning@pnnl.gov
[2]Environmental Molecular Sciences Laboratory, Pacific Northwest National Laboratory, Richland, WA, 99352, USA
[3]Energy and Environmental Directorate, Pacific Northwest National Laboratory, Richland, WA, 99352, USA

The rapidly growing field of high energy density rechargeable batteries for large-scale renewable energy applications has generated a wide range of *in-situ/operando* experimental techniques that can provide significant insights into the battery operation. In particular, the recent development of *in-situ* liquid electrochemical stages for (scanning) transmission electron microscopes (*in-situ* liquid ec-(S)TEM) enables the fabrication of a "nano-battery" to study the details of electrochemical processes providing real-time information on the dynamic structural changes and processes that occur locally at the electrode/electrolyte interface during charge/discharge cycles [1]. In addition to providing insights into battery operation, the in-situ cells allow the details of electrolyte stability and degradation to be mimicked using radiation

damage – providing a means to test new systems independent of the electrochemistry taking place [2]. Here, we demonstrate the application of an *in-situ* ec-(S)TEM cell to quantitatively image the electrochemical processes occurring and study the formation and decomposition mechanisms in both Li-ion, and alternative beyond Li designs for next generation batteries [3].

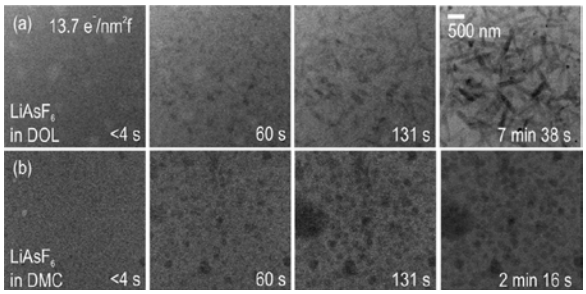

Fig. 1. The stability and breakdown of two different battery electrolytes under in-situ e-beam illumination

1. M. Gu et al, Nano Letters 13, 6106-6112 (2013)
2. P. Abellan et al, Nano Letters 14, 1293-1299 (2014)
3. This work was supported in part by the Joint Center for Energy Storage Research (JCESR), an Energy Innovation Hub funded by DOE, Office of Science, Basic Energy Sciences. The work involving development of in situ stages was supported by the Chemical Imaging Initiative; under the Laboratory Directed Research and Development Program at Pacific Northwest National Laboratory (PNNL). PNNL is a multi-program national laboratory operated by Battelle for the U.S. Department of Energy (DOE) under Contract DE-AC05-76RL01830. A portion of the research was performed using the Environmental Molecular Sciences Laboratory (EMSL), a national scientific user facility sponsored by the Department of Energy's Office of Biological and Environmental Research and located at Pacific Northwest National Laboratory.

GE-06 (Invited Talk)
Thin films for Li and Li-ion all-solid-state batteries

Brigitte Pecquenard[1], Frédéric Le Cras[2], D. Poinot[1,2], M. Ulldemolins[1,2],Vincent Pelé[1,2], Florian Flamary[1,2]

[1]CNRS, Univ. Bordeaux, ICMCB, UPR 9048, F-33600 Pessac, France
Email:pecquen@icmcb-bordeaux.cnrs.fr

[2]Univ. Grenoble Alpes, F-38000 Grenoble, France
CEA, LETI, Minatec Campus, 17 rue des Martyrs, F-38054 Grenoble cedex, France

With the continuous miniaturization of electronic devices and components, the need for efficient microscale power sources is ever increasing. As a consequence, all-solid-state microbatteries are of growing interest both at the academic and industrial levels. The special features of these microsystems mainly lie in their size, the use of an ionic conducting inorganic solid electrolyte and their processing route. Microbatteries are build up through the deposition by PVD techniques of current collectors, the positive electrode, the electrolyte and the negative electrode (metallic lithium is often used) on a rigid or flexible substrate, followed by the deposition of protective layers. Each of these different layers is a few micrometers thick. Finally, about ten layers are stacked to form a complex system with a total thickness of about 10 µm. The choice of the active materials (electrodes, electrolyte) appears quite different from the one for conventional Li-ion batteries due to the specific applications of these micro-power sources and their manufacturing process.

Our aim is to tailor thin film properties by tuning the sputtering parameters in order to improve the performance of each active constituent of the cell and the overall behavior of the microbattery. Hence, we are focusing our work on:

- the composition, the structure and the morphology of the films (Rutherford

Backscattering Spectroscopy, EPMA, ICP, XRD, Raman spectroscopy, SEM,TEM)

- the ionic and electronic properties (conductivity measurements by impedance spectroscopy or 4-probe set-up, study of redox mechanism occurring during lithium insertion/deinsertion processes by XPS spectroscopy)
- the nature of the interfaces (nature of the interphases formed at the electrode/electrolyte interface characterized by XPS spectroscopy, Auger spectroscopy and AFM, contribution to the internal resistance)

As for positive electrode materials, most studies focused up to now on intercalation compounds ($LiCoO_2$, $LiMn_2O_4$, V_2O_5…) despite their limited capacity (65-115 $\mu Ah.cm^{-2}.\mu m^{-1}$)[1]. A mean to improve the capacity of the microbattery consists to study compounds reacting with lithium according to a conversion reaction (M_aX_b +(b.n)Li $\leftrightarrow$ aM + bLi_nX (M = metal; X = O, N, F, S, P, H)), hence having a far larger theoretical capacity. Thin films of CuO [2, 3] or FeS_2 in particular were found to deliver reversible capacities above 300 $\mu Ah.cm^{-2}.\mu m^{-1}$. On the negative side, a limitation of the lithium electrode is its low melting temperature (T_f~180°C) which is incompatible with the solder-reflow operation (T_{max}~260°C) usually used to connect electronic components. As a consequence, elements forming alloys with Li and having melting temperatures above 300°C are interesting substitutes. Among them, Si and Ge were studied due to their high volumetric specific capacity (834 $\mu Ah.cm^{-2}.\mu m^{-1}$for $Li_{15}Si_4$ and 737 $\mu Ah.cm^{-2}.\mu m^{-1}$ for $Li_{15}Ge_4$) and their ability to insert Li at a low potential. Despite the large volume expansion of the silicon thin film electrode no evidence of cracks or damage was observed in the SEM images, even after 1500 cycles [4]. Concerning the solid electrolyte, alternative materials to the widely used LiPON are investigated in order to get higher ionic conductivity.

1. J. B. Bates, N. J. Dudney et al., *J. Power Sources* **54**, 58 (1995).
2. L. Martin, H. Martinez , D. Poinot, B. Pecquenard, F. Le Cras, *J. Phys. Chem. C,* **117** 4421 (2013)
3. B. Pecquenard, F. Le Cras, D. Poinot, O. Sicardy, J.P. Manaud , *ACS Applied Mater. Interfaces*, **6** 3413 (2014)
4. V. P. Phan, B. Pecquenard, F. Le Cras, *Adv. Funct. Mater.*, **22,** 2580 (2012)

GE-07 (Invited Talk)
High energy density positive electrode materials for Lithium-ion batteries

Laurence Croguennec[1], Hideyuki Koga[1,2], Jean-Marcel Ateba Mba[1,3], Matteo Bianchini[1,3,4], Michel Ménétrier[1], François Weill[1], Claude Delmas[1], Dany Carlier[1], Emmanuelle Suard[4] and Christian Masquelier[3]

[1]ICMCB - Institut de Chimie de la Matière Condensée de Bordeaux, Université de Bordeaux, Pessac, France
Email:crog@icmcb-bordeaux.cnrs.fr, web site: http://www.icmcb-bordeaux.cnrs.fr/groupes/lp-groupe2.html

[2] TOYOTA MOTOR EUROPE NV/SA, Zaventem, Belgium

[3] LRCS - Laboratoire de Réactivité et de Chimie des Solides, Université de Picardie Jules Verne, Amiens, France

[4] ILL - Institut Laue-Langevin, Grenoble, France

The development of new materials for high energy density batteries is critical since batteries are still facing limitations to power a wide range of applications. Intense academic and industrial research activities are devoted to the development of better performing materials with in particular high voltage and safety. We will discuss results obtained recently in our groups for Lithium and Manganese rich layered oxide and Tavorite-like phosphate materials, $LiVPO_4F$ and $LiVOPO_4$, in Li-ion batteries. We will also show that *in-situ* techniques proved to be exceptional useful tools to follow structural changes and redox processes involved in these electrode materials.

The lithium and manganese-rich layered oxides deliver a large specific capacity, with deintercalation of Li^+ ions during the first charge (over 4.5 V vs. Li^+/Li) although all the transition metal ions are already at the tetravalent state. The mechanism of lithium deintercalation and reintercalation in these materials is unconventional. We have proposed that oxygen participates to the redox processes, with reversible oxygen oxidation, more in the bulk, and an irreversible oxygen loss, more at the surface. [1-5]

Polyanionic materials attract great interest in the field of Li and Na-ion batteries research thanks to the wide range of possible available compositions, resulting in a great amount of different properties. [6] Tavorite type compositions offer very rich crystal chemistry, among which $LiVPO_4F$ offers the highest theoretical energy density. [7] $LiV^{III}PO_4F$ and the homeotypic composition $LiV^{IV}OPO_4$ have revealed the ability to exploit two redox couples upon Li^+ extraction and insertion, in different voltage domains. [7-9] The two materials show interesting marked differences, both in the electrochemical signature and in the phase diagram. These will be discussed in details, considering especially differences in the chemical bond around vanadium.

The authors thank Toyota, the European Research Institute Alistore and the French Network on Electrochemical and Energy Storage (RS2E) for funding.

[1] Koga H., Croguennec L., Mannessiez P., Ménétrier M., Weill F., Bourgeois L., Duttine M., Suard E. and Delmas C., *J. Phys. Chem. C* 2012, 116(25), 13497-13506.

[2] Koga H., Croguennec L., Ménétrier M., Mannessiez P., Weill F. and Delmas C., *J. Power Sources* 2013, 236, 250-258.

[3] Koga H., Croguennec L., Ménétrier M., Douhil K., Belin S., Bourgeois L., Suard E., Weill F. and Delmas C., *J. Electrochem. Soc.* 2013, 160(6), A786-A792.

[4] Koga H., Croguennec L., Ménétrier M., Mannessiez P., Weill F., Delmas C. and Belin S., *J. Phys. Chem. C* 2014, 118(11), 5700-5709.

[5] Genevois C., Koga H., Croguennec L., Ménétrier M., Delmas C. and Weill F., *submitted*

[6] Masquelier C. and Croguennec L., *Chem. Rev.* 2013, 113, 6552-6591.

[7] Ateba Mba J.M., Masquelier C., Suard E. and Croguennec L., *Chem. Mater.* 2012, 24, 1223-1234.

[8] Ateba Mba J.M., Croguennec L., Basir N.I., Barker J. and Masquelier C., *J. Electrochem. Soc.* 2012, 159(8), A1171-A1175.

[9] Bianchini M., Ateba-Mba J.M., Dagault P., Bogdan E., Carlier D., Suard E., C. Masquelier, and L. Croguennec, *J. Mater. Chem. A* 2014, 26, 10182-10192.

GE-08 (Invited Talk)
On the insertion mechanism of A_xFePO_4 (A=Li, Na) through the combination of experiments and DFT calculations, the importance of the $A_{2/3}FePO_4$ composition

Florent Boucher,[1,3] Joël Gaubicher,[1,3] Philippe Moreau,[1,3] Marine Cuisinier,[2] Patrick Soudan,[1,3] and Dominique Guyomard[1,3]

[1]*Institut des Matériaux Jean Rouxel (IMN), Université de Nantes - CNRS, UMR 6502, 2 rue de la Houssinière, BP 32229, 44322 Nantes Cedex 3, France*
Email:Florent.Boucher@cnrs-imn.fr

[2]*University of Waterloo, Department of Chemistry, 200 University Avenue West, Waterloo, Ontario, Canada*

[3]*Réseau sur le Stockage Electrochimique de l'Energie (RS2E), FR CNRS 3459, 33 rue Saint Leu, 80039 Amiens Cedex, France*

Based on transmission electron microscope experiments, synchrotron X-ray diffraction, Mössbauer spectroscopy, and DFT calculations, a unified understanding of the Na and Li intercalation process in $FePO_4$ is proposed. The key to this lies in solving the highly sought-after intermediate $A_{2/3}FePO_4$ (A=Na, Li) superstructures [1–3] that are characterized by alkali ions as well as Fe^{II}/Fe^{III} charge orderings in

a monoclinic 3-fold supercell (Figure 1). Formation energies and electrochemical potential calculations confirm that $Na_{2/3}FePO_4$ and $Li_{2/3}FePO_4$ are stable and metastable, respectively, and that they yield insertion potentials in fair agreement with experimental values.

The 2/3 Na(Li) and 1/3 vacancy sublattice of the intermediate phases forms a dense (1 0 -1) $_{Pnma}$ plane in which the atom/vacancy ordering is very similar to that predicted for the most uniform distribution of 1/3 of vacancies in a 2D square lattice. Structural analysis strongly suggests that the key role of this dense plane is to constrain the intercalation in the diffusion channels to operate by cooperative filling of $(\mathbf{bc})_{Pnma}$ (Figure 2). From a practical point of view, this generalized mechanism highlights the fact that an interesting strategy for obtaining high rate $FePO_4$ materials would consist in designing grains with an enhanced (101) surface area, thereby offering potential for substantial improvements with respect to the performance of rechargeable Li and Na batteries.[4]

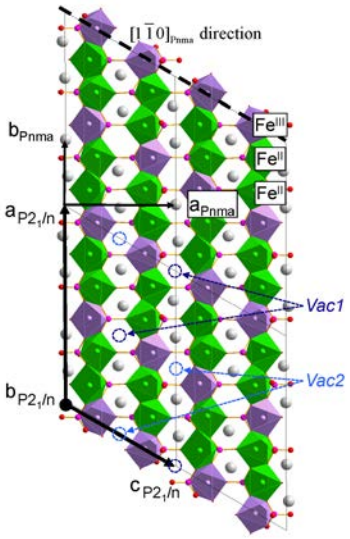

Fig. 1. Structure of $Na_{2/3}FePO_4$ phase viewed along the $\mathbf{c}_{Pnma}$ direction showing the sodium/vacancy and the Fe^{II}/Fe^{III} charge orderings.

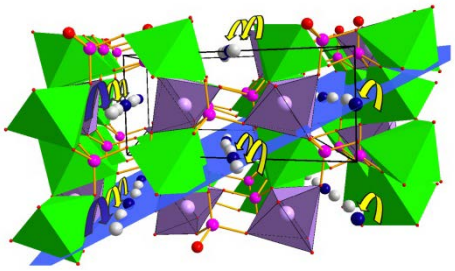

Fig. 2. Schematic view of the cooperative sodium insertion mechanism in $FePO_4$

[1] P. Moreau, D. Guyomard, J. Gaubicher, and F. Boucher, Chem. Mater. **22**, 4126 (2010).

[2] M. Casas-Cabanas, V. V. Roddatis, D. Saurel, P. Kubiak, J. Carretero-Gonzalez, V. Palomares, P. Serras, and T. Rojo, J Mater Chem **22**, 17421 (2012).

[3] M. Galceran, D. Saurel, B. Acebedo, V. V. Roddatis, E. Martin, T. Rojo, and M. Casas-Cabanas, Phys. Chem. Chem. Phys. (2014).

[4] F. Boucher, J. Gaubicher, M. Cuisinier, D. Guyomard, and P. Moreau, J. Am. Chem. Soc. **136**, 9144 (2014).

GE-09 (Invited Talk)
PVD processes for energy applications

Alain Billard[1], Mohammad Arab Pour Yazdi[1], Pascal Briois[1]

[1]LRC CEA-UTBM LIS-HP, Université de Technologie de Belfort-Montbéliard, Site de Montbéliard, 90010 Belfort Cedex, France

Solid electrolytes and mixed conductors are often complex oxides widely used in numerous applications in the fields of energy and environment such as fuel cells, microbatteries, catalysts, sensors etc. Among the methods able to allow the synthesis of these various materials, reactive co sputtering appears as an interesting and powerful alternative. This is particularly true when in situ optical methods are used to control either the deposition rate or the coating transparency.

In this presentation, we will first describe the structural features of the main solid

electrolytes and mixed conductors which often present fluorite, perovskite or close-perovskite structures. Hence, we will discuss the deposition conditions for high rate deposition of those materials, either as dense coatings such as required for electrolyte coatings or as porous layers such as required for mix conductors in numerous applications. In each case, the relation between deposition conditions and coating morphology and structure will be established. Some examples of coating intrinsic performance owing to their ionic or electrical conductivity or catalytic activity will then be presented in relation with their deposition conditions. Finally, some recent examples of applications will be given in the fields of solid oxide fuel cells, depollution catalysts or gas sensors.

GE-10 (Invited Talk)
Oxide Thin Films for Thermoelectricity

Hanns-Ulrich Habermeier, Petar Yodanov and S. Heinze

Max-Planck-Institute for Solid State Research, Stuttgart, Germany
Email:huh@fkf.mpg.de, web site: http://www.fkf.mpg.de

Worldwide activities in thermoelectricity have been snowballing during the past 5 years mainly initiated by a wide spread of applications ranging from room temperature based cooling devices, energy harvesting from waste heat, power generation from the lower frequency range of the spectrum of visible light to radioisotope thermoelectric generators in space. Most strategies, however, are restricted to prepare bulk thermoelectric nanocomposites based on semiconductors by investigating the possibilities of improving the power factor arising from the combined effect of introducing additional carrier scattering mechanisms and modifications in the electronic structure. The goal is the formation of systems acting as electron crystal and phonon glass and thus to enhance the powerfactor as well as the thermoelectric figure of merit. While substantial progress has been made in recent years using semiconductor-based materials their drawback is seen in their limitations for high temperature applications as well as the toxicity of their constituents.

In this contribution the potential of oxides for high temperature thermoelectric applications is explored and two strategies are pursuit. One includes the investigation of single layer complex oxide thin films, e.g. cobaltites, due to their stability in a temperature range from ambient to 1000^0C. Amongst them, layered cobaltites such as $Ca_3Co_4O_9$, $LaCoO_3$ and $Na_{1-x}CoO_2$ deserve special attention. We have investigated ultrathin PLD grown $Ca_3Co_4O_9$ films and observed power factors up to 4 $mW/m*K^2$ at high temperatures and interpreted the results as an interplay of intrinsic and dimensionality related effects.

The other strategy is the attempt to tailor the thermoelectric properties of heterostructures and superlattices composed of transition metal oxides with strong electron correlation. They offer a unique opportunity to design new artificial materials whose electrical, magnetic and optical properties can be manipulated by tailoring the occupation of the 3d-orbitals of the transition metal in the compound. This possibility is an implication of symmetry constraints at interfaces resulting in a delicate interplay of spin-, charge-, orbital and lattice interactions of electrons by modifications of the electronic structure of the heterointerfaces. In a case study the system $LaCaMnO_3$ and $YBa_2Cu_3O_7$ is studied. Characterizing their charge and entropy transport properties we observed a tremendous change of the thermoelectric power, S (T), in the superlattices which can't be described by a simple superposition of those of the components. Different possible mechanisms such as interfacial strain, charge transfer, oxygen deficiency and electronic reconstruction at the interface are discussed to explain these findings.

The material properties of the strongly correlated oxides are sensitive to external perturbations such as strain, electrical and magnetic fields and photon flux as well. As an example for applications we use photon flux exposure to explore the consequences of superlattice formation of $YBa_2Cu_3O_{7-\delta}/La_{2/3}Ca_{1/3}MnO_3$ on the entropy transport,

especially on the Seebeck coefficient. In addition to the investigation of the fundamental aspects of entropy transport in oxide superlattices, the driving force for this work is the development of optical sensing devices. The method applied is based on the off-diagonal thermoelectric effect (ODTE) appearing in films deposited on substrates with a vicinal cut. This well-known principle serves as a technique to investigate the anisotropic transport properties and the components of the Seebeck tensor in these superlattices. It could be shown that the normalized ODTE signals scale linearly with the number of interfaces in the structures. We observed an enhancement of the ODTE signals by a factor of four due to superlattice formation. The results are discussed with respect to cross-plane coherent backscattering of phonon waves at the superlattice interfaces and the thermal boundary resistance at the $YBa_2Cu_3O_{7-\delta}/La_{2/3}Ca_{1/3}MnO_3$ interfaces.

GE-11 (Invited Talk)

Strategies for the Synthesis of New Nanoscale Materials used as Electrode Materials for Li or Na ion Batteries

Valerie Pralong

Laboratoire CRISMAT, CNRS ENSICAEN, 6 bd Maréchal Juin, 14050 CAEN, France
Email:valerie.pralong@ensicaen.fr, web site: http://www.crismat.ensicaen.fr/index.php

Regarding the field of energy storage, the design of new materials that provide high energy densities and long cycle life together with being economic and environmental benign is crucial [1, 2]. Therefore, the soft chemistry used to prepare the original frameworks, new structures is in perfect appropriateness with such a target. Moreover, one of the primordial properties needed for the new materials to be a good candidate for such a challenge is the property of good ionic conduction. Our research is focused on the synthesis by soft chemistry of new "metastable" frameworks with large tunnels or layered structures at low temperature. We will discuss on our strategies to generate original framework showing ionic conductivity. The first approach is based on topotactic reactions starting from existing ionic conductors with a compact anionic framework. In this case, we will show that the lithium/sodium insertion leads to new nanoscale rock salt type structure (Fig. 1). The second approach is related to polyanionic frameworks. In order to favor reactivity, we are using protonic materials, either as precursors or as matrix for intercalation, containing transition elements with adequate redox potential (Fe, Mn, V, Ti). This matrix presents two types of polyhedra, i.e. hydroxyphosphate or hydroxysulfate tetrahedra and transition metal octahedra. Tetrahedral hydroxyl groups favour the formation of open frameworks at rather low temperature. Transition metal octahedra will ensure the generation of mixed valence and consequently electrochemical intercalation/deintercalation process in an adequate range of redox potential values. Then, structure-properties relationships are studied and the possibility to use these materials as electrode materials for power generation systems is evaluated. We will discuss our recent results on iron, manganese and vanadium based materials ($Li_xFeOHSO_4$, $Li_2Mn(SO_4)_2$, Li_2VO_3, Na_2VO_3, $Li_5W_2O_7$,…) [3].

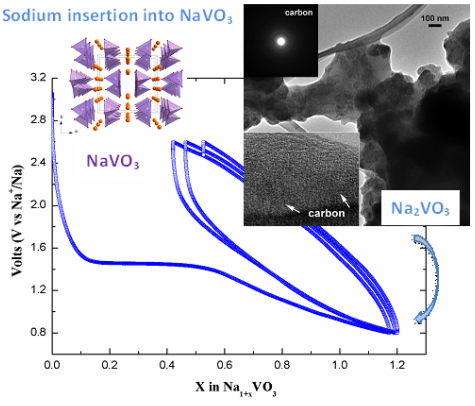

Fig. 1. $NaVO_3$ as a precursor for the synthesis of a Na-rich amorphous phase $Na_{1.5+y}VO_3$, the potential-composition curve of $Na_{1.5+y}VO_3$ is showing a reversible capacity of 150 mAh/g at 1.8V vs. Na+/Na.

1. J.M. Tarascon, M. Armand, *Nature*, 2001, 414, 6861, 359-367; M. S. Whittingham, *Chem. Rev*., 2004, 104, 4271; J. M. Tarascon, N. Recham, M. Armand, et al., *Chem. Mater*., 2010, 22, 3, 724
2. B. L. Ellis, K. T. Lee, L.F. Nazar, *Chem. Mater*., 2010, 22, 3, 691; M. I. Saiful, L.F. Nazar, *J. Mat. Chem*., 2011, 21, 27, 9810
3. M. A. Reddy, V. Pralong, V. Caignaert, et al., *Electrochem. Com.*, 2009, 11 1807; V. Pralong, V. Caignaert, B. Raveau, *J. Mater. Chem*., 2011, 21, 12188; V. Pralong, V. Gopal, V. Caignaert, et al., *Chem. Mat. Com.*, 2012, 24, 12; V. Pralong, *Progress in Solid State Chem*., 2009, 37, 4, 262-277; V. Gopal, V. Pralong, et al., *Electrochem. Com*., 40, 100-102, 2014

GE-12 (Contributed Talk)

All-solid-state lithium-ion microbatteries using a silicon negative electrode for microelectronic systems

Frédéric Le Cras[1], Brigitte Pecquenard[2], Vincent Dubois[2,3], Delphine Guy-Bouyssou[3]

[1] CEA LETI, Minatec Campus, F-38054 Grenoble Cedex 9, France
Email:frederic.lecras@cea.fr

[2] CNRS, Université de Bordeaux, ICMCB, Pessac, F-33608, France

[3] STMicroelectronics, F-37071 Tours Cedex 2, France

All-solid state microbatteries are innovative energy storage solutions for powering microelectronic devices such as ICs, real-time clocks, memories, sensors. Today, most microbatteries available on the market are based on the Li/LiPON/$LiCoO_2$ active core developed by Bates and *al.* [1]. Nevertheless this system is no longer adapted to emerging applications, which now require lower operating voltages (1 to 2 V) and the possibility to connect the microbattery as a conventional electronic component, i.e. using the reflow soldering (SR) process. Thus, two options are possible to get rid of metallic lithium which melts around 180°C: the development of Li-free cells [2] or efficient all-solid-state Li-ion cells. The difficulty to control the morphology of plated lithium in Li-free cells, which is often detrimental to the cycle life, promotes the choice of robust Li-ion cells.

This work reports on the development of '2 V' lithium-ion cells, comprising an amorphous silicon film as the negative electrode and amorphous lithium titanium oxysulfide film as the positive electrode, both obtained by sputtering. Silicon thin film electrode was previously found to have excellent cycle life in all-solid-state half-cells [3]. As for TiO_yS_z, these materials exhibit high volumetric capacities, which may vary with composition. Their electrochemical activity involves highly reversible redox processes on both sulfur and titanium around 2V/ Li^+/Li [4,5]. In order to obtain Li-ion cells, new lithiated titanium oxysulfide films $Li_xTiO_yS_z$ were synthesized and characterized. The electrochemical behavior of electrode materials, especially the one of new positive electrode materials, and of the complete Li-ion cells was studied (figure 1a). The positive material and the cells exhibit excellent cycle life at room temperature when operated up to 130 $\mu A.cm^{-2}$ (figures 1b & 1c). Higher sulfur content in the positive electrode was found to enhance its specific capacity. EIS measurements showed it also slightly increases the electrode polarization. This polarization was found to sharply increase at the end of the charge for all $Li_xTiO_yS_z$ compositions. Depending on cycling conditions (voltage window, current density), reversible slow-fading phenomena, as the memory effect related to the Li_xSi negative electrode, were highlighted [6]. Finally, no detrimental effect of three successive SR thermal treatments at 260°C on the active core was evidenced.

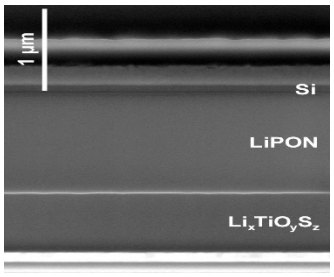

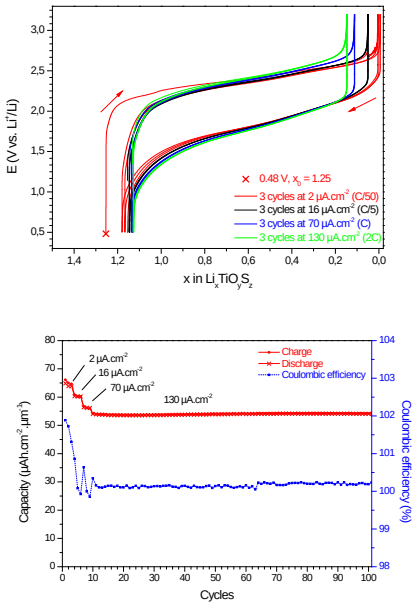

Fig. 1. (a) cross section of the of $Li_xTiO_yS_z$/LiPON/Si cells, (b) voltage curves and (c) capacity retention of Li-ion microbatteries during cycling at various current densities

1. B. Wang, J. B. Bates, F. X. Hart, B. C. Sales, R. A. Zuhr et al., *J. Electrochem. Soc.*, **143**, 2203 (1996)
2. B. J. Neudecker, N. J. Dudney, J. B. Bates, *J. Electrochem. Soc.*, **147**, 517 (2000)
3. V.P. Phan, B. Pecquenard, F. Le Cras, *Adv. Funct. Mater.*, **22**, 2580 (2012)
4. M.H. Lindic, H. Martinez, A. Benayad, B. Pecquenard et al., *Solid State Ionics*, **176**, 1529 (2005)
5. B. Fleutot, B. Pecquenard, F. Le Cras, B. Delis, H. Martinez et al., *J. Power Sources*, **196**, 10289 (2011)
6. M. Ulldemolins, F. Le Cras, B. Pecquenard, *Electrochem. Comm.*, **27**, 22 (2013)

GE-13 (Contributed Talk)

GeO_2/Multiplates graphene composite based cathode electrodes for magnesium-ion battery

E. Sheha, Atef Bassyouni

Physics Department, Faculty of Science, Benha University, Benha 13518, Egypt

Email: ISLAM.SHIHAH@fsc.bu.edu.eg,

Tel:+201007414705

The aim of the contribution is to introduce a high performance cathode for magnesium-ion batteries. A simple ball mill process is employed to synthesize GeO_2/Multiplates graphene composites. The synthesized samples are characterized using x-ray diffraction (XRD) and scanning electron microscope (SEM). The maximum conductivity was found to be 9.89×10^{-1} S/cm for optimum composite film (30 wt. % GnP) at room temperature. The spex-milled composites exhibit better electrochemical performance with higher reversible capacity and excellent cyclability. The excellent electrochemical performance of GeO_2/Multiplates graphene composites can be attributed to their unique structures, which intimately combine the conductive graphene nanosheets network with GeO_2 nanoparticles and possess the characteristic parallel channels running along the [101] orientation, which allow easy Mg^{+2} transport. A prototype cell was constructed using non aqueous liquid electrolyte with Mg anode and a GeO_2 cathode. The Mg/GPE/ GeO_2 cell showed low initial discharge capacity of 58 mAh/g. The combination of ion-exchanged GeO_2 with magnesium is DMSO/Glyme electrolyte system proposed in this work provides a low-cost and practical rechargeable magnesium battery with high energy density.

GE-14 (Invited Talk)

Triple-phase boundary and power density enhancement in thin solid oxide fuel cells by controlled etching of the nickel anode.

Rabi Ebrahim[1,2], Mukhtar Yeleuov[4], Ainur Issova[4], Serekbol Tokmoldin[4],and Alex Ignatiev[1,2,3,4]

[1]*Center for Advanced Materials, University of Houston, Houston, TX 77204-5004, USA*

[2]*Department of Physics, University of Houston, Houston, TX 77204-5005, USA*

Email: rebrahim@central.uh.edu

[3]*Department of Electrical and Computer Engineering, University of Houston, Houston, TX 77204-4005, USA*

[4]*Institute of Physics and Technology, Almaty 050032, Kazakhstan*

Fabrication of microporous structures for the anode of a thin film solid oxide fuel cell (SOFC(s)) using controlled etching process has led us to increased power density and increased cell robustness. Micropores were etched in the nickel anode by both wet and electrochemical etching processes. The samples etched electrochemically showed incomplete etching of the nickel leaving linked nickel islands inside the pores. Samples which were wet- etched showed clean pores with no nickel island residues. Moreover, the sample with linked nickel islands in the anode pores showed higher output power density as compared to the sample with clean pores. This enhancement is related to the enlargement of the surface of contact between the fuel-anode-electrolyte (the triple-phase boundary).

1. Rabi Ebrahim, et al Nanoscale Res Lett. 2014; 9(1): 286.

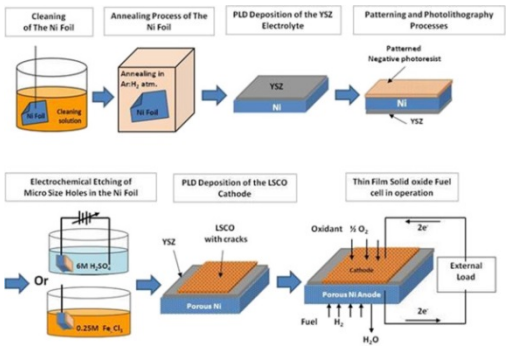

Fig. 1. Schematic diagram for LSCO/YSZ/Ni thin SOFC(s) fabrication process flow [1].

GE-15 (Invited Talk)
Metal-organic frameworks for hydrogen storage applications

Myunghyun Paik Suh[1]

[1]*Department of Chemistry, Hanyang University, Seoul 133-791, Republic of Korea*
E-mail: mpsuh@snu.ac.kr, website: http://mpsuh.snu.ac.kr

Metal-organic frameworks (MOFs) have great potentials in hydrogen storage applications due to their high surface areas and tunable pore properties [1]. However, several problems still remain unsolved, such as low gas uptake capacities at ambient temperature and low stability against water, limiting the practical applications. To enhance hydrogen storage capabilities of MOFs, we have synthesized MOFs and modified their pore spaces by various strategies.

The H_2 uptake capacities of MOFs could be increased by creation of vacant coordination sites at the metal ions, incorporation of crown ether as the guests, and fabrication of metal (Pd, Mg) nanoparticles in the pores [2][3]. In particular, the MOF embedded with Mg nano crystals stores H_2 gas by physical adsorption at low temperatures and by chemical absorption at high temperatures, and two different components of the material exhibit synergistic effects on H_2 adsorption [4]. We have also synthesized Zn-MOF incorporating a crown ether moiety in the struts of the framework, which provides the specific binding sites for K^+, NH_4^+, and methylviologen (MV^{2+}). The MOF incorporating K^+ ion exhibits significantly enhanced H_2 adsorption [5].

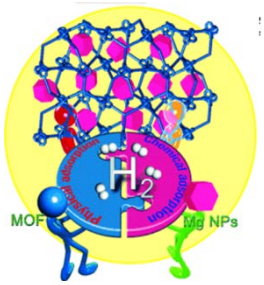

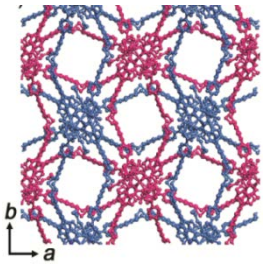

1. Myunghyun Paik Suh, Hye Jeong Park, Thazhe Kootteri Prasad, Dae-Woon Lim, *Chem. Rev.* **112**, 782-835 (2012).
2. Hoi Ri Moon, Dae-Woon Lim, and Myunghyun Paik Suh, *Chem. Soc. Rev.* **42**, 1807-1824 (2013).
3. Young Eun Cheon and Myunghyun Paik Suh, *Angew. Chem. Int. Ed.* **48**, 2899-2903 (2009).
4. Dae-Woon Lim, Ji Woong Yoon, Keun Yong Ryu, and Myunghyun Paik Suh, *Angew. Chem. Int. Ed.* **51**, 9814-9817 (2012).
5. Dae-Woon Lim, Seung An Chyun, and Myunghyun Paik Suh, *Angew. Chem. Int. Ed.* **53**, 7953-7956 (2014).

GE-16 (Invited Talk)
Theory and modeling of lithium-ion battery electrode materials

Khang Hoang

Center for Computationally Assisted Science and Technology, North Dakota State Univ., Fargo, North Dakota, USA

Email:khang.hoang@ndsu.edu

Materials for lithium-ion battery electrodes are often structurally and chemically complex transition-metal oxides, where intrinsic point defects can be either essential or detrimental to their functioning. A detailed understanding of the defect physics and chemistry is key to controlling charge and mass transport and structural stability. First-principles density-functional theory calculations have been established as an important tool in investigations of complex phenomena and processes at the electronic and atomic level. In such calculations, certain processes can be isolated and studied more easily than in experiments.

In this talk, I will present a comprehensive computational approach based on first-principles defect calculations and illustrate how it helps uncover the defect physics and chemistry, electronic and ionic conduction mechanisms, and mechanisms for lithium extraction and insertion. Specific examples will be taken from recent studies of complex oxides for intercalation electrodes [1–4]. Through these examples, I will also provide guidelines for defect characterization and defect-controlled synthesis in which defect concentrations can be tuned by tuning the experimental conditions during materials preparation.

1. K. Hoang and M. Johannes, *Chemistry of Materials* **23**, 3003 (2011).
2. M. D. Johannes, K. Hoang, J. L. Allen, and K. Gaskell, *Physical Review B* **85**, 115106 (2012).
3. K. Hoang and M. D. Johannes, *Journal of Materials Chemistry A* **2**, 5224 (2014).
4. K. Hoang, *Journal of Materials Chemistry A* **2**, 18271 (2014).

GE-17 (Invited Talk)
Efficient solar water-splitting using a nanocrystalline CoO photocatalyst

Jiming Bao

Department of Electrical and Computer Engineering, University of Houston, Houston, TX 77204, USA
Email:jbao@uh.edu, web site: http://nano.ee.uh.edu

The generation of hydrogen from water using sunlight and photocatalysts not only can provide renewable fuel to meet the world's energy demands but can also mitigate climate change by reducing carbon emissions. As such, there has been great interest in developing highly efficient photocatalysts since the discovery of water splitting using platinum as cathode and TiO_2 as photoanode in a photoelectrochemical cell in 1972. However, the development of overall water-splitting photocatalysts, especially those that can be efficiently driven by the visible spectrum of solar radiation, remains a great challenge due to many concurrent materials requirements. In this talk, I will describe our recent discovery of a new photocatalyst: CoO

nanoparticle. The new photocatalyst can decompose water under visible light without any co-catalysts or sacrificial reagents.[1] Although CoO nanoparticles are synthesized from non-active CoO micropowders, they have demonstrated a remarkable 5% solar-to-hydrogen energy conversion efficiency. Details about material synthesis, characterizations, water-splitting experiments and new challenges will be presented.

1. L. Liao, et al. "Efficient solar water-splitting using a nanocrystalline CoO photocatalyst" Nature Nanotechnology 9, 69 (2014).

GE-18 (Invited Talk)
Advanced photovoltaic approaches to increase efficiency and reduce cost

Gavin Conibeer[1], Ivan Perez-Wurfl[1], Santosh Shrestha[1], Shujuan, Huang[1], Supriya Pillai[1], Robert Patterson[1], Yu Feng[1], Lingfeng Wu[1], Hongze Xia[1], Xuguang Jia[1], Binesh Puthen-Veettil[1]

[1] *Centre for Advanced Photovltaics, University of New South Wales, Sydney, NSW, 2052, Australia*
Email:g.conibeer@unsw.edu.au

Truly large scale implementation of photovoltaics will require further significant reductions in cost. These will necessarily also involve significant increases in efficiency. The ability to do both of these in the same device can be reaslised through the use of multilple energy levels in nanostructures, whether coupled to existing cells in transitional technologies to boost efficiency, or in freshly engineered disruptive technologies on a longer timescale.

The ability to tune the properties of materials using nanostructures gives much greater freedom in designing materials and structures for such high efficiency devices. Modification of energy bands in quantum well and quantum dot structures can be used to tune the band gap of materials for tandem solar cells. Quantum dot materials, in which Si QDs are embedded in a dielectric matrix can be used to fabricate such structures.

Nanostructures can also confine vibrational modes. In nanowell and quantum dot superstructures this can lead to a modulation of phonon energies. This can be used in hot carrier cells to interrupt the loss of energy to phonons from a photogenerated hot carrier population to give higher photovoltaic voltages. Plasmonic modes excited in metal nanoparticles can be used to couple light more effectively into or out of nanostructure materials. In addition near field effects can be used to massively increase local fields t give concentrating effects.

Light trapping also requires nanostructures to give effective non-coherrent interference that can increase the optical thickness of materials dramatically.

These nanostructure approaches to modifying electronic, optical or vibrational properties give a great deal more flexibility in materials design for solar cells. Other options for such exploitation, such as intermediate band solar cells and up or down conversion, will be briefly discussed and their potential to radically decrease costs per Watt investigated.

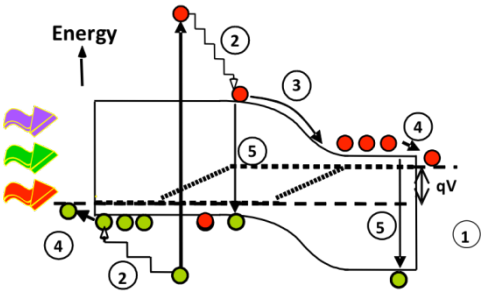

Fig. 1. Major loss mechanisms in single junction PV cell.

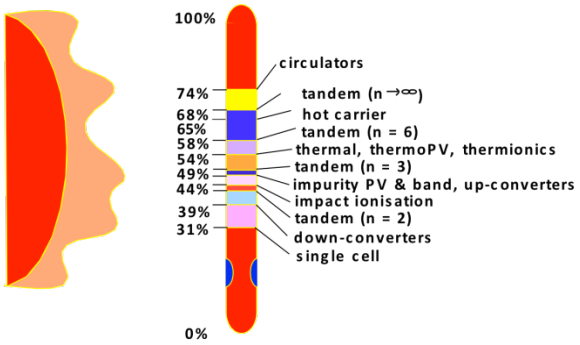

Fig. 2. Possible multiple energy level approaches for higher efficiency.

GE-19 (Invited Talk)
Molecular Design of Donor-π-Acceptor Type Organic Dyes for Efficient Dye-Sensitized Solar Cells

Vinich Promarak

School of Chemistry, Institute of Science, Suranaree University of Technology, Muang District, Nakhon Ratchasima, 30000 Thailand
E-mail:pvinich@sut.ac.th, web site: http://chem.sci.ubu.ac.th/adom

Dye-sensitized solar cells (DSSCs) have been intensively investigated since the report of highly efficient ruthenium complex-sensitized TiO_2 solar cells by the Swiss scientists. To date, overall conversion efficiencies of up to 12% were achieved from the ruthenium complex device. However, pure organic dyes exhibit not only higher extinction coefficient, but simple preparation and purification procedure with a low cost. Recently, enormous progress has been made in this field and the highest overall photoelectric conversion efficiency of solar cells sensitized by organic dyes containing an electron donor (D) and an electron acceptor (A), separated by a π-conjugation bridge (π) has reached 13%. This indicates the promising perspective of metal-free organic dyes [1].

In my talk, a series of novel D-π-A type organic dyes bearing carbazole or porphyrin as electron donor moiety (D), oligothiophene segments with number of thiophene units from one to three units as π-conjugated spacers (π) and cyanoacrylic acid as the electron acceptor (A) have been synthesized and characterized as dye sensitizers for DSSCs [2-6]. These compounds exhibit high thermal and electrochemical stability. Detail investigations of these dyes reveal that both peripheral donor moieties not only can contribute electron injection into TiO_2 upon photo-excitation, either directly or indirectly by internal conversion to the lowest excited state, but also inhibit aggregation between dye molecules and prevent iodide/triiodide in the electrolyte from recombining with injected electrons in the TiO_2, leading to increased overall conversion efficiency. The overall efficiencies of the corresponding devices reach 98% with respect to that of the N3-based device fabricated and measured under similar conditions. This work suggests that the organic dyes based on this type of donor moiety or donor molecular architecture are promising candidates for improvement of the performance of the DSSCs.

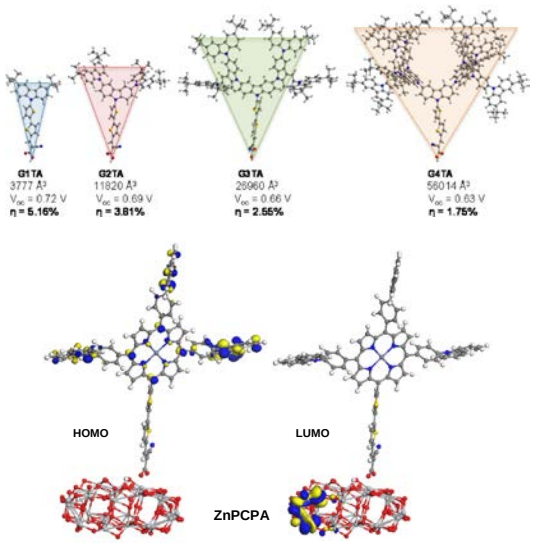

Fig. 1. D-π-A type dyes and the DFT calculation.

1. M. Liang and J. Chen, *Chem. Soc. Rev.* **42**, 3453 (2013).
2. S. Namuangruk, R. Fukuda, M. Ehara, J. Meeprasert, T. Khanasa, S. Morada, T. Kaewin, S. Jungsuttiwong, T. Sudyoadsuk and V. Promarak, *J. Phys. Chem. C* **116**, 25653 (2012).

3. P. Thongkasee, A. Thangthong, N. Janthasing, T. Sudyoadsuk, S. Namuangruk, T. Keawin, S. Jungsuttiwong and V., Promarak, *ACS App. Mater. Interfaces* **6**, 8212 (2014).
4. T. Sudyoadsuk, S. Pansay, S. Morada, R. Rattanawan, S. Namuangruk, T. Kaewin, S. Jungsuttiwong and V. Promarak, *Eur. J. Org. Chem.* **13**, 5051 (2013).
5. T. Khanasa, N. Jantasing, S. Morada, N. Leesakul, R. Tarsang, S. Namuangruk, T. Kaewin, S. Jungsuttiwong, T. Sudyoadsuk and V. Promarak, *Eur. J. Org. Chem.* **13**, 2608 (2013).
6. K. Sirithip, N. Prachumrak, R. Rattanawan, T. Keawin, T. Sudyoadsuk, S. Namuangruk, S. Jungsuttiwong and V. Promarak, *Chem.-An Asian J.* Accepted (2014)

GE-20 (Contributed Talk)
Interfacial Effect of Charge Carriers on Stabilizing Zinc Oxide in Poly(vinylidene fluoride) and study their Enhanced Dielectric Properties for Electro-mechanical Applications

Radhamanohar Aepuru[1], H. S. Panda[1]

[1]*Materials Engineering Department, Defence Institute of Advanced Technology (D. U.), Pune, Maharashtra, India.*
Email:radhamanohar.aepuru@gmail.com, web site: http://www.diat.ac.in

Conventional electro-active materials are based on ceramics and polymers. The selection of materials depends upon the application of the final product. Generally, ceramics poses higher piezoelectric and dielectric constants than any other materials. Nevertheless, their processing routes, high density and brittleness limited their wide spread usage. On the other hand, polymers which have advantages like easy processing, low cost and their flexible nature make them attractive for many applications for electromechanical devices such as actuators, sensors and energy harvesters. Despite their excellent physical properties, polymers often have low dielectric and piezoelectric constants compared to the inorganic metal oxides. Thus a vital issue is to enhance the dielectric and piezoelectric properties, while maintaining their excellent physical and mechanical properties. At present, Polymer nanocomposite which poses synergetic effect have been recognized with high dielectric and piezoelectric properties. These novel polymer nanocomposites were promising substitute materials for conventional electromechanical devices. [1][2].

In the present study, Polyvinylidene fluoride (PVDF) – Zinc Oxide (ZnO) composites with enhanced dielectric properties were successfully prepared by modifying ZnO fillers with adsorption charge carriers (Polyaniline). The structural morphology of the fillers was examined using powder X-ray diffraction and then correlated with high-resolution transmission electron microscopy. For the first time, maximum adsorption limit was studied by performing solvent relaxation nuclear magnetic resonance experiments, and the results suggested that a maximum of 10% PANI is adsorbed onto the ZnO. Electron spin resonance (ESR) analysis was carried out to know the significant difference between ZnO and modified ZnO fillers. The adsorbed PANI acts as an interface and stabilized the ZnO in PVDF solution leads to strong interactions between the matrix and fillers. Further, Dielectric studies of the modified fillers in polymer matrix were studied over the wide range of frequencies and temperatures. An enhanced dielectric constant with decrease in dielectric loss caused by adsorption of PANI on ZnO leads to the strong interaction between matrix and fillers and enhances the interfacial polarization in PVDF [3].

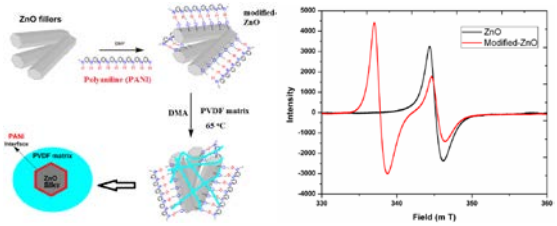

Fig1. (a) Schematic view of Composites preparation (b) ESR analysis of ZnO and modified ZnO [3].

References:

1. Radhamanohar; Sukla, R.; Sahoo,P.k.; Panda,H.S. *Adv.Sci.Eng.Med.* 6, 166 (2014).
2. Wu, W.; Huang, X.; Li, S.; Jiang, P.; Toshikatsu, T. *J. Phys. Chem. C*, 116, 24887 (2012).

3. Radhamanohar Aepuru and H. S. Panda, *J. Phys. Chem. C.* **118**, 18868 (2014).

GE-21 (Contributed Talk)
Study of CZTS nanocrystaline thin films by using electrodeposition for solar cell application

Sachin V. Mukhamale[1], Priyanka Tabhane[2], Vilas A. Tabhane[1]*

[1]*Department of Physics, Savitribai Phule Pune University, Pune, Maharashtra, INDIA*

[2]*Department of Physics, SDMC College of Commerce &Science, Silvasa, D &NH-396230, INDIA*
**Email:yash.goaldriven@gmail.com, web site: http://physics.unipune.ernet.in/~Tabhane/*

CZTS thin films have been deposited on conducting glass plate / substrates using low cost electrodeposition method. Solar energy is largest source of energy which if harnessed can provide 1000 times the current energy demand. Converting this energy into electricity through solar cell is one of the best ways. Initially CuS is optimized, then different deposition techniques for CZTS absorber layer electrodeposition is an effective and low cost alternative deposition method. CZTS solar cell can prove a substitute for those solar cell as they contain novel and earth abundant material which are easily at low cost. [1].

The synthesis of CZTS thin film using electroplating method was carried out by deposing Sn, Cu, Zn one after the other on a single substrate. The aim of this study is to fabricate Cu_2ZnSnS_4 (CZTS) thin film by electrodepositing the metal precursor. All of conditions of the electrodeposition including temperature, pH, solution composition. The process is in two steps a) comprised the electroplating of metallic precursors. As all precursors were first fabricated on stainless steel for optimization of process then it was synthesized on ITO coated glass. b) Second process step was sulphurization of precursors. The SEM and EDS gives the concentration then XRD shows the particle size.[2].

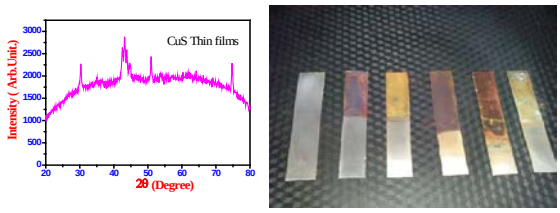

Fig1. X-ray diffraction (XRD) of CuS thin films with deposited by electrode position method.

1. S.Thanikaikarasan, T. Mahalingam, A. Kathalingam, Hosun Moon, and Yong Deak Kim, *Journal of New Materials for Electrochemical Systems 13, 29-33 (2010)*).
2. M.I. Khalil, R. Bernasconi, S. leffa, and L. Magagnin (Politecnico di Milano), *Journal of Electrochrmical society, 9, (2014)*

GE-22 (Contributed Talk)
Study of the effect of silicon substrate on the performance of organic-inorganic hybrid solar cells

Viney Saini, Shawn Bourdo, Omar Abdulrazzaq, Ganesh Kannarpady, Alexandru S. Biris

Center for Integrative Nanotechnology Sciences, University of Arkansas at Little Rock
Email: vxsaini@ualr.edu

In this work, single-walled carbon nanotube (SWCNT)/n-silicon based hybrid solar cells have been fabricated and characterized in order to investigate the effect of different doping levels/charge carrier concentrations in silicon. The effect of charge carrier concentration in silicon has been observed and the corresponding influence on the solar cell efficiencies is reported. The SWCNT films were characterized by UV-VIS-NIR spectroscopy for optical absorption, photoluminescence spectroscopy for chirality determination, and resistivity measurements. The n-type silicon substrates were characterized by

Hall-effect measurements for mobility of charges, charge carrier concentration, and resistivity measurements. The solar cells were characterized by current-voltage measurements under AM 1.5 solar irradiance, and scanning electron microscopy was employed to study the morphology of SWCNT films. We have found that a heavily doped silicon substrate does not result in a functional solar cell, whereas lightly doped silicon substrate produces much less photocurrent. The SWCNT/n-Silicon solar cells with silicon substrate resistivity of 1.82 Ω-cm and change carrier concentration of 2.33 x 10^{15} produce the best power conversion efficiency of 2.35%. These studies provide sufficient insight into material selection parameters for the SWCNT/n-silicon solar cell architectures to optimize device efficiencies.

GE-23 (Contributed Talk)
Hybrid nanomaterials and new designs for energy storage applications

Leela Mohana Reddy Arava
Department of Mechanical Engineering, Wayne State University, Detroit, MI, USA

In response to the ever increasing energy demands of modern society and in view of emerging ecological concerns, it is now essential to provide efficient, cost-effective, and environmental friendly energy storage devices. Rechargeable Lithium-ion batteries and Supercapacitors are amongst the most promising candidates in terms of their wide spread applicability, and tremendous potential owing to their high energy and power densities. The performance of these devices is inherently tied to the properties of materials used to build them. This talk will focus on the enhancement of these properties for next generation energy devices through nanoscale engineering and novel designs. Research efforts in miniaturizing the conventional Li-ion battery configurations through tailored designs such as three-dimensional and nano-wire batteries will be presented. Improving the performance of Li-ion batteries by using next generation electrode materials such as Si nanostructures will also be presented.

With growing concerns about the ecological footprint of energy industry, more sustainable and environmental friendly approaches are being called for. Recent efforts addressing these issues, including, recycling used silicon wafers into flexible battery components and transforming biodegradable plant extract to green batteries, will also be discussed.

Session FM
FUNCTIONAL MATERIALS

FM-01 (Contributed Talk)
In Situ TEM Analysis of Low-Temperature Creep of Si Nanowires Grown with Sn-Catalysts

Soumyadeep Misra[1], Wanghua Chen[1], Shengyi Qian[2], Jean-Luc Maurice[1], Linwei Yu[1,2], Erik Johnson[1] and Pere Roca iCabarrocas[1]

[1]*Laboratoire de Physique des Interfaces et Couches Minces, LPICM, UMR7647, CNRS, Ecole Polytechnique, Palaiseau, France*
Email:jean-luc.maurice@polytechnique.edu, web site: http://www.lpicm.polytechnique.fr/

[2]*School of Electronics Science and Engineering/National Laboratory of Solid State Microstructures, Nanjing University, 210093, Nanjing, China*

Si nanowires (SiNWs) are studied as promising building blocks for high-efficiency radial junction solar cells [1]. They are grown by the vapor-liquid-solid (VLS) mechanism, here at 425°C using Plasma Enhanced Chemical Vapor Deposition (PECVD) with Sn or In catalyst. It was shown that these metals may be an order of magnitude more soluble in the nanowires than in bulk Si [2]. It was also shown that tin tends to coat the SiNW walls during growth [3].

The presence of Sn in Si may significantly modify the properties of the nanowire. At the surface of the nano-object in particular, it may decrease its surface tension and correlatively change its thermodynamic properties. Here, we have investigated the latter *in situ*, in the transmission electron microscope (TEM). We show that, in these Sn-containing SiNWs, creep becomes active at temperatures as low as 620 °C in irradiated wires (electron irradiation due to 200-keV TEM observation in standard conditions).

As the crystalline structure of the wires remains unaffected during the large changes of shape observed (Fig1), we infer that the creep is due to surface diffusion of silicon atoms that would be enhanced by the presence of Sn. The effect of irradiation would be to further increase this (creep also occurs in areas not under investigation, but at higher temperature).

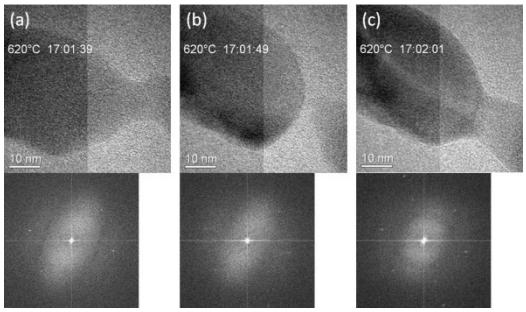

Fig. 1. Top row: TEM lattice images of a SiNW first obtained with Sn catalyst by PECVD at 425 °C. In (a) the SiNW has been annealed in situ for 15 min 700°C and 40 min at 600°C, without irradiation, then 20 s at 620°C under electron irradiation. In (b), after 10 additional seconds at 620°C, the SiNW is separated after a significant movement of silicon matter. In (c), after another 10 seconds at 620°C, the SiNW is welded together again. Bottom row: Fourier transforms of corresponding images, indicating that the Si remains a single crystal.

1. L. Yu, *et al., Sci. Rep.* **4**, 4357 (2014).
2. W. Chen, *et al., Nat Commun.* **5**, 4134 (2014).
3. S. Misra, *et al., J. Phys. Chem. C* **117**, 17786 (2013).

FM-02 (Contributed Talk)
Tuning the Work Function of Polyaniline via Camphorsulfonic Acid; XPS Study

Omar Abdulrazzaq, Shawn Bourdo, Viney Saini, Fumiya Watanabe, Bailey Barnes, Alexandru S. Biris

Center for Integrative Nanotechnology Sciences, University of Arkansas at Little Rock, Little Rock, Arkansas, USA.
Email: oaabdulrazza@ualr.edu

Polyaniline is a potential hole/electron transport layer for organic solar cells. It can be doped with dopants such as camphorsulfonic

acid. This work demonstrates the first study of the work function tunability of polyaniline using various levels of camphorsulfonic acid as a protonic acid dopant and *m*-cresol as a solvent. Optical, thermal, structural, and electronic properties along with elemental analysis of doped polyaniline were studied in detail to investigate the effect of camphorsulfonic acid on the work function of polyaniline. Results showed that increasing camphorsulfonic acid induces a gradual transformation in PANI structure from an emeraldine base to emeraldine salt phase, which is associated with an increase in electrical conductivity and an improvement in crystallinity. X-ray photoelectron spectroscopy (XPS) was used to evaluate the work function values and to determine the elemental composition on the surface and underneath. Results showed that raising camphorsulfonic acid from quarter protonated to fully protonated leads to an increase in the work function of polyaniline from 4.42 ±0.14 to 4.78 ±0.13 eV, respectively. Aside from the effect of doping on work function of polyaniline, we postulated that surface roughness and contamination can play a significant role in changing the work function at the surface.

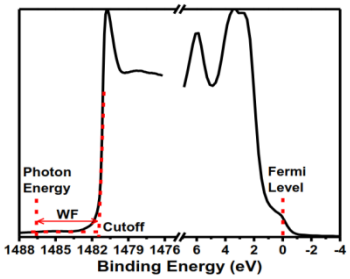

Fig. 1. The two parts of the survey spectrum from gold (i.e., low and high binding energy regions) acquired from XPS.

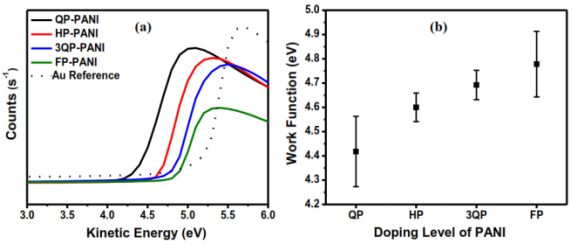

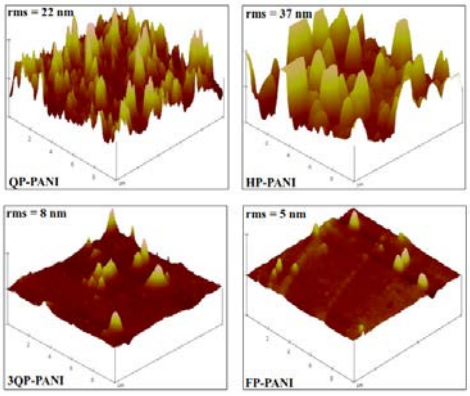

Fig. 2. Work function of PANI:CSA determined from XPS measurements (upper panel, a and b). AFM images for PANI:CSA (lower panel).

FM-03 (Contributed Talk)
A Novel Growth Process for the Deposition of $CH_3NH_3PbI_{3-x}Cl_x$ Perovskite Films

Chaminda Hettiarachchi, Nicholas Valdes, Pritish Mukherjee, Sarath Witanachchi[1]

[1]*Department of Physics, University of South Florida, Tampa, FL, 33620, USA*
Email:lakmal@mail.usf.edu, web site:labs.cas.usf.edu/lamsat/

Perovskite solar cell technology was selected as one of the top ten science breakthroughs in 2013 by the editors of Journal Science. Power conversion efficiency (PCE) of perovskite solar cells rose steeply from 3 % in 2009 to 17.9 % confirmed efficiency in early 2014. So far there have been four different fabrication techniques of organometal lead halide perovskites namely one-step precursor solution deposition [1]; two-step sequential deposition [2]; dual-source vapor deposition [3] and vapor assisted solution process [4]. The conventional method of making mixed halide perovskite $CH_3NH_3PbI_{3-x}Cl_x$ is reacting excess CH_3NH_3I with $PbCl_2$ but one must synthesize the first compound.

We demonstrate a novel one-step solution approach to prepare perovskite $CH_3NH_3PbI_{3-x}Cl_x$ films by adding CH_3NH_3Cl (or MACl) to PbI_2. The use of nebulizer assisted spray (NAS) process strongly affects the crystallization process of forming highly crystalline pure $CH_3NH_3PbI_{3-x}Cl_x$, leading not only to enhanced absorption of $CH_3NH_3PbI_{3-x}Cl_x$ but also to significantly improved coverage of $CH_3NH_3PbI_{3-x}Cl_x$ on a planar substrate. Compared to the standard spin coating method, nebulizer assisted spray approach enhances crystallinity and the mobility of charge carriers of $CH_3NH_3PbI_{3-x}Cl_x$ films. These results suggest that this new one-step solution approach is promising for controlling $CH_3NH_3PbI_{3-x}Cl_x$ growth to achieve high-performance perovskite solar cells.

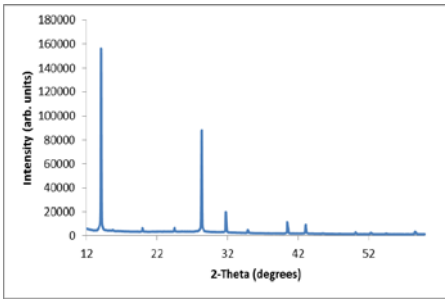

Fig. 1. X-ray diffraction pattern of NAS deposited $CH_3NH_3PbI_{3-x}Cl_x$ perovskite film.

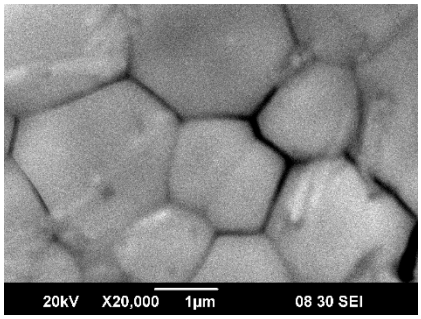

Fig. 2. SEM image of NAS deposited $CH_3NH_3PbI_{3-x}Cl_x$ perovskite film.

1. H. S. Kim, C. R. Lee, J. H. Im, K. B. Lee, T. Moehl,A. Marchioro, S. J. Moon, R. Humphry-Baker, J. H. Yum, J. E. Moser, M. Gratzel and N. G. Park, Sci. Rep., 2, 591 (2012).

2. J. Burschka, N. Pellet, S. J. Moon, R. Humphry-Baker,P. Gao, M. K. Nazeeruddin and M. Gratzel, Nature, 499, 316–319 (2013).

3. M. Liu, M. B. Johnston and H. J. Snaith, Nature, 501, 395–398 (2013).

4. Q. Chen, H. Zhou, Z. Hong, S. Luo, H. S. Duan, H. H. Wang, Y. Liu, G. Li and Y. Yang, J. Am. Chem. Soc., 136, 622–625 (2014).

FM-04 (Invited Talk)
Studies of Polymer-Like Behaviour in Ultrathin Nanowires

B. Yuan[1], S.Shaw[1], L.Cademartiri[1,2,3]

[1]*Department of Materials Science & Engineering, Iowa State University of Science and Technology, 2220 Hoover Hall, Ames, IA, 50011*
[2] *Department of Chemical & Biological Engineering, Iowa State University, Sweeney Hall, Ames, IA, 50011*
[3] *Ames Laboratory, US Department of Energy, Iowa State University, Ames, IA, 50011*

Recent years have seen a growing interest in the behaviour of ultrasmall colloidal nanocrystals[1-7]. The remarkable and still unclear transition between the cluster regime and the nanocrystal regime has become more tractable experimentally as better synthesis have yielded ultralarge clusters and ultrasmall nanocrystals.[6]
Interesting opportunities arise when ultrathin nanowires are considered[8]. The behaviour of these ultrathin and ultralong objects can be compared to that of polymer molecules.
Polymer molecules owe their unique properties to a combination of aspect ratio and spontaneous flexibility[9]. The combination yields a large contribution of the conformational entropy to the free energy of the polymers[10]. That entropic term is largely responsible for the unique properties of polymers. Because of the fact that large aspect ratios in crystals are difficult to obtain and that crystals are rigid, crystal have never displayed large conformational entropies and therefore have remained separate from the realm of applications of polymers (when not considered as fillers of composites)[2].

We here show our latest results on a kind of ultrathin nanowires that display remarkable flexibility[10, 11]. We will show preliminary results that strongly indicate that the nanowires are indeed spontaneously flexible and that, therefore, possess a non-negligible conformational entropy.

References

1. S. Hu and X. Wang, *Chem. Soc. Rev.*, 2013, **42**, 5577-5594.
2. A. Repko and L. Cademartiri, *Can. J. Chem.*, 2012, **90**, 1032-1047.
3. G. C. Xi, S. X. Ouyang, P. Li, J. H. Ye, Q. Ma, N. Su, H. Bai and C. Wang, *Angew. Chem. Int. Edit.*, 2012, **51**, 2395-2399.
4. M. McEachran, D. Keogh, B. Pietrobon, N. Cathcart, I. Gourevich, N. Coombs and V. Kitaev, *J. Am. Chem. Soc.*, 2011, **133**, 8066-8069.
5. G. X. Zhu, S. G. Zhang, Z. Xu, J. Ma and X. P. Shen, *J. Am. Chem. Soc.*, 2011, **133**, 15605-15612.
6. L. Cademartiri and V. Kitaev, *Nanoscale*, 2011, **3**, 3435-3446.
7. G. Z. Shen, B. Liang, X. F. Wang, H. T. Huang, D. Chen and Z. L. Wang, *ACS Nano*, 2011, **5**, 6148-6155.
8. L. Cademartiri, R. Malakooti, S. Petrov, A. Migliori and G. A. Ozin, *Abstr. Pap. Am. Chem. S.*, 2007, **234**.
9. M. Rubinstein and R. H. Colby, *Polymer Physics*, Oxford University Press, 2003.
10. S. Shaw and L. Cademartiri, *Adv. Mater.*, 2013, **25**, 4829-4844.
11. L. Cademartiri, G. Guerin, K. J. M. Bishop, M. A. Winnik and G. A. Ozin, *J. Am. Chem. Soc.*, 2012, **134**, 9327-9334.

FM-05 (Invited Talk)
Advanced laser ablation techniques for ferroelectric and multiferroic heterostructures of perovskite-oxides

Devajyoti Mukherjee[1], S. Witanachchi[1], P. Mukherjee[1]

[1]Center for Integrated Functional Materials and Department of Physics, University of South Florida, Tampa, Fl, USA
Email:dmukherj@usf.edu

Multiferroic heterostructures of ferroelectric (FE) and ferromagnetic (FM) perovskite-oxides have attracted considerable attention for their multifunctional properties and potential applications in non-volatile memory devices. Pulsed laser deposition (PLD), although quite successful in the growth of complex-oxide thin films, is complicated in the synthesis of multilayered FE/FM heterostructures. This is primarily associated with the dissimilar ablation conditions of the insulating FE and the conducting FM phases in such heterostructures. Here, we address some of the challenges in the laser ablation of epitaxial multilayered thin films of the FE perovskite $PbZr_{0.52}Ti_{0.48}O_3$ (PZT) with the FM oxide $La_{0.7}Sr_{0.3}MnO_3$ (LSMO) [1] and how they can be overcomed using a unique dual-laser ablation process. In this process, the energy output from the KrF excimer laser (typically used in PLD) is spatially overlapped and temporally synchronized (to within 100 ns) with that of a pulsed CO_2 laser. The optimum coupling of the laser energies lead to enhanced excitation of the laser-ablated species; resulting in highly-crystalline, particulate-free and smooth films with uniform thicknesses. Using the dual-laser process, epitaxial PZT/LSMO thin films were deposited on single-crystal $SrTiO_3$ (100) and MgO (100) substrates. Structural analyses using X-ray diffraction, atomic force microscopy and transmission electron microscopy revealed their single crystalline nature, smooth particulate-free surfaces and atomically sharp and flat interfaces. Magnetic and polarization measurements showed enhanced room temperature FE and FM properties in PZT/LSMO heterostructures as compared to those grown using traditional PLD [2]. Further, using the dual-laser process the incorporation of an ultra-thin hard-magnetic $CoFe_2O_4$ (CFO) sandwich layer in PZT/LSMO heterostructures was achieved. Structural characterization of the PZT/CFO/LSMO heterostructures revealed their single-crystalline nature, defect-free interfaces and smooth surface morphologies. With the introduction of the CFO sandwich-layer, the low magnetic coercivity of PZT/LSMO as well as the remanent polarization were increased; thus making PZT/CFO/LSMO films desirable for multiferroic device applications. In a different direction, we report on a novel combined physical/chemical methodology

using PLD and solvothermal process that has been quite successful in the growth of nanostructured films of the classic FE perovskite PZT [3] as well as the emergent Pb-free non-centrosymmetric FE oxide $LiNbO_3$-type (LN-type) $ZnSnO_3$ [4]. In this combined physical/chemical technique, a seed-layer of a lattice-matched material (i.e. PZT seed-layer for PZT nanostructured film and ZnO seed-layer for LN-type $ZnSnO_3$ nanostructured film) is initially deposited on a suitable substrate using PLD. This is followed by the chemical synthesis of the FE nanostructures on the pre-orientating seed-layers. The similar crystal symmetry between the seed-layers and FE phase facilitated the growth of well-aligned and self-supported FE nanostructured arrays. The structural integrity and high density of the nanostructures allowed a direct measurement of the intrinsic FE polarization of PZT and LN-type $ZnSnO_3$ from the resulting nanostructured device without the using of any dielectric fillers to prevent shorting of the device. Detailed study on the structural and FE properties of PZT and LN-type $ZnSnO_3$ nanostructured films will be presented. The results presented here highlight the recent advances in laser ablation techniques for the growth of multiferroic heterostructures and FE nanostructures which is crucial for the coherent design of future memory devices based on these composite systems.

1. D. Mukherjee et al., *J. Appl. Phys.* **112**, 064101 (2012).
2. D. Mukherjee et al., *J. Appl. Phys.* **111**, 064102 (2012)
3. A. Datta, D. Mukherjee et al., *Adv. Funct. Mater.* **24**, 2638 (2014).
4. A. Datta, D. Mukherjee et al., *Small*, (2014).

FM-06 (Invited Talk)
Recent Progress in Studies of Magnetic Microwires

Arcady Zhukov[1,2, 3], Mihail Ipatov[1,2], Ahmed Talaat[1,2], Alexandr Chizhik[1,2], Juan M. Blanco[2], Sergei Gudoshnikov[4] and Valentina Zhukova[1,2]

[1]Dpto. de Fís. Mater., UPV/EHU San Sebastián 20018, Spain
[2]Dpto. de Física Aplicada, EUPDS, UPV/EHU, 20018, San Sebastian, Spain

[3]IKERBASQUE, Basque Foundation for Science, 48011 Bilbao, Spain
[4]National University of Science and Technology «MISIS», Moscow, 119049, Russia

Amorphous Co-rich soft magnetic microwires exhibiting Giant magnetoimpedance (GMI) effect and Fe-rich microwires exhibiting fast magnetization switching have been proposed for promising applications in magnetic microsensors and smart tuneable composites[1,2]. Taylor-Ulitovsky technique allows fabrication of glass-coated microwires consisting of metallic nucleus with diameters from 0.05 μm to 100 μm. Overall shape of hysteresis loop and GMI effect of Co- and Fe-rich glass-coated microwires are rather different. This difference is usually attributed to the complex internal stresses arising during fast solidification of thin metallic nucleus surrounded by the glass coating.

The magnetostriction coefficient, λ_s, plays decisive influence on magnetic properties of amorphous materials. In the case of metallic glasses λ_s depends mostly on the chemical composition, achieving vanishing values in amorphous Fe-Co based alloys with Co/Fe ≈70/5. Additionally, the magnetostriction coefficient changes with the stress.Therefore tailoring of magnetic properties using either annealing or glass coating removal is essentially relevant and observed changing of magnetic properties are quite noticeable [3].

We present our last results on comparative studies of soft magnetic properties and magnetostriction coefficient of Co-Fe-rich microwires with vanishing magnetostriction coefficient. We found that the hysteresis loop of Co-Fe rich samples drastically changes after annealing (see Fig.1). Varying either annealing time, t_{ann}, or the annealing temperature, T_{ann}, we observed changes of the character of hysteresis loops. After annealing at high enough

temperature or long enough annealing time the hysteresis loop becomes rectangular typical for Fe-rich microwires. But in spite of rectangular character of hysteresis loop annealed Co-Fe-rich samples present considerable GMI effect. The study of the surface magnetization reversal has been performed using the magneto-optical Kerr effect (MOKE) in two microwires of the following compositions Sample 1 ($Co_{69.2}Fe_{4.1}B_{11.8}Si_{13.8}C_{1.1}$) and Sample 2 ($Fe_{70.8}Cu_1Nb_{3.1}Si_{14.5}B_{10.6}$). From MOKE studies we can conclude that studied Co-rich microwire (Sample 1) has helical magnetic structure and Fe-rich microwire (Sample 2) has axial magnetic structure.We also performed studies of the annealing conditions on the magnetostriction coefficient of Co and Fe-rich microwires and compared observed changes with hysteresis loops. We observed that drastic changes of the hysteresis loop are correlated with change of the sign of the magnetostriction coefficient.

We interpreted observed correlation with internal stresses dependence of the magnetostriction coefficient. Internal stress relaxation and can be tailored by the annealing.

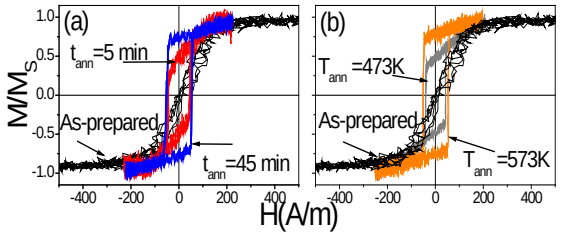

Fig. 1. Effect of annealing time, t_{ann}, at T_{ann}= 523 K (a) and annealing temperature at t_{ann} =5 min (b) on hysteresis loops of $Co_{69.2}Fe_{4.1}B_{11.8}Si_{13.8}C_{1.1}$ microwires.

1. M. Vazquez, H. Chiriac, A. Zhukov, L. Panina, and T. Uchiyama, *Phys. Status Solidi A*, 208, 493 (2011)
2. D.C. Jiles, *Acta Materialia*, 51 5907v(2003)
3. Y. Konno, K. Mohri, *IEEE Trans Magn* Vol. 25, No.5 3623, (1989)

FM-07 (Invited Talk)
The nano revolution and its impact in materials for energy applications

Victor Castaño,
Centro de Física Aplicada y Tecnología Avanzada, Mexico

The fundamental physical and chemical principles of Nanotechnology will be revised, in terms of the opportunities for energy applications that they offer. Then, some of the main challenges for energy generation and storage will be analyzed along with a review of the methods that have been tested so far, along with their limitations. Finally, a number of examples, including quantum dots with non-semiconductor materials, nanostructures batteries and others, will be explained and discussed as potential short and long-term nanotechnologies for energy applications.

FM-08 (Invited Talk)
Tandem Photovoltaics Using Transparent Conducting Photonic Crystal Contacts

Nazir P. Kherani[1,2,*], Joel Y. Y. Loh[1], Paul G. O'Brien[2,3], Andrew G. Flood[1], Brett Ramautarsingh[2]
[1] *Dept. of Electrical & Computer Engineering, University of Toronto, Toronto, Canada*
[2] *Dept. of Materials Science & Engineering, University of Toronto, Toronto, Canada*
[3] *Dept. of Chemistry, University of Toronto, Toronto, Canada*
[*] *kherani@ecf.utoronto.ca*

With recent advances in various photovoltaic material systems the prospect of attaining ultra-high efficiency terrestrial solar cells using tandem photovoltaics has been of increasing interest with an emphasis on integrating coherent light trapping structures that provide the required spectral and directional utilization of solar irradiation. Within this framework, both two and four terminal devices are of interest subject to the complexity of device

integration and properties of the light trapping structures. In the context of two terminal devices, effective incorporation of conducting optical-photonic structures as intermediate contacts enables current matching and efficient extraction of photogenerated carriers across multiple junctions in a tandem photovoltaic device. In the context of four terminal tandem devices, transparent conducting optical-photonic structures are advantageous because they can be located directly adjacent to the active region of a photovoltaic cell, thereby enabling the design of light trapping architectures in the coherent light trapping regime [1].

Photonic crystals are periodic nanostructures that exhibit bandgaps within which the propagation of certain frequencies of the electromagnetic spectrum are disallowed. Accordingly, photonic crystal constructs can enable control over reflection, transmission and trapping of light upon device integration. Recently, the synthesis of photonic crystals from transparent conducting materials has opened the potential of simultaneously designing nanostructures that afford light modulation and electrical conduction [2]. The advent of conducting photonic crystals enables intimate coupling of active photovoltaic absorbing materials and photonic crystal elements for optimal light trapping, absorption and photogenerated charge extraction [3].

This talk will present a recently developed novel class of one-dimensional photonic crystals, called selectively transparent and conducting photonic crystal (STCPC), which amalgamates optical tunability and electrical conductivity [4]. These nanoparticle based photonic crystals provide effective wavelength selective broadband reflectance along with the transmissive and electrical properties of transparent conducting oxides. The stop-gap of these STCPCs can be tuned to extend over the visible and near infrared part of the spectrum with the PCs exhibiting electrical conductivity suitable for device integration. Herein we report on a range of successful device integrations [5-8] as well as explore their potential within novel tandem photovoltaic material systems.

1. Mallick, S. B, et al., *Coherent light trapping thin-film photovoltaics*, 2011.36(06): p. 453-460.
2. Bielawny, A., et al., *3D photonic crystal intermediate reflector for micromorph thin-film tandem solar cell.* Physica Status Solidi a-Applications and Materials Science, 2008. **205**(12): p. 2796-2810.
3. O'Brien, P.G., et al., *Silicon photovoltaics using conducting photonic crystal back-reflectors.* Advanced Materials, 2008. **20**(8): p. 1577-1582.
4. O'Brien, P.G., et al., *Selectively transparent and conducting photonic crystals.* Advanced Materials, 2010. **22**(5): p. 611-616.
5. Heiniger, L.P., et al., *See-through dye-sensitized solar cells: Photonic reflectors for tandem and building integrated photovoltaics.* Advanced Materials, 2013. **25**(40): p. 5734-5741.
6. Yang, Y. et al., *See-through amorphous silicon solar cells with selectively transparent and conducting photonic crystal back reflectors for building integrated photovoltaics.* Applied Physics Letters (accepted), 2013.
7. Puzzo, D.P., et al., *Organic light-emitting diode microcavities from transparent conducting metal oxide photonic crystals.* Nano Letters, 2011. **11**(4): p. 1457-1462.
8. O'Brien, P.G., et al., *Selectively transparent and conducting photonic crystal solar spectrum splitters made of alternating sputtered indium-tin oxide and spin-coated silica nanoparticle layers for enhanced photovoltaics.* Solar Energy Materials and Solar Cells, 2012. **102**: p. 173-183.

FM-09 (Invited Talk)
Piezoelectric MEMS Energy Harvesters

Susan Trolier-McKinstry, H. G. Yeo, X. Ma, J. I. Ramirwz, K. G. Sun, C. Rahn, and T. N. Jackson

[1]Department of Materials Science and Engineering, Penn State, University Park, PA, USA
Email: STMcKinstry@psu.edu

The development of self-powered wireless microelectromechanical (MEMS) sensors hinges on the ability to harvest adequate energy from the environment. When solar energy is not available, mechanical energy from ambient vibrations, which are typically low frequency, is of particular interest. Piezoelectric thin films enable MEMS devices to convert mechanical to electrical

energy. Here higher power levels were approached by better coupling energy into the harvester, using improved piezoelectric layers, and efficiently extracting energy through the use of voltage rectifiers. MEMS structures (end-loaded cantilevers) with natural frequencies below 50 Hz were designed to demonstrate energy harvesting of low frequency vibrations. Two approaches were utilized for preparing low frequency harvesters: composite membranes with polymer passive elastic layers, and Ni foil-based substrates. In both cases, lead zirconate titanate (PZT) was chosen as the piezoelectric layer. Strongly {001} oriented PZT could be deposited by RF magnetron sputtering and ex situ annealing on (100) oriented $LaNiO_3$ / HfO_2 / Ni foils. The comparatively high thermal expansion coefficient of the Ni facilitates development of a strong out-of-plane polarization. 31 mode cantilever beam energy harvesters were fabricated using strongly {001} textured 1~3 micron thick PZT films on Ni foils with dielectric permittivity of ~ 350 and low loss tangent (<2%) at 100Hz. The resonance frequency of the cantilevers (50~75 Hz) were tuned by changing the beam size and proof mass. The cantilever beam with 3 micron thick PZT films and 0.4 g proof mass exhibited a maximum output power of 64.5 micro-Watts at 1 g acceleration vibration with a 100 k-Ohm load resistance. At 0.3g, the average power was 9 micro-Watts at resonance. Excellent agreement between the measured and modeled data was obtained using a linear analytical model for an energy harvesting system, using an Euler-Bernoulli beam model. It was also demonstrated that up to an order of magnitude more power could be harvested by more efficiently utilizing the available strain using a parabolic mode shape for the vibrating structure. Additionally, voltage rectifying electronics in the form of ZnO thin film transistors are deposited directly on the cantilever. This relieves the role of voltage rectification from the interfacing circuitry and provides a technique improved harvesting relative to solid state diode rectification because the turn-on bias can be reduced to zero.

FM-10 (Contributed Talk)
Surface wrinkling of shape memory polymers

Yu Wang[1], Jianliang Xiao[1]

[1]*Department of Mechanical Engineering, University of Colorado, Boulder, CO, USA*
Email:Jianliang.Xiao@colorado.edu

Shape memory polymers (SMPs) can remember two or more distinct shapes, and therefore can have a lot of potential applications. We here present combined experimental and theoretical studies on the wrinkling of stiff thin films on SMPs. Experimental results show well-defined, wavy profiles of the thin films (see Fig. 1). Time and temperature dependent wrinkle formation and evolution were observed. It was shown that both wrinkling wavelength and amplitude increase with SMP relaxation. This is different from previous observations of thin film wrinkling on soft substrates, which show decreasing wavelength and increasing amplitude when compression increases. Finite element simulations accounting for the thermomechanical behavior of SMPs were used to study wrinkling of thin films on SMPs, which show good agreement with experiments. This study can have important implications in surface engineering, stretchable electronics and advanced manufacturing.

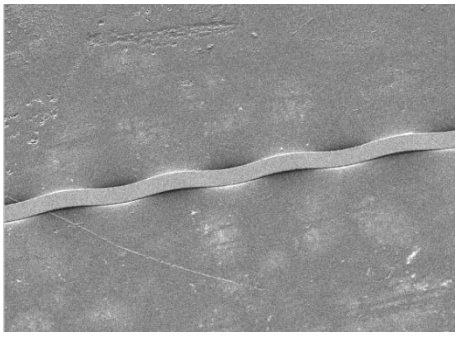

Fig. 1. SEM image of silicon wrinkling on SMP

FM-11 (Contributed Talk)
Influence of Crystal Defects on the Martensitic Transformation in Ni-Mn-Ga Alloy

Anna Kosogor[1,2], V.V. Sokolovskiy[1,3], V.A. L'vov[2], V.V. Khovaylo[1,4]

[1]*National University of Science and Technology "MISiS," Moscow, Russia*
Email:annakosogor@gmail.com

[2]*Institute of Magnetism, Kyiv, Ukraine*

[3]*Chelyabinsk State University, Chelyabinsk, Russia*

[4]*ITMO University, St. Petersburg, Russia*

Shape memory alloys (SMAs) exhibit a number of unique features, such as giant (up to 12 %) reversible deformation and shape memory effect, which give rise to numerous industrial and medical applications of these alloys. The functional properties of the shape memory alloys strongly depend on the concentration of crystal defects, and change with time due to the spatial reconfiguration of crystal defects. [1] In spite of intensive experimental studies of defect effect on SMAs properties, the theoretical works elucidating this effect are missing. In the present communication two different theoretical approaches to the description of defect influence on martensitic transformation (MT) in Ni-Mn-Ga alloy are presented. The numerical Monte Carlo method was advanced for the microscopic modeling of the defect impact on the MT temperature. This method was combined with macroscopic Landau theory describing MT in a crystal with defects. [2] The emphasis is given to the spatial reconfiguration of crystal defects during alloy aging.

Figure 1(a) shows the temperature dependencies of the structural order parameter calculated using the Monte Carlo method for the fresh and aged Ni-Mn-Ga alloy with different defect concentrations. The jump of the structural parameter value characterizes martensitic transformation. As can be seen from the figure, the reverse MT temperature computed for the aged alloy is larger than that for the fresh one and the magnitude of the MT temperature shift depends on the defect concentration, which is in accordance with experiments on alloy aging. In the Figure 1(b) the concentration dependence of the reverse MT temperature of the fresh alloy computed using Monte Carlo method and Landau theory is presented.

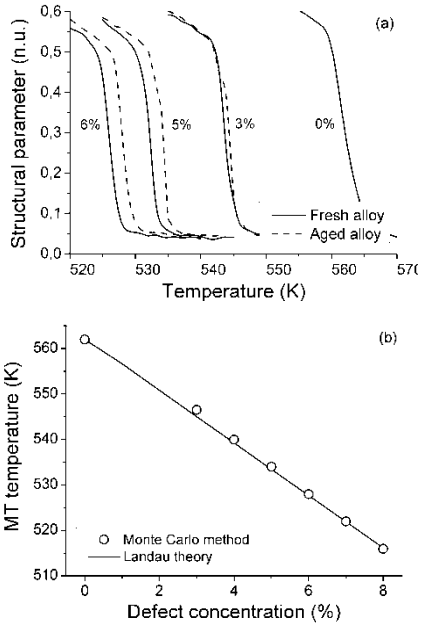

Fig. 1. (a) Temperature dependencies of the structural parameter calculated by the Monte Carlo method for the reverse MT of the fresh and aged Ni-Mn-Ga alloy for the different defect concentrations. (b) Concentration dependence of the reverse MT temperature of the fresh alloy computed using Monte Carlo method (circles) and Landau theory (line).

The Landau theory describes the thermodynamic characteristic of the SMA, but says nothing about the defects types and concentration, while the Monte Carlo simulations deal with certain types of crystal defects and its concentration, but do not involve the thermodynamic characteristics of the alloy, which are widely studied in numerous experiments. The combination of the Landau theory and the Monte Carlo simulations bridges a gap between the macroscopic and microscopic approaches to the description of the transformational properties of real (with defects) shape memory alloys.

1. X. Ren and K. Otsuka, *Nature* **389**, 579 (1997).

2. A. Kosogor, V.A. L'vov, O. Söderberg and S-P. Hannula, *Acta Mater*. **59**, 3593 (2011).

FM-12 (Invited Talk)
Magnetic shape memory thin films and nano-disks: effects of size reduction on magnetism, structure and microstructure

F. Albertini[1], M. Campanini[1], P. Ranzieri[1], R. Ciprian[1], V. Chiesi[1], S. Fabbrici[2,1], F. Casoli[1], L. Nasi[1], L. Righi[3,1], V. Grillo[4,1], F. Celegato[5], P. Tiberto[5,,1], G. Barrera[5]

[1]*Intitute of Materials for Electronics and Magnetism-National Research Council, Parma, Italy. Email:franca.albertini@imem.cnr.it web site: http://www.imem.cnr.it/mmm/Home.html*
[2]*Mist E-R Lab., Bologna, Italy.*
[3]*Chemistry Department, Parma University, Parma, Italy.*
[4]*NANO-CNR, Modena, Italy.*
[5]*INRIM, Torino, Italy.*

Magnetic shape memory are multi-functional materials exhibiting a coupling between magnetic and structural order arising from the presence of a martensitic transformation and leading to a rich phenomenology (e.g. "giant" magnetomechanical, magnetocaloric, elastocaloric properties) [1]. Low-dimensional materials, mainly thin films, have recently attracted much interest for the promising applications (e.g. microactuators, valves, solid-state microrefrigerators) [2]. With respect to the bulk, they offer the further possibility of tuning properties by thickness and by the choice of suitable substrates and underlayers [3]. The present paper is aimed at deepening these effects, extending the study to laterally confined nanostructures.

Epitaxial thin films of NiMnGa of thickness ranging from 10 to 200 nm were grown by sputtering r.f. on MgO substrate with and without a Cr underlayer. Patterned thin films were obtained by polystyrene-nanosphere lithography, a large-scale and inexpensive nanostructuring method. Freestanding nano-disks (d=160 and 650 nm) were subsequently obtained by removing Cr underlayer by selective chemical etching.

A multiscale structural and magnetic study was performed on nanodisks and continuous thin films by means of electron transmission microscopy (HREM, STEM-HAADF, electron diffraction, Lorentz microscopy), X-ray diffraction and reflectivity, atomic and magnetic force microscopy, AGFM and SQUID magnetometry and susceptometry.

It was noticeably shown that nanodisks (free standing and on substrate) preserve the salient martensitic and magnetic properties of continuous films for both the investigated sizes, and are then exploitable in multifunctional applications. On the other hand the twin structure and its temperature dependence can be influenced by lateral confinement and release from substrate. This fact, mainly exploitable in shape memory and magnetic shape memory applications, paves the way to the realization of shape-controlled nano-actuators.

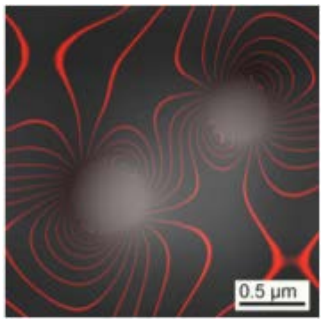

Fig. 1. In-line Lorentz microscopy of NiMnGa free-standing nano-disks.

1. M. Acet, L. Mañosa, and A. Planes, *Handbook of Magnetic Materials* 19 (Elsevier, Amsterdam), 231 (2011).
2. A. Backen et al., *Adv. Eng. Mat.* **14**, 696 (2012).
3. P. Ranzieri et al., *Acta Mater.* **61**, 263 (2013).

FM-13 (Invited Talk)
Voltage-controlled exchange bias and exchange bias training

Christian Binek, Will Echtenkamp

Department of Physics & Astronomy and Nebraska Center for Materials and Nanoscience, University of Nebraska-Lincoln, USA
Email:cbinek@unl.edu, web site: http://physics.unl.edu/~cbinek/

Voltage-controlled exchange bias (EB) is a seminal achievement in nanomagnetism. It enables dissipationless electric control of interface magnetic states with major implications for room temperature spintronic applications. Numerous prototypical solid-state spintronic devices rely on switchable interface magnetism, enabling spin-selective transmission or scattering of electrons. Controlling magnetism at thin-film interfaces, preferably by purely electrical means, i.e. in the absence of electric currents, is a key challenge to better spintronics. Currently, most attempts to voltage-control magnetism focus on potentially large magnetoelectric (ME) effects of multiferroics.

Here, we report on the use of antiferromagnetic (AF) ME Cr_2O_3 (chromia) for voltage-controlled magnetism [1,2]. Electrically switchable boundary magnetization (BM) can overcome the weak linear ME susceptibility of bulk ME antiferromagnets. Voltage-controlled BM is the key property enabling isothermal voltage-controlled switching of exchange bias (EB) which emerges at the interface of adjacent ferromagnetic (FM) and the ME antiferromagnetic (AF) thin film. The inter-layer exchange alters the magnetization reversal shifting the FM hysteresis loop along the magnetic field axis. In this presentation I introduce voltage-control of EB and EB training [2]. Electric switching between stable EB fields is investigated in heterostructures based on single crystal Cr_2O_3(0001)/PdCo heterostructures and compared with recent results in MBE grown all thin film EB heterostructures. In addition to voltage-switching of EB we electrically and isothermally tune chromia into distinct AF multi-domain states (see figure). As a result, EB training, which originates from triggered rearrangements of the AF interface magnetization during consecutively cycled hysteresis loops, is tuned between zero and sizable effects. We quantify and interpret the peculiar voltage-controlled training effect in Cr_2O_3(0001)/PdCo by adapting our recently developed theory which is based on a discretized Landau-Khalatnikov dynamic equation [3].

We acknowledge the Center for NanoFerroic Devices, C-SPIN, part of STARnet, a SRC program sponsored by MARCO and DARPA for partial funding of this work.

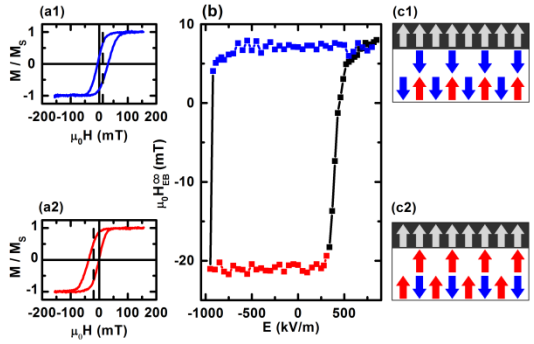

Fig. 1: a1) Hysteresis loop of pinned CoPd thin film after ME annealing of the sample. a2) Hysteresis loop of pinned CoPd thin film after electrically switching the spin configuration of chromia. b) Hysteretic behavior of equilibrium EB with respect to applied electric field, a constant magnetic field of 100 mT is simultaneously applied. c1,2) Cartoons of the spin structure for positive (c1) and negative (c2) EB.

[1] Xi He, Yi Wang, N. Wu, A. N. Caruso, E. Vescovo., K. D. Belashchenko, P. A. Dowben, and Ch. Binek, Nature Mater. 9, 579 (2010).
[2] W. Echtenkmap, Ch. Binek, Phys. Rev. Lett. **111**, 187204 (2013).
[3] Ch. Binek, et al., Phys. Rev. Lett. **96**, 067201 (2006).

FM-14 (Invited Talk)
Organic Spintronic Devices

Luis E. Hueso[1,2], M. Gobbi[1,2], A. Bedoya-Pinto[1], X. Sun[1], F. Golmar[1], F. Casanova[1,2]

[1]*CIC nanoGUNE, San Sebastian, Spain*
Email:l.hueso@nanogune.eu, web site: http://nanodevices.nanogune.eu

[2]*IKERBASQUE, Basque Foundation for Science, Bilbao, Spain*

Materials based on carbon have recently caught the attention of spintronics, and significant efforts are being made towards their integration in this field [1,2]. One of their most attractive aspects for spintronic applications is the weakness of their spin scattering mechanisms, implying that the spin polarization of the carriers can be maintained for a very long time in these materials. Moreover, molecular materials might have tunable chemical properties, opening a way for the integration of synthetic chemistry into spintronic devices.

In this talk, I will present results with a prototypical spintronic device (the spin valve), in which a molecular active layer was sandwiched between two ferromagnetic materials (see Figue 1 for a scheme of such device and an electron microscopy image). I will show how two very different molecules, namely C_{60} fullerene and bathocuproine or BCP, are capable or maintaining the coherence of the spin of the injected carriers for more than 60 nm at room temperature.

In the case of the fullerene, the room temperature magnetoresistance data is consistent with a multistep tunneling regime [3, 4]. In the case of the BCP, we highlight the differences between spin tunneling and transport in molecular levels. The chemical stability of this molecule, even under ambient conditions, could make it very attractive for potential molecular spintronic

We expect our results to be reproduced by other molecular semiconductors, opening novel pathways for the further development of molecular spintronics.

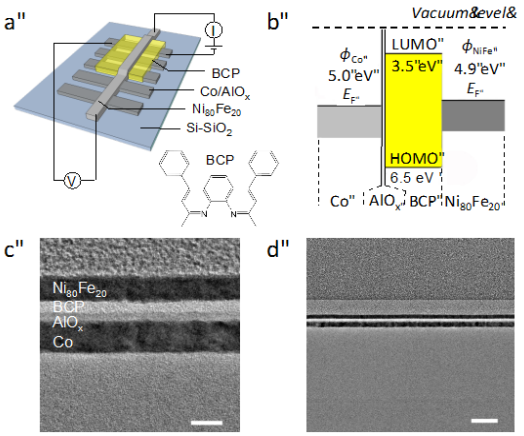

Fig. 1. **a)** Schematic representation of a molecular spin valve **b)** Rigid energy diagram for a $Co/AlO_x/BCP/Ni_{80}Fe_{20}$ stack. **c)** and **d)** Transmission Electron Microscopy cross section images of a BCP-based spin valve structure. Scale bars in c) and d) represent 10 nm and 50 nm, respectively.

1. L.E. Hueso, M.A. Pruneda, V. Ferrari, G. Burnell, J. Valdes, B. Simons, P.B. Littlewood, A. Fert and N.D. Mathur, *Nature* **445**, 410 (2007); Wei Han et al., *J. Magn. Magn. Mater.* **324**, 369 (2012).
2. V.A. Dediu, L.E. Hueso, I. Bergenti, C. Taliani, *Nature Mater.* **8**, 707 (2009).
3. M. Gobbi, F. Golmar, R. Llopis, F. Casanova, L.E. Hueso, *Adv. Mater.* **23**, 1609 (2011).
4. M. Gobbi, A. Bedoya-Pinto, F. Casanova, L.E. Hueso, *Appl. Phys. Lett.* **101**, 102404 (2012); *Nature Commun.* **5**, 4161 (2014).
5. X. Sun, M. Gobbi, A. Bedoya, F. Golmar, F. Casanova, L.E. Hueso, *Nature Commun.* **4**, 2794 (2013).

FM-15 (Invited Talk)
Evolution of a Disordered Nanoparticle Network into Boolean Logic

Wilfred G. van der Wiel

MESA⁺ Institute for Nanotechnology, University of Twente, P.O. Box 217, 7500 AE Enschede, The Netherlands
Email: W.G.vanderWiel@utwente.nl, web site: http://www.nano-electronics.nl

Present-day computers are based on integrated circuits, constructed according to fixed design rules and making use of well-defined components. Living systems, however, are able to achieve extraordinary feats of computation without the need for a specific design. Darwinian evolution has resulted in sophisticated information processing systems in which the emergent properties and huge parallelism of complex networks are exploited. Inspired by this, we here report on an artificial system of randomly assembled gold nanoparticles coupled via molecular tunnel barriers, acting as a disordered network of single-electron transistors at low temperature [1]. Using artificial evolution, we demonstrate that this designless system can be configured into any basic Boolean logic gate with a very high degree of stability and reproducibility. Our results comprise the first experimental demonstration of fully reconfigurable logic based on randomly distributed nanoscale components, and bear direct relevance for future unconventional computer architectures.

1. S.K. Bose, C.P. Lawrence, Z. Liu, K.S. Makarenko, R.M.J. van Damme, H.J. Broersma and W.G. van der Wiel, *manuscript submitted* (2014).

FM-16 (Invited Talk)
Transition metal based magneto caloric materials

Ekkes Brück, Yibole Yibole, Van Thang Nguyen, Xuefei Miao, Maurits Boeije, Luana Caron, Lian Zhang, Francois Guillou, Niels Van Dijk

Fundamental Aspects of Materials and Energy, Department of Radiation Science and Technology, Faculty of Applied Sciences, Delft University of Technology, Delft, The Netherlands
Email:e.h.bruck@tudelft.nl, web site: http://www.rst.tudelft.nl/fame

Large adiabatic temperature changes and large isothermal entropy changes in low magnetic fields are of great interest for heat pumps and energy conversion.

Magnetocaloric materials are being studied with magnetic measurements for decades. With the advent of giant magnetocaloric effects (MCE) that occur in conjunction with magneto-elastic or magneto-structural phase transition of first order (FOT), room temperature applications became more feasible.

In this context the MnFe(P,X) system appears to be an ideal playground. This material family derives from the Fe_2P compound, a prototypical example known since a long time to exhibit a sharp but weak (the latent heat L is only 0.25 $kJkg^{-1}$) FOT at 210 K.

In this hexagonal system, the Fe atoms occupy two inequivalent atomic positions referred as 3*f* (in a tetrahedral environment of non-metallic atoms) and 3*g* (pyramidal). One intriguing aspect is the disappearance of the magnetic moments of the irons on the 3f sites when crossing T_C, whereas there is only a limited decrease on the 3*g* site. This observation has led to a cooperative description of the FOT linking the loss of long range magnetic order at TC with the loss of local moments on 3*f*. This mechanism has recently been shown to be at the origin of the G-MCE observed in MnFe(P,Si)[1].

The disappearance of the magnetic moments has been ascribed to a conversion from non-bonding 3f d electrons into a distribution with a pronounced hybridization with the surroundings Si/P atoms. Therefore, one can expect to adjust the properties of these compounds by substitutions on the non-metallic site. This solution has been used to optimize the properties of MnFe(P,Si) materials: (1) The first improvement is related to the control of the hysteresis. (2) The second target is to solve the mechanical stability problem observed in MnFe(P,Si) materials. In these latter, even if the cell volume change at the FOT is limited ($\Delta V \leq$ 0.2%), crossing the transition still frequently leads to a destruction of bulk samples. (3) The last objective is to provide materials having a large MCE in intermediate fields, i.e. reachable by permanent magnets. A strategy to achieve this goal is to involve most of the FOT latent heat into

the MCE. It requires an optimization of the shift of the transition due to the field (dT_C/dB) while keeping the width of the transition limited [2].

1. Nguyen H. Dung et al., *Mixed Magnetism for Refrigeration and Energy Conversion*. Adv. Energ. Mater. 1 (6), 2011 pp. 1215-1219.
2. Guillou F. et al., *Taming the First-Order Transition in Giant Magnetocaloric Materials.* Advanced Materials 26 (17), 2014 pp. 2671–2675.

FM-17 (Invited Talk)
Caloric effects in ferroic materials

Lluís Mañosa

Departament d'Estructura i Constituents de la Matèria. Facultat de Física. Universitat de Barcelona. Catalonia.
Email:lluis@ecm.ub.edu

Many ferroic materials undergo first order phase transitions with an associated large entropy change which confer to these materials giant caloric properties. These giant caloric properties make ferroic materials excellent candidates for environmental friendly solid-state refrigerating devices [1]. Particularly interesting are those materials with strong coupling between degrees of freedom. Their cross-response to external applied fields opens-up the possibility of inducing more than one caloric effect in a single material by the application of diverse external fields (mechanic, magnetic and electric). In my talk I will present examples of magnetocaloric, elastocaloric, barocaloric and electrocaloric effects for a number of illustrative ferroic materials.

1. L. Mañosa, A. Planes and M. Acet, *J. Mater. Chem. A* **1**, 4925 (2013).

FM-18 (Invited Talk)
Emerging Functional properties in Cobalt based Oxides

Chandrima Mitra[1]

[1]*Material Science and Technology Division, Oak Ridge National Laboratory, Oak Ridge, TN, USA*
Email:mhc@ornl.gov

The discovery and design of new materials for next generation energy devices are a crucial step towards addressing various energy-related issues. $ABO_{3-\delta}$ type perovskite oxides have emerged as promising candidates for cathode/electrolyte materials in solid oxide fuel cells (SOFC's). Among them those which crystallize in the orthorhombic brownmillerite-phase ($ABO_{2.5}$) are particularly interesting due to their promising crystal structure which contains ordered channels of oxygen vacancies. In this work we examine the cobalt based brownmillerite oxide $SrCoO_{2.5}$ (BM-SCO). Earlier experiments had demonstrated the improvement of catalytic oxygen reduction kinetics by two orders of magnitude in epitaxial $SrCoO_{2.5}$ films [1]. Furthermore the epitaxial stabilization of $SrCoO_x$ was shown to lower the redox temperature to ~200^{o}C [2]. The goal of this work is to provide a detailed understanding of oxygen transport properties within BM-SCO .In this work we first perform a theoretical investigation of the electronic structure and magnetic ground state properties of $SrCoO_{2.5}$ employing density functional theory [3]. Building on this we then investigate in detail oxygen transport properties within BM-SCO [4]. Employing quantum mechanical simulations a quantitative picture of the exact mechanisms of oxygen diffusion pathways within BM-SCO is provided. Our study finds that the ordered vacancy channels would provide the fastest diffusion pathways for oxygen diffusion with a migration barrier of 0.62 eV. This can be further lowered, by as much as 30%, upon application of epitaxial strain thereby provide a crucial route towards designing of efficient cathode materials for SOFC's.

1. H. Jeen, Z. Bi, W. S. Choi, M. F. Chisholm, C. A. Bridges, M. P. Paranthaman, and H. N. Lee, Adv.

Mater. **25**, 6459–6463 (2013).A.B. Green, C.D. Black, *Book title* (Publisher), 135 (2006).
2. H. Jeen, W. S. Choi, M. D. Biegalski, C. M. Folkman, I. C. Tung, D. D. Fong, J. W. Freeland, D. Shin, H. Ohta, M. F. Chisholm, and H. N. Lee, Nat. Mater. 12, 1057–1063 (2013).
3. C. Mitra, R. S. Fishman, S. Okamoto, H. N. Lee, and F. A. Reboredo, J. Phys.: Condens. Matter **26**, 036004 (2014).
4. C. Mitra, T. Meyer, H.N. Lee and F.A. Reboredo, J. Chem. Phys. **141**, 084710 (2014).

FM-19 (Invited Talk)
Near-Infrared Emitting Nanoparticles for Applications in Biology

Fiorenzo Vetrone

Institut National de la Recherche Scientifique - Énergie, Matériaux et Télécommunications, Université du Québec, Varennes, Québec, CANADA
Email: vetrone@emt.inrs.ca, web site: http://www.inrs.ca/fiorenzo-vetrone OR www.nanocrystalresearch.com

Nanoparticles with emissions in the near-infrared (NIR) are quickly emerging as useful tools in diagnostic and therapeutic medicine. In particular, the usefulness of these nanomaterials for applications in biology stems primarily from the fact that NIR light is silent to tissues thus minimizing autofluorescence, possesses greater tissue penetration capabilities, reduced scattering, and does not cause photodamage to the specimen under investigation. Moreover, tailoring of the nanoparticles' absorption and emission wavelengths allow them to operate within the so-called "biological windows", regions of the spectrum in which tissues are partly transparent.

In this regard, lanthanide (Ln^{3+})-doped nanoparticles (LnNPs) are at the vanguard since they posses multiple absorption and emissions in the three "biological windows" (approximately 750-1000, 1100-1450, and 1500-1700 nm). Thus, it is feasible to excite within one window and observe emission in another window. Moreover, with LnNPs, it is possible to induce multiphoton excited luminescence (known as upconversion) where both the excitation (typically 980 nm) and emission lie within the biological windows. This multiphoton excitation process differs from what occurs in conventional multiphoton excited materials where the absorption of photons is simultaneous. In the case of LnNPs, the multitude of long-lived "real" electronic energy states of the Ln^{3+} ions (from the partially filled 4*f* shell) allow for sequential absorption of multiple NIR photons eliminating the need for complex and expensive optical excitation. Thus, upconverted luminescence can be observed using an inexpensive commercial continuous wave diode laser.

Here, we present the synthesis and surface functionalization of various NIR excited and NIR emitting nanoparticles and demonstrate how they can be used for biological applications. Furthermore, we show how they can be used as the cornerstone in the development of a multifunctional nanoplatform for the potential diagnostics and therapeutics of disease.

FM-20 (Contributed Talk)
Internal Friction and Impact Toughness of Superelastic FeMnAlNi Alloys

V. V. Khovaylo[1], I. S. Golovin[1], A. A. Komissarov[1], M. V. Lyange[1], T. Omori[2], R. Kainuma[2]

[1]National University of Science and Technology "MISiS", Moscow 119049, Russia
Email:khovaylo@misis.ru

[2]Department of Materials Science, Graduate School of Engineering, Tohoku University, Sendai 980-8579, Japan

Recently, it has been found that FeMnAl-based ferrous alloys demonstrate well-defined superelastic properties in a wide temperature range due to stress-induced martesnitic transformation [1]. The uniqueness of these materials is a weak dependence of the superelastic stress on temperature which is thought to originate from a small transformation entropy change. The weak temperature dependence of the superelastic properties is very

beneficial for practical applications. Moreover, a low cost and a high workability of FeMnAlNi imply that these alloys are suitable for the use in large-scale applications.

Superelastic properties of FeMnAlNi have been characterized for the specimens in the form of sheets [1] and wires [2]. Results of these studies have revealed that superelastic response of the FeMnAlNi alloys depends on the relative grain diameter which can be manipulated by thermal treatment conditions. Considering practical applications of these alloys, e.g., as damping materials, it is necessary to evaluate their ability to dissipate/absorb energy of external mechanical loadings. For this aim we studied internal friction and impact toughness of these materials. Samples for the measurements were prepared as described in Ref. [1]. Nominal chemical composition of the samples studied was Fe43.5Mn34Al15Ni7.5 (at.%).

The internal friction was studied by a Dynamic Mechanical Analysis (DMA) instrument at different frequencies of external load and at temperatures up to 473 K. Experimental results obtained for Fe43.5Mn34Al15Ni7.5 samples showed that internal friction in the sample quenched from 1200°C and in the sample subjected to the subsequent aging at 200°C for 6 h is essentially the same. In both the samples, internal friction drastically increases when the applied strain ε exceeds 0.1% (Fig. 1). This increase is due to the stress-induced martensitic transformation. Since such a strain can be attributed to the onset of the stress-induced martensitic transformation [1] it can be suggested that the internal friction shall further increase for larger magnitudes of the applied strain ε. Thus, a very large damping, exceeding that reported in R-phase of a TiNi(Fe) alloy [3] is reasonably to expect in the FeMnAlNi alloys.

Impact toughness of $Fe_{43.5}Mn_{34}Al_{15}Ni_{7.5}$ was studied by an impact testing machine Instron SI-1M over temperatures ranging from –196°C to +80°C. In this experiment, $Fe_{43.5}Mn_{34}Al_{15}Ni_{7.5}$ samples quenched from 1473 K were used. It was found that the impact toughness increases with the increase of temperature. The largest impact toughness, ~27.8 J/cm^2, was observed at T = 80°C. This value is larger than that in representatives of shape memory alloys (e.g., in CuAlBe alloys the largest impact toughness was reported to be ≈15.4 J/cm^2 [4]) and comparable with that observed in some stainless steels [5].

1. T. Omori, K. Ando, M. Okano, X. Xu, Y. Tanaka, I. Ohnuma, R. Kainuma, and K. Ishida, *Science* **333**, 68 (2011).
2. T. Omori, M. Okano, and R. Kainuma, *APL Mat.* **1**, 032103 (2013).
3. G. Fan, Y. Zhou, K. Otsuka, and X. Ren, *Appl. Phys. Lett.* **89**, 161902 (2006).
4. V. H. C. de Albuquerque, T. A. de Melo, R. M. Gomes, S. J. G. de Lima, and J. M. R. S. Tavares, *Mater. Sci. Eng. A* **528**, 459 (2010).
5. C. C. Silva, V. H. C. Albuquerque, C. R. O. Moura, W. M. Aguiar, and J. P. Farias, *J. Mater. Eng. Perform.* **18**, 324 (2009).

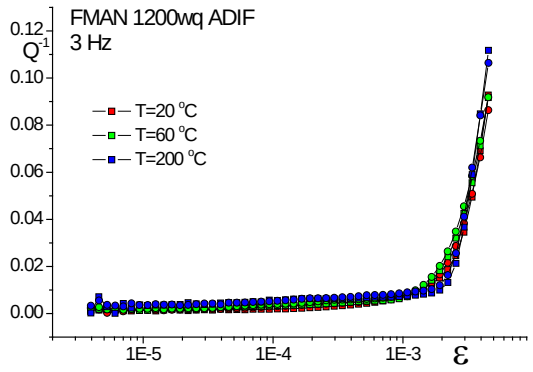

Fig. 1. Internal friction in the Fe43.5Mn34Al15Ni7.5 sample quenched from 1473 K.

FM-21 (Invited Talk)
Perovskite materials for energy related applications

Riad Nechache

Institut Nationale de la Recherche Scientifique, Canada

The perovskites ABO_3, with A and B cations of different valences, are multifunctional materials. Depending on their chemical composition they can behave very differently, showing properties specific to metals, dielectrics, ferroelectrics, ferro(ferri)magnetics or super- and semiconductors. Most of these materials are inorganic, such as well-known ferroelectrics $BiFeO_3$ or Bi_2FeCrO_6 (BFCO). Since the discovery of the bulk photovoltaic (PV) effect in ferroelectrics, there has been a growing interest in perovskite materials for energy related applications, including PV and water splitting. In such materials, the spontaneous polarization-induced electric field promotes the required separation of photo-excited carriers and allows photovoltages higher than their bandgap, which lead to efficiencies that can exceed the maximum possible in a semiconductor p–n junction solar cells. Among these materials, Bi_2FeCrO_6 (BFCO) is highly promising because it exhibits a conversion efficiency of about 8.1% under 1 Sun illumination in thin film form. Other perovskites can be hybrid, if the cation A is replaced with an organic radical. This is the case for halide perovskite compounds (CH3NH3PbX), with X=Br, Cl, I, found recently to possess excellent light absorbing properties in the visible-near infrared spectrum. The use of these materials in solar cells had led to a rapid increased of the photovoltaic conversion efficiency (PCE) in the last year up to about 19 %. The combination of the relatively high PCE with the low cost technologies makes perovskite photovoltaic solar cells very attractive for future development. Here we review recent progress of our group in the exploration of perovskite materials – both thin film and nanostructures – in pursuit of two major research thrusts: Semiconducting perovskite and their energy-related applications. We will present, the controlled growth and characterization of BFCO and $CH3NH3PbI_3$ thin films and nanostructures via pulsed laser deposition and physical vapor transport technique. The optimization of PV properties of such systems and the performance of their related devices will be also discussed.

FM-22 (Invited Talk)
An STM-Guided Search For 2D Organic Ferroelectrics and Co-Crystals

Axel Enders[1]

[1]Department of Physics and Astronomy and Nebraska Center for Materials and Nanoscience, University of Nebraska, Lincoln, NE, USA
Email:aenders2@unl.edu, web site: http://www.physics.unl.edu/enders

I will present a comprehensive study on the self-assembly and electronic properties of the organic ferroelectrics, croconic acid (CA), 3-hydroxyphenalenone (3-HPLN), and the related compound rhodizonic acid (RA) on crystalline coinage metal surfaces. Importantly, the bond polarization of the selected organics is highly planar. This provides the foundation for the development of 2D polarization patterns by design, including rather complex ones like the honeycomb pattern recently discovered by our group [1]. What is remarkable about those honeycomb networks of CA is that the interaction with the substrate determines the ferroelectric switching barriers. The structurally related 3-HPLN forms linear chains on surfaces that are identical to those found in bulk crystals where they exhibit ferroelectric polarization along the chains. On substrate surfaces, the molecular arrangement can, however, be manipulated considerably by the growth conditions. We have identified a variety of structural phases, including a new, chiral phase of hydrogen-bonded trimers of 3-HPLN [2] and a Kagome lattice [3]. This surface-science approach was also key to the first reported synthesis of RA crystalline structures [4].

Here we present an overview over the structural phases of select organic ferroelectrics on surfaces and how ordered 2D polarization states can emerge. Importantly, we discovered by co-deposition of CA and 3-HPLN on Au(111) surfaces that they form ordered 2D co-crystalline phases. The structure of the resulting networks can be tuned by varying the relative concentration of the organics. Namely, for equal ratios of CA and 3-HPLN two polymorphs are observed, while for 2/1 CA/3-HPLN ratio, only a single structure is found (Figure 1). Transitions from CA rich structures to CA poor structures can be induced through weak annealing, where the smaller CA desorbs before the 3-HPLN. Similar discoveries were made for other combinations of organic molecules, such as quinonoid zwitterions with CA. Guided by these findings we were able to crystallize co-crystals in solution, as bulk crystals and micrometer thin films. X-ray diffraction studies indicate that the unit cell in those bulk crystals is identical to the unit cell found on surfaces, and piezo response force microscopy studies have confirmed that these crystals are ferroelectric at room temperature. The significance of this study is therefore in the demonstration that surface science studies, specifically scanning tunneling microscopy (STM), can help accelerate co-crystal discovery.

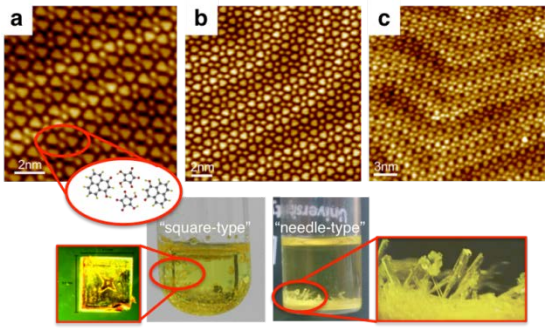

Figure 1: *(a-c) Scanning tunneling microscopy images of 2D co-crystals of croconic acid and 3-HPLN. (a) and (b) have a stoichiometric ratio CA:3-HPLN = 1:1, but are polymorphs of different crystal structure. The network in (c) has a stoichiometric ratio CA:3-HPLN = 2:1 Inset: structure model of the bowtie tetramers in (a). Bottom: photographs of two types of co-crystals (squares and needles) prepared by wet-chemical synthesis.*

1. D. A. Kunkel, et al. Phys. Rev. B **87**, 041402 (2012).
2. J Hooper et al. Surface Science, (2014) DOI: 10.1016/j.susc.2014.04.015.
3 S. Beniwal, et al. Chem. Commun., 2014, 50 (63), 8659 - 8662; DOI:10.1039/c4cc03523b
4. D. A. Kunkel, et al. J. Phys. Chem. Lett. **4**, 3413 (2013).

FM-23 (Invited Talk)
The role of surfaces and interfaces in multifunctional materials

F. Rosei

INRS Centre for Energy, Materials and Telecommunications
Email: rosei@emt.inrs.ca

The bottom–up approach is considered a potential alternative for low cost manufacturing of nanostructured materials [1]. It is based on the concept of self–assembly of nanostructures on a substrate, and is emerging as an alternative paradigm for traditional top down fabrication used in the semiconductor industry. We demonstrate various strategies to control nanostructure assembly (both organic and inorganic) at the nanoscale. Depending on the specific material system under investigation, we developed various approaches, which include, in particular: (i) control of size and luminescence properties of semiconductor nanostructures, synthesized by reactive laser ablation [2]; (ii) we developed new experimental tools and comparison with simulations are presented to gain atomic scale insight into the surface processes that govern nucleation, growth and assembly [3-6]; (iii) we devised new strategies for synthesizing multifunctional materials for electronics and photovoltaics [7-14]; (iv) we developed a nanoscale surface modification which allows to control cell growth [19], including antibacterial effects [20].

[1] F. Rosei, *J. Phys. Cond. Matt.* **16**, S1373 (2004);
[2] D. Riabinina et al., *Phys. Rev. B* **74,** 075334 (2006);

[3] K. Dunn et al., *Phys. Rev. B* **80**, 035330 (2009); [4] F. Ratto et al., *Small* **2**, 401 (2006); [5] F. Ratto et al., *Phys. Rev. Lett.* **96**, 096193 (2006); [6] F. Ratto et al., *Nanotechnology* **19**, 265703 (2008); [7] F. Ratto, F. Rosei, *Mater. Sci. Eng. R* **70**, 243 (2010); [8] O. Moutanabbir et al., *Phys. Rev. B* **85**, 201416 (2012); [9] C. Yan et al., *Adv. Mater.* **22**, 1741 (2010); [10] R. Nechache et al., *Adv. Mater.* **23**, 1724 (2011); [11] R. Nechache et al., *Appl. Phys. Lett.* **98**, 202902 (2011); [12] G. Chen et al., *Chem. Comm.* **48**, 8009 (2012); [13] T. Dembele et al., *J.Power Sources* **233**, 93 (2013); [14] S. Li et al., *Chem. Comm.* **49**, 5856 (2013); [19] F. Vetrone et al., *Nanoletters* **9**, 659 (2009) [20] O. Seddiki et al., submitted.

FM-24 (Invited Talk)
Using Micro-Origami Techniques to Create Functional Materials with Complex Architectures

Leszek Malkinski, Rahmatollah Eskandari

Department of Physics and the Advanced Materials Research Institute, University of New Orleans, New Orleans, Louisiana, USA
Email: lmalkins@uno.edu

Micro-origami technique is a convenient tool for self-assembly of multifunctional composites to form complex three-dimensional architectures. This technology takes advantage of residual stresses in the thin film patterns which cause them to bend, fold, twist or self-roll when released from a substrate by selective removal of a sacrificial underlayer. These free-standing structures gain new functions. They can be used as sensors or actuators in Micro-Electro-Mechanical Systems (MEMs) and microfluidic systems or create metamaterials with interesting responses to electromagnetic radiation.

In our initial studies, several bi-layered and tri-layered polycrystalline systems were grown on top of 50 nm thick Cu sacrificial layer [1-3]. Rectangular patterns of Au/Fe, Co/Al, Ni/Ti, Au/Ni/Ti, Au/FeGa/Ti and FeCo/AlN self-rolled and formed multiwall tubes with 3 to 4 turns. For the patterns with the thickness of the layers ranging from 30 to 60 nm diameters of the microtubes were from 1 to 10 μm. An example of magnetic microtubes of Au/FeGa/Ti is presented in Fig 1. Magnetic properties and microwave absorption of the microtubes depend on the diameter of the tubes. Correlation between the shape and static magnetic properties is presented in Fig 1c. The hysteresis loops are affected by both the magnetic shape anisotropy and by the stresses in the bent magnetostrictive film. Oxidation of Ti layer produced additional stresses due to expansion of Ti-oxide which resulted in 50% reduction of diameter of the tubes (blue triangles in Fig 3c).

In order to reduce the radius of the mirco-origami patterns to sub-micrometer or nanometer range it is necessary to grow ultrathin and atomically smooth films and use lattice mismatch between dissimilar layers. This requires epitaxial growth of layers of various materials including the sacrificial layer. We have recently proposed to use single crystalline Zn films as a sacrificial layer for the films of Co, Ru, Ti and other elements and compounds with hexagonal lattice constants. Zn films were grown by electron beam evaporation on sapphire substrates with Ru or Ti buffer layers. Sacrificial layer of Zn was removed in vacuum chamber via sublimation by heating the sample stage to 200°C. Single crystal films of NaCl were deposited by e-beam evaporation on MgO substrates at 350°C to serve as sacrificial layers for Fe, Cr, Au, Ag and other cubic crystals. NaCl layer can be dissolved by water or water vapor. The advantage of the new sacrificial layers of Zn and NaCl is that they are both biocompatible and eco-friendly and can be used in biotechnological and medical applications.

The current work is funded by the NSF EPSCoR LA-SiGMA project under award #EPS-1003897

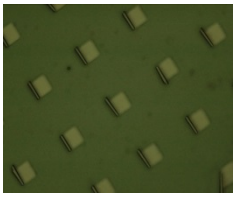
(a)

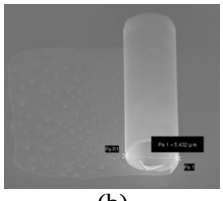
(b)

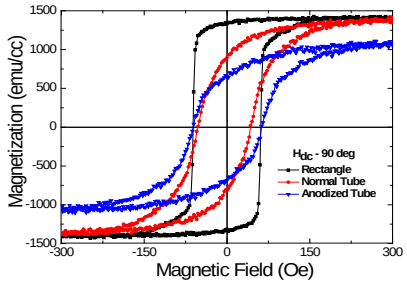

(c)

Fig. 1. (a) Optical microscope image of an array of Au/FeGa/Ti microtubes. (b) Scanning electron microscope image of the individual scroll. (c) A comparison of hysteresis curves of the FeGa film before rolling (black squares), after formation of microtubes (red circles) and after oxidation of Ti film (blue triangles).

References

1. S. Min, J.H, Lim, J. Gaffney, K. Kinttle, J. B. Wiley and L. Malkinski, *J. Appl. Phys.*,111, 07E518 (2012)
2. S.-G. Min., J. Gaffney, R. Eskandari, J. Tripathy, J.-H. Lim, J. B. Wiley and L. Malkinski, *Magnetics Letters,* 3, 4000304 (2012)
3. L. Malkinski, "Magnetics with a twist", *Magnetics Technology International Magazine,* pp 8-14 (2013)

FM-25 (Invited Talk)
Controlling electrons through a single atom one at a time

Giuseppe C. Tettamanzi, Joost van der Heijden, and Sven Rogge

School of Physics and Australian Centre of Excellence for Quantum Computation and Communication Technology,
The University of New South Wales, Sydney, Australia.
Email: g.tettamanzi@unsw.edu.au, web site: https://research.unsw.edu.au/people/dr-giuseppe-carlo-tettamanzi

The main task of the electrical branch of quantum metrology is the development of reliable quantized electron pumps (QEPs) [1,2] and, as a consequence, the full implementation of the quantum metrology triangle [1-2]. The QEP approach to metrology was introduced in the early 1990s [3] and, since then, many interesting schemes have been proposed, i.e. see the examples discussed in references 1 and 2. The strong focus on QEP-based metrology is justified by its ability to generate currents in which capture and emission processes can be controlled at the single electron level [1-3]. This can be obtained by taking advantage of Coulomb blockade (CB) effects [1-3] as QEPs are often single electron transistor (SET) based [1-3]. Recently, a new kind of quantised charge pumping has been demonstrated (see G. C. Tettamanzi et al, 2014 New J. Phys., 16 063036) by using a single dopant atom quantised electrons pump (SDA-QEP). The characteristics of the SDA-QEP were found to be quite different from the more conventional quantum dot charge pumps (QD-QEPs) [2]. This difference originates from the intrinsic dissimilarity in the confinement potential that traps the electrons during the pumping cycle and results in a lower non-adiabatic excitation error rate for the SDA-QEP [1]. In my talk, I will discuss how the experimentally determined performance of the SDA-QEP can be compared to a new model that describes the behavior in terms of frequency, power and the position of the dopant in the channel.

ACKNOWLEDGMENT

The devices used in this work have been designed and fabricated in the AFSiD Project, see http://www.afsid.eu. G. C. Tettamanzi acknowledges financial support from the ARC-Discovery Early Career Research Award (ARC-DECRA) scheme, project title: Single Atom Based Quantum Metrology and ID: DE120100702 and from the UNSW under the GOLDSTAR Award 2013 scheme. SR acknowledges the ARC FT scheme, project ID: FT100100589.

REFERENCES

1. Tettamanzi, G. C. and Wacquez R. and Rogge S., New J. Phys. 2014, 16, 063036.

2. Rossi A. and Tanttu T. and Tan K. Y. and Iisakka I. and Zhao R. and Chan K. W. and Tettamanzi G. C. and Rogge S. and Dzurak A. S. and Mottonen M., *Nano Letters* 2014, 14, 3405.

3. Pothier H et al 1992 Europhys. Lett., 17 249.

FM-26 (Invited Talk)
From "smart" Material to "smart" Devices: Novel Applications based on the Insulator-to-Metal Transition in VO_2

Ali Hendaoui[1], Nicolas Émond[1], Mohamed Chaker[1]

[1] INRS-Énergie, Matériaux et Télécommunications, 1650 Boulevard Lionel Boulet, Varennes, Québec J3X 1S2, Canada
Email: hendaoui@emt.inrs.ca

Vanadium dioxide (VO_2) is a particularly interesting "smart" material because of its first-order reversible insulator-to-metal transition (IMT) that occurs near room temperature ($T_{IMT} \approx$ 68 °C) on ultrafast timescales ($<10^{-12}$ s). This IMT is associated with a structural transition from a low-temperature (insulator) monoclinic phase to a high-temperature (metallic) tetragonal phase, and is characterized by a sharp change of the electrical resistivity together with a dramatic modification of the infrared and terahertz (THz) optical properties. The IMT can be triggered electrically, optically, or thermally. Furthermore, it is possible to shift the VO_2 IMT temperature and/or tailor the transition over a wide range of temperatures by doping with donors and/or acceptors of appropriate concentration. Therefore, VO_2 is an excellent candidate for future electronic and optical switching devices. The "smart" exploitation of this material for advanced applications requires a thorough understanding of the IMT mechanisms, including the relationship between the microstructure and the IMT characteristics. This full understanding would pave the way to the exploration of new application opportunities of the IMT of VO_2 thin films.

In this perspective, our group has conducted several studies aimed to optimize the characteristics of VO_2 thin films in view of developing new technological applications of this material. For example, we demonstrated that doping VO_2 with a mixture of tungsten and titanium remarkably influences both optical and resistivity characteristics of the IMT, which can be exploited for applications in uncooled infrared and THz bolometers. More recently, we developed VO_2-based multilayer smart coatings that are able to respond to the temperature by adapting their thermal emittance to radiate more heat at high temperature and less at low temperature. This behavior is quite interesting for a number of applications such as smart radiator devices (SRDs) for an energy-efficient light-weight thermal control of spacecrafts. By adapting the thickness of a SiO_2 layer being part of this multilayer structure, we were able to achieve an unprecedented temperature-dependent emittance variation at wavelengths ranging from 3 to 5 µm, known as Mid-Wave Infrared (MWIR) range. This variation offers the possibility to dramatically modify the so-called IR signature of the coating. In the present talk, we will present an overview of our recent investigations on controlling the IMT features of VO_2 thin films towards the development of "smart" devices.

FM-27 (Invited Talk)
Nanostructured magneto-plasmonic metamaterials: a promising route for label-free molecular sensing applications

P. Vavassori[1,2], N. Maccaferri[1], K. Gregorczyk[1], T. V. A. G. De Oliveira[1], Mato Knez[1,2], Z. Pirzadeh[3], A. Dmitriev[3], M. Kataja[4], S. Van Dijken[4], and J. Akerman[5]

[1] CIC Nanogune, San Sebastian, Spain

[2] Ikerbasque, Basque Foundation for Science, Bilbao, Spain

[3] Applied Physics, Chalmers University of Technology, Göteborg, Sweden

[4] Applied Physics, Aalto University, Espoo, Finland

[5] *Materials Physics, Royal Institute of Technology, Kista, Sweden*

Magneto-plasmonics materials combine magnetic and plasmonic functionalities and are an emerging field of intense research as they would allow the design of a new class of magnetically controllable optical nano-devices. Magneto-plasmonics studies have mainly focused on hybrid multilayered nanoantennas consisting of noble metals and ferromagnetic materials. Plasmon properties of pure ferromagnetic nanoantennas are a widely unexplored terrain, although they offer the advantage of stronger magnetic polarization and less demanding fabrication. Here we explore the opportunities arising from direct excitation of localized surface plasmon resonances (LSPRs) in metasurfaces based on purely ferromagnetic nanoantennas due to the intertwined optical and magneto-optical properties. [1]

We then investigate the spectral magneto-optical (MO) response of such nanoantennas using different Kerr effect configurations. [2-5] We extended present theoretical models based on generalized ellipsoidal nanoparticles in order to account for both plasmonic and MO effects. [4,5] Guided by these experimental findings and the results of our modeling efforts, we combine the excitation of LSPRs together with polarizability anisotropy to tune the phase difference between the optical and MO induced polarizabilities beyond what is offered by constituent material intrinsic properties and to manipulate the reflected light's polarization. [3,6]

Such magneto-plasmonic nanoantennas could be a building block for future biotechnological and optoelectronic applications. In particular, systems allowing label-free molecular detection are expected to have enormous impact on biochemical and biomedical research, and are therefore subject to intense investigation. We show that magneto-plasmonic nanoantenna based metasurfaces allow for unprecedented sensitive label-free detection, clearly outperforming recently reported plasmon based sensors. Such extreme sensitivity was achieved exploiting the above mentioned light phase control offered by magnetoplasmonic nanoantenna-based metasurfaces. In detail, we demonstrate a manifold improvement of refractometric sensing figure-of-merit performance. [7] Most remarkably, we achieved a local surface sensitivity of two orders of magnitude higher than the best values reported for surface plasmon resonances based sensors. Such sensitivity corresponds to a mass of ~0.8 ag/nanoantenna of polyamide-6.6 (n=1.51).

1. J. Chen et al., *Small* **7**, 2341 (2011)
2. V. Bonanni et al., *Nano Lett.* **11**, 5333 (2011)
3. N. Maccaferri et al., *Phys. Rev. Lett.* **111**, 5333 (2013)
4. N. Maccaferri et al., *Opt. Express* **21**, 9875 (2013)
5. N. Maccaferri et al., *Physica Status Solidi A* **211**, 1067 (2014)
6. K. Lodewijks et al., submitted to *Nat. Comm.*
7. N. Maccaferri et al., submitted to *Nature Nanotech*.

FM-28 (Contributed Talk)
Europium Tetrakis Dibenzoylmethide Triethylammonium: A Bright Functional Material for Smart Sensors

Ross Fontenot[1*], Kamala Bhat[2], William Hollerman[1], and Mohan Aggarwal[2]

[1]*Physics Department, University of Louisiana at Lafayette, Lafayette, LA, USA*
[*]*Email:rsfontenot@hotmail.com*

[2]*Department of Physics, Chemistry and Mathematics, Alabama A&M University, Normal, AL, USA*

Since 2003, the authors have been pushing the boundaries on a special type of functional material, i.e., a material that gives off light when it is stressed, strained, and/or fractured [1]. This unique class of materials have been proposed for the active element of impact sensors, earthquake detectors, and stress sensors [2]. While there are a number of techniques currently being used for damage detection and monitoring of civil, aerospace, and military structures and aircraft, they do not provide in-situ and distributed sensing. Wiedemann and Schmidt defined triboluminescence (TL) as the emission of light produced by the fracturing of materials [3]. In recent years, triboluminescent materials have

been proposed for use as the active element in smart structural sensors. To sense damage, these materials would be embedded into the structure [4,5]. If damage occurs to this structure, the embedded triboluminescent material would give off visible light. This light could be transferred by lightweight fiber optics or wireless detector to a computer-based detection system to warn occupants in real time that a significant impact event has occurred. In addition, the triboluminescent based sensor could allow for real-time monitoring of both the magnitude and location of damage with influence to the host structure. However, in order for this concept to go from the lab to real world applications, the light emission from these functional materials must be bright so that inexpensive light detectors can be used. One of the brightest materials found thus far is europium tetrakis dibenzoylmethide triethylammonium (EuD_4TEA) [6]. This material has a luminescent emission so bright that it can be observed in daylight. In 2014, the authors discovered that the addition of dibutyl phosphate (DBP) produces a six fold increase on the triboluminescence of EuD_4TEA. This talk will provide an overview on the synthesis and characteristics of EuD_4TEA.

[1] R.S. Fontenot, K.N. Bhat, W.A. Hollerman, M.D. Aggarwal, in:, M.S.A. Moustafa (Ed.), Eur. Synth. Charact. Potential Appl., 1st ed., Nova Science Publishers Inc., 2013, pp. 85–160.

[2] D.O. Olawale, T. Dickens, W.G. Sullivan, O.I. Okoli, J.O. Sobanjo, B. Wang, J. Lumin. 131 (2011) 1407–1418.

[3] A.J. Walton, Adv. Phys. 26 (1977) 887–948.

[4] I.C. Sage, R. Badcock, L. Humberstone, N.J. Geddes, M. Kemp, G. Bourhill, Smart Mater. Struct. 8 (1999) 504.

[5] I.C. Sage, G. Bourhill, J. Mater. Chem. 11 (2001) 231–245.

[6] R.S. Fontenot, K.N. Bhat, W.A. Hollerman, M.D. Aggarwal, Mater. Today 14 (2011) 292–293.

Session SS

SMART SENSOR MATERIALS AND TECHNOLOGIES

SS-01 (Invited Talk)
About Processes and Performance of Integrated Gas Sensor Components

Lado Filipovic, Siegfried Selberherr

Institute for Microelectronics, Technische Universität Wien, Gußhausstraße 27-29/E360 Wien, Austria
Email: filipovic|selberherr@iue.tuwien.ac.at, web site: http://www.iue.tuwien.ac.at

The integration of gas sensor components into smart phones, tablets, and wrist watches will revolutionize the environmental health and safety industry by providing individuals the ability to detect harmful chemicals and pollutants in the environment using always-on hand-held devices. However, in order for this goal to be achieved the fabrication of gas sensors and, more precisely, the deposition of gas sensing metal-oxide materials, must be performed using a cost-effective technique which is integrable in the full CMOS sequence [1]. A sensor array requires a combination of MEMS and CMOS analog and digital circuitry in order to generate a useful product, as shown in Fig. 1.

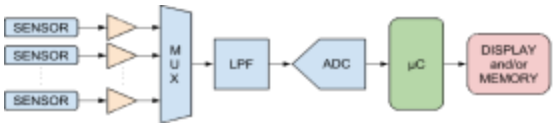

Fig. 1: Sensor array with interface electronics blocks

Spray pyrolysis has proven to be an inexpensive technique which can be used to deposit the metal oxide sensing material at the backend of a CMOS process. A model for the spray pyrolysis deposition of tin oxide (SnO_2) has been developed and is described by the Arrhenius expression $d(t,T)=A\cdot t\cdot e^{-E/k_bT}$, where A=3.1µm/s, E=0.427eV, k_b is the Boltzmann constant, and T is the temperature in Kelvin. The growth of the metal oxide grains is characterized by the Volmer-Weber growth model [2], which can lead to residual stress development due to the interaction between the expanding grains. The grain growth after thin film deposition at 400ºC has been simulated, resulting in a residual stress of approximately 30MPa at a 50nm thickness. The stress distribution along the grains is shown in Fig. 2(a) while Fig. 2(b) shows the stress development during film growth. After coalescence, the minimum residual stress reached is about 15.5MPa.

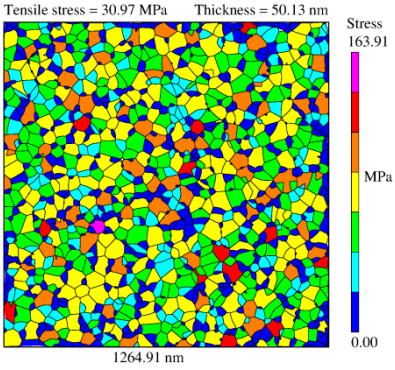

(a)

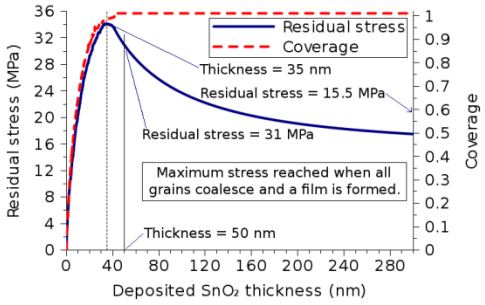

(b)

Fig. 2: (a) Stress distribution along the grains of a deposited tin oxide layer with a 50nm thickness. 1000 grains were used for the simulation.
(b) Average residual stress development during the growth of the tin oxide thin film.

After cooling the device to room temperature following deposition, the SnO_2 experiences further stress due to a difference in the coefficients of thermal expansion between SnO_2 ($4\cdot10^{-6}K^{-1}$) and the oxide ($0.5\cdot10^{-6}K^{-1}$). The final stress at room temperature for a 50nm thick SnO_2 film with 100µm×5µm dimensions is 500MPa.

The sensor operates at temperatures between 150°C and 400°C by oxygen being

adsorbed at the SnO_2 surface. After exposure to a target gas, the resistivity of the metal oxide is reduced by an amount which depends on the temperature and concentration of the target gas in the atmosphere. A relationship which relates the H_2 concentration (C_{H2} in ppm), a gas used for fire and smoke detection, to the SnO_2 resistance is described by the expression $R_{norm}=R_0-m\cdot ln(C_{H2})$, where R_0 and m are geometry-dependent variables in Ω.

1. M. Ortel et al., *Solid-State Electronics* **86**, 22 (2013).
2. J. Boltz, *Sputtered tin oxide and titanium oxide thin films as alternative transparent conductive oxides*. PhD diss. (2011).

SS-02 (Invited Talk)
Effect of Magnetic Field in Organic Semiconductor Devices

Tho Nguyen

Physics and Astronomy Department, University of Georgia, Athens, Georgia, USA
Email:ngtho@uga.edu, web site: https://www.physast.uga.edu/research/nguyen/

Organic semiconductors have been used as active layer in devices such as organic light-emitting diodes (OLEDs), photovoltaic cells, field-effect transistors. Recently there has been a growing interest in spin and the effect of magnetic field in OSEC devices. These include OLEDs, where substantive magneto-electroluminescence and magneto-resistance (OMAR) were obtained;[1] organic spin valves (OSV) where spin injection, transport and detection of holes were demonstrated; this leads to the so-called giant magneto-resistance (GMR) in OSVs;[2] and bipolar OSVs or spin-OLEDs,[3] where spin aligned holes and electrons are simultaneously injected into organic spacer causing electroluminescence, whose intensity depends on the relative spin polarization direction of the carriers. The interest in spin transport in organic semiconductors has been motivated by the weak spin-orbit interaction (SOC) that is caused by the light-weight building block elements such as carbon and hydrogen, and the relatively small hyperfine interaction (HFI) of the π-electrons with the adjacent nucleus. In this talk the status of the young field of 'Organic Spintronics' will be reviewed. The necessary ingredients needed for the success of this field will be summarized and evaluated by recent experiments. In particular the role of the HFI in magneto-transport will be elucidated via the isotope effect.[3,4]

1 Mermer, Ö. *et al.* Large magnetoresistance in nonmagnetic π-conjugated semiconductor thin film devices. *Physical Review B* **72**, 205202-205213 (2005).
2 Xiong, Z. H., Wu, D., Vardeny, Z. V. & Shi, J. Giant magnetoresistance in organic spin-valves. *Nature* **427**, 821-824 (2004).
3 Nguyen, T. D., Ehrenfreund, E. & Vardeny, Z. V. Spin-Polarized Light-Emitting Diode Based on an Organic Bipolar Spin Valve. *Science* **337**, 204-209 (2012).
4 Nguyen, T. D. *et al.* Isotope effect in spin response of [pi]-conjugated polymer films and devices. *Nat Mater* **9**, 345-352 (2010).

SS-03 (Invited Talk)
Design and Fabrication of Magnetic Tips for High Resolution Magnetic Force Microscopy

Masaaki Futamoto, Mitsuru Ohtake

Faculty of Science and Engineering, Chuo University, Bunkyo-ku, Tokyo, Japan
Email:futamoto@elect.chuo-u.ac.jp, web site: http://www.elect.chuo-u.ac.jp/futamoto/

Magnetic force microscopy (MFM) has been used in the investigations of magnetization structure of various magnetic devices such as magnetic recording media, magnetic heads, permanent magnets, etc. Magnetic sensor tip, which detects the magnetic interaction between the tip and a magnetic sample, is the key component. There are several requirements for the sensor tip; high spatial resolution, high sensitivity, high magnetic switching field, mechanical durability, corrosion resistance, etc. Figure 1 shows the trend of MFM spatial resolution through improvements of sensor tips [1]. It is currently becoming possible to observe

the magnetization structures with resolutions below 10 nm. The present paper briefly discusses the design and fabrication of magnetic tips for high-resolution magnetic force microscopy.

MFM sensor tips are prepared by coating magnetic materials on nonmagnetic sharp tips typically made of silicon or silicon nitride. Various magnetic materials including elemental and alloy materials (Fe, Co, Ni, Ni-Fe, Co-Fe, Fe-B, Co-Pt-Cr), ordered structure materials ($L1_0$-FePd, $L1_0$-FePt, $L1_1$-CoPt), multilayers (Co/Pt, Co/Pd, Co/Ni), and soft/hard hybrid magnetic layers (Fe/$L1_1$-CoPt) are applied as the coating magnetic materials on nonmagnetic Si tips with 3 – 5 nm in radius by changing the layer thickness in a range 10 – 200 nm. The spatial resolution and the switching field have been systematically investigated [2]. Higher resolution is realized by employing a magnetic material of higher magnetic moment and by optimizing the coating thickness, whereas higher switching field is related with a coating material of high magnetic anisotropy. A very high spatial resolution below 7 nm and a high magnetic switching filed greater than 1 kOe are realized. Figure 2 shows the structure and a transmission electron micrograph of MFM tip. A very small volume of magnetic material (1000 – 5000 nm^3) around the top part of MFM tip plays an important role in the detection of magnetic flux emanating from a sample surface. The mechanical strength and the corrosion resistance of MFM tip need to be enhanced for practical MFM applications, since the magnetic material is generally softer than the base material of Si or silicon nitride and easily deforms and oxidizes when used and/or kept in a normal condition. These properties are, however, improved by coating a thin protective layer (2 nm) on the magnetic material [3]. Such improvements of MFM performance pave ways toward easier and more accurate magnetization structure observation of various magnetic devices with very high spatial resolution. Examples of high-resolution MFM observation will be shown at the conference.

1. M. Futamoto, T. Hagami, S. Ishihara, K. Soneta, M. Ohtake, *IEEE Trans. Magn.*, **49**, 2748 (2013).
2. M. Futamoto, M. Ohtake, *Abst. IC-MAST 2014* (Bilbao, June 2014). (to appear in *Key Eng. Mater.*).
3. K. Kato, M. Ohtake, M. Futamoto, N. Inaba, F. Kirino, *Ann. Conf. Mag. Soc. Japan.*, 4pA-8 (Sept. 2014).

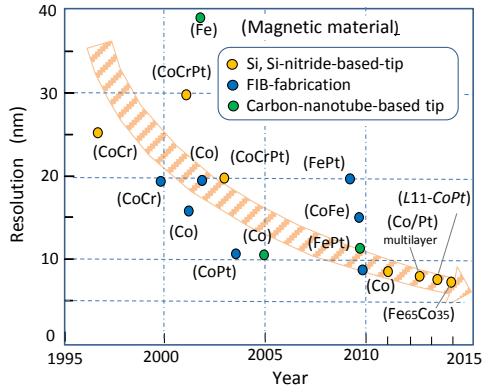

Fig. 1: Improvement of MFM spatial resolution

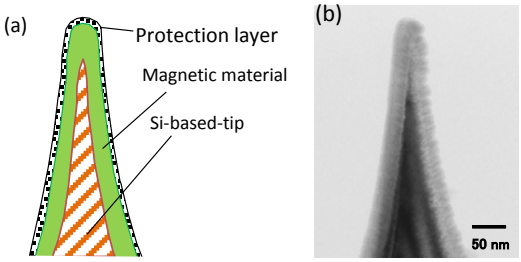

Fig. 2: Cross-sectional structure of practical MFM sensor tip with mechanical strength and corrosion resistance (a). Transmission electron micrograph of MFM tip prepared by coating 20 nm thick magnetic material on sharp Si-based nonmagnetic tip (b).

SS-04 (Invited Talk)
Laser Spectroscopic Techniques for Remote Probing of Trace Species

Dennis K. Killinger

Department of Physics, University of South Florida, Tampa, FL 33620
Email: killinge@usf.edu, web site: http://physics.usf.edu/faculty/dkillinger/

Lasers spectroscopic techniques can be used for remote probing and detection of trace species in the environment and in complex media. There are a multitude of different spectroscopic techniques including differential absorption, fluorescence, Raman, breakdown emission, and thermal emission which can be used under selected conditions. Some examples of several of these techniques will be shown including tunable laser detection of global CO2 using differential absorption lidar, laser induced fluorescence of trace species in drinking water, laser induced breakdown spectroscopy of distant species, and mapping of water vapor blobs in the atmosphere.[1] Their common laser spectroscopy requirements and common S/N detection limits will be briefly covered. Of importance is the role that background interferences play in defining the minimum concentration of the trace species that can be detected, and the importance that differential spectroscopic techniques such as laser tuning and multiple spectral samples play. As an example, Fig. 1 shows the techniques of multiple laser wavelengths used for discrimination for remote differential-absorption lidar detection of a selected trace gas in the atmosphere while still having large numbers of nearby spectral lines from other background gases. Some of the spectroscopic techniques to improve the detection S/N will be covered.

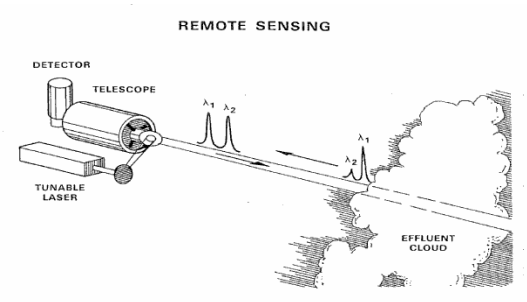

Fig. 1: Schematic of laser spectroscopic sensing of distant trace species showing need for multi-wavelength laser pulses or tunable laser spectroscopy for enhanced S/N detection.

1. D. K. Killinger, *Laser Spectroscopy for Sensing* (Woodhead Publishing), 292 (2014)

SS-05 (Invited Talk)
Sensing RF and microwave energy with fiber Bragg grating heating via soft ferromagnetic glass-coated microwires

Philip Colosimo[1], A. Chen[1], J. Devkota[2], H. Srikanth[2], M. H. Phan[2]

[1]Applied Physics Laboratory, University of Washington, Seattle, Washington, USA
Email:philip.colosimo@gmail.com, web site: http://www.apl.washington.edu/people/profile.php?last_name=Colosimo&first_name=Philip

[2]Department of Physics, University of South Florida, Tampa, Florida, USA

Results from a fiber Bragg grating-based microwave energy sensor are presented. The sensor relies on a soft ferromagnetic glass-coated microwire that is bonded to the cladding of the grating. The microwire absorbs microwave energy and heats up thus raising the temperature of the fiber Bragg grating. Compared to a similar sensor that uses gold to absorb electromagnetic radiation, the microwire yields a sensor with greater sensitivity (~10 times at f = 3.25 GHz) relative to the perturbation of the microwave field. With the sensor reported here, the best sensitivity to electromagnetic radiation corresponds to AC electric fields that have an average electric energy density of approximately 1.3 μJ/m^3 [1].

1. P. Colosimo and A. Chen, J. Devkota, H. Srikanth, and M.H. Phan, *Sensors and Actuators A: Physical* 210, 25 (2014)

SS-06 (Invited Talk)

Rapidly Quenched Amorphous and Nanocrystalline Bilayer Ribbons for Energy and Sensor Applications

Ivan Škorvánek[1], Jozef Marcin[1], Marek Varga[1], Igor Maťko[2], Peter Švec[2]

[1]Institute of Experimental Physics, Slovak Academy of Sciences, Watsonova 47, 04001 Košice, Slovakia Email: skorvi@saske.sk

[2] Institute of Physics, Slovak Academy of Sciences, Dúbravská cesta 7, 842 28 Bratislava, Slovakia

Bilayer ribbons consisting of different magnetic phases are subject of continuing interest both to physicists and technologists, who may wish to exploit them in specific applications. In order to optimize the magnetic performance of these systems it is important to deepen knowledge about the influence of composition and processing techniques that can be used to tailor their properties. One possible technique, often employed for this purpose in a variety of soft magnetic materials, is thermal treatment under presence of external magnetic field.

This work deals with the study of the influence of longitudinal (LF) or transversal (TF) magnetic field annealing on the magnetic properties and magnetoimpedance of rapidly solidified ribbons in the form of monolayers and bilayers. Bilayer ribbons have been prepared by planar flow casting from a single crucible with two nozzles close to each other and with a partition between them forming two separate vessels. Such an arrangement allowed us to obtain ribbons with two homogeneous amorphous layers, one on top of the other, along the ribbon length with a high quality surface and with a contact interlayer having submicron thickness. The composition of the individual layers was chosen from the Fe-Co-Si-B, Fe-Cu-Nb-Si-B, Fe-Ni-Nb-B and Fe-Co-Nb-B alloy systems, respectively. Depending on the subsequent heat treatment, it was possible to transform selected layers or entire bilayers to the (nano)crystalline state.

A special attention was devoted to amorphous/nanocrystalline bilayers composed of ferromagnetic layers with different magnetic and magnetoelastic properties. An example of such system is $Fe_{40.5}Co_{40.5}Nb_7B_{12}/Co_{72.5}Si_{12.5}B_{15}$ composite where, the nanocrystalline $Fe_{40.5}Co_{40.5}Nb_7B_{12}$ layer with the high Curie temperature shows strong response to field annealing while the amorphous $Co_{72.5}Si_{12.5}B_{15}$ layer with the low Curie temperature is only weakly affected by thermal processing in magnetic field. We have shown that besides the effects of field-annealing, the magnetic reversal process in such bilayers is strongly influenced by interlayer stresses, which are induced in material due to different thermal expansion of two mechanically solid connected individual layers with positive and negative magnetostriction coefficients.

The heat treatment in longitudinal or transverse magnetic field was found to be a very powerful tool for tuning of domain structure and GMI characteristics in selected amorphous and nanocrystalline FINEMET-type and $(Fe_{0.5}Ni_{0.5})_{78}Nb_7B_{15}$ bilayer ribbons. The bilayers provide higher magnetoimpedance ratio values, which can be explained by the increased ratio of the thickness to the penetration depth as compared to their thinner monolayer counterparts. The observed sensitivity of the GMI response in bilayer ribbons to field annealing can be used for tailoring their sensor characteristics for potential applications.

Acknowledgement - This work has been supported by the project MNT-ERA.NET II STREAM. It was also supported by the Slovak Agency for the Research and Development (projects APVV-0492-11 and APVV-0266-10).

SS-07 (Invited Talk)
Triboluminescent Materials: Uses in Smart Sensors and Technology

William Hollerman and Ross Fontenot

Department of Physics, University of Louisiana at Lafayette, Lafayette, LA, USA
Email:hollerman@louisiana.edu

There are a number of techniques currently being used for damage detection and monitoring [1]. However, the major drawbacks of the current techniques are that they do not provide in-situ and distributed sensing. Wiedemann and Schmidt defined triboluminescence (TL) as the emission of light produced by the breaking of a material [2]. In recent years, triboluminescent materials have been proposed for use as the active element in smart structural sensors [3,4]. To sense damage, these materials would be embedded into the structure. If damage occurs to this structure, the embedded triboluminescent material would give off visible light. This light could be transferred by fiber optics or by wireless to a computer-based detection system to warn occupants in real time that a significant impact event has occurred. In addition, the triboluminescent-based sensor could allow for real-time monitoring of both the magnitude and location of damage with influence to the host structure. However, for this sensor to become reality, the triboluminescent emission must be bright so that inexpensive light detectors can be used. To date, there are only a handful of materials capable of meeting the criteria. The relative triboluminescent emission yield ratios for a variety of tested materials are shown Table 1 [5]. This presentation will provide an overview of triboluminescence and new potential applications for this class of materials.

Table 1. Comparison of the triboluminescent yields for a selection of materials [5].

Base Material and Dopant	Mass (g)	Lot	Manufacturer	Grain Size (μm)	Yield Ratio*
ZnS:Mn	1	1	CINT†	0.005	0.000
	1.0/0.1	15248	Phosphor Technology, Limited of Great Britain	7.5	1.000/1.000
	1	17112		8.5	1.223
		19252		8.5	1.092
		20223		10.5	1.107
		20056		11.5	0.004
		20054		16.2	0.127
		09029		19.8	1.766
		20131		24.1	1.023
		19275		30.0	0.982
ZnS:Cu		19017		2.0	0.005
		14159		9.0	0.056
		19018		30.0	0.019
ZnS:Mn,Cu		19010		21.9	1.130
		19010		22.0	1.519
		20267			1.585
		20268			1.337
		20269			1.038
		20270			1.496
ZnS:Cu,Pb		15027		19.0	0.034
ZnS:Cu,Pb,Mn		17002		19.3	1.017
MgF_2:Mn		09147			0.029
La_2O_2S:Eu		10185			0.004
Y_2O_2S:Eu		19145			0.000
EuD_4TEA	0.1	None	SNL‡		0.960
		3	Alabama A&M University of Huntsville, Alabama		2.063
EuD_4TEA + 1.25 mL DMMP		10			3.196
EuD_4TEA + 4 mol % Uranyl Acetate		75			1.796

* Ratio based on the TL light yield for both the 1 g and 0.1 g samples of 7.5 μm ZnS:Mn set equal to 1.000.
† The Center for Integrated Nanotechnologies (CINT) is located in Albuquerque, New Mexico USA.
‡ The Sandia National Laboratories (SNL) branch is located in Livermore, California USA.

[1] D.O. Olawale, T. Dickens, W.G. Sullivan, O.I. Okoli, J.O. Sobanjo, B. Wang, J. Lumin. 131 (2011) 1407–1418.

[2] A.J. Walton, Adv. Phys. 26 (1977) 887–948.

[3] I.C. Sage, R. Badcock, L. Humberstone, N.J. Geddes, M. Kemp, G. Bourhill, Smart Mater. Struct. 8 (1999) 504.

[4] I.C. Sage, G. Bourhill, J. Mater. Chem. 11 (2001) 231–245.

[5] W.A. Hollerman et al., Opt. Mat. 34, 9 (2012) 1517-1521.

SS-08 (Invited Talk)
Development of highly sensitive magneto-impedance sensor and its Application to P300 brainwaves measurement

Tsuyoshi Uchiyama[1], Shinsuke Nakayama[2]

[1]*Department of Electrical Engineering and Computer Science, Graduate school of Engineering, Nagoya University, Nagoya, Aichi, Japan*
Email:*tutiyama@nuee.nagoya-u.ac.jp*

[2] *Department of Cell Physiology, Graduate school of Medicine, Nagoya University, Nagoya, Aichi, Japan*
Email: *h44673a@cc.nagoya-u.ac.jp*

The tension-annealed amorphous wires with a circular domain structure show large impedance change due to applying external magnetic field. The micro magnetic sensors referred to as “MI sensor” based on the magneto-impedance effect in amorphous wires have been used for electric compass. [1] The magnetization dynamics due to pulse excitation in such amorphous wire is limited by the magnetization rotation in the surface layer. We have constituted highly sensitive linear micro magnetic-field sensors due to Off-diagonal Magneto-Impedance effect. [2] Use of pick-up coil has an advantage to realize of high performance linear magnetic field sensor. [3] Recently we have succeeded in producing pico-Tesla (10^{-8}Oe) resolution MI sensors, utilizing ultra-low intrinsic magnetic noise of amorphous wire. The pico-Tesla MI sensor would be useful especially for bio-magnetic

measurements without any magnetic shielding at room temperature.

Detecting and analysing biosignals of the human brain could be beneficial for us to figure out the brain construction and operational function. The application of brain signals detection also was developed in various fields. In medicine area, it could be implemented in such as brain injury inspection, diagnosis of neocortical epilepsy, telemedicine or cognitive functions research. And with advances in sensing technology, neuroprosthetics applications based on brain computer interfacing (BCI) could be improved and used to restore damaged hearing, sight or movement. Event-related potentials (ERP) is one of the important biosignals of the brain which has a wide application in examining brain activity and cognitive functions. The P300 (or P3) is one of the ERP components which

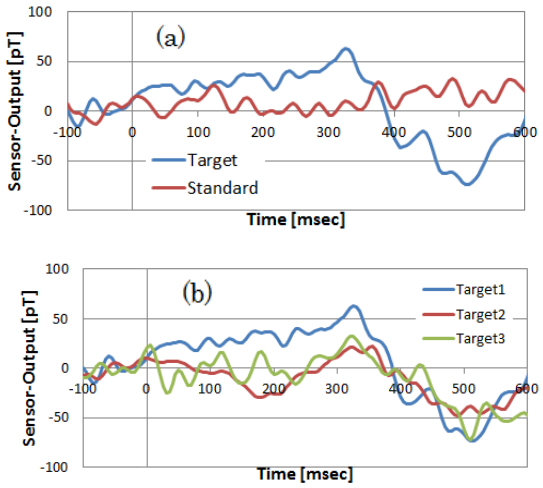

Fig.1. The waveforms of ERP we reported in past work. (a) displays the waveforms of mean P300 ERP elicited by target and standard stimuli in occipital region; (b) displays the waveforms of 3 times repeated measurement of the same subject.

normally elicited in the process of making decisions. It surfaces as a positive deflection with a latency of roughly 250 to 500 ms. ERPs have been mostly measured and monitored in two methods, Electroencephalography (EEG) and Magnetoencephalography (MEG).

Comparing with the EEG electrodes and the SQUIDs, Magneto-Impedance sensor (MI sensor) is smaller, lower cost and no need for magnetic shielding. Fig. 1(a) and (b), which we reported in the past work, display the waveforms of mean P300 ERP elicited by target and standard stimuli in occipital region and the waveforms of 3 times repeated measurement of the same subject. [4]

1. K. Mohri and Y. Honkura, *Sensor Letters* **5**, 267-270, (2007).
2. S. Sandacci, D. Makhnovskiy, L. Panina, K. Mohri, and Y. Honkura, *IEEE Trans. Magn.*, **40**, 6, 18–23, (2008).
3. S. Gudoshnikov, N. Usov, A. Nozdrin, M. Ipatov, A. Zhukov and V Zhukova, "Phys. Status Solidi A, DOI 10.1002/pssa.201300717 ,(2014).
4. S. Tajima, et.al. , The 7th International Conference on Sensing Technology, Wellington, New Zealand, (2013).

SS-09 (Invited Talk)
Design and Synthesis of Hierarchical Nanostructured Materials for Gas Sensing Applications

Sunkara V Manorama

Nanomaterials Laboratory, Inorganic and Physical Chemistry Division,

CSIR-Indian Institute of Chemical Technology, Hyderabad-500 007. Telangana. India. Email:manorama@iict.res.in and manorama.s.v@gmail.com, web site: http://www.iictindia.org

Development of materials for chemical sensing has been the topic of widespread research over the last few decades as evidenced by the literature on this topic. In spite of this it is also currently one of the thrust areas being pursued by different schools of expertise. Chemical sensing demands materials that have a large surface area facilitating high response to the test gas and specific functionalities to impart selectivity over other interfering analytes. In addition inclusion of noble metals in the matrix results in a reduction of operating temperature by the catalytic action.

Further, it has been now been proven beyond doubt that nanostructured materials because of their inherent small size and corresponding large surface to volume ration meet the above criteria, along with exhibiting superior physical, chemical and electronic properties meeting the prerequisites for several niche applications. Moving forward in this quest for better and high performance nanoarchitectures, the design of hierarchical structures has opened up a new area in materials synthesis for chemical sensing and for other application areas like catalysis, biomedical etc.

Tailored hierarchical structures could be obtained by a comprehensive understanding of the chemistry of the synthetic procedures, the interfacial properties etc. that would lead to tailored structures with desired morphologies. The use of surface directing agents and the dynamics of the reaction lead to structures whose surface properties could be tailored for the application in chemical sensing. The last few years our group has been successful in obtaining morphologies which exhibit excellent gas sensing properties for the detection of gases like CO, H_2 etc. In this endeavor we have been successful with SnO_2, SnO/SnO_2, In_2O_3, ZnO etc. with different architectures and we have been able to control the surface structure along with the electronic properties and all this by controlling the synthesis parameters like type and ratio of solvent, temperature, time of reaction, pressure etc.

The present talk deals with recent trends in materials synthesis methodologies being adopted to realize smart, multifunctional materials for a wide range of applications with special emphasis on highlighting the requirement for materials suitable for chemical sensing. Characterization of the structure, morphology and studying the electrical properties in the context of sensing behavior and its response to specific analytes throws light on the mechanism of sensing and this understanding leads to the design of better materials for the desired application.

SS-10 (Contributed Talk)

Study of zinc sulphide (ZnS) nanocrystaline thin films prepared by varying complexing agent for biosensing application

Sachin V. Mukhamale[1], Vilas A. Tabhane[1]*

[1] Department of Physics, Savitribai Phule Pune University, Pune, Maharashtra, INDIA*
**Email:yash.goaldriven@gmail.com, web site: http://physics.unipune.ernet.in/~Tabhane/*

The control of size and shape ZnS thin films has been prepared successfully, with varying molar concentrations of complexing agent and capping agent around for possible tunning band gap of materials. The phase transformation from Zinc blende structure to Wurtizite structure ZnS nanocrystals. They have been used in all the fields from material science to medical. The zinc sulphide semiconducting nanocrystals were synthesized, by colloidal solution method, by taking zinc sulphate as a precursor with sodium sulphide or thiourea. The particle growth and size is controlled and tuned by using suitable complexing agent. [1].

ZnS nanoparticles were characterized by ultra violet visible (UV-VIS) spectroscopy, Photoluminescence (PL-spectra), X-Ray diffraction (XRD), scanning electron microscopy (SEM), transmission electron microscopy (TEM), and fourier transform infrared spectroscopy (FTIR) gives well response. This paper contains a general view of current approaches to the synthesis, characterizations and composite of nanocrystalline thin films and their applications in medical sciences. Now a day such nanocrystalline thin films have been used in Photovoltaic's, biosensing materials such as DNA labeling, cholesterol deficiency in blood, and protein zinc deficient detection etc. By studying further they can be used for more applications. [2].

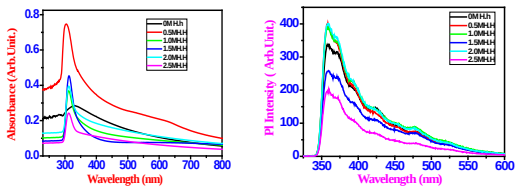

Fig. 1. Absorption spectra and Photoluminescence (PL) spectra of ZnS thin films deposited by chemical bath deposition method.

1. Masao Sato, Yasushi Nagai. *Springer of open journal*, 587, (1989).
2. Koichi Yamaguchi, Tsukasa Yoshida, Daniel Lincot, and Hideki Minoura. *Journal of physical chemistry B.*, 107 (2003).

Session GN

EMN GENERAL WORKSHOP ON NANOTECHNOLOGY

GN-01 (Invited Talk)
Green synthesis and characterization of gold nanoparticles and their sensing for antioxidant activity based on rapid colorimetric measurement

Ju Chou[1], X. Li, Y. Yin, N. Indrisek

Department of Chemistry and Physics, Florida Gulf Coast University, Fort Myers, FL, USA
Email:jchou@fgcu.edu

It is well known that free radicals in human bodies potentially can lead to diseases such as stroke, heart attack, and cancers [1]. Antioxidants can fight against these free radicals to protect cells from damage caused by free radicals and can reduce the risk of these diseases [2]. Plants (such as tea) and fruit or fruit juices are natural sources of antioxidants. Since the antioxidant composition and the matrix varies, a diverse array of analytical methodologies are required to measure antioxidant concentration or reducing power.

Since Au nanoparticles (AuNPs) have many sensing applications, they have been used to evaluate antioxidant activity in foods, plants and beverages [3]. Antioxidants present in plants and fruits can act as reductants. In this study, a simple and green synthesis of AuNPs has been achieved in tea leaves and fruit juices with auric tetra chloride ($HAuCl_4$). Natural antioxidants present in tea leaves and fruit juices were able to reduce Au^{3+} ions to AuNPs as shown in Fig.1. Citrate solution was added to cap AuNPs in the above synthesis to prevent the AuNPs from their aggregation. A colorimetric determination of antioxidants based on the formation of citrate capped AuNPs has been developed and the colorimetric response of AuNPs was dependent on the concentration of antioxidants tested. The colorimetric method developed was compared with the reference assay, Folin-Cicolteau method for validation and a perfect correlation (R^2 = 0.996) between the two methods was observed. Total antioxidant capacity of five fruit juices was determined and expressed as gallic acid equivalent (GAE).

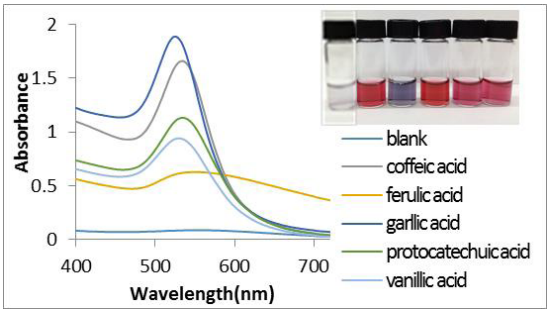

Fig. 1. UV-vis absorbance spectra and color images (upper insets) of AuNPS produced in citrate and different antioxidant solutions. Spectra and images were taken after 10 minutes heating at 70 ºC of the mixture containing 0.5 mM of $HAuCl_4$ and 1.6 mM citrate in the absence (a), and the presence of 100 μM of, coffeic acid (b), ferulic acid (c), gallic acid (d), protocatechuic acid (e) and vanillic acid (f). All solutions were prepared in 10 mM phosphate buffer at pH 7.0.

1. M. Valko, D. Leibfritz, J. Moncol, M. T. Cronin, and J. Telser, *Int. J. Biochem. Cell Biol.* **39**, 44, (2007).
2. L.A. Pham-Huy, H. He and C. Pham-Huy, *Int J Biomed Sci*. **4 (2)**, 89, (2008).
3. C. López-Alarcón, A.Denicola, *Anal. Chim. Acta* **763**, 1, (2013).

GN-02 (Invited Talk)
Novel Nanoparticles and Nanowires using Polyol/alcohol-based Synthesis Techniques

Balachandran Jeyadevan

Department of Material Science, The University of Shiga Prefecture, Hikone, JAPAN
Email:jeyadevan.b@mat.usp.ac.jp, web site: http://metal1.mat.usp.ac.jp/~metal-labo/index.html

Synthesis of metallic particles(MPs) using polyol as reducing agent was demonstrated by Fievet et al. over two decades ago [1]. At the beginning, the main focus was on the synthesis of metallic Ni, Co and their alloys. Besides, the

synthesis of pure metallic Fe was also attempted but, with little success [2]. But later, the synthesis of pure metallic Fe and Fe-based alloys such as FeCo and FeNi was demonstrated by our group using ethylene glycol as the reducing agent along with some additives such as hydroxyl ions, to accelerate the reduction process [3-5]. The accumulated know-how was subsequently introduced in the development of alcohol-based synthesis techniques for relatively easily reducible conducting and magnetic metals such Cu[6], Ag and Ni [7]. Though several metals and alloy nanoparticles have been produced using either polyol or alcohol, little has been done to understand the reduction mechanism.

The role of polyol as a reducing agent in the case of ethylene glycol(EG) was proposed in 1989[8]. However, the proposed reaction was not considered universal and it required further detailed investigation. Since then, little have been done to understand either the oxidation scheme of polyols or the metal complex transformation taking place during the formation of various metal particles. This has been an impediment for the researchers to get actively involved in the development of novel materials using polyol or alcohol-based reduction process in spite of its immense potential.

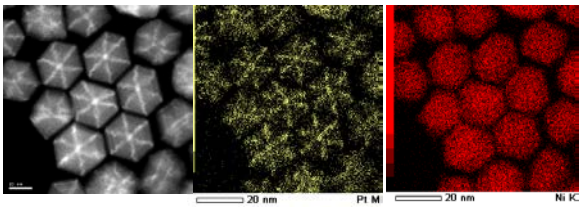

Fig. 1. STEM-HAADF image and EDS elemental mapping images of the Ni-Pt NPs.

In this presentation, we discuss about the dissolution and reduction of cobalt ions in ethylene glycol, and propose a universal reaction scheme for the synthesis of metal nanoparticle in polyol/alcohol-based synthesis technique. Then, we present the synthesis of novel bi-metallic and tri-metallic particles such as Ni-Pt [9] and Ni-Pd-Pt [10] using long chain alcohol. STEM-HAADF image and EDS elemental mapping images of the Ni-Pt NPs is shown in Fig. 1.Then, discuss the formation mechanism of these nanostructures and forecast the possibilities of applying this technique for the synthesis of other novel nanostructures. And also, discuss about their potential as chemical catalysts. Finally, we also present the one-step and one-pot process to prepare Cu-Ni nanowires with different diameters and length using long chain alcohols.

1. F. Fievet, J.P. Lagier, B. Blin, B. Beaudoin, M. Figlarzs, *Solid State Ionics* **1989**, 32-3, 198-205.
2. G. Viau, F. Fiévet-Vincent and F. Fiévet, J. Mat. Chem. **1996**, 6 1047-1053
3. R. J. Joseyphus, et al. *J. Magnetism and Magnetic Materials* **2007**, 310(2), 2393-2395
4. D. Kodama, et al., *Advanced Materials* **2006**, 18, 3154-3159
5. D. Kodama, et al., *J. Appl. Phys.* 2010, 107, 09A320-23
6. J. L. Cuya H., K. Sato, S. Kurita, T. Matsumoto and B. Jeyadevan, J. Mater. Chem., **2011**, 21, 7062-7069
7. J. L. Cuya H., N. Hironaka, K. Shinoda, H. Miyamura, B. Jeyadevan, *CrystEngComm*, **2013**, *15*, 7299.
8. Fievet, F., Lagier, J. P., Figlarz, M., *MRS Bull.*, **1989**, 29-34.
9. Jhon L. Cuya Huaman, S. Fukao, K. Shinoda and B. Jeyadevan, *CrystEngComm*, **2011**, 13, 3364-3369
10. B. Jeyadevan, et al., RSC Advances, **2014**, 4 (51), 26667 - 26672

GN-03 (Invited Talk)

Facile Fabrication of Tungsten Bronze Nanoparticles for Heat-ray Shielding via Solvothermal Reaction

Tsugio Sato, Chong-shen Guo, Shu Yin

Institute of Multidisciplinary Research for Advanced Materials, Tohoku University, 2-1-1 Katahira, Aoba-ku, Sendai 980-8577, Japan
Email:tsusato@tagen.tohoku.ac.jp, web site: http://www.tagen.tohoku.ac.jp/center/CENIM/eng/field_eimc.html

There has been a great demand to shield the near-infrared (NIR) radiation (heat rays) by employing visible light transparent coating on the windows, since such coating can reduce energy consumption for the air conditioning. The tungsten bronze compounds, such as Cs_xWO_3

possess the ability as a NIR filter. The traditional solid state reactions to synthesize tungsten bronze compounds often resulted to form agglomerated and/or irregular shaped particles, therefore, the post-synthesis milling process is required to produce nanocrystals. In the present paper, the monodispersed nanocrystals of tungsten cesium were directly synthesized by the solvothermal reaction using an ethanol-acetic acid mixed solvent.

After dissolving a certain amount of WCl_6 in the dehydrate ethanol, CsOH was introduced to produce a homogeneous suspended solution, followed by adding a certain amount of acetic acid into the solution, where the amount of acetic acid in the solvent was adjusted to 0-40 mol.%, and final concentration of WCl_6 was adjusted to 0.015 M with nominal Cs/W atomic ratio of 0.5. After that, the solutions were transferred into a Teflon-lined autoclave of 100 ml internal volume, followed by the solvothermal reactions in an electric oven at 240ºC for 20 h.

During the solvothermal reaction, the esterification reaction between ethanol and acetic acid proceeded to form water, which plays an import role on the crystallization of the product. By controlling the amount of acetic acid, it was possible to control the amount of water generated, and consequently, control the particle size, morphology and agglomeration of the products (Fig. 1). The Cs_xWO_3 nanocrystals with well-dispersed homogeneous morphology showed visible light transparency and excellent NIR shielding performance as shown in Fig. 2. The simulated experimental results confirmed the heat-shielding performance of Cs_xWO_3 is superior to commercial ITO glass, indicating their high-potential as a solar filter. It was also confirmed that the nanoparticles of various tungsten bronze compounds, such as Na_xWO_3, K_xWO_3, $(NH_4)_xWO_3$ and $W_{18}O_{49}$ could be synthesized via similar solvothermal reactions, and all of them showed excellent NIR shielding ability.

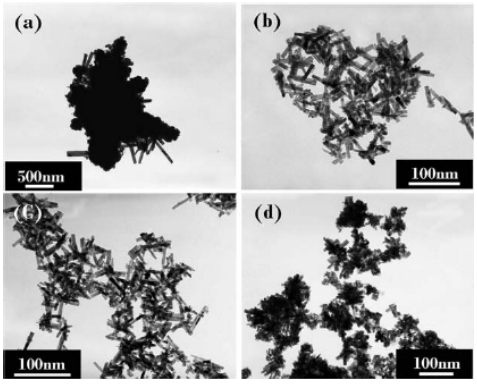

Fig. 1. Cs_xWO_3 formed by the solvothermal reaction in C_2H_5OH solutions containing (a) 0, (b) 10, (c) 20 and (d) 40 vol.% of CH_3COOH at 240ºC for 20 h.

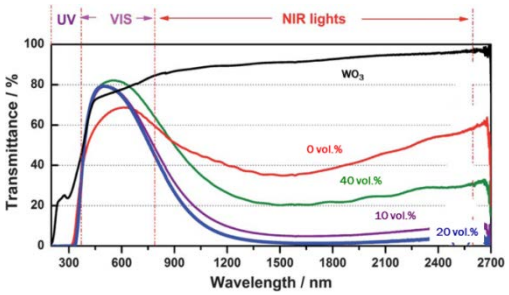

Fig. 2. Transmittance of the thin film of Cs_xWO_3 formed by the solvothermal reaction in C_2H_5OH containing various amounts of CH_3COOH at 240ºC for 20 h.

GN-04 (Invited Talk)
Detonation nanodiamond as attractive building block for nanotechnology

A. Vul, A.Alexenskii, M. Baidakova, A. Dideikin, E. Eidelman, S. Kidalov, V. Osipov, K.Reich, F. Shakhov

Ioffe Physical-Technical Institute, St.Petersburg, Russia
E-mail: alexandervul@mail.ioffe.ru

This presentation is a review addressed the new features of technology, the structure, properties and applications of a member of the nanocarbon family, namely, detonation

nanodiamond (DND). The main results included in the presentation have been obtained by Ioffe Institute nanodiamond group [1-3].

It is well known that a non-vanishing amount of residual metal impurities in DND, mainly 3*d*- transition metals is an important and unsolved problem of industrial DND technology for several DND applications. We demonstrate a method for super-purification of the industrial DND and EPR as an effective characterization method for control the purity of DND destined for biomedical applications.

A commercial powder of DND and their aqueous suspensions consist of submicron agglomerates of 4 - 5 nm crystalline diamond grains. We have recently submitted a method for disaggregation and production of stable hydrosol of 4 nm isolated DND particles. The properties of the hydrosols and gels obtained by concentration of hydrosols up to 6 wt. % are submitted here for the first time. We have demonstrated that 4 nm DND hydrosols produced by annealing in air and hydrogen atmospheres differ from each other by sign of their zeta potentials and submit a model of this effect.

One of the attractive features of DND is possibility for surface functionalization by metal using ion exchange, and we demonstrated a possibility of surface modification DND agglomerate by Cu, Co, Ni, Fe as well as rare metals. One of unusual properties of DND, we revealed is oriented attachment growth of submicron diamond crystals from 4 nm grains after high pressure and high temperature (HPHT) sintering This HPHT treatment has an affects to thermal conductivity and concentration impurities and defects in sintered microcrystals.

In view of the unique combination of DND properties, it appeared only reasonable to assume that this material would find broad application in various areas of technology. Probably the first DND application was associated with development of abrasive compositions for ultrafine mechanical polishing of hard surfaces, including optical elements, semiconductor substrates. Another rapidly expanding area of DND application is the technology of seeding at CVD diamond film growth. Progress in the technology of formation of crystallization centers based on the use of suspensions of 4-nm DND particles permits one presently to prepare diamond photonic crystals.

First reports on the use of DND as catalyst carrier have recently appeared. By using a neutral, chemically resistant phase in the form of particles on which a thin film of catalyst, primarily a metal of the platinum group, was deposited, one can enhance substantially the catalysis efficiency, while at the same time cutting noticeably the consumption of noble metals.

A promising application of DND as biomarker is based on using its luminescent properties deriving from nitrogen-vacancy defects in the crystal structure of its particles. High-pressure sintering of DND reveals the presence of nitrogen luminescent centers $(N\text{-}V)^-$ in concentrations as high as 10-20 cm^{-3}.

Production of isolated single-crystal 4 nm particles of DND opens the door for targeted delivery of drugs in living organisms. The rich surface chemistry of ND, the absence of toxic properties and small size make nanodiamonds a very convenient object for biomedical applications.

Participation at the conference supported by the Russian Science Foundation (grant 14-13-00795)

1. A Vul', M. Baidakova, A. Dideikin. Nanocrystalline Diamond. In: Carbon Nanomaterials, Second Edition. Ed. Yury Gogotsi, Volker Presser. CRC Press (2013)
2. Detonation nanodiamonds - Science and Technology. Ed. Alexander Vul' and Olga Shenderova. Pan Stanford Publishing (2014).
3. A.Ya.Vul', A. T. Dideikin, A.E. Aleksenskiy, M. V. Baidakova. Detonation Nanodiamonds. Synthesis, Properties and Applications. In: "Nanodiamond". Ed. O. A Williams, Cardiff University, UK Royal Society of Chemistry (2014).

GN-05 (Invited Talk)

Probing structure and dynamics of nanoparticles for energy applications

Thomas E. Ashton[1], Serena A. Corr[1*]

[1]*School of Chemistry, University of Glasgow, Glasgow, G12 8QQ, Scotland*
Email:serena.corr@glasgow.ac.uk, web site: http://corrgroupglasgow.wordpress.com/

Critical for advances in functional nanoparticles is an understanding of how the properties of materials operate on such limited length scales. Their complexity demands a combination of characterization methods in order to fully evaluate their behavior. We have prepared a host of vanadate- and olivine-structured nanoparticles, which have potential applications as energy efficient materials and insertion electrodes. We can use a variety of bottom-up synthetic approaches including hydrothermal synthesis, co-precipitation, sol-gel and recently developed microwave-assisted methods, which allow us to prepare size- and shape-tailored nanoparticles of desired phases in a controlled manner.

To intimately understand the structure-property-function relationships in these materials, we make full use of a host of physical characterisation tools and facilities-based local structure techniques including muon spin relaxation and x-ray absorption spectroscopy (XAS). [1] Such methods allow us to monitor, in detail, lithium diffusion processes and magnetic ordering in these nanoparticles, together with changes in local structure. Recently, we have employed *in-situ* XAS to investigate the structural changes ongoing in the insertion electrode VO_2 (B) during electrochemical lithiation which will also be presented (see Figure 1). The combination of this variety of techniques builds a more complete picture of such nanostructured materials and is of huge importance in elucidating mechanistic information.

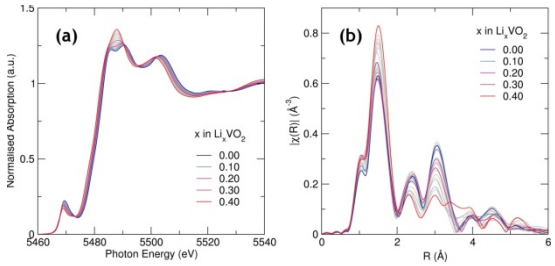

Fig. 1. *In-situ* vanadium K-edge XAS conducted on a VO_2 (B) Li-ion cell showing (a) XANES spectra oxidation state changes and (b) EXAFS spectra changes indicating changes inter-atomic distance.

1. T. E. Ashton, J. Vidal Laveda, D. MacLaren, P. J. Baker, A. Porch, M. O. Jones and S. A. Corr, *J. Mater. Chem. A* **2**, 6238 (2014)

GN-06 (Invited Talk)

Plasma Nanocoatings for Preventing/Inhibiting Biofilms

QS Yu[1], J Jones[1], M Chen[2], YX Xu[3], Y.B. Ma[3], HM Sun[3]

[1]*Center for Surface Science and Plasma Technology, Department of Mechanical and Aerospace Engineering, University of Missouri, Columbia, MO 65211, USA*

[2] *Nanova, Inc., 1005 Brook Trout Ct., Columbia, MO 65203, USA*

[3] *Department of Internal Medicine, University of Missouri, Columbia, MO 65211, USA*

** E-mail: yuq@missouri.edu*

Biofilm formation on implantable medical and dental devices such as pacemakers, catheters, artificial heart valves is causing serious infection problems in clinical care.[1] *S. aureus* and *S. epidermidis* infections are the leading causes of biofilm formation on indwelling devices. *S. mutans* are the major cariogenic bacteria that form biofilms on teeth and dental implants.[2] Biofilm-associated bacteria are particularly resistant to antibiotic treatment, which in combination with the increasing prevalence of antibiotic resistance among human pathogens further complicates treatment of biofilm-related device infections.

In this study, non-thermal plasma coating technology was used to fabricate novel anti-biofilm nano-scale coatings for preventing and/or inhibiting biofilm formation on biomaterials. Plasma nanocoatings from trimethylsilane (TMS) with thickness of 20 – 30 nm were deposited on substrates of 316L stainless steel and grade 5 titanium alloys, which are widely used in implantable medical and dental devices. The surface chemistry and surface properties of the TMS plasma nanocoatings were characterized in terms of chemical composition and structure, surface roughness, and surface hydrophilicity, etc. Biofilm assay results showed that TMS plasma nanocoatings significantly decreased biofilm formation of *S. epidemidis* and *S. mutans* by inhibiting the attachment of bacterial cells to the coated 316L stainless steel and titanium surfaces. The results suggest that plasma coatings have shown their capability and potential in reducing and inhibiting biofilm formation. It was also found that bacterial cells on the plasma nanocoating surfaces were more susceptible to antibiotic treatment than their counterparts on uncoated surfaces. These findings suggested that TMS coating could result in a surface that is resistant to biofilm development and also in a bacterial community that is more sensitive to antibiotic therapy than typical biofilms.

Acknowledgements: This study was supported by US NIH with grant number of 5R44DE019041.

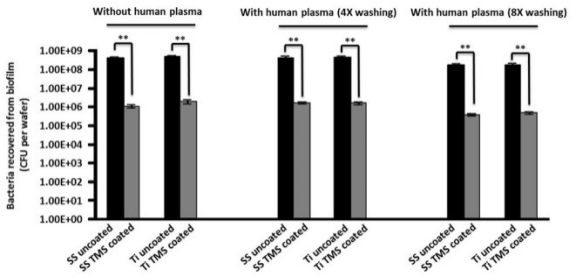

Fig. 1. Viable cell counts from biofilms on TMS coated and uncoated 316 stainless steel (SS) and grade 5 titanium alloy (Ti) wafers. ** denotes $P < 0.01$.

1. H. J. Busscher, M. Rinastiti, W. Siswomihardjo, and H.C. van der Mei. J. Dent. Res. Vol. 89, p. 657-665, 2010.
2. R. Huang, M. Li, and R. L. Grdgory, Virulence, Vol 2, p. 435-444, 2009.

GN-07 (Contributed Talk)

Nanomaterials: A key tool for improvising waste water technologies

Shivani Bhardwaj Mishra, Sadanand Pandey, Sourabh Thakur, Ajay Kumar Mishra

Department of Applied Chemistry, University of Johannesburg, Johannesburg, Gauteng, South Africa
Email:smishra@uj.ac.za

Different types of wastewater technologies have been developed and commercialized to combat the challenges of variety of pollutants. The new generation of wastewater treatment methodologies are being designed to improve treatment efficiency and reusability. The pollutants in all forms such as heavy metals, organics, dyes and pathogens provide different response to different technologies. Nanomaterials and nanocomposites have been identified to play a key role for improvising the wastewater treatment methods. The recent research in this field show an enormous potential by these nanomaterials and nanocomposites. In our research theme, the material in nanoscale have been used for adsorption, chemical and photochemical degradation of pollutants. Besides, organic – inorganic hybrid systems and magnetic nanocomposites are being investigated for the uptake of contaminants [1-4].

2. S. Pandey and S. B Mishra, *J. Colloid and interface science*, **361**, 509 (2011).
2. M. M. Mahlambi, A.K. Mishra, S. B. Mishra, R. W. Krause, B.B. Mamba and A.K. Raichur, *Industrial and engineering chemistry research*, **52**, 1783 (2013).
3. H. Mittal and S.B. Mishra, *Carbohydrate polymers*, **101**, 1255 (2014)
4. N. Ballav, H. G. Choi, S.B. Mishra and A. Maity, *Industrial and engineering chemistry research*, Accepted manuscript (2014).

GN-08 (Contributed Talk)

Enzymatic grafting: A Novel Approach to Develop Multifunctional Materials of Interest

Hafiz M.N. Iqbal*[1] Godfrey Kyazze[1], Thierry Tron[2] and Tajalli Keshavarz[1]

[1] *Applied Biotechnology Research Group, Department of Life Sciences, Faculty of Science and Technology, University of Westminster, London W1W 6UW, United Kingdom*

[2] *Aix Marseille Université, CNRS, Centrale Marseille, iSm2 UMR 7313, 13397, Marseille, France*

**Corresponding author E-mail address: hafiz.iqbal@my.westminster.ac.uk*

Today more than 99% of plastics are petroleum-based because of the availability and cost of the raw material. The durability of disposed plastics contributes to the environmental problems as waste and their persistence in the environment causes deleterious effects on the ecosystem. Environmental pollution awareness and the demand for green technology have drawn considerable attention of both academia and industry into biodegradable polymers. In this regard green chemistry technology has the potential to provide solution to this issue. Enzymatic grafting has recently been the focus of green chemistry technologies due to the growing environmental concerns, legal restrictions, and increasing availability of scientific knowledge.

Over the last several years, research covering various applications of robust enzymes like laccases and lipases has been increased rapidly, particularly in the field of polymer science, to graft multi-functional materials of interest. In principle, enzyme-assisted grafting may modify/impart a variety of functionalities to the grafted composites which individual materials fail to demonstrate on their own. The modified polymers through grafting have a bright future and their development is practically boundless.

In the present study series of graft composites with poly(3-hydroxybutyrate) (P(3HB) as side chain and cellulose as a backbone polymer were successfully synthesised by introducing enzymatic grafting technique where laccase and lipase were used as model catalysts [1-3]. Subsequently, the resulting composites were removed from the casting surface under ambient environment and characterised by Fourier-transform infrared spectroscopy (FT-IR), scanning electron microscopy (SEM), and X-ray diffraction (XRD) in detail. Moreover, the thermo-mechanical behaviours of the grafted composites were investigated by differential scanning calorimetry (DSC) and dynamic mechanical analyser (DMA) measurements, respectively. In addition, hydrophobic and hydrophilic characteristics of the grafted polymers were studied through drop contour analysis using water contact angle (WCA).

In comparison to the individual counterparts improvement was observed in the thermo- mechanical properties of the composites to varied extent. The tensile strength, elongation at break, and Young's modulus values of the composites reached their highest levels in comparison to the films prepared with pure P(3HB) only which was too fragile to measure any of the above said characteristics. Interestingly, untreated P(3HB) was hydrophobic in nature and after lipase treatment P(3HB) and P(3HB)-EC-based graft composite attained higher level of hydrophilicity. This is a desired characteristic that enhances the biocompatibility of the materials for proper cell adhesion and proliferation therefore suggesting potential candidates for tissue engineering/bio-medical type applications [3]. The present research will be a first step in the biopolymer modification. To date no report has been found in literature explaining the laccase/lipase assisted grafting of P(3HB) [1-3]. The newly grafted composites exhibit unique functionalities with wider range of potential applications in bio-plastics, pharmaceutical, and cosmetics industries, tissue engineering, and biosensors.

[1] H.M.N. Iqbal, G. Kyazze, T. Tron and T. Keshavarz, *Cellulose* **21**, 3613-3621 (2014).

[2] H.M.N. Iqbal, G. Kyazze, T. Tron and T. Keshavarz, *Carbohydrate Polymers* **113**, 131-137 (2014).

[3] H.M.N. Iqbal, G. Kyazze, T. Tron and T. Keshavarz, *Polymer Chemistry* **In-Press**, DOI: 10.1039/C4PY0 0857J (2014).

GN-09 (Invited Talk)

Controlled Synthesis and Properties of Cu- and Bi-based Functional Semiconductor Nanomaterials

Guanjun Xiao, Bo Zou*

State Key Laboratory of Superhard Materials, Jilin University, Changchun 130012, China
Email:zoubo@jlu.edu.cn; xguanjun@jlu.edu.cn

Much effort has so far been dedicated to achieving rational control over the morphology, assembly and their related applications.[1] However, improvement in manipulating their shape, size and properties is still a significant challenge in modern materials physics and chemistry. Herein, we first of all developed a solution route to synthesize shape- and structure-controlled copper selenide nanocrystals (NCs) including CuSe nanosheets, $Cu_{2-x}Se$ nanoparticles and $Cu_{2-x}Se$ nanorods.[2] The electrical transport properties of as-prepared products were systematically investigated. In addition, we demonstrated the synthesis of monodispersed hollow $Cu_{2-x}Te$ NCs with tunable interior volume based on the nanoscale Kirkendall effect, as shown in Figure 1.[3] The as-prepared hollow $Cu_{2-x}Te$ NCs exhibited greatly enhanced gas sensitivity owing to the small grain size and large surface-to-volume ratio. The hollow $Cu_{2-x}Te$ nanostructures may serve as microreactors in catalytic applications and it is highly probable to provide new functional blocks for the design of gas sensors. Moreover, we reported that Bi_2S_3 hierarchical architectures (HAs) with controllable sizes and shapes were successfully prepared *via* a facile one-step strategy.[4] Crystal splitting behavior was believed to be responsible for the formation of Bi_2S_3 HAs. It was worth nothing that the products are potential candidate for photoswitch and light-sensitive devices. Finally, we experimentally fabricated nanostructured hierarchical architectures of the topological insulator Bi_2Te_3 without the introduction of any exotic magnetic dopants, in which intriguing room-temperature ferromagnetism was identified.[5] First-principles calculations demonstrated that the intrinsic point defect with respect to the antisite Te site is responsible for the creation of a magnetic moment. Such a mechanism, which is different from that of a vacancy defect, provides new insights into the origins of magnetism. Our findings may pave the way for developing future Bi_2Te_3-based dissipationless spintronics and fault-tolerant quantum computation.

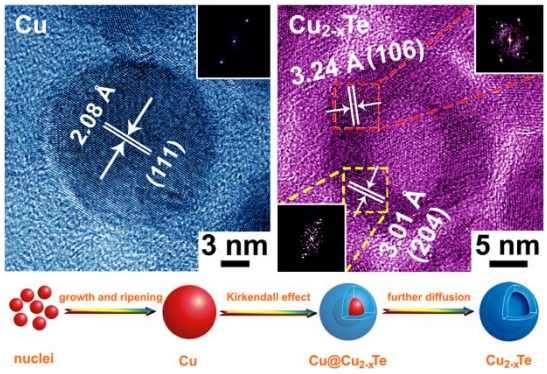

Fig.1. Controlled synthesis of hollow $Cu_{2-x}Te$ nanocrystals based on the nanoscale Kirkendall effect.

1. Guanjun Xiao, Yingnan Wang, Jiajia Ning, Yingjin Wei, Bingbing Liu, William W. Yu, Guangtian Zou and Bo Zou, *RSC Adv*., **3**, 8104 (2013).
2. Guanjun Xiao, Jiajia Ning, Zhaoyang Liu, Yongming Sui, Yingnan Wang, Qingfeng Dong, Wenjing Tian, Bingbing Liu, Guangtian Zou and Bo Zou, *CrystEngComm*, **14**, 2139 (2012).
3. Guanjun Xiao, Yi Zeng, Yueyue Jiang, Jiajia Ning, Weitao Zheng, Bingbing Liu, Xiaodong Chen, Guangtian Zou and Bo Zou, *Small*, **9**, 793 (2013).
4. Guanjun Xiao, Qingfeng Dong, Yingnan Wang, Yongming Sui, Jiajia Ning, Zhaoyang Liu, Wenjing Tian, Bingbing Liu, Guangtian Zou and Bo Zou, *RSC Adv*. **2**, 234 (2012).
5. Guanjun Xiao, Chunye Zhu, Yanming Ma, Bingbing Liu, Guangtian Zou and Bo Zou, *Angew. Chem., Int. Ed.*, **53**, 729 (2014).

GN-10 (Invited Talk)

Ultrahigh density arrays of semiconducting nanotubes for high performance logic electronics

Qing Cao[1]

[1]IBM T.J. Watson Research Center, Yorktown Heights, NY 10598, USA

Email:qcao@us.ibm.com

Single-walled carbon nanotubes (SWNT) could replace silicon in high-performance electronics with their exceptional electrical properties and intrinsic ultra-thin body. However, a major challenge to make nanotube electronics a practical technology is to assemble these nanotubes into regular arrays with both minuscule and uniform pitch for sufficient device packing density and homogeneity. We will discuss our latest progress on producing well aligned, ultrahigh density nanotube arrays based on enriched semiconducting tubes. With the Langmuir-Schaefer method, full surface coverage aligned arrays of semiconducting nanotubes can be assembled with their pitch self-limited by the nanotube diameter plus ver der Waals separation.[1] However, the assembled nanotube arrays exhibit a double layered structure, which could be unfavorable for device operations. To overcome this limitation, we recently developed a method in which the alternating voltage fringing electric field formed between surface microelectrodes and the substrate is utilized to assemble semiconducting nanotubes into well-aligned, ultrahigh density, and sub-monolayered arrays, with a consistent pitch as small as 21nm.[2] The pitch is determined by a self-limiting mechanism based on the unique field focusing and screening effects of the fringing field. Devices based on such ultrahigh density aligned arrays demonstrate record high performance, at both transistor and single tube level.

1. Q. Cao, S.J. Han, G.S. Tulevski, Y. Zhu, D.D. Lu, W. Haensch, *Nature Nanotech.* **8**, 180 (2013).
2. Q. Cao, S.J. Han, G.S. Tulevski, *Nature Commun.* in press (2014).

GN-11 (Invited Talk)

Metal-Semiconductor Hybrid Nanostructures with Plasmon-Enhanced Photocatalytic Activities

Can Xue[1], Zhenyi Zhang[1], Jun Fang[1], Shao-Wen Cao[1]

[1]School of Materials Science and Engineering, Nanyang Technological University, Singpaore
Email: cxue@ntu.edu.sg Web site: http://www.ntu.edu.sg/home/cxue/

We present the preparation of hybrid nanostructures, including core-shell nanoparticles, hetero-nanoparticles, nanoframes, and composite nanofibers, which are consisting of Au/Pt nanoparticles and different semiconductor nanostructures such as TiO_2, Fe_2O_3, $BiVO_4$ and $InVO_4$.[1-5] The obtained hybrid nanostructures exhibit high photocatalytic activities for water splitting and dye degradation. Our observations suggest that the surface plasmon resonance (SPR) of the conjugated gold nanoparticles might contribute significantly to the visible-light-driven activities through plasmon-enhanced charge separation. Furthermore, we demonstrate the direct evidence of SPR-enhanced photocatalytic hydrogen generation through a strategy of dual-beam irradiation. By finely controlling the irradiation wavelengths, we observe that the enhancement factor on hydrogen generation is directly correlated with the plasmon absorption band of the Au nanoparticles in the hybrid nanostructures. The control experiments with different sacrificial agents suggest that the hot plasmonic electrons of Au are responsible to the enhanced photocatalytic activity that can be magnified when the semiconductor is simultaneously excited.

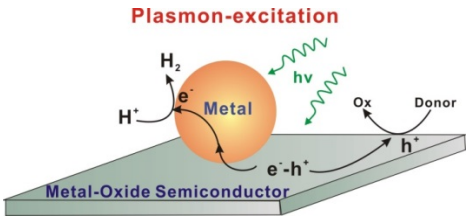

Fig. 1. Schematic illustration on the plasmon-enhanced photocatalytic activity by the gold nanoparticles conjugated on semidoncutor surfaces.

1. Z. Y. Zhang, A. Li, S. W. Cao, M. Bosman, S. Li, C. Xue*, *Nanoscale*, **6**, 5217 (2014)..
2. M. M. Shahjamali, M. Bosman, S. W. Cao, X. Huang, X. H. Cao, H. Zhang, S. S. Pramana, and C. Xue, *Small* **9**, 2880 (2013).
3. Z. Y. Zhang, Z. Wang, S. W. Cao, and C. Xue, *J. Phys. Chem. C* **117**, 25939 (2013),
4. J. Fang, L. Xu, Z. Y. Zhang, Y. P. Yuan, S. W. Cao, Z. Wang, L. S. Yin, Y. S. Liao, and C. Xue, *ACS Appl. Mater. Interfaces* **5**, 8088 (2013).
5. M. M. Shahjamali, M. Bosman, S. W. Cao, X. Huang, S. Saadat, E. Martinsson, D. Aili, Y. Y. Tay, B. Liedberg, S. C. J. Loo, H. Zhang, F. Boey, and C. Xue, *Adv. Funct. Mater.* **22**, 849 (2012).

GN-12 (Invited Talk)
Lattice dynamics of bismuth nanoislands and nanoparticles studied by ultrafast electron diffraction

Ahmed R. Esmail, Aleksey Bugayev, Hani E. Elsayed-Ali

Department of Electrical and Computer Engineering and the Applied Research Center, Old Dominion University, Norfolk, VA 23529, USA.
Email: helsayed@odu.edu, web site: http://www.eng.odu.edu/arc/

The lattice response of bismuth nanoparticles and nanoislands to femtosecond laser excitation is probed by ultrafast electron diffraction (UED). The UED gun produced 35 keV electron pulses of ~1.4 ps duration at the photocathode excitation level used. For both morphologies, the transient decay time after laser excitation is observed to be longer for diffraction from the (012) lattice planes compared to that from (110). These results indicate that different energy coupling mechanisms to the lattice occur for both types of samples depending on the crystal direction. For the nanoparticles, with most-probable size ~16 nm, changes in the position of the (012) diffraction peak shows a transient lattice contraction due to hot electron blast force that lasts over several picoseconds followed by expansion [1]. For nanoislands, fabricated by deposition of 5-nm Bi on carbon grid, no hot electron blast force effects were observed.

Figure 1 shows the time-resolved normalized diffraction intensity of the (012) Bragg peak of and the relative change in ring radius $\Delta r(t)/r_o$ along the <012> direction obtained for nanoparticles. The lattice contracts ~0.05% immediately after photoexcitation (first contraction from 0 < time < 10 ps reaching maximum at ~5 ps). Following this contraction, the lattice expands to ~0.22%. After the lattice reaches its maximum expansion, it contracts again to a certain position. The magnitude of the contraction and expansion is fluence-dependent. The results are interpreted by nanoparticle vibration model initiated by a gradient in electron kinetic pressure generating hot electron blast force.

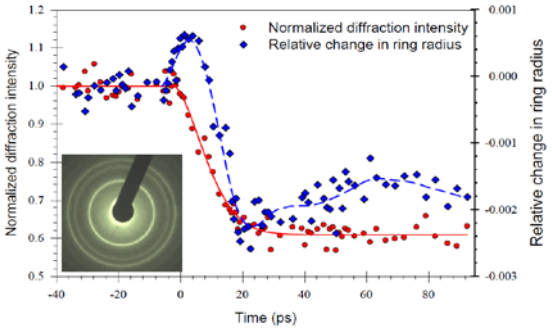

Fig. 1. Time evolution of the normalized change in intensity of Bragg peaks due to femtosecond laser excitation pulses of fluence 2.9 mJ/cm^2 and the corresponding relative change in ring radius $\Delta r(t)/r_o$ for the (012) Bragg peak. The inset shows transmission UED pattern.

1. Ahmed R. Esmail, Aleksey Bugayev, and Hani E. Elsayed-Ali, *J. Phys. Chem. C* **117**, 9035 (2013).

GN-13 (Invited Talk)

In situ synchrotron studies of reactivity at model complex oxide surfaces

D.D. Fong[1], C.M. Folkman[1], S.-H. Chang[1], J.A. Eastman[1], J.W. Freeland[2], H. Zhou[2], N. M. Markovic[1], H. Jeen[3], and H.-N. Lee[3]

[1]*Materials Science Division, Argonne National Laboratory, Argonne, IL, USA*
Email:fong@anl.gov

[2] *X-Ray Science Division, Advanced Photon Source, Argonne National Laboratory, Argonne, IL, USA*

[3] *Materials Science and Technology Division, Oak Ridge National Laboratory, Oak Ridge, TN, USA*

Oxide materials are known to be active in a variety of redox reactions, making them important for many energy technologies. Unfortunately, the complex interactions between such reactions and the structural/chemical evolution of the oxide surface are not well-understood. This has hindered progress in many areas, including solid oxide fuel cells, corrosion, and the development of new heterogeneous catalysts. With the advent of high precision growth techniques, epitaxial oxide heterostructures can now be synthesized with controlled strain, orientation, and surface termination. When combined with the unique capabilities of the APS, this permits *in situ* studies of redox reactions on model oxide surfaces and can therefore lead to the development of much needed structure-reactivity relationships for this important class of materials.

In this presentation, I will discuss recent *in situ* x-ray results on epitaxial $SrCoO_x$ films and their behavior during oxidation and CO oxidation, as well as epitaxial $SrRuO_3$ films and their behavior during the oxygen evolution reaction. We find significant structural changes during reaction as well as a large dependence of reaction rates on crystal orientation.

GN-14 (Invited Talk)

Functional thin films using nanotechnology: epitaxy anywhere.

Dave H.A. Blank and Gertjan Koster

MESA+ Institute for Nanotechnology, P.O. Box 217, 7500 AE, Enschede, the Netherlands
Email:d.h.a.blank@utwente.nl and g.koster@utwente.nl website: http://www.utwente.nl/mesaplus/daveblank

In nanotechnology a tremendous synergy can be achieved as a result of a combination of different fields. Here we would like to discuss an example in the realm of epiaxial thin films. The past decade has seen numerous examples of novel physical phenomena observed in complex oxide electronics that were realized by the atomic scale precision with which metal oxide thin films can be formed, and originating from the crystallographic orientation, epitaxial stress and strain, and/or artificial interfaces. Commercialized application of perovskite-based materials has for an important part been hindered by the challenge to combine the technology with current (Si-based) processes or even glassy substrates lacking any translation symmetry, and is related to the challenge to retain control over crystal growth that is achieved on lattice-matching crystals. Ideally, such control should also be scaled-down in order to achieve miniaturization. Because of their single crystalline nature, (sub)-µm lateral sizes, and broad variety, inorganic nanosheets are promising candidates to achieve this goal. By utilizing inorganic nanosheets to orchestrate thin film growth, we fabricated perovskite oxide thin films in which strain and crystallographic orientation was patterned. I will give any overview of the possibilities for epitaxy of functional materials offered by nanosheets.

As an example, Pulsed laser deposition was used to grow thin films of $SrRuO_3$ on Si substrates that were covered by two different types of nanosheets to direct crystal growth: $Ca_2Nb_3O_{10}$ was used to realize $(001)_c$ oriented films and $Ti_{0.87}O_2$ to realize epitaxial growth in the $[110]_c$ direction (label c is used to refer to a

(pseudo-)cubic crystal symmetry). The ferromagnetic conducting perovskite was selected for two reasons: To illustrate our ability to locally tailor magnetic behavior and because of the importance of this material as electrode in all oxide heterostructures. Moreover, we will show that different oriented thin films on layers depend on the type of nanosheets as well as the thickness of the nanosheet layer. Considering for example magnetic behavior like the Curie temperature or anisotropy different properties are found depending on the used nanosheet template. By micro-patterning various types of nanosheets, these properties were combined into a single sample, illustrating that this approach allows to locally control growth and properties of thin films. In terms of for instance roughnesses or resistivities, these films showed strong resemblance to fully oriented counterparts, making them potentially relevant in future heteroepitaxial multilayered materials.

GN-15 (Invited Talk)
Fatigue Crack Growth and Retardation in Nanostructured Materials

Ming Dao[1]

[1]*Department of Materials Science and Engineering, Massachusetts Institute of Technology, Cambridge, MA, USA*
Email:mingdao@mit.edu, web site: http://www.mit.edu/~mingdao/

When characteristic microstructure dimensions go below 100 nm, materials may exhibit superior mechanical, electrical, magnetic, catalytic or biological properties [1-4]. For any potential structural applications of these advanced materials, understanding the size-dependent fatigue damage and failure mechanisms is critical for better microstructural design and optimization with improved fatigue properties against crack initiation and growth. In this presentation, several optimization strategies and related mechanisms will be reviewed and discussed. Introducing nanoscale twins was found to be such a successful strategy for improving fatigue properties in addition to providing higher strength with reasonable ductility [5-7]. As another example, fatigue-induced nanocrystallization in an Al-based metallic glass, observed using high-resolution in situ TEM, was found to slow down fatigue crack growth and bridging [8]. In discussing these strategies and related mechanisms, critical differences between monotonic and cyclic loading conditions will be emphasized, correlations between improved fatigue properties versus microstructural evolution will be carefully examined, and possible size-dependent and/or orientation dependent deformation mechanisms will be discussed.

Figure 1 shows the microstructure evolution of $Al_{88}Fe_7Gd_5$ metallic glass under fatigue loading [8]: (A) High-resolution TEM images of the notch-tip area for the untested, cyclically strained, and monotonically strained specimens. (B) Fatigue crack tip morphology after 980, 1,470, and 1,960 fatigue loading cycles, respectively. Selected area diffraction patterns (Inset) confirmed nanocrystallization ahead of the crack tip. Grain growth, crack bridging and crack-tip blunting were observed.

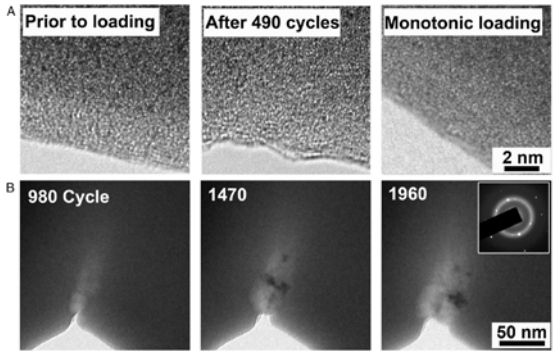

Fig. 1. Microstructure evolution of $Al_{88}Fe_7Gd_5$ metallic glass under fatigue loading [8].

1. M. Dao, L. Lu, R.J. Asaro, J.T.M. De Hosson and E. Ma, *Acta Materialia* **55**, 4041 (2007).
2. K. Lu, L. Lu and S. Suresh, *Science* **324**, 349 (2009).
3. T. Zhu and J. Li, *Progress in Materials Science* **55**, 710 (2010).
4. K. Tai, M. Dao, S. Suresh, A. Palazoglu and C. Ortiz, *Nature Materials* **6**, 454 (2007).

5. A. Singh, L. Tang, M. Dao, L. Lu and S. Suresh, *Acta Materialia* **59**, 2437 (2011).
6. A. Singh, M. Dao, L. Lu and S. Suresh, *Acta Materialia* **59**, 7311 (2011).
7. A. Singh, N.R. Tao, M. Dao and S. Suresh, *Scripta Materialia* **66**, 849 (2012).
8. C.-C. Wang, Y.-W. Mao, Z.-W. Shan, M. Dao, J. Li, J. Sun, E. Ma and S. Suresh, *Proc. Natl. Acad. Sci. USA* **110**, 19725 (2013).

GN-16 (Invited Talk)
Size, shape, stability and plasmonic properties of metal nanoparticles

Cecilia Noguez

Instituto de Física, Universidad Nacional Autónoma de México, Apartado Postal 20-364, México D.F. 01000 MÉXICO
Email: cecilia@fisica.unam.mx, web site: http://www.fisica.unam.mx/cecilia.htm

Metal nanoparticles (NPs) exhibit remarkable physical and chemical properties, which are morphology-dependent. Particular interest has been paid in their surface plasmon excitations that play an important role in fluctuation-induced interactions. At the nanoscale, this physical property conducts to new phenomena because these surface plasmon resonances are localized and consequently they enhance the near electromagnetic field. This latter can be important for controlling the interaction among diverse nanostructures. In this presentation, we discuss surface plasmon in metal NPs, their localization, the electromagnetic field enhancement of such plasmons and their possible application in TERS.

GN-17 (Invited Talk)
Revisiting Aluminum for Li-ion Battery Anodes: core-shell $NiSi_x$-Al nanowire structures.

Didier Pribat, Hung Tran Nguyen, Mihai Robert Zamfir and Eric Moyen.

Department of Energy Science, Sungkyunkwan University, Suwon, 440-746, Korea.
Email:didier53@skku.edu

Li-ion batteries (LIBs) are a great success of modern material science. They are based on insertion materials at both the anode and the cathode. However, in spite of more than 20 years of commercialization, LIBs still exhibit a low capacity, they can only deliver low powers and their lifetime is limited to about 1000 charge-discharge cycles depending on the way they are used. Typically, graphite is used at the anode, because Li ions can easily penetrate inside its lamellar structure, inducing only slight strain. While graphite is an interesting material in terms of cycling behavior and reliability, it exhibits a modest capacity of only ~ 370 mAh/g. Because they can provide higher capacities as well as larger charge-discharge rates, lithium alloys are currently being studied for the potential replacement of graphite. However, none of these alloys have made their way to the market place yet, because of fast electrode degradation problems due to the large volume change upon lithiation-delithiation.

Although the major contenders are tin or silicon, aluminum is also an interesting anode material since it can make a series of solid solutions and intermetallic compounds with Li, culminating at a capacity of 2235 mAh/g for the Li_9Al_4 compound of the equilibrium phase diagram. Moreover, Al is the third most abundant element on earth, it is environment-friendly and relatively cheap and it can be easily deposited by various techniques, such as thermal evaporation or sputtering, chemical vapor deposition (CVD) from organometallic compounds or even electrodeposition in electrolytes based on ionic liquids [1]. However, the use of Al has so far been largely unsuccessful, even when

nanostructures are employed [1], a behavior which contrasts with Sn or Si [2].

In this talk, we shall revisit the use of nanostructured Al-based anodes and show that indeed, such nanostructures can withstand a large number of charge-discharge cycles, making them attractive for the potential replacement of graphite. Typically, we use random arrays of core-shell nanowires (NWs), with a $NiSi_x$ core and an Al shell. The $NiSi_x$ NWs are first grown by CVD, using SiH_4 decomposition over a thin film Ni catalyst and Al is subsequently evaporated on top of the $NiSi_x$ NWs. We shall present the anode evolution as a function of charge-discharge cycling at various rates and discuss the viability of such core-shell structures.

1. N. S. Hudak, D. L. Huber, *J. Electrochem. Soc.* **159**, A688 (2012).
2. M. R. Zamfir, H. T. Nguyen, E. Moyen, Y. H. Lee, D. Pribat, *J. Mater. Chem.* A, **1**, 9566 (2013).

GN-18 (Contributed Talk)
Toward Roll-to-Roll Production of Nanomaterials Using Microwave

Xinyu Zhang, Jonathan Cook, Selcuk Poyraz

Polymer and Fiber Engineering Department, Auburn University, Auburn, AL, USA
Email:xzz0004@auburn.edu, web site: http://www.eng.auburn.edu/users/xzz0004/

Nanomaterials, such as carbon nanotubes (CNT), metal oxides, and polymers, possess superior mechanical, thermal and electrical properties, lead to broad applications in composite materials, smart structures, chemical sensors, energy storage and nano-electronic devices. However, the high cost and difficulty in getting large scale, high quality nanomaterials remain challenges. We demonstrate for the first time an affordable and scalable microwave approach for the direct growth of CNT, nanostructured metal oxides on a wide range of substrates, including carbon fibers, glass fibers, Kevlar, and Basalt fibers (Figure 1). The microwave initiated nanomaterial growth will take only 20-30 seconds under the microwave irradiation at room temperature in the air, no need of any inert gas protection, and additional feed stock gases, usually required in CVD approach.

Demonstrated by the preliminary testing through Scanning Electron Microscope (SEM) and Transmission Electron Microscope (TEM), the as-produced CNTs possess hollow centers, with the diameter ranging from 10-100 nanometers, and the length varies from several to tens of micrometers. Although the type of the CNT is not yet determined, it's reasonable to predict the majority of the product should be multiwalled nanotubes (MWNT), based on the diameter range. The image below shows CNT growth on glass fibers. [1,2]

1. X. Zhang, and Z. Liu, *Nanoscale*, **4**, 707 (2012).
2. Z. Liu, and X. Zhang, *et al.*, *Chemical Communications*, **47**, 9912 (2011)

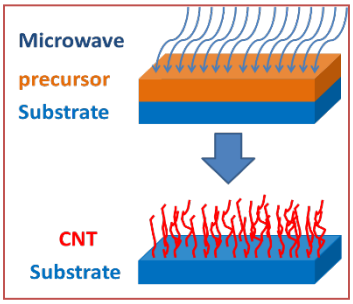

Fig. 1. Microwave initiated carbon nanotube growth.

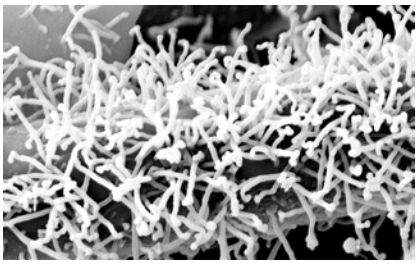

Fig. 2: CNT on glass fibers

GN-19 (Contributed Talk)

Composites and nanocomposites: An application towards wastewater treatment

Ajay Kumar Mishra

Department of Applied Chemistry, University of Johannesburg, Johannesburg, Gauteng, South Africa
Email:amishra@uj.ac.za

Composites and nanocomposites have shown an exemplary performance for uptake of contaminants from wastewater. Different industries discharge different type of pollutants that can cause sever health related problems. With ever growing industrial developments, it is extremely necessary to investigate materials that can effectively remove a broad range of contaminants with high uptake level and low desorption activity to resist secondary pollution. The pollutants in all forms such as heavy metals, organics, dyes and pathogens has been treated with different type of composites and nanocomposites using physicochemical, chemical, photochemical and biological methods. The recent research in this field show an enormous potential by these nanomaterials and nanocomposites. In our filed of research, the polymer composites, nanocomposites and other nanomaterials have been investigated for the uptake of heavy metals and organics and dyes [1-4].

1. E. Vunain, A.K. Mishra and R.W. Krause, *J. Inorganic and organometallic polymers and materials*, **23**, 293 (2013).
2. M. M. Mahlambi, A.K. Mishra, S. B. Mishra, R. W. Krause, B.B. Mamba and A.K. Raichur, *Industrial and engineering chemistry research*, **52**, 1783 (2013).
3. D.S. Dlamini, A.K. Mishra and B.B. Mamba, *Water SA*, **40**, 369 (2014)
4. G. Mamba, XY Mbianda and A.K. Mishra, *Environmental Science and Pollution Research*, **21**, 5597 (2014).

GN-20 (Contributed Talk)

Characterization of Functionalized Multiwalled - Carbon Nanotubes / Kevlar Fiber Hybrid Reinforced Epoxy Composites Using Vacuum Resin Infusion Process

M. Bassyouni[1,2], Saud A. Gutub[3], M.H. Abdel-Aziz[1,4], S.M.-S. Abdel-Hamid[2] and Umair Javaid [1]

[1]Department of Chemical and Materials Engineering, King Abdulaziz University, Rabigh, Saudi Arabia
Email: mbassyonie@kau.edu.sa & migb2000@hotmail.com , web site: http://fer-che.kau.edu.sa/Pages-wordCME.aspx
[2]Department of Chemical Engineering, Higher Technological Institute, 10th of Ramadan city, Egypt
[3]Department of Chemical and Materials Engineering, King Abdulaziz University, Rabigh, Saudi Arabia
[4]Department of Civil Engineering, King Abdulaziz University, Jeddah, Saudi Arabia

Epoxy composites were synthesized in the presence of multiwall functionalized carbon nanotubes (MWCNTs) with weight percentage (0.2- 0.5%). Five layers commercial woven Kevlar fabric (0/90) are prepared for each experimental set. The vacuum resin infusion process (VRI) was followed in the samples preparation. Epoxy-Kevlar fiber composites and MWCNTs hybrid reinforced using VRI technique was investigated. Dynamic mechanical analysis (DMA) was applied as illustrated in figure 1 to measure (a) the storage modulus (E'); (b) the loss modulus(E") (c) loss factor (tan d) ratio E'/E" representing mechanical damping and (d) glass transition temperature of the neat epoxy, epoxy-kevlar composites and nanocomposites. The measurements were carried out using three point bending with frequency of 1 Hz an amplitude of 30 μm and a heating rate of 2 ^{o}C/min from 25 to 170 ^{o}C. Comparison study of commercial epoxy Kevlar composites and Epoxy Kevlar MWCNTs –COOH functionalized (EKMF) composites were carried out using Cambridge Engineering Selector program. Remarkable improvement in mechanical properties of EKMF reflects opportunities for manufacture wind turbine blades with improved mechanical properties.

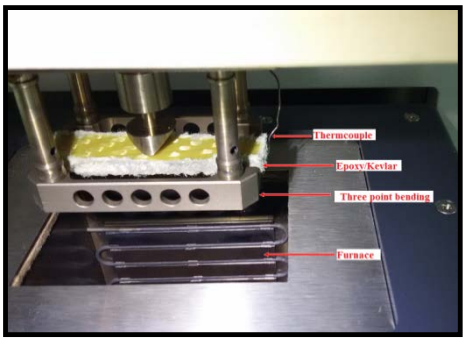

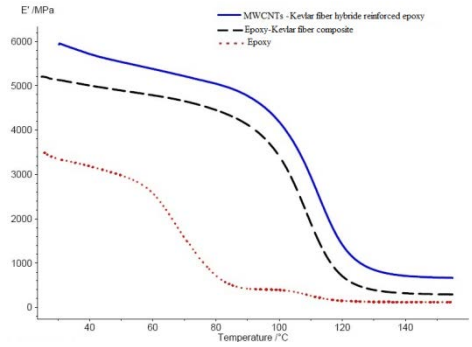

Fig. 1. DMA analysis of neat epoxy and epoxy-Kevlar -MWCNTs nanocomposites using three point bending.

Session MT

METAMATERIALS AND TRANSFORMATION OPTICS

MT-01 (Invited Talk)
Metamaterials for Terahertz Photonics

M. A. Hoeh[1], J. Neu[1,2], K. Schmitt[1,2], and M. Rahm[1]

[1]*Department of Electrical and Computer Engineering and Research Center OPTIMAS, University of Kaiserslautern, Germany*
Email:marco.rahm@eit.uni-kl.de, web site: http://www.eit.uni-kl.de/mmt

[2]*Physics Department and Research Center OPTIMAS, University of Kaiserslautern, Germany*

In the course of the last few years, metamaterials have proven to be almost ideally suited for the design and implementation of tailored optics for THz radiation. In particular, significant progress has been made in the development of passive components as e.g. passive bandpass filters, gradient index lenses and much more [1]. As an intriguing feature, the electromagnetic properties of metamaterials can be actively controlled by electronic or optical means, thus rendering them as a new type of adaptive THz optics [2]. For tuning, semiconductors are embedded into the plasmonic metamaterial structure. Due to a mutual coupling of the electromagnetic fields in the semiconductor and the metamaterial, the hybrid properties of the system can be changed by photo-excitation of free carriers in the semiconductor. So far, most semiconductor embedding techniques rely on the incorporation of thick substrates which suffer from loss and induce disturbing spectral interferences that corrupt the spectroscopic information obtained from THz time-domain spectroscopy.

Here, we present a new approach for the embedding of ultra-thin silicon into plasmonic structures. As an example, we designed and fabricated an ultra-thin, mechanically flexible and optically tunable bandpass filter with a total thickness of 25 µm (see Fig. 1(a)). Fig. 1(b) shows the amplitude transmission of the filter with a peak amplitude transmittance of 85%. Upon optical tuning, the amplitude transmission could be modulated by 98% at an operating frequency of 0.65 THz. Furthermore, the transmission peak blue shifted for increased photo-excitation energy. Our fabrication technique makes use of a combination of thinning processes and bonding of commercially available silicon wafers and is therefore a budget-priced method for fabrication of ultra-thin, optically tunable metamaterial membranes that are mechanically flexible. Since the fabrication method is not linked to a specific metamaterial structure, the presented approach can be generally applied.

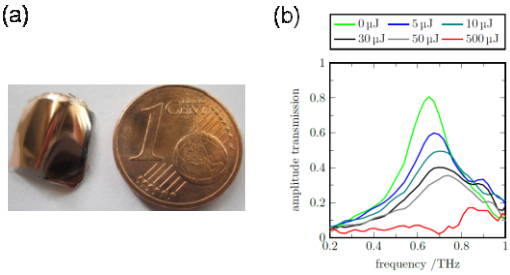

Fig. 1. (a) Metamaterial membrane on the left, (b) measured amplitude transmission spectra for different tuning powers.

1. J. Neu, B. Krolla, O. Paul, B. Reinhard, R. Beigang, and M. Rahm, Opt. Express 18, 27748 (2010).
2. H. T. Chen, W. J. Padilla, J. M. O Zide, A. C Gossard, A. J Taylor, R. D Averitt, Nature 444 (7119), 597-600.

MT-02 (Invited Talk)
Storage and manipulation of electromagnetic waves in metamaterials

Toshihiro Nakanishi[1*], Yasuhiro Tamayama[2], and Masao Kitano[1]

[1]*Department of Electronic Science and Engineering, Kyoto University, Kyoto, Japan*
[*]*Email:t-naka@kuee.kyoto-u.ac.jp*

[2]*Department of Electrical Engineering, Nagaoka University of Technology, Nagaoka, Japan*

Electromagnetically induced transparency (EIT) is a nonlinear optical phenomenon, which renders opaque medium transparent in a narrow spectral region by an incidence of auxiliary light. In addition to the transparency, the group velocity of light is extremely reduced in the transparent region. The slow-light effect has been developed to the storage of light, which can be realized by dynamically modulating the group velocity of light. The EIT effects have been originally investigated in atomic physics. Recently, the realization of the EIT effect with metamaterials composed of artificial structures, or "*meta-atoms*," have attracted much attention in wide frequency regions from microwave to visible light [1-3]. Various types of metamaterials, which implement the functions attributed to the EIT effects such as narrow-band transparency and slow propagation, have been proposed, but the storage of electromagnetic (EM) waves with metamaterials has not been reported.

For storage of EM waves in an EIT metamaterial, it is necessary to dynamically control the properties of the EIT effects in a similar fashion to the case of atomic EIT. In this paper, we propose a tunable EIT metamaterial and demonstrate storage of EM waves in the metamaterial in microwave region [4]. The unit structure of the metamaterial is shown in Fig. 1(a). It contains two lumped elements; a capacitor with the capacitance of C=1.2pF and a varactor diode, whose capacitance C_D can be controlled by bias voltage V. Figure 1(b) represents measured transmission spectra for V=-0.4V and V=-3.6V. A sharp transparent window due to the EIT effect can be observed for V=-0.4V, while there is no transparent region for V=-3.6V.

In a first step of EM storage, the bias voltage is set to be V=-0.4V. In this period, the EM pulse slowly travels in the metamaterial due to the EIT effect. In a next step, the EIT effect is turned off by changing the bias voltage to V=-3.6V, and then the EM energy is stored in the metamaterial. After some period T, the EIT effect is reintroduced, and the stored energy is released into the free space. The solid line in Fig. 1(c) represents an output signal passing through three-layered metamaterial under modulation of the metamaterial states, which are displayed just above the axis. The signal observed before the EIT OFF state corresponds to the part that was not captured. On the other hand, the signal growing after the reintroduction of the EIT effect is the retrieved signal that was stored in the metamaterial during the EIT OFF state. We have also achieved the frequency control of the stored waves and the extension of the storage time by introducing parametric amplification.

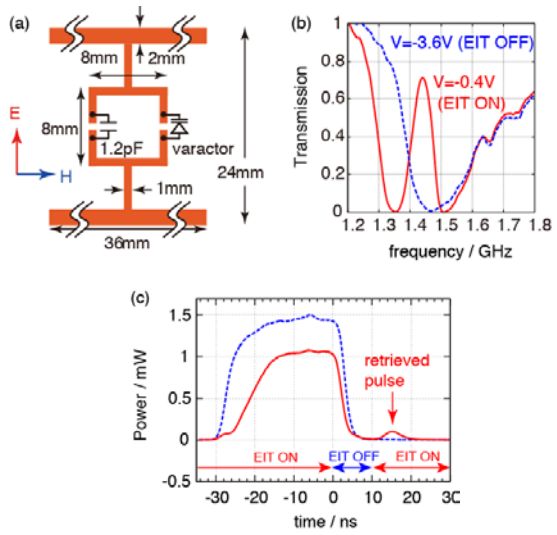

Fig. 1. (a) Unit cell. (b) Transmission spectra for V=-0.4V and V=-3.6V. (c) Demonstration of EM storage.

1. V. A. Fedotov, M. Rose, S. L. Prosvirnin, N. Papasimakis, and N. I. Zheludev, *Phys. Rev. Lett.* **99**, 147401 (2007).
2. S. Zhang, D. A. Genov, Y. Wang, M. Liu, and X. Zhang, *Phys. Rev. Lett.* **101**, 047401 (2008).
3. N. Liu, L. Langguth, T. Weiss, J. Kästel, M. Fleischhauer, T. Pfau, and H. Giessen, *Nat. Mater.* **8**, 758 (2009).
4. T. Nakanishi, T. Otani, Y. Tamayama, and M. Kitano, *Phys. Rev. B* **87**, 161110 (2013).

MT-03 (Invited Talk)
Bistability in nonlinear metamaterials

Sinhara Silva, Jiangfeng Zhou

Department of Physics, University of South Florida,Tampa, Florida, USA
Email: jiangfengz@usf.edu

Nonlinear (NL) effects have an important role in modern photonics, but observed nonlinearities in conventional optical materials are extremely weak. Metamaterials (MMs) have the functionalities to help resolve this problem, i.e. enhance the electromagnetic (EM) field to allow nonlinear response at low input intensity. EM metamaterials are man-made, typically periodically-arranged, metallic resonant structures with size (a) much smaller than the EM wavelength (λ) [1, 2]. With appropriately engineered ε and μ values, MMs can realize fascinating EM properties that do not exist in nature, such as a negative refractive index [3], and EM invisibility cloaking [4]. The nonlinear MM (NL-MM) research began with Pendry's original paper proposing the first MM [5] in 1999, where he showed that the field in the gap of the split-ring resonators (SRRs) can be significantly enhanced. The enhanced field can be used to improve nonlinear effects. Recently, a number of nonlinear phenomena based on the SRRs have been studied including second harmonic generation [6] and four-wave mixing [7]. Here we report a nonlinear metamaterial exhibiting bistability, which is a nonlinear effects enables applications such as optical switching and optical memory.

We designed a nonlinear MM working at microwave frequency range based on a SRR structure with embedded varactor diode in the gap. Our experimental results show that the resonance frequency of the SRR is tunable while applying a separate pump signal. As shown in Fig. 1(a), as we change the intensity of the pump signal, the resonance frequency changes between 0.74 to 0.81 GHz. More importantly, as we increase or decrease the pump intensity, the resonance frequency fellows two different paths, showing a clear hysteresis. In the hysteresis region, the NL-MM exhibits two stable resonance states. The NL-MM stays on either state 1 or state 2 depending on the history of the pump signal. The transition between bistable states can be controlled by the pump signal. For example, as shown in Fig. 1(b), at 0.75GHz, the transition between low transmission (state 1) and high transmission (state 2) can be controlled by the intensity of the pump signal. Thus by applying a programmable pump signal, we are able to switch on and off the transmission response, which writes "0" or "1" into this NL-MM as a memory device.

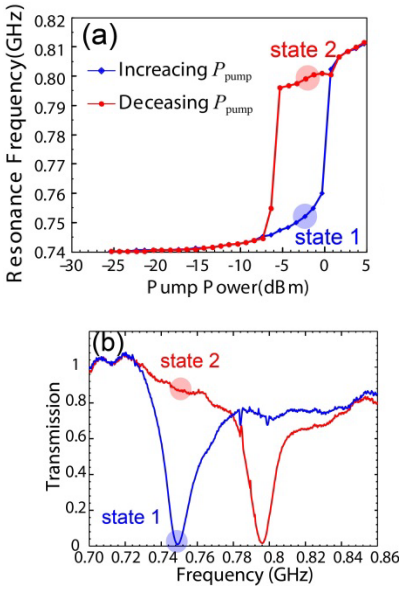

Fig. 1. (a) The resonance frequency of SRR follows different paths depending on increasing (blue) or decreasing (red) the intensity of the pump signal, showing a clear hysteresis. (d) The transmission spectra of the NL-MM show two stable states in the hysteresis region.

[1] D. R. Smith, J. B. Pendry, and M. C. K. Wiltshire, Science **305**, 788 (2004).
[2] C. M. Soukoulis and M. Wegener, Nature Photonics **5**, 523 (2011).
[3] R. A. Shelby, D. R. Smith, and S. Schultz, Science **292**, 77 (2001).
[4] J. B. Pendry, D. Schurig, and D. R. Smith, Science **312**, 1780 (2006).
[5] J. B. Pendry, A. J. Holden, D. J. Robbins, and W. J. Stewart, Ieee T Microw Theory **47**, 2075

[6] A. Rose, D. Huang, and D. R. Smith, Phys Rev Lett **107**, 063902, 063902 (2011).
[7] A. Rose, D. Huang, and D. R. Smith, Phys Rev Lett **110**, 063901, 063901 (2013).

Session AB
ADVANCED NANOMATERIALS AND NANOTECHNOLOGY FOR BIOMEDICAL APPLICATIONS

AB-01 (Invited Talk)
Potential of graphene as nanomaterial for biomedical applications

Subhra Mohapatra

Department of Molecular Medicine, Nanomedicine Research Center, Morsani College of Medicine, University of South Florida, Tampa, FL, 33612, USA

Two-dimensional graphene has received considerable attention in biomedical applications in the past few years owing to its high conductivity, mechanical strength, pH sensitivity and photosensitivity. Graphene shows higher photothermal sensitivity than carbon nanotubes and is highly effective in photothermal therapy for cancer. Graphene has also been used to control fate of stem cell differentiation. However, use of graphene-based nanomaterials in biomedicine is still limited due to poor solubility and potential toxicity. My lab has developed various graphene-functionalized nanomaterials for drug delivery applications and modulation of stem cell differentiation. This presentation will discuss potential of use of chemically reduced graphene oxide for on demand drug release and graphene-based hydrogel for stem cell differentiation and regenerative medicine.

AB-02 (Invited Talk)
Multifunctional nanoparticles for lung cancer therapy

Jyothi U. Menon[1,2], Aneetta E. Kuriakose[1,2], Roshni Iyer[1,2], Shanrong Zhang[3], Masaya Takahashi[3], Zhang Zhang[4,5], Debabrata Saha[4,5], Kytai T. Nguyen[1,2 *]

[1] Department of Bioengineering, University of Texas at Arlington, Arlington, TX 76019, Email: knguyen@uta.edu*

[2] Department of Biomedical Engineering, [3]Department of Radiology, [4]Department of Radiation Oncology, [5]Simmons Comprehensive Cancer Center, The University of Texas Southwestern Medical Center, Dallas, TX, 75390

INTRODUCTION: Lung cancer is a leading cause of cancer-related mortality in the United States, with a quarter of cancer-related deaths in 2014 expected to be attributed to this disease (1). Conventional treatments are limited by temporary remission, systemic toxicity, radio-resistance and lack of specificity (2). To improve combined chemo- and radiation-therapy, we have developed a novel multi-functional dual-responsive nanoparticle (MDNP) consisting of a poly(lactic-co-glycolic acid)–superparamagnetic iron oxide (PLGA-SPIO) core and a poly(N-isopropylacrylamide-carboxymethyl chitosan) (PNIPAAm-CMC) shell to provide a temperature- and pH-sensitive controlled release of radiation sensitizers and chemotherapeutic agents and to assist for imaging and hyperthermia therapy if needed. The MDNP core contains NU7441, a highly potent radio-sensitizer, while the shell contains gemcitabine hydrochloride, an FDA approved chemotherapeutic lung cancer drug. The MDNPs are also surface-conjugated with folic acid (FA) to actively target lung cancer cells.

RESULTS: The MDNPs showed good stability, super-paramagnetic properties, and temperature- and pH-dependent releases of encapsulated therapeutic reagents. In addition, the MTS viability assays revealed that the nanoparticles were cytocompatible with both HDFs and Type 1 alveolar cells up to 1 mg/ml concentration. The presence of folate receptors was confirmed by western-blot and Resonant Sensors Inc. (RSI) Bioassay system. Additionally, the uptake of these nanoparticles by lung cancer cells was dose- and magnetic-field dependent. There were significantly lower IL-6, IL-8 and IL-10 and TNF-α production in cells exposed to MDNPs, indicating that MDNP uptake did not cause significant cell activation or initiate significant inflammatory reactions in the lung cells. Colony forming studies further established that our drug-loaded particles caused

significant cancer cell death *in vitro*. Moreover, visualization of our FA-MDNPs *in vivo* was possible by MRI (Fig.1 A-E). Prussian blue staining of tissue sections from animal studies revealed more iron in tumor sections treated with FA-MDNPs, indicating a higher uptake of the FA-MDNPs at the tumor site (Fig. 1 F-H). These nanoparticles also showed good therapeutic efficacy by slowing down tumor growth when administered in combination with radiation treatment (RT) in nude athymic mice (Fig.1 I-J).

CONCLUSION: Our results thus demonstrate the potential use of FA-MDNPs as theranostic reagents for cancer therapy as they could be visualized using MRI and be able to provide targeted simultaneous radiotherapy and chemotherapy for effective lung cancer treatment.

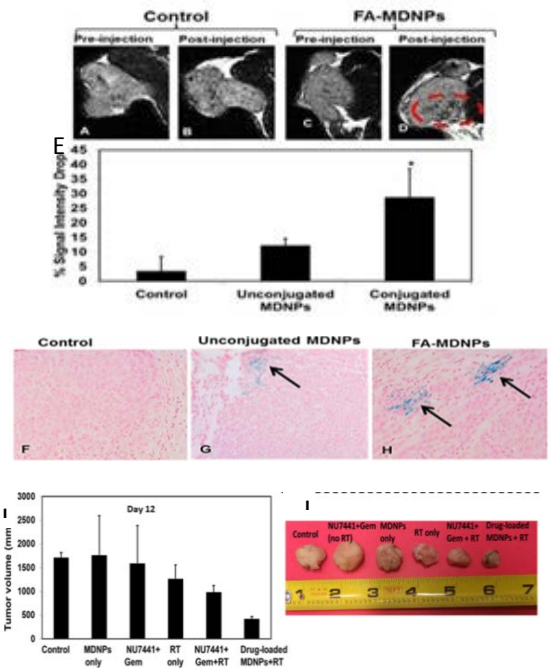

Fig. 1. **(A-D)** MR images show distinct darkening of tumors treated with FA-conjugated NPs 24 h post-injection. **(E)** Significantly higher r2 relaxivity in the FA-MDNPs indicate greater negative contrast due to presence of iron oxide in the tumor, which is supported by Prussian blue staining **(F-H)** showing more blue regions (arrows) in tumors administered with FA-MDNPs indicating the presence of a greater amount of iron oxide in these tumors. **(I-J)** Demonstrate reduction in tissue volume after treatment with drug-loaded MDNPs and RT.

1. Siegel R, et.al. CA: A Cancer Journal for Clinicians; 64(2014).
2. Siegel R, DeSantis C, et al.; *CA: A Cancer Journal for Clinicians*; 62(2012).

AB-03 (Invited Talk)
Study of the Interaction of Superparamagnetic Nanoparticles with Cells: Targeting and Mechanochemical Response

G. U. Lee, D. Kilinc, A. Lesniak, A. Blasiak, B.M. Szydlowska, A. von Kriegsheim, and W. Kolch

University College Dublin, Dublin, Ireland

Regeneration of central nervous system (CNS) axons into hostile environments such as the glial scar that forms after the spinal cord injury is a crucial medical problem. Successful therapeutic approaches will combine pharmaceutical interventions with engineering methods that control the mechanical and chemical environment along the axon path. Axon growth cones are highly motile regions that constantly probe the surrounding tissue and integrate external chemotactic stimuli into motility decisions such as elongation, retraction or turning. While a range of chemical guidance molecules and subsequent signaling pathways are well established, the effect of mechanics on axon elongation is largely unknown. Magnetic nanoparticles (NPs) have been suggested as a means to mechanically stimulate axonal regeneration for therapeutic purposes. Here, we present an experimental model system that enables microfluidic compartmentalization and mechanochemical stimulation of primary CNS neurons. We describe the synthesis and use of multifunctional nanoparticles (NPs) for targeting growth cones towards magnetic-tweezers based force application as well as for studying NP internalization and transport. On one hand, we aim to dissect the roles of signaling pathways in the motility of growth cones, which are pulled towards a source of Sema3A. On the other hand, we aim to characterize NP-neuron interactions in

flow condition, mimicking *in vivo* dynamics.

AB-04 (Invited Talk)
Graphene-based biosensors and graphene synthesis

Kenzo Maehashi

The Institute of Scientific and Industrial Research, Osaka University, Japan
Email:maehashi@sanken.osaka-u.ac.jp

Label-free electrical monitoring of biorecognition events provides a promising platform, which is simpler, less expensive and requires less energy. Rapid testing of different proteins is required in various applications, including clinical diagnostics, environmental testing, food analysis, bioterrorism detection technologies, etc.

Graphene, a single honeycomb-like sheet of carbon atoms, have been intensively investigated in most recent due to its extraordinary high mobility even at room temperature [1]. Since graphene has a perfect two-dimensional structure, electrical characteristics in graphene FETs are very sensitive for modulation of surface potentials in graphene channels. In this study, we have demonstrated highly sensitive electrical detection of chemical and biological molecules based on graphene FETs.

Solution-gated graphene FETs showed good transfer characteristics in buffer solution (Fig. 1) [2]. To selectively detect targets such as ions or protein, receptors were modified on graphene channels [3-7]. Atomic force microscopy images revealed that receptors were successfully immobilized on the graphene channel. The receptor-modified graphene FET showed selective electrical detection of targets. The target concentration dependence of the drain currents revealed that graphene FETs effectively detected targets with concentration from several pM to several hundred nM (Fig. 2).

The chemical and biological molecules were detected with high sensitivity based on graphene FETs. When a different kind of receptor is functionalized on each graphene channel in the graphene FET array, many kinds of biomolecules can be electrically detected simultaneously. Therefore, the graphene FET array can be useful for the fabrication of multiplex hand-held chemical and biological sensors for home medical care.

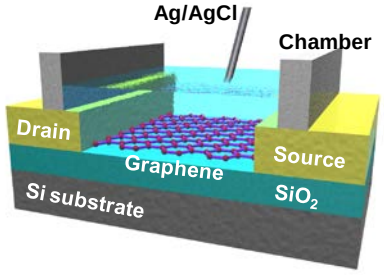

Fig. 1. Graphene-based biosensor.

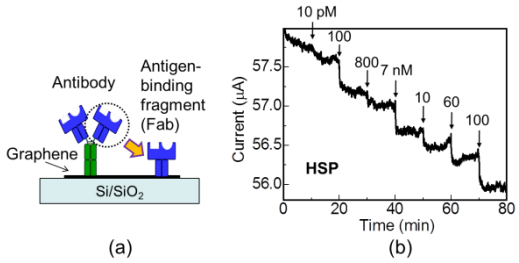

Fig. 2. (a) Fab modified on graphene, (b) target protein concentration dependence.

1. K. Novoselov, A. Geim, S. Morozov, D. Jiang, Y. Zhang, S. Dubonos, I. Grigorieva and A. Firsov, *Science* **306**, 666 (2004).
2. Y. Ohno, K. Maehashi, and K. Matsumoto, *Biosens. Bioelectron*. **26,** 1727 (2010).
3. Y. Ohno, K. Maehashi, Y. Yamashiro, and K. Matsumoto, *Nano Lett*. **9**, 3318 (2009).
4. K. Maehashi, Y. Sofue, S. Okamoto, Y. Ohno, K. Inoue and K. Matsumoto, *Sensors and Actuators* B **187**, 45 (2013).
5. Y. Ohno, K. Maehashi, and K. Matsumoto, *J. Am. Chem. Soc*. **132**, 18012 (2010).
6. S. Okamoto, Y. Ohno, K. Maehashi, K. Inoue, and K. Matsumoto, *Jpn. J. Appl. Phys*. **51**, 06FD08 (2012).
7. N. B. M. Zaifuddin, S. Okamoto, T. Ikuta, Y. Ohno, K. Maehashi, M. Miyake, P. Greenwood, K. B. K. Teo, and K. Matsumoto, *Jpn. J. Appl. Phys*. **52**, 06GK04 (2013).

AB-05 (Invited Talk)
Fundamentals and Applications of Zinc Oxide Nanorods in Enhanced Optical Bioassays

J. Hahm

Department of Chemistry, Georgetown University, Washington, DC, USA
Email: jh583@georgetown.edu, web site: http://chemistry.georgetown.edu/people/hahm.html

This talk presents an overview of our ongoing nanomaterials research, aiming to provide more rapid, sensitive, and accurate detection of genetic and protein markers. Current research efforts pertaining to the synthesis and applications of various nanotubes, nanorods, nanowires, and polymeric nanodomains will be highlighted. Following the introduction of various nanomaterials research in our group, this talk will focus on the remarkably enhanced optical detection of DNA and proteins enabled by the use of nanoscale zinc oxide (ZnO) platforms. Without any chemical or biological amplification processes, ZnO nanorods enable much improved fluorescence detection of biomolecules when compared to other commonly used substrates. Such ultrasensitive detection is possible due to the unique optical properties of ZnO nanomaterials which contributes greatly to the increased signal to noise ratio of biomolecular fluorescence. The easy integration potential of ZnO nanostructures into periodically patterned platforms will be also discussed. Combined with their high sensitivity, this useful capability of ZnO nanorods will promote easy assembly and seamless integration of these materials into multiplexed, high-throughput, optical sensor arrays. Our efforts will be extremely beneficial in accomplishing highly sensitive and specific detection of biological samples involving nucleic acids, proteins and cells, particularly under detection environments involving ultratrace analyte concentrations, large scale population tests, and early biomarker development.

AB-06 (Invited Talk)
Protein Hydrogel Photonic Crystal Sensors for Chemical and Biological Analytes

Sanford A. Asher

Chemistry Department, University of Pittsburgh, Pittsburgh, Pennsylvania, USA
Email: asher@pitt.edu, web site: http://www.pitt.edu/~asher/homepage/index.html

In the work here, we describe sensing motifs that utilize 2-D and 3-D arrays and monolayers of particles embedded onto a molecular recognition polymer hydrogel network. The 2-D arrays alter their visually evident diffraction color because the hydrogel network swells or shrinks in response to analyte concentration changes. We developed 2-D photonic crystals for molecular recognition and chemical sensing applications. We prepared close packed 2-D polystyrene particle arrays by solvent evaporation of an assembling monolayer on a mercury surface or by lifting off the array from a water surface. We then transfer the 2-D arrays onto a hydrogel thin film that showed a hydrogel volume phase transition in response to a specific analyte. This alters the array spacing, changing the array diffraction wavelength. These 2-D array photonic crystals exhibit ultrahigh diffraction efficiencies that enable them to be used for visual detection of analyte concentrations. The 3-D arrays undergo 3-D volume changes to shift the diffraction wavelength. We developed novel protein hydrogels that are highly selective for charged species binding. These protein hydrogels act as a Coulometer that senses binding of individual charged species.

AB-07 (Invited Talk)
Lipid nanotechnologies for drug screening and biosensor microarrays

Steven Lenhert

Department of Biological Science, Florida State University Tallahassee, Florida 32306-4370, USA
Email:lenhert@bio.fsu.edu, web site: http://www.bio.fsu.edu/lenhertgroup/

Lipids are biological molecules that spontaneously self-organize in water to form 5nm lipid bilayers that function as microscopic and sub-microscopic compartments such as cells and organelles. Fabrication of lipid multilayer nanostructures on surfaces allows the recreation of this compartmentalization function in semi-synthetic environments. Encapsulation of different lipophilic materials into fluid lipid multilayer microarrays has applications as sensor arrays [1] and high throughput drug screening microarrays [2]. These applications require lipid multilayer microarrays of controllable thickness that are composed of multiple materials on the same surface. For this purpose we have developed a new mode of micro-contact printing which we refer to as nanointaglio (Figure 1A).[3] Recent progress in the fabrication, characterization and application of lipid multilayer nanostructures on surfaces will be presented.

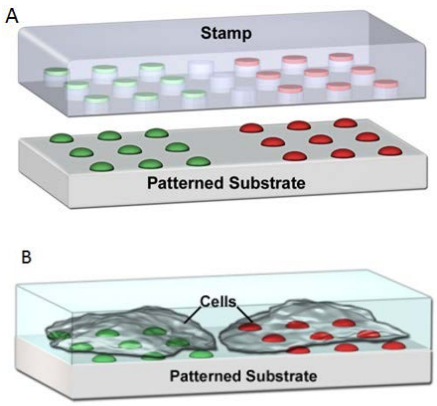

Fig. 1: Lipid multilayer nanostructure fabrication and application. A. Nanointaglio – lipid multilayer micro and nanostructures are produced from a microcontact printing stamp in an intaglio mode where the ink is transferred from the recesses of the stamp resulting in multi-layered structures. B. Microarray screening – cells are cultured on drug-encapsulated lipid multilayer microarrays and used to measure drug efficacy.

References

[1] S. Lenhert, F. Brinkmann, T. Laue, S. Walheim, C. Vannahme, S. Klinkhammer, M. Xu, S. Sekula, T. Mappes, T. Schimmel, H. Fuchs, *Nature Nanotechnology* "Lipid multilayer gratings," 5, 275-279 (2010).

[2] A. E. Kusi-Appiah, N. Vafai, P. J. Cranfill, M. W. Davidson, S. Lenhert, *Biomaterials* "Lipid multilayer microarrays for in vitro liposomal drug delivery and screening," 33, 4187-4194 (2012).

[3] Lowry TW, Kusi-Appiah A, Guan J, Van Winkle DH, Davidson MW, Lenhert S, *Advanced Materials Interfaces* "Materials Integration by Nanointaglio," 1, 5, 1300127, (2014).

AB-08 (Contributed Talk)
The CdS nanocrystals prepared by colloidal solution method for biosensing application

Sachin V.Mukhamale[1], Archana A. Meshram[2]*, Vilas A. Tabhane[1]*

[1]*Department of Physics, Savitribai Phule Pune University, Pune-411007, Maharashtra, INDIA*

[2]*Department of Zoology, Dr. Ambedkar college, Nagpur-440010, Maharashtra, INDIA*

[1]**Email:yash.goaldriven@gmail.com, web site: http://physics.unipune.ernet.in/~Tabhane/*

[2]**Email:drarchanameshram4517@ gmail.com.*

The CdS nanoparticles size with around 1-15 nm are known as nanocrystals, since last few years, they have been used in all the fields from material science to medical. The cadmium sulphide semiconducting nanocrystals were synthesized, by colloidal solution method, by taking cadmium sulphate as a precursor with sodium sulphide or thiourea. The particle growth and size is controlled and tuned by using suitable capping agent. [1].

Synthesized nanoparticles were characterized by ultra violet visible (UV-VIS) spectroscopy, Photoluminescence (PL-spectra), X-Ray diffraction (XRD), scanning electron microscopy (SEM), transmission electron microscopy

(TEM), and fourier transform infrared spectroscopy (FTIR) gives well response. These particles have properties due to which they can be used in biomedical applications, bio sensing applications, etc. This paper contains a general view of current approaches to the synthesis, characterizations and functionalization of quantum dots and their applications in medical sciences.[2].

1. Yu Zou, Dongsheng Li and Deren Yang, *Springer of open journal*, 1 (2011).
2. Matteo Amellia, Rebacca Flamini and Loredana Lateterini, *Journal of American chemical society*, 10129 (2010).

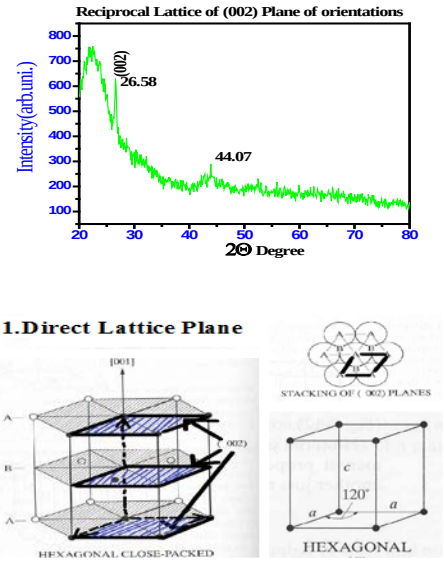

Fig1. X-ray diffraction (XRD) of CdS nanoparticles with reciprocal (002) orientations, HCP structure of direct lattice, stacking of (002) planes and bravice lattice of HCP by colloidal solution method.

AB-09 (Contributed Talk)

Erbium-doped $Y_3Ga_5O_{12}$ nano-garnet as optical nanothermometer in bioassays

M.L. Fanarraga[1], I. Temiño[2], V. Monteseguro[3], S.F. León-Luis[3], J. González[4], R. Valiente[2], V. Venkatramu[5], U.R. Rodríguez-Mendoza[3] and V. Lavín[3]

[1] *Department of Molecular Biology, Universidad de Cantabria-IDIVAL.39011 Santander, Spain.*
[2] *Department of Applied Physics, Universidad de Cantabria. 39005 Santander, Spain.*
[3] *Department of Physics, and MALTA Consolider Team, Universidad de La Laguna.38200 San Cristóbal de La Laguna, Santa Cruz de Tenerife, Spain.*
Email: vlavin@ull.edu.es
[4] *CITIMAC Department, and MALTA Consolider Team, Universidad de Cantabria. 39005 Santander, Spain.*
[5] *Department of Physics, Yogi Vemana University. 516 003 Kadapa, India.*

Nanothermometry aims to extract knowledge of the local temperature of a given system with nanometric spatial resolution and whose dynamics and performance are strongly determined by temperature [1,2]. Nowadays, the emergence of nanotechnology has opened new research lines for the use of the luminescence of rare earth ions as temperature nanosensors. This is especially important in medicine, where the majority of biological microorganisms (cell, bacteria,…) have dimensions of several microns. In this case, the traditional thermal probes cannot be used. Alternatively, rare-earth doped inorganic materials in the nanoscale can be used as nanothermometers for "*in vivo*" and "*in vitro*" biomedical applications. Moreover, they have the advantage of a better biologic compatibility and smaller cytotoxicity compared to quantum dots, and they do not need functionalization to enter in the cells.

Optical nanothermometers are based in different parameters (changes in lifetime, polarization, bandwidth, etc.), although the most widely used is the relative intensities changes of the emissions from two thermalized closed-energy levels. The intensity ratio of the emission peaks is related with the temperature of the nanoparticle environment. In this work we

analyze the temperature dependence of emissions of Erbium(III) in $Y_3Ga_5O_{12}$ nano-garnet, with sizes ranging from 40 to of 60 nm [3], for its use in optical temperature nanosensing. The green luminescence can be obtained by infrared-to-visible energy upconversion processes just in the biological window, of particular interest in medical applications. The dependence of the thermal sensitivity on the Er^{3+} concentration and their application in cells are also analyzed in detail.

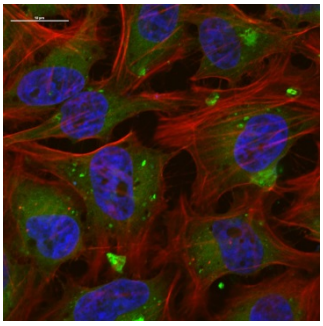

Fig. 1. Confocal microscopy image of HeLa cells containing bright green emitting Er^{3+}-doped $Y_3Ga_5O_{12}$ nanogarnets. The cell nuclei (blue channel), cytoplasms (green channel) and cell cortex (red channel) are labelled.

1. D. Jaque and F. Vetrone, *Nanoscale* **4**, 4301 (2012).
2. C.D.S. Brites, P.P. Lima, N.J.O. Silva, A. Millán, F. Palacio and L. D. Carlos, *Nanoscale* **4**, 4799 (2012).
3. V. Venkatramu, S.F. León-Luis, U.R. Rodríguez-Mendoza, V. Monteseguro, F.J. Manjón, A.D. Lozano-Gorrín, R. Valiente, D. Navarro-Urrios, A. Muñoz and V. Lavín, *J. Mater. Chem.* **22**, 13788 (2012).

AB-10 (Contributed Talk)

Optical Labels Based on Depolarized Light Scattering from Plasmonic Nanoparticles

George Chumanov, John Heckel, Kyle Dukes

Department of Chemistry, Clemson University, Clemson, SC 29634
Email: gchumak@clemson.edu

Optical properties of silver nanoparticles (AgNPs) in the visible spectral range are determined by the excitation of plasmon resonances, the collective oscillations of the free electron density. The frequency of plasmon resonances can be tuned by changing the size, shape, and dielectric environment of the NPs. The excitation of plasmon resonances represents the most efficient mechanism for the interaction of light with matter leading to either absorption or scattering of light. For 100 nm AgNPs, the scattering efficiency in the visible spectral range approaches 90% with the scattering cross section more than six times exceeding the particle's geometric cross section. This fact makes100 nm AgNPs the brightest light scattering objects. Such high light scattering efficiency as well as the outstanding photochemical stability makes AgNPs excellent candidates as optical labels. In addition, AgNPs are capable of depolarizing scattered light: when excited with linearly polarized light they scatter light of the orthogonal polarization [1]. This property is of immense importance for labeling applications because it enables high contrast observation and detection of these labels on zero background. The depolarized scattering diagram is highly anisotropic with well defined directions of the maximum and nearly zero scattering intensity (Fig. 1). When these NPs are allowed to undergo free rotational diffusion in solutions, the scattered light appears 'blinking'. Blinking stops when the NPs bind to targets. Optical labels based on the depolarized light scattering from 100 nm AgNPs were used for cell analysis by flow cytometry and light microscopy [2]. In the case of flow cytometry, labeled cells exhibited two orders of magnitude enhancement of the scattering intensity compared to unlabeled cells. Single NPs attached to cell surfaces via specific

antibody binding were easily seen and discriminated on individual cells when views in a microscope using two crossed polarizers.

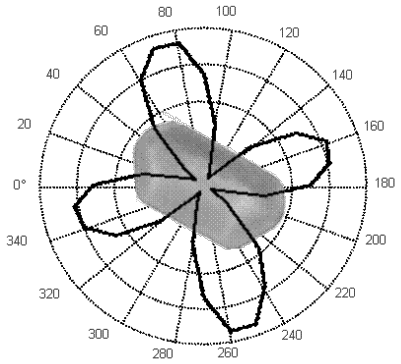

Fig1. Depolarized scattering diagram from a single AgNP. The longest particle axis is about 150 nm.

1. J. C. Heckel, G. Chumanov "Depolarized Light Scattering From Single Silver Nanoparticles" *J. Phys. Chem. C*, **115**, 7261-7269 (2011).
2. K. D. Dukes, K. A. Christensen, G. Chumanov, "Silver Nanoparticles for Optical Labeling of Cells" *Bioanalytical Chemistry*, **458**, 43-48 (2014).

AB-11 (Invited Talk)
Nanomagnetic Remote Control of Cell Signaling and Gene Expression

Jon Dobson

J Crayton Pruitt Family Department of Biomedical Engineering, Department of Materials Science and Engineering, Institute for Cell Engineering and Regenerative Medicine – ICERM, University of Florida, Gainesville, Florida, USA
Email:jdobson@ufl.edu, web site: http://www.bme.ufl.edu/people/dobson_jon

The use of magnetic micro- and nanoparticles for biomedical applications was first proposed in the 1920s as a way to measure the rehological properties of the cytoplasm. Since that time, particle synthesis techniques and functionality have advanced significantly. Magnetic micro- and nanoparticles are now used in a variety of biomedical applications such as targeted drug delivery, MRI contrast enhancement, gene transfection, immunoassay and cell sorting. More recently, magnetic micro- and nanoparticles have been used to investigate and manipulate cellular processes both *in vitro* and *in vivo*.

This talk will focus on our work developing Magnetically Activated Receptor Signaling (MARS) – a magnetic nanoparticle-based technique for activating cell surface receptors and controlling the activity of biomolecules such as growth factors. The technology has applications in regenerative medicine, drug screening and cell engineering. Other nanomagnetic technologies for biomedical applications will also be discussed.

AB-12 (Invited Talk)
Magnetic nanoparticles and the influence of their magnetic properties for biomedical applications

C.L. Dennis[1]

[1]*Material Measurement Laboratory, National Institute of Standards and Technology, Gaithersburg, MD, USA*
Email:cindi.dennis@nist.gov

In recent years, there has been significant progress in both the development of magnetic nanoparticle syntheses and in their applications, especially in biomedicine. With regards to synthesis, it is now possible to highly control the physical properties (size, shape, composition, crystallinity, etc.) of nanoparticles [1-3]. As the physical properties also influence the magnetic properties, this synthetic control now enables tailoring of magnetic nanoparticles for their intended application. With regards to applications, the number of diverse applications is increasing, and our knowledge about what properties have the most influence on the desired outcome, including diagnostic or treatment efficacy is becoming ever more detailed.

Here, we will discuss three different biomedical applications: magnetic resonance imaging (MRI) [4], magnetic nanoparticle hyperthermia [5-6], and magnetic nanoparticle imaging (MPI) [7-8]. For each, we will review the fundamental physics underlying the technique followed by a discussion of the dominant magnetic properties. In MRI, these include interparticle interactions and saturation

magnetization. In hyperthermia, these include interparticle interactions, magnetic anisotropy, and internal magnetic domain structure. In MPI, these include magnetic anisotropy, size, and saturation magnetization. Finally, we will conclude with a discussion on ways to tailor the magnetic properties for each application, while considering the physiological limitations inherent in biomedicine.

1. S. Sun, et al., *J. Am. Chem. Soc*. **126**, 273 (2004).
2. J. Park, et al. *Nature Mater*. **3**, 891 (2004).
3. W.W. Yu, et al, *Chem. Comm*. **20**, 2306 (2004).
4. T. Geva, J. Cardiovascular Magn. Resonance **8**,573–580 (2006).
5. R.K. Gilchrist, et al., *Ann. Surgery* **146**, 596-606 (1957).
6. C.L. Dennis and R. Ivkov, *International J. Hyperthermia* **29**, 715-729 (2013).
7. B. Gleich and J. Weizenecker, *Nature*, **435**, 1214 (2005).
8. D. Eberdeck, et al., *IEEE Trans. Magn*. **49**, 269-274 (2012).

AB-13 (Invited Talk)
Microfluidic Biosensors using Magnetic Nanoparticles

Ioanna Giouroudi

Institute of Sensor and Actuator Systems, Vienna University of Technology, Austria
Email: ioanna.giouroudi@tuwien.ac.at

The development of portable, sensitive and fully automated on-chip diagnostic systems that directly translate the presence of certain bioanalyte (e.g., pathogens, cells and viruses) into an electronic signal gain interest increasingly. In such systems all necessary sample handling and analysis steps are performed within the biochip without the need for established laboratory infrastructure or well-trained personnel [1]. Microfluidic systems are ideally suited for the development of such inexpensive and disposable biochips. They usually consist of a set of units which guarantee the manipulation, detection and recognition of bioanalyte in a reliable and flexible manner. Additionally, the use of magnetic fields for performing the aforementioned tasks has been steadily gaining interest. Some of the merits of such combined systems are that magnetic fields can be well tuned and applied either externally or from a directly embedded solution in the biochip. In combination with these applied magnetic fields, magnetic nanoparticles (MNPs) are utilized. The advantages of MNPs, among others, are the possibility of manipulating them inside microfluidic channels by utilizing high gradient magnetic fields, of detecting them by integrated magnetic microsensors, and the fact that they can be used to label bioanalyte by means of surface modification and specific binding. Their multi-functionality is what makes them ideal candidates as the active component in miniaturized on-chip biosensing systems [2].

In this paper, we present a simple microfluidic diagnostic system which combines magnetic separation and either optical or magnetic detection of pathogens without flow, without the need to use fluorophore or quantum dot labels and without complicated microfluidic structrures (see Fig. 1). We also present a microfluidic system for trapping and counting of rare circulating tumor cells (CTCs). Preliminary experiments for both systems will be presented and discussed.

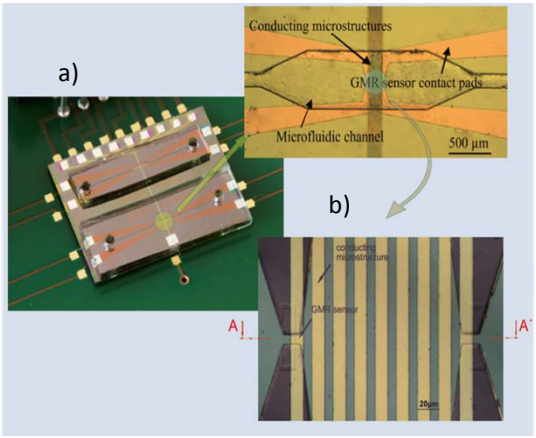

Fig. 1. Photograph of the developed diagnostic microsystem consisting of the GMR sensors, the conducting microstructures and the microfluidic channels b) Microscope photograph of the GMR

sensor with the conducting microstructures and the microfluidic channel.

References

1. I.Giouroudi and F. Keplinger, *Int. J. Mol. Sci.* **14**(9), 18535; doi:10.3390/ijms140918535 (2013)
2. G. Kokkinis, F. Keplinger and I. Giouroudi, *Biomicrofluidics* **7**, 054117; doi: 10.1063/1.4826546 (2013)

AB-14 (Invited Talk)
Magnetically Barcoded Microcarriers Detection with TMR and Asymmetric Giant Magneto-Impedance sensors

Pratap Kollu[1], Adrian Ionescu[1], David M. Love[1], C. Cimorra[1], Justin Llandro[1] and C.H.W. Barnes[1]

[1]*Cavendish Laboratory, University of Cambridge, Cambridge CB3 0HE, UK*
Email:ai222@cam.ac.uk, web site: http://www.tfm.phy.cam.ac.uk/

We are working towards a novel lab-on-a-chip technology based on suspended magnetically encoded microcarriers [1,2]. Our newest generation of microcarriers consist of up to fourteen individual magnetic elements encapsulated within a SU8 polymer and gold layer (Fig. 1.b), which both provide routes to bio-functionalization through surface epoxide groups and thiol chemistry [3]. The writing/reading of the digital magnetic codes is obtained through coercivity engineered magnetic elements (Fig. 1.a), while the detection is performed by means of a tunneling magneto-resistance (TMR) sensor. The global address-ability of these bits is achieved by utilizing magnetic shape anisotropy. The possibility of attaching different fluorescent labels to each side of the microcarriers enables a positive control in binding assays. Potential applications for this platform range from DNA/protein analysis for genotyping and point-of-care diagnostics to drug development and combinatorial chemistry.

Alternative magnetic detection platforms include asymmetric giant mageto-impedance (GMI) thin film sensor [4,5], which possess a high sensitivity and are currently under development. Films are deposited at room temperature using dc magnetron sputtering. Test sensor are patterned by UV photo-lithography and lift-off processes to form strips 0.2 mm wide and 10 mm long on glass/silicon wafers. The films consist of a symmetrical multilayer structure of the following composition: Ti(10 nm)/NiFe(5 nm)/IrMn(15 nm)/NiFe(40 nm)/Cu(100 nm)/NiFe(40 nm)/IrMn(15 nm)/NiFe(5 nm)/Ti(10 nm). The thin film structure gives a significant GMI response as will discussed. Linear GMI behaviour can be obtained around zero external field by tuning the frequency, without the need for external biasing fields or additional coils.

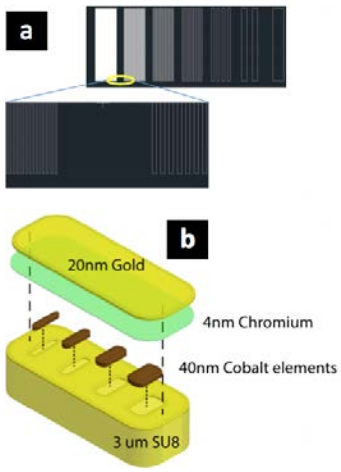

Fig. 1. **a**, Illustration of composite magnetic elements. **b**, Constituents of bi-functional microcarriers.

1. J. Llandro *et al.*, *Medical & Biological Engineering & Computing* **48**, 977 (2010).
2. B. Hong *et al.*, in "Biomagnetism and Magnetic Biosystems Based on Molecular Recognition Processes", edited by J.A.C. Bland and A. Ionescu, *AIP Conf. Proc.* **1025** (2008).
3. K.N. Vyas *et al.*, Lab on a Chip **12**, 5272 (2012).
4. C. Garcia *et al.*, Applied Physics Letters 96, 232501 (2010).
5. S.S. Yoon, P. Kollu *et al.*, IEEE Trans. Magn. 45, 2727(2009)

AB-15 (Invited Talk)
The Next Generation of Multifunctional Magnetic Nanoparticles for Biomedical Engineering Applications

Hafsa Khurshid, Manh-Huong Phan, Pritish Mukherjee, and Hariharan Srikanth

Physics Department, CIFM, University of South Florida, Tampa FL 33620
Email:khurshid@usf.edu

Magnetic nanostructures form the basic building blocks in various technological and biomedical applications, as well as energy storage. When used as a potential multifunctional clinical tool, they can provide cancer cell detection in magnetic resonance imaging (MRI) contrast agents as well as therapy by targeted drug delivery or local hyperthermia generation by heating the cancer cells in the vicinity of nanoparticles via an alternating magnetic field. These applications rely on their spin structure and spin dynamics that can be easily tuned by controlling their microstructure, size, shape and morphology. We have developed a novel chemical synthesis technique of decomposing organometallic compounds at high temperature, to manipulate these parameters. We demonstrate that the nanoparticles can be grown in either isotropic or anisotropic shapes, depending upon a chemical reaction scheme that is controlled kinetically or thermodynamically [1]. A large class of monodisperse core/shell and hollow nanoparticles with controlled shapes (sphere, cube, octopod, triangle, etc.) has been successfully synthesized [1-3]. Inductive heating experiments performed on these nanoparticles reveal that they are very promising candidates for enhanced magnetic hyperthermia. We have also exploited the intriguing phenomena of exchange bias and surface spin disorder in the core/shell and hollow morphologies, using a wide range of experimental probes such as DC and AC magnetometry, and radio-frequency transverse susceptibility, as well as theoretical models [3-6]. In this talk we will mainly discuss about the novel synthesis techniques and related parameters for the growth of magnetic nanoparticles with unique morphologies, as well as the important roles of surface spin disorder and finite size effects in controlling exchange bias in these nanostructures for future spintronics and biomagnetics applications.

Acknowledgement: our research was supported by USAMRMC through grant numbers W81XWH-07-1-0708 and W81XWH1020101/3349.

References

1. H. Khurshid and H. Srikanth et al. *Nanoscale* 5 (2013) 7942-7952.
2. H. Khurshid, and H. Srikanth et al. *Journal of Materials Chemistry C* 1 (2013) 6553.
3. H. Khurshid, and H. Srikanth et al. *Applied Physics Letters 101* (2012) 022403.
4. S. Chandra, H. Khurshid and H. Srikanth et al. *Physical Review B* 86 (2012) 014426.
5. H. Khurshid and H. Srikanth et al. *Applied Physics Letters 104* (2014) 072407.
6. B. Duong, H. Khurshid and M. H. Phan et al. *Small 10* (2014) 2840.

AB-16 (Contributed Talk)
New Class of Magnetic Bioceramics for Biomedical Applications

A.S.Kamzin[1], M.V.Tkachenko [2], K.Romachevsii[1]

[1]Ioffe Physical-Technical Institute of RAS, St.-Petersburg, Russia
Email: kamzin@mail.ioffe.ru web site: http://membership.sciencepublishinggroup.com/kamzin

[2]Karazin Kharkiv National University, Kharkiv, Ukraine

Magnetic nanoparticles, due to their properties, are attracting attention for applications in the medical and biological fields. One of the cancer treatment research directions is magnet hyperthermia with the help of biocomposite consisted of bioactive component, usually it is bioglass or ceramics based on calcium phosphates and ferrimagnetic particles. Such implant introduced in the malignant tissue makes it possible to heat it without wire connections up to the temperatures dependent on the applied power of the external alternating

magnet field. Generating temperatures of 42 °C can damage and kill cancer cells, usually with minimal injury to normal tissues.

In this report we present the first experimental ceramic implants based on calcium phosphates, modified by hexagonal ferrites M-type magnetic particles for strengthening the processes of osteogenesis in human hard tissue which have been created and tested in medical and biological experiments. The heat generation effect in alternating magnetic fields is appropriate for performing magnetotherapy treatment. Implants were compounds of apatite structure consisted of carbonated hydroxyapatite (CHA) as a bioactive matrix and biocompatible ferrimagnetic oxide $BaFe_{12}O_{19}$ as a magnetic component which content in the composite ceramic was from 10 to 50 wt%.

The improved bioactive properties and biocompatibility of the magnetic bioceramics are due to chemical and structural similarity of the matrix with mineral component of bone that promotes formation of strong chemical bonds between the implant and living tissue on the bone-implant boundary. The magnetic properties required for optimal magneto therapy and thermal effects were achieved by introducing microparticles of the M-type ferrites magnetic particles. It was found that the Curie point of ceramics with a concentration of the magnetic phase above 20 wt.% is the same as that of barium ferrite. The $BaFe_{12}O_{19}$ particles plays role of thermoseeds. This is confirmed by the Mössbauer data.

It is shown that a significant concentration of magnetic filler has not substantially influenced the phase composition of the bioactive matrix of CHA both on the structural and molecular levels; therefore, the created ceramics has preserved the high bioactive properties. The obtained bioceramics gives promises for application in medicine as thermoseeds at hyperthermal treatment. The resulting composite ceramic is a new class of magnetic bioceramic, combining excellent bioactivity of CHA and high magnetic characteristics of M-type hexaferrite.

AB-17 (Invited Talk)

Glucose-driven "Organic Engine" with enzyme membrane for autonomous drug release system as self-sustainable artificial pancreases for diabetes

H. Takagi[1], M. Munkhjarga[1], K. Toma[1], T Arakawa[1], K Mitsubayashi[1]

[1]*Institute of Biomaterials and Bioengineering, Tokyo Medical and Dental University, Tokyo, Japan*
Email:m.bdi@tmd.ac.jp

INTRODUCTION

In living being, constituent levels of body fluid are self-regulated by functions of some organs (i.e. blood sugar level by pancreas with insulin release). Many glucose sensors have been developed for monitoring blood sugar level in diabetic in order to inject the insulin by hand or electric power. On the other hand, we have reported a chemo-mechanical energy conversion device, which induced pressure change dependent on glucose concentration. In this study, a self-regulation system of glucose level was developed using chemo-mechanical drug release function with bio-energy of glucose.

METHODS

A self-regulation system of glucose level consisted of chemo-mechanical decompression unit and periodic drug release unit (Fig). In the decompression unit, a glucose oxidase (GOD) immobilized membrane functioned as a separating diaphragm between liquid and gas cells. The GOD enzyme reaction with glucose in the liquid cell would induce the oxygen consumption, thus resulting in the active decompression in the gas cell. The periodic drug release unit also had other gas and liquid cells, which connected with those of the decompression unit, respectively. After drawing drug into a pre-chamber by the decompression, the pressure would return periodically to the atmosphere pressure by a pressure regulator, and the drug simultaneously release to the liquid cell with glucose solution. In this study, glucose dehydrogenase (GDH) instead of insulin was used for the glucose decomposition with NAD+.

RESULTS and DISCUSSION

By circulating glucose solution in the liquid cell, the chemo-mechanical decompression unit showed the periodical pressure change (gradual decrease and quick return) between 0 to -500 Pa. The periodical GDH release induced the glucose decomposition in the liquid cell. The glucose decrease means the energy deficiency for the decompression, thus successfully self-regulating the glucose level without any power. This is a first artificial system for bio-energetic self-regulation of chemical level.

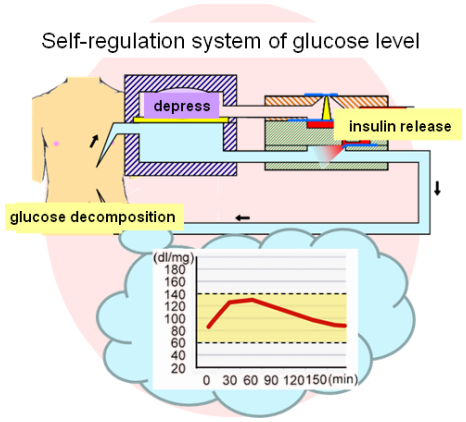

Fig. 1. Schematic diagram of autonomous drug release system with glucose-driven "Organic Engine".

1. R. Kato, M. Munkhjargal, D. Takahashi, T. Arakawa, H. Kudo, K. Mitsubayashi, *Biosensors and Bioelectronics*, 26, 1455-1459, (2010)

AB-18 (Invited Talk)

New insights into the picosecond dynamics of water and solvated proteins

N. Q. Vinh

Physics Department, Virginian Tech, Blacksburg, Virginia 24061, USA
Email:vinh@vt.edu, web site: http://www.phys.vt.edu/~vinhnq

According to computer simulations, the slowest, largest-scale harmonic motions of solvated biomolecules and the relaxation times of water occur on the picosecond regime. Experimental methods for the characterization of these collective vibrational modes, however, have been severely lacking. In response, I have developed the world's highest precision, highest sensitivity and highest frequency terahertz-dielectric spectrometer. Operating over the frequency range from 4.5 GHz up to 1.12 THz, this spectrometer provides an unparalleled ability to probe the dynamics of water and aqueous proteins over the 100 fs to 10 ps timescale. Using this spectrometer to characterize the collective dynamics of solvated lysozyme I find that the collective vibrational modes of this protein are characterized by a hitherto unrecognized cutoff at 250 GHz (corresponding to 0.6 ps) arising due to the finite size of the molecule. Employing an effective medium approximation to describe the complex dielectric response of the protein in solution I find that each molecule is surrounded by a tightly held layer of 164 ± 5 water molecules that behave as if they are an integral part of the protein. Following studies of the spectra of water and of aqueous salt solutions I identify three Debye relaxations with the characteristic times of 8.56, 1.1 ps and 179 fs (at 25˚C). Of note, while the relative strengths of these relaxation modes depend in a systematic way on solute concentration, their relaxation times do not. The observation sheds new light on the femtosecond to picosecond collective dynamics of water and solvated biomolecules.

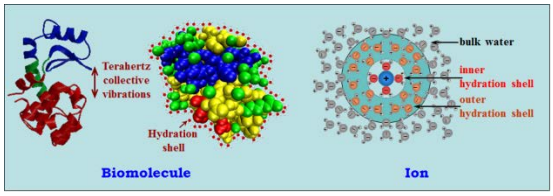

AB-19 (Invited Talk)
Single cell endoscopy

Surya Cheemalapati,[1] Mikhail Ladanov,[1] AnnaPyayt[1*]

[1]*Chemical and Biomedical Engineering Department, University of South Florida, Tampa, FL, USA*
Email:pyayt@usf.edu, web site: http://www.pyayt.com

Currently analysis of individual cells instead of cell colonies is a growing area of research, and one of an important directions in this area is a single-cell endoscopy [1]. Information obtained from a single cell response to a stimulus can be quite different from an average response of the cell colony [2]. This difference can be caused by variety of reasons including the phase of cell division [3], stochasticity, or noise, in gene expression [4-6], ion concentrations [7] and many others. Use of nanoscale probes that can be inserted inside of an individual cell and analyze the content is necessary for the detailed single-cell analysis and for better understanding real time biochemical processes happening in the cell. We proposed a new design of a single-cell endoscope [1] based on combination of optical fiber, nanowire waveguide and a plasmonic coupler between those two (Figure 1).

One of the reason to use nanowires for single-cell endoscopy is that they are minimally invasive, and based on our experiments cells can function well at least for 50-60 min after initial insertion. This is a long enough period of time to conduct many interesting single cell studies. Since coupling of light in the nanowire is a very challenging task, we conducted 3D FDTD simulations and maximized coupling efficiency using plasmonic field enhancement.

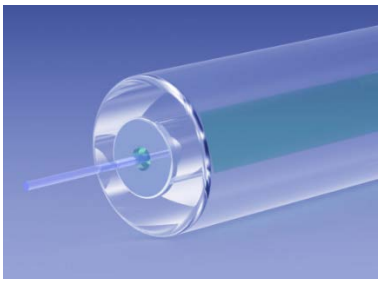

Fig. 1. Model of a nano-scale endoscope.

1. Mikhail Ladanov, Surya Cheemalapati, and Anna Pyayt,, *Optics Express* **21** (23), 28001 (2013).
2. H. Andersson and A. van den Berg, *Current Opinion in Biotechnology* **15**, 44 (2004).
3. J. E. Ferrell and E. M. Machleder, *Science* **280**, 895 (1998).
4. J. S. Marcus, W. F. Anderson, and S. R. Quake, *Anal. Chem.* **78**, 3084 (2006).
5. W. J. Blake, M. KÆrn, C. R. Cantor, and J. J. Collins, *Nature* **422**, 633 (2003).
6. M. B. Elowitz, A. J. Levine, E. D. Siggia, and P. S. Swain, *Science* **297**, 1183 (2002).
7. M. N. Teruel and T. Meyer, *Science* **295**, 1910 (2002).
8. S. Lindström and H. Andersson-Svahn, *Biochimica et Biophysica Acta (BBA) - General Subjects* **1810**, 308 (2011).

Session GM
EMN GENERAL WORKSHOP ON MATERIALS

GM-01 (Invited Talk)
High Pressure-Induced Polymorphic Transformation of Maleic Hydrazide

Kai Wang, Bo Zou*

State Key Laboratory of Superhard Materials, Jilin University, Changchun 130012, P. R. China
E-mail: zoubo@jlu.edu.cn

Maleic hydrazide, a unique example of polymorphic structures, was analyzed at pressure up to 5 GPa using *in situ* high pressure Raman scattering and synchrotron X-ray diffraction techniques. Changes in the Raman spectra at 2 GPa indicates that a pressure-induced phase transition is occurring. The transition was further analyzed with angle dispersive X-ray diffraction, which demonstrated that maleic hydrazide underwent a polymorphic transformation from the form III to the form II. Moreover, the observed transformation was partially reversible when the system was brought back to ambient pressure. This work suggests that the high pressure polymorphic transformation is caused by changes in the hydrogen-bonded ribbons which lead to supramolecular rearrangements in the crystal structure.

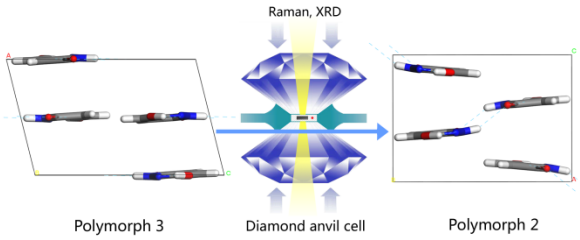

Fig1. Polymorphic transformation of maleic hydrazide under high pressure.

1. K. Wang, J. Liu, K. Yang, B. B. Liu, and B. Zou,* *The Journal of Physical Chemistry C* **118**, 8122 (2014).
2. K. Wang, J. Liu, K. Yang, B. B. Liu, and B. Zou,* *The Journal of Physical Chemistry C* **118**, 18640 (2014).

GM-02 (Contributed Talk)
Effects of flexible spacing coating on macroscopic supramolecular assembly

Mengjiao Cheng, Feng Shi*

State Key Laboratory of Chemical Resource Engineering, Beijing University of Chemical Technology, Beijing, China USA
Email:kisswind22@163.com, web site: http://www.shifgroup.com/en

Macroscopic supramolecular assembly is a promising bottom-up strategy for manufacturing macroscopic, ordered structures for various applications, especially in biological field as complex scaffold and template for induced cell differentiation. However, except for reports related to microscale rigid objects or millimeter-scale soft materials, there are no reports on the supramolecular assembly of rigid building blocks with macroscopic features because of surface effects on large building blocks. Therefore, we propose the concept of a 'flexible spacing coating' under the host-guest layer not only to compensate for the surface roughness of large building blocks but also to provide a flowing coating for the assembly process that leads to complementary assembly through supramolecular host-guest interactions. The macroscopic assembly mechanism is based on multivalency; hence, the flexible spacing coating deforms when two surfaces contact, adapts to the surface morphology of the substrates, increases the interactive chances, and enhances the apparent binding constant. Our hypothesis was proven by introducing highly competitive guest molecules to the assembled system, which led to disassembly. Moreover, we developed a quantified characterization method for the *in situ* measurement of the dissociating force between the building blocks; we demonstrated that the dissociation force for the host-guest pair with flexible spacing coatings was 16-fold larger than that for the pair without the flexible spacing coating.

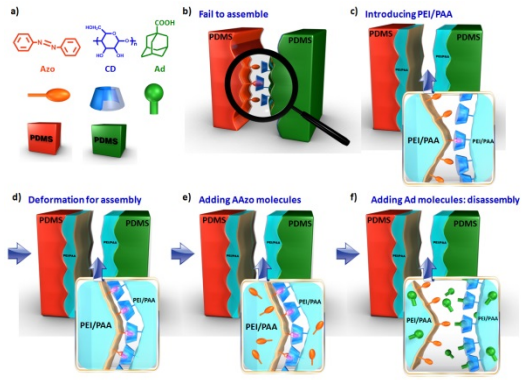

Fig. 1. Supramolecular assembly of macroscopic building blocks through multivalency based on the flexible spacing coating of PEI/PAA multilayer.

1. M. J. Cheng, F. Shi, J. S. Li, Z. F. Lin, C. Jiang, M. Xiao, L. Q. Zhang, W. T. Yang and T. Nishi, *Adv. Mater.* **26**, 3009 (2014).
2. M. J. Cheng, H. T. Gao, Y. J. Zhang, W. Tremel, J.-F. Chen, F. Shi and W. Knoll, *Langmuir* **27**, 6559 (2011).
3. M. J. Cheng, G. N. Ju, Y. W. Zhang, M. M. Song, Y. J. Zhang and F. Shi, Small DOI: 10.1002/smll.201400922 (2014).
4. M. J. Cheng, Q. Liu, Y. M. Xian and F. Shi, *ACS. Appl. Mater. Interfaces* **6**, 7572 (2014).

GM-03 (Invited Talk)
High pressure Supramolecular Chemistry: Pressure Induced Assembly and Their Functions

Bo Zou[1]

[1] *State Key Lab of Superhard Materials, Jilin University, Changchun 130012, China*
Email: zoubo@jlu.edu.cn
Web site: http://nlshm-lab.jlu.edu.cn/show.aspx?id=39893e96-3af0-470a-80df-2588f8863eae

Pressure is an essential physical method in exploring new structures and new properties of condensed materials. Compared to covalent bonds, high pressure has more significant influences on noncovalent bonds. Recently, we systematically studied the high pressure behavior of supramolecular systems based on noncovalent bonds and the cooperative effects between different noncovalent bonds. [1] We found some new supramolecular assembly systems can be formed under high pressure.

At the same time, investigations of high pressure phase of functional supramolecular materials are helpful to obtain new functional materials. For example, we can prepare the high density phase of energy materials using high pressure technique.[2] Moreover, high pressure is a powerful tool to fabricate and analyze the polymorphism phenomenon of organic crystals. Furthermore, we can achieve high pressure chemical reaction based on supramolecular pre-organization. In addition, we also studied the relationship between high pressure and milling effects on organic luminescent materials.[3]

Acknowledgments:
This talk is supported by NSFC (91227202) and RFDP (20120061130006).

References:

[1] S. Li, K. Wang, M. Zhou, Q. Li, B. Liu, G. Zou, B. Zou, *The Journal of Physical Chemistry B*, **115**, 8981 (2011); Q. Li, S. Li, K. Wang, W. Li, J. Liu, B. Liu, G. Zou, B. Zou, *The Journal of Chemical Physics*, **137**, 184905 (2012)

[2] R. Wang, S. Li, K. Wang, D. Duan, L. Tang, T. Cui, B. Liu, Q. Cui, J. Liu, B. Zou, G. Zou, *The Journal of Physical Chemistry B*, **114**, 6765 (2010); S. Li, Q. Li, K. Wang, X. Tan, M. Zhou, B. Li, B. Liu, G. Zou, B. Zou, *The Journal of Physical Chemistry B*, **115**, 11816 (2011); S. Li, Q. Li, K. Wang, M. Zhou, X. Huang, J. Liu, K. Yang, B. Liu, T. Cui, G. Zou, B. Zou, *The Journal of Physical Chemistry C*, **117**, 152 (2013)

[3] Y. Dong, B. Xu, J. Zhang, X. Tan, L. Wang, J. Chen, H. Lv, S. Wen, B. Li, L. Ye, B. Zou, W. Tian, *Angewandte Chemie International Edition*, **51**, 10782 (2012); H. Yuan, K. Wang, K. Yang, B. Liu, B. Zou, *The Journal of Physical Chemistry Letters*, **5**, 2968 (2014)

GM-04 (Invited Talk)
Heavy Metals fluoride glasses and fibers

Mohammed Saad, Ph.D.

Glass & Fiber Senior Scientist
Thorlabs, Newton, USA
msaad@thorlabs.com; www.thorlabs.com

There are many infrared materials available, but no one of these materials can fulfill all infrared application needs. Engineers have to make some compromise when choosing the right material for the right application. Heavy metal fluoride glasses are among the infrared materials list. They show some outstanding properties that make them the material of choice for some applications. They are the only material that transmits light from the UV to the mid-infrared. They can be used in applications as diverse as medical, military, high power delivery, fiber lasers and amplifiers, supercontinuum sources, sensing and spectroscopy. Tremendous progress has been made in fluoride fiber technology during the last two decades. Almost all type of fibers have been made with fluoride glasses, including single mode multimode fibers, rare-earth doped fibers Some exotics shapes have been made as well, such as hexagonal, D-shapes, square…. High quality optical fibers and assemblies are now available and being used in very demanding environment. So far fluoride fiber technology is the second mature technology after silica. The current commercial fluoride fibers have low loss, the lowest loss among all infrared optical fibers, and high strength. The loss is ranging from 50 to 100 dB/km and the strength from 50 to 100 kpsi.

The presentation will focus on the latest development in fluoride fiber technology and applications.

GM-05 (Contributed Talk)
Properties of Zigzag Silicene Nanoribbons

Nam B. Le[1], Lilia M. Woods[1]

[1]Department of Physics, University of South Florida, Tampa, FL, USA
Email: nble@mail.usf.edu, web site: http://shell.cas.usf.edu/~lwoods2/index.htm

Silicene has been recently considered as a great replacement for graphene in practical electronic applications due to its compatibility with the current silicon-based electronics. Silicene nanoribbons are studied using *ab initio* simulations methods. Our density functional theory calculations show that the electronic and magnetic properties of these structures are influenced by several factors, such as the magnitude of the width, edge spin polarization, spin-orbit coupling, and extended topological defects. It is obtained that while defect free silicene nanoribbons experience an antiferromagnetic-ferromagnetic transition as a function of the width, all defective nanoribbons are ferromagnetic. At the same time, the spin-orbit coupling role is significant as it leads to spin dependent energy gaps in the electronic structure. The origin of edged spin polarization is also studied in terms of the balance between the exchange-correlation and kinetic energy contributions. The uncovered unique spin-dependent properties may be useful for the application of silicene nanoribbons in spintronic applications.

GM-06 (Invited Talk)
A Band Alignment of Tunnel-FET Heterojunction by Internal Photoemission

Nhan V. Nguyen

Semiconductor and Dimensional Metrology Division
Physical Measurement Laboratories,
National Institute of Standards and Technology,
Gaithersburg, MD 20899, USA

In this talk, I will provide an overview of internal photoemission (IPE) and the significance

of this technique when combined with spectroscopic ellipometry (SE) to investigate the interfacial electronic properties of semiconductor heterostructures. The principles of IPE will be described and discussed leading to a simple interpretation and modeling of electron and/or hole emission over the interface barrier. Not until recently, IPE and SE have become important metrology tools in electronic band offset characterization. A few material systems that are technologically important will be used to demonstrate the power of the IPE technique. In the early day of high-k search to replace SiO_2 in the traditional CMOS, we were successful to determine the interfacial energy barriers of an important ternary metal stack on a high-k/oxide stack. However, I will focus most on a system of materials of recent great interest to tunnel field effect transistor application. I will show a unique way to measure the energy band offset at heterojunction by manipulating the light absorption under visible-ultraviolet internal photoemission. Recently, we have made a significant progress in IPE measurement technique by exploiting the unique properties of graphene to detect hole injection resulting the determination of the small band offset of a broken gap of a tunnel FET structure. Lastly, I will discuss a direct measurement of the Dirac point, the Fermi level, and the work function of graphene by a unique optical-cavity enhanced test structure.

GM-07 (Invited Talk)
Silicon Nanoparticles as Potential Light Emitters: Synthesis, Separation by Color, and Applications

Naoto Shirahata[1,2]

[1]WPI-MANA, National Institute for Materials Science (NIMS), 1-2-1 Sengen, Tsukuba 305-0047, [2]PRESTO, Science and Technology Agency (JST), 4-1-8 Honcho Kawaguchi, 332-0012, Japan E-mail: shirahata.naoto@nims.go.jp

Optical use of colloidal nanoparticles of silicon (npSi) and germanium (npGe) has gained increasing attention for its possible contributions to building a sustainable society that ideally uses resources and energy with high efficiency without causing damage to the environment or human health. Full control in nanostructures such as crystalline phase, surface and size of the NPs allows the tuning the color in a very broad range of emission wavelength from near-UV (300 nm~) through full color of visible to near-IR (~1100 nm for npSi and ~1300 nm for npGe). However, the story does not end here. Unlike the direct bandgap semiconductors, PL origin of npSi is still not very clear and under debate. The yet-to-be-defined mechanism becomes a big obstacle for ease in access to emission tuning. As a result, research on luminescent Si is a matter for fundamental study. A lot of reports regarding the emission is very interesting counter-intuitive and even confusing and to reach in a unified conclusion. From the reported literatures emission of npSi can be divided into two distinct regions. First region is in the emission range from near-UV to Aqua (λ_{em}= 300−500 nm), and another region is Green to NIR (λ_{em}= 500−1100 nm) region. There is a discontinuity or wall between these two regions. These two kind of different emission zone, covered by npSi are being prepared by fundamentally different preparation approaches. Unfortunately, there are no reports which break this barrier or discontinuity smoothly by a single preparation method. In the first decade after discovery, the emission from silicon and its related-research had been almost restricted in the red-NIR region. Emissions in the Red-NIR were tuned with size of the npSi covered with amorphous silica shells. In the later time, npSi emitting the lights in the NUV-Blue-Aqua region have also been emerging out, respectively. While the Red-NIR emissions are commonly believed to appear due to the quantum confinement effect, the NUV-Blue emission is still controversial. According to the previous papers, there are a variety of factors that affect the emission properties of npSi, such as core size, stabilizers including surface monolayers, defect states, and interface of oxide-shell/silicon-core. All the phenomena must be considered in order to get an overall idea about the origin and to control over emissions in a whole of NUV-VIS-NIR range. In order to provide a direct evidence of size-

emission relationship, we demonstrate an interesting work showing a minimum size that forms the diamond cubic lattice structure of Si. Next, we succeed in observing the reliable relationship between emission wavelengths and sizes of diamond cubic Si. The emission can be tuned in the ranging from 530 nm to 1100 nm by only control over size of diamond cubic Si. On the other hand, we see the size-dependent NUV-Aqua emissions when npSi has a nanocluster structure unlike diamond cubic structure. As a result, the discovery of color-tunable emission from free-standing npSi kindled the development and study of luminescent forms of silicon for its potential applications. I will show herein several applications including light-emitting diodes.

1. For recent reviews, see: a) B. Ghosh and N. Shirahata, "Solution-Processable White-Light-Emitting Germanium Nanocrystals", *Sci. Technol. Adv. Mater.* 2014, 15, 014207 (1-14) b) N. Shirahata, "Colloidal Si nanocrystals: A controlled organic-inorganic interface and its implications of color-tuning and chemical design toward sophisticated architectures", *Phys. Chem. Chem. Phys.* 2011, 13, 7284-7294.
2. B. Ghosh, Y. Masuda, Y. Wakayama, Y. Imanaka, J. Inoue, K. Hashi, Deguchi, H. Yamada, Y. Sakka, S. Ohki, T. Shimizu, and N. Shirahata, "Hybrid White Light Emitting Diode Based on Silicon Nanocrystals", *Adv. Funct. Mater.* 2014 (DOI: 10.1002/adfm.201401795)
3. N. Shirahata, D. Hirakawa, Y. Masuda, and Y. Sakka, "Size-Dependent Color-Tuning of Efficiently Luminescent Germanium Nanoparticles", *Langmuir* 2013, 29, 7401-7410
4. J. Zhou, N. Shirahata, H. Sun, B. Ghosh, M. Ogawara, Y. Teng, S. Zhou, S. C. R. Gui, M. Fujii, and J. Qiu, "Efficient Dual-Modal NIR-to-NIR Emission of Rare-earth Ions Co-doped Nanocrystals for Biological Fluorescence Imaging", *J. Phys. Chem. Lett.* 2013, 4, 402-408
5. N. Shirahata, "Solution-Processable White-Light-Emitting Germanium Nanocrystals"*J. Sol. Stat. Chem.* 2014, 214, 74-78
6. B. Ghosh, Y. Sakka, and N. Shirahata, "Efficiently Green-Luminescent Germanium Nanocrystals", *J. Mater. Chem. A* 2013, 1, 3747-3751

GM-08 (Invited Talk)

On the nature of organic semiconductors: Improving the mobility and stability of organic devices

Jin-Peng Yang[1], Fabio Bussolotti[1], Alexander Hinderhofer[1,2], Satoshi Kera[1,3], and Nobuo Ueno[1]

[1]Graduate School of Advanced Integration Science, Chiba University, Inage-ku, Chiba 263-8522, Japan

[2]Institut für Angewandte Physik, Universität Tübingen, Auf der Morgenstelle 10, Tübingen 72076, Germany

[3] Institute for Molecular Science, Myodaiji, Okazaki 444-8585, Japan

Email:uenon@faculty.chiba-u.jp, web site: http://ulab-www.tf.chiba-u.jp/

Charge carrier transport, which is central to the performance of various organic-based devices, is strongly affected by localized electronic gap states originating from structural defects, impurities and/or chemical interactions with the gaseous environment. Detailed investigations of gap states energy distribution are therefore of paramount importance to understand the energy level alignment at interfaces and the intrinsic limits of transport in organic semiconductors [1]. We use ultrahigh-sensitivity ultraviolet photoelectron spectroscopy (UPS) to demonstrate that even exposure to seemingly innocuous inert gases such as N_2 and Ar can have a significant impact on the electronic properties of pentacene films [2], while F_{16}Cu-phthalocyanine films are stable against the gas exposure [3]. We found furthermore that the density of structural defects (thus electronic states in the gap) of an organic film can be controlled by inserting organic template layer between the organic over layer and the substrate [4]. The defects in organic transistor films decrease also device stability. In this talk we will present results obtained by direct measurements of the density-of-states in the gap and the structural defects, which are induced by weak physical perturbations, using the UPS and X-ray scattering. The results are of fundamental importance for a better understanding of the nature of organic semiconductors, but are also of

high practical importance, given that current processing steps in organic devices always include exposure to inert N_2 atmosphere. Furthermore we will present a successful application of the gap-state (trap-state) control [4] to fabricate higher performance C_{60} transistor with C_{60} films prepared on diindenoperylene (DIP) template layer (Fig.1). The C_{60} transistor with the DIP shows much higher electron mobility and device stability with less trap states [5](Figs.1 and 2).

References:

1. T. Sueyoshi, H. Fukagawa, M. Ono, S. Kera, and N. Ueno, Appl. Phys. Lett. **95** 183303 (2009).
2. F. Bussolotti, S. Kera, K. Kudo, A. Kahn, and N. Ueno, Phys. Rev. Lett. **110**, 267602 (2013).
3. F. Bussolotti, J-P. Yang, A. Hinderhofer, Y. L. Huang, W. Chen, S. Kera, A. T.S. Wee, and N.Ueno, Phys. Rev. B **89**, 115319 (2014).
4. A. Hinderhofer, A. Gerlach, K. Broch, T. Hosokai, K. Yonezawa, K. Kato, S. Kera, N. Ueno, and F. Schreiber, J. Phys. Chem. C, **117**, 1053 (2013).
5. J.-P. Yang, Q.-J. Sun, K.Yonezawa, A. Hinderhofer, F. Bussolotti, X. Gao, N. Ueno, S.-D.Wang, and S. Kera, Org Electronics **15**, 2749 (2014).

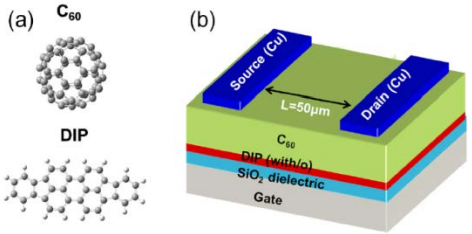

Transistors	μ_n[a] ($cm^2 V^{-1} s^{-1}$)	I_{ON}/I_{OFF}	V_T (V)
C_{60} with DIP	2.62 ± 0.32	4×10^5	5
C_{60} without DIP	0.21 ± 0.10	3×10^4	17

[a] The average mobilities with standard deviation were calculated from the results from 6 OFETs.

Fig. 1. Molecular structures of C_{60} and DIP (a), C_{60} organic field effect transistor (OFET) structure (b) (with DIP as template layer) and the transistor parameters (with/without DIP). μ_n: Electron mobility.

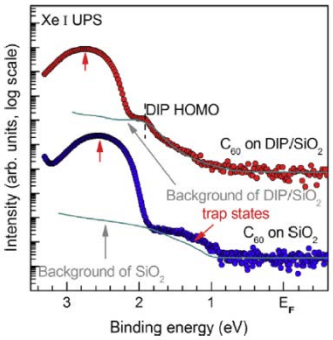

Fig. 2. Xe I UPS (log scale) of the C_{60}(15nm)/SiO_2 and C_{60}(15nm)/DIP(3nm) /SiO_2 thin films. Density of charge-trap states decreases in C_{60} film on DIP film.

GM-09 (Invited Talk)
Nanomaterials for excitonic solar cells

Alberto Vomiero[1]

[1]Luleå University of Technology, 971 98 Luleå, Sweden.
Email:alberto.vomiero@ltu.se

The typical photoanode in dye- and quantum dot- sensitized solar cells is composed of a wide band gap semiconductor, which acts as electron transporter for the photoelectrochemical system. Anatase TiO_2 nanoparticles are one of the most used oxides and are able to deliver the highest photoconversion efficiency in this kind of solar cells, but intense research in the last years was also addressed to ZnO and other composite systems. Modulation of the composition and shape of nanostructured photoanodes is key element to tailor the physical chemical processes regulating charge dynamics and, ultimately, to boost the efficiency of the end user device, by favoring charge transport and collection, while reducing charge recombination.

We investigated several systems: (i) TiO_2 nanoparticles / ZnO nanowires [1]; (ii) Multiwall carbon nanotubes (MWCNTs) / TiO_2 nanoparticles [2]; (iii) TiO_2 nanotubes [3]; (iv) Hierarchically self-assembled ZnO sub-microstructures [4]. Both dye molecules and semiconducting quantum dots were applied as light harvesters. Possible tailoring of structure and morphology of the photoanodes, and their

implication in improving the functional properties of these kinds of excitonic solar cells will be discussed in detail.

In addition, we will discuss the mechanisms of charge transfer between semiconducting nanocrystals (quantum dots, QDs) and wide band gap oxide semiconductors, which ultimately affect photoconversion efficiency in QD solar cells. In particular, we will examine colloidal and non-colloidal QDs, highlighting the peculiarities and illustrating benefits and drawbacks of the two different systems.

1. A. Vomiero, I. Concina, M.M. Natile, E. Comini, G. Faglia, M. Ferroni, I. Kholmanov, G. Sberveglieri, *Applied Physics Letters* 95 (2009) 193104.
2. K.T. Dembele, G.S. Selopal, C. Soldano, R. Nechache, J.C. Rimada, I. Concina, G. Sberveglieri, F. Rosei, A. Vomiero, *Journal of Physical Chemistry C* 117 (2013) 14510-14517.
3. A. Vomiero, V. Galstyan, A. Braga, I. Concina, M. Brisotto, E. Bontempi, G. Sberveglieri, *Energy and Environmental Science* 4 (2011) 3408–3413.
4. N. Memarian, I. Concina, A. Braga, S. M. Rozati, A. Vomiero, G. Sberveglieri, *Angewandte Chemie In Ed* 50 (2011) 12321-12325.

GM-10 (Invited Talk)
From Point Defects to Defect Superstructures in Complex Oxides

Peter V. Sushko[1], Ryan Comes[1], K. Hongliang L. Zhang[1], Robert Colby[2], Yuingge Du[2], Mark E. Bowden[2], Scott A. Chambers[1]

[1]*Fundamental and Computational Sciences Directorate, Pacific Northwest National Laboratory, Richland, WA, USA*
Email:peter.sushko@pnnl.gov, web site: http://www.pnl.gov/science/

[2]*Environmental Molecular Sciences Laboratory, Pacific Northwest National Laboratory, Richland, WA, USA*

The ability to control materials properties is critical to the development of new technologies. Complex oxides exhibit a wide range of structural, compositional, and functional properties, which can be further tuned or even drastically transformed by means of judicious defect engineering, providing the underlying atomic scale mechanisms of defect-induced phenomena are well understood. Exploiting collective behavior of defects in order to generate novel structures and functions remains a challenging goal.

Here we first give several examples, pertinent to energy applications, of how defects and defect aggregates in complex oxides induce detrimental or desirable effects, including voltage suppression in Li-ion batteries, [1] red-shifting of optical absorption in solid solutions, [2] formation of low-resistance Ohmic metal-semiconductor contacts, [3] and room temperature conversion of CO_2 to CO. [4] Then, we focus on two systems, which exhibit correlated behavior of defects in the anion and cation sublattices, respectively. In particular, we discuss how epitaxial strontium chromite films can be transformed, reversibly and at low temperature, from cubic, metallic perovskite $SrCrO_{3-\delta}$ ($\delta<0.1$) to rhombohedral, semiconducting $SrCrO_{2.8}$. [5] As the concentration of oxygen vacancies in $SrCrO_{3-\delta}$ increases, they aggregate into {111}-oriented SrO_2 planes interleaved between layers of tetrahedrally-coordinated Cr. In turn, these planes form ordered arrays so as they are separated by ~1 nm (Figure 1). Using *ab initio* simulations, we reveal the atomic scale mechanisms leading to this ordering, and show that the structural motifs of the oxygen-deficient SrO_2 planes allow for the Grotthuss-type mechanism of the O^{2-} ion diffusion with the potential energy barrier for this diffusion path being significantly lower than that in the cubic $SrCrO_{3-\delta}$. This property is of considerable importance in solid oxide fuel cells where fast O^{2-} diffusion reduces the required operating temperature. Quite differently, oxygen vacancies can be detrimental in the case of photovoltaic devices. Yet, when a host oxide lattice is doped with a photo-active cation, oxygen vacancies are often generated as a natural compensating defect. We demonstrate that in the case of thin $SrTiO_3$ (STO) films, it is possible to suppress the formation of oxygen vacancies by

co-doping STO with La and Cr in equal amounts. Moreover, we find that appropriate growth conditions promote correlated spatial distribution of the substitutional La and Cr defects and the reduction of the STO band gap by as much as 0.9 eV. We discuss the atomic scale mechanisms responsible for this behavior.

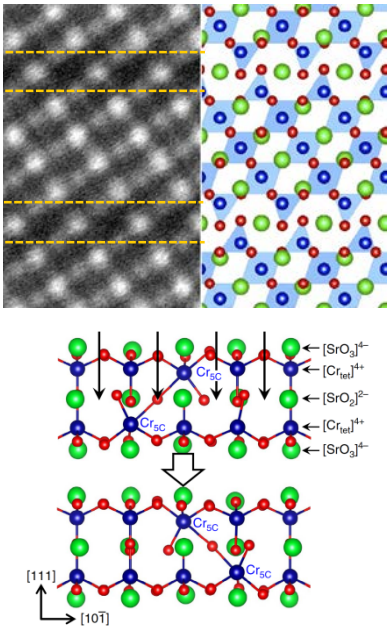

Fig. 1. Ordered oxygen deficient planes in $SrCrO_{2.8}$: HAADF-STEM matched with the computed structural model (left). Mechanism of concerted oxide ion transfer along the oxygen deficient planes (right).

1. P. V. Sushko, *et al.*, *Adv. Funct. Mater.* **23**, 5530 (2013).
2. S. E. Chamberlin, *et al.*, *J. Phys.: Condens. Matter* **25**, 392002 (2013).
3. S. A. Chambers, *et al.*, *Adv. Mater.* **25**, 4001 (2013).
4. Y. Toda, *et al.*, *Nature Commun.* **4**, 2378 (2013).
5. K. H. L. Zhang, *et al.*, *Nature Commun.* **5**, 4669 (2014).

GM-11 (Invited Talk)
Applications of Density-Functional and Tight-Binding Theory in Complex Materials

D. Papaconstantopoulos, A. Koufos, J. McGrady
Computational Materials Science Center
George Mason University, Fairfax, VA USA

We present results of density functional theory calculations and tight-binding parametrizations for the complex materials FeSeTe, Boron and KBH4. We have used the linearized augmented plane wave method (LAPW) in the local density approximation. For the FeSeTe superconductor, we have applied the Gaspari-Gyorffy-McMillan theory and found support for an electron-phonon mechanism of superconductivity. We have also fitted our LAPW results to a tight-binding (TB) basis and studied the composition dependence of the densities of states via the coherent potential approximation. We also present a TB study of predicting the complex allotrope structures of the element Boron. In Boron crystal structures with many atoms in the unit cell are common and they are computationally difficult to calculate using the LAPW method; so the NRL-TB approach is suitable and facilitates the prediction of complex crystal structures. We have created a set of TB parameters based on a fit to LAPW results for the fcc, bcc, sc, dhcp, and Rhombohedral 12 atom alpha Boron. Our TB non-orthogonal Hamiltonian using s and p orbitals, accurately predicts the total energy for other boron allotropes which were not fitted to LAPW data. Additionally, a study of the formation energy of charged hydrogen vacancies in the compound KBH4 will be presented.

GM-12 (Invited Talk)
Multiscale modeling of layered electroactive materials

William Parker[1], Lydie Louis[2], Olle Heinonen[1], Dmitry Karpeev[1], Seungbum Hong[1], Rafal Korlacki,[3] James M. Takacs[3], Stephen Ducharme[3] and Serge Nakhmanson[2]

[1]Argonne National Laboratory, Lemont, IL, USA
[2]Department of Materials Science and Engineering & Institute of Materials Science, University of Connecticut, Storrs, CT, USA
Email: smn@ims.uconn.edu, web site: http://satori.ims.uconn.edu/

[3] *Nebraska Center for Materials and Nanoscience, University of Nebraska-Lincoln, Lincoln, NE, USA*

Electroactive materials for future technological applications should display excellent polar properties, combined with high mechanical stability and low environmental impact. Ferroic and ferroelectric oxides, which are a backbone of modern piezoelectric technology, can only partially fulfill the above requirements. Electroactive nanotube and polymer compounds, like ferroelectric polyvinylidene fluoride (PVDF), $[-CH_2-CF_2-]_n$, are highly attractive for such technological applications due to their low weight, flexibility, and chemical inertness coupled with substantial piezoelectric and pyroelectric response. Furthermore, conceptually, these structures can be regarded as simple models for macromolecular piezo- and ferroelectricity that lend themselves well to studies with predictive computational methods. Therefore, they can be used as a basis for detailed understanding of more complicated materials, as well as to design novel electroactive compounds with advanced properties.

We have combined large-scale *ab initio* computer simulations and modern polarization theory to evaluate the properties of promising electroactive polymers and layered-oxide materials, predicting intriguing behavior in a variety of cases that involve quasi-2D arrangement of electroactive layers [1-4].

We are also exploring ways to distill the results of first-principles computations into simple energy expressions that can be used to study mesoscale-level behavior of nano- and microstructures made out of these functional compounds. For conducting such simulations, we are developing a highly scalable real-space finite-element code (Ferret) that can treat systems with coupled polar and elastic degrees of freedom. This computational toolchain is built on MOOSE, Multiphysics Object Oriented Simulation Environment [5] that is being developed at Idaho National Laboratory. In this presentation we will provide an overview of our approach and some examples of applications we are working on in collaboration with experimental groups [6-7].

This work was supported in part by the U.S. Office of Naval Research, the U.S. Department of Energy EPSCoR Laboratory Partnerships Program under grant number DE-FG02-08ER46498 and the Nebraska Research Initiative. Work at Argonne National Laboratory was supported by the U.S. Department of Energy, Office of Science, Office of Basic Energy Sciences and by American Recovery and Reinvestment Act (ARRA) funding through the Office of Advanced Scientific Computing Research. Argonne National Laboratory is operated under Contract No. DE-AC02-06CH11357 by UChicago Argonne, LLC.

1. S. M. Nakhmanson, R. Korlacki, J. Travis Johnson, S. Ducharme, Z. Ge and J. M. Takacs, *Phys. Rev. B* **81**, 174120 (2010).
2. S. M. Nakhmanson and I. Naumov, *Phys. Rev. Lett.* **104**, 097601 (2010).
3. W. D. Parker and S. M. Nakhmanson, *Phys. Rev. B* **88**, 035203 (2013).
4. J. H. Lee, G. Luo, I. C. Tung, S. H. Chang, Z. Luo, M. Malshe, M. Gadre, A. Bhattacharya, S. M. Nakhmanson, J. A. Eastman, H. Hong, J. Jellinek, D. Morgan, D. D. Fong, and J. W. Freeland, *Nature Mater.* **13,** 879-883 (2014).
5. http://www.mooseframework.org/
6. D. J. Li, S. Hong, S. Gu, Y. Choi, S. Nakhmanson, O. Heinonen, D. Karpeev and K. No, *Appl. Phys. Lett.* **104**, 012902 (2014).
7. B. Lee, S. M. Nakhmanson and O. Heinonen, *Appl. Phys. Lett.* **104**, 262906 (2014).

GM-13 (Invited Talk)
All oxide piezo-MEMS devices: the role of clamping on piezo electric properties

Guus Rijnders

MESA+ Institute for Nanotechnology, University of Twente, Enschede, the Netherlands
Email:a.j.h.m.rijnders@utwente.nl, web site: http://www.utwente.nl//tnw/ims/

I will focus on the recent progress in the fabrication of all-oxide piezo-MEMS devices by pulsed laser deposition. In our devices, we use $Pb(Zr,Ti)O_3$ (PZT) as the piezoelectric material.

The ferro- and piezoelectric properties are strongly related to the crystal orientation as well as the strain state of the PZT layer. Successful integration of these devices into silicon technology is therefore not only dependent on the ability of epitaxial growth on silicon substrates, but also the control of the crystallographic orientation as well as the strain state. We have fabricated all-oxide piezoMEMS devices and studied the resulting properties, such as piezomechanical actuation and sensor properties.

In the contribution, I will further highlight our recent progress on large area deposition by PLD. Currently, we are able to fabricate piezoMEMS devices using a 200 mm technology, see fig 1. Using this technology, biosensors and actuators for use in ink jet printing have been fabricated end characterized. The outcome of these studies will be presented.

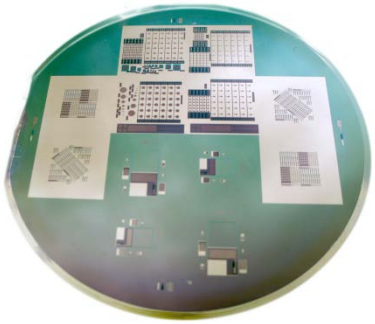

Fig. 1. Full wafer scale PiezoMEMS devices.

GM-14 (Invited Talk)

Phase Change of Ba-substituted Sodium Bismuth Titanate Ferroelectrics with Bi Deficiency

Hirotaka Fujimori, Tomonori Yamatoh

Department of Applied Chemistry, Yamaguchi University, Ube, Yamaguchi, Japan
Email: hiro@hiro-fuji.net, web site: http://www.cera.chem.yamaguchi-u.ac.jp/

Sodium bismuth titanate, $Na_{0.5}Bi_{0.5}TiO_3$ (NBT), is considered to be an excellent candidate of lead-free piezoelectric materials. NBT contains sodium and bismuth, which are easier to evaporate at high-temperature sintering. It is of vital importance to synthesize it at lower temperature. The polymerizable complex (PC) method often allows the crystallization at relatively lower temperature. $(Na_{0.5}Bi_{0.5})_{1-y}Ba_yTiO_3$ is more focused by Takenaka *et al.* [1]. They pointed out that at the room temperature rhombohedral-tetragonal morphotropic phase boundary (MPB) exists at y = 0.06-0.07, where the system shows outstanding electric properties of all the lead-free ceramic resources. Previously Ba-doped NBTs have been synthesized by the PC method in our group. However, the composition of MPB was located at y = 0.10. Other researchers reported that the composition near the MPB was y = 0.06 as well as Takenaka *et al.*. They sintered the samples over 1120 °C. Therefore, sodium and bismuth are guessed to be evaporated from those samples, which leads to Na and/or Bi deficiency. In this study, Bi deficient Ba-doped NBT was intentionally synthesized to keep an initial composition of starting materials by means of relatively low temperature sintering using the PC method. The variation of MPB with Bi deficiency was studied.

First, 6 mol% Ba-doped NBTs with various amounts of Bi deficiency were synthesized. The 002 reflection peak of tetragonal phase appeared at a lower angle of the rhombohedral 220 one and its intensity increased up to 3 mol% of Bi deficiency. Tetragonal phase did not increase over 4 mol% Bi deficiency because of production of an impurity, indicating 3 mol% is a possible maximum of Bi deficiency. Thus, 0-10 mol% Ba-doped NBTs with 3 mol% of Bi deficiency were synthesized. Any impurities were not observed in those samples. Mole fraction was evaluated by Rietveld analysis as shown in Fig. 1. Single rhombohedral phase existed between y = 0 and 0.04. Coexistence of rhombohedral and tetragonal phases was seen at y = 0.06. Single tetragonal phase was observed over y = 0.08. The composition of MPB was detected at y = 0.068 although the composition with no deficiency lay at y = 0.10 in our previous study. The MPB of y = 0.068 in samples with 3 mol% of Bi deficiency consists with that reported by other researchers.

This result suggests that they decided the value of MPB using samples with Bi deficiency.

1. T. Takenaka, K. Maruyama and K. Sakata, *Jpn. J. Appl. Phys.*, **30** [9B], 2236–39 (1991).

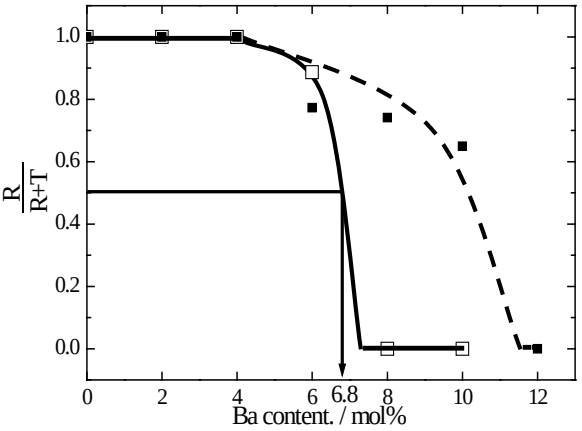

GM-15 (Invited Talk)
Magneto-optical Material and its Application to Silicon Photonics

Tetsuya Mizumoto, Yuya Shoji

Department of Electrical and Electronic Engineering, Tokyo Institute of Technology,2-12-1 Ookayama, Meguro-ku, Tokyo, Japan
Email:tmizumot@pe.titech.ac.jp, web site:

Optical nonreciprocal devices, such as isolators and circulators, provide a unique function that they permit a lightwave to propagate in a pre-designated direction in a photonic circuit. Preventing a reflected lightwave from launching into an optical active device is essential in stabilizing its operation [1]. In order to obtain the optical nonreciprocity, magneto-optical materials play an essential role. The author's group has developed a surface activated direct bonding technique for integrating magneto-optical garnets on semiconductors such as silicon and III-V compound semiconductors, which are commonly used in photonic integrated circuits [2]. Reduction of bonding temperature was the most crucial for avoiding the difference of thermal expansion between dissimilar crystals. The author's group has achieved lowering the bonding temperature down to 200 ^{o}C. Oxygen or nitrogen plasma exposure is effective to realize tight bonding between the garnet and silicon as well as the garnet and III-V compound semiconductors.

The author's group fabricated optical isolators on silicon and GaInAsP/InP optical waveguides by directly bonding a magneto-optical garnet $(CeY)_3Fe_5O_{12}$ (Ce:YIG) single crystal. Figure 1 shows the fabricated silicon waveguide optical isolator. The measured fiber-to-fiber transmittances of the isolator are shown in Fig. 2 as a function of wavelength. An isolation, which is defined by the transmittance ratio of forward to backward propagation, is one of the important characteristics of nonreciprocal devices. An isolation of ~30 dB was obtained in optical isolators fabricated in silicon and GaInAsP/InP waveguides [3,4]. Also, a 4-port optical circulator was demonstrated with an isolation of 33.5 dB in a silicon waveguide [5]. Both isolator and circulator are based on the Mach-Zehnder interferometer (MZI) configuration in which magneto-optical phase shifters are implemented in a push-pull manner in two arms of the interferometer. With this configuration, a crucial issue of TE-TM mode phase matching can be circumvented, which is inevitable in conventional waveguide devices.

The insertion loss of devices was ~13 dB excluding fiber-to-waveguide coupling losses. Annealing the garnet is known to be effective to reduce its optical absorption. Also, the scattering loss can be minimized by reducing the refractive index mismatch between the garnet clad of devices and the clad of access waveguides.

1. K. Petermann, *IEEE J. Sel. Top. Quantum Electron.* **1**, 480 (1995).
2. R. Takei, K. Yoshida, T. Mizumoto, *Jpn. J. Appl. Phys.* **49**, 086204 (2010).
3. Y. Shoji, T. Mizumoto, *Sci. Technol. Advanced Mat.* **15**, 014602 (2014).
4. Y. Sobu, Y. Shoji, K. Sakurai, T. Mizumoto, *Optics Express*, **21**, 15373 (2013).

5. T. Mizumoto, Y. Shoji, K. Mitsuya, *Proc. SPIE*, **8988**, 89880C (2014).

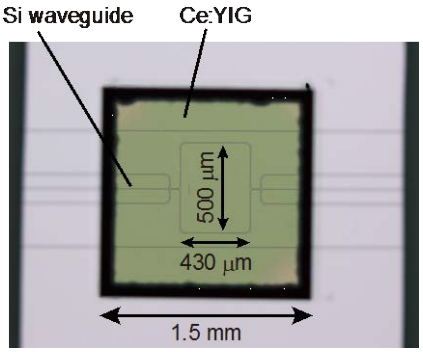

Fig. 1. Optical isolator fabricated on a silicon waveguide platform [3].

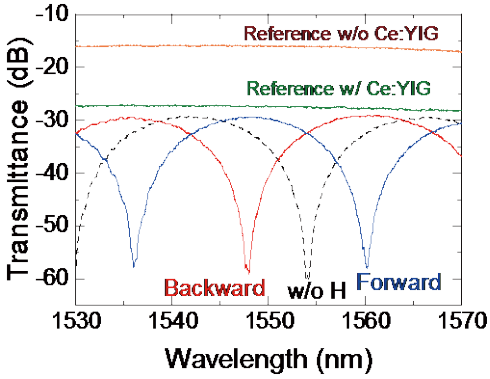

Fig. 2. Measured fiber-to-fiber transmittance of the silicon waveguide optical isolator [3].

GM-16 (Invited Talk)
Nanocomposite Materials for Energy Applications

Jackie Y. Ying

Institute of Bioengineering and Nanotechnology
31 Biopolis Way, The Nanos, Singapore 138669
www.ibn.a-star.edu.sg
E-mail: jyying@ibn.a-star.edu.sg

Nanocrystalline materials are of interest for a variety of applications. This talk describes the design and synthesis of metallic, metal oxide and semiconducting nanocrystals of controlled size and morphology. The nanocrystalline building blocks are used to create multifunctional nanocomposites and heterodimers with unique properties. They are successfully tailored towards energy conversion and storage applications, such as fuel cells and batteries.

GM-17 (Invited Talk)
Small Scale Energy Harvesting by Magnetic Shape Memory Alloys

Manfred Kohl[1], Ruizhi Yin[1], Hinnerk Ossmer[1], Makoto Ohtsuka[2], Hiroyuki Miki[2], Toshiyuki Takagi[2], and Marcel Gueltig[1]

[1]*Karlsruhe Institute of Technology (KIT), Institute of Microstructure Technology, Karlsruhe, Germany*
Email:manfred.kohl@kit.edu, web site: http://www.imt.kit.edu/english/214.php

[2]*Tohoku University, Sendai, Japan*

Miniature energy harvesting devices are needed for the development of novel self-sustaining microsystems such as sensor nodes in wireless networks, where power supply by cables or batteries is not desirable. New emerging applications on small scales include mobile, wearable and implantable devices. Magnetic shape memory alloys (MSMAs) offer interesting solutions as they show multiple coupling effects of their physical properties as well as large abrupt changes of strain and magnetization due to a first order phase transformation [1]. Owing to their multifunctional properties, these materials may perform different tasks while keeping the design simple, which is important for downscaling.

The presentation gives an overview on material properties, engineering and fabrication of miniature MSMA energy harvesting devices.

One class of devices is designed to harvest vibrational energy by using the stress-induced reorientation of martensite variants and of magnetic moments in a Ni-Mn-Ga single crystalline foil [2]. Laboratory demonstrators

based on this so-called magnetic shape memory effect (Fig. 1) show broadband non-resonant operation at a power output of 2.5 mW/cm^3.

Another class of devices are thermal microgenerators based on ferromagnetic and metamagnetic shape memory alloy films [3]. Different options for energy conversion and intrinsic actuation are possible. The thermally induced abrupt change in magnetization in these materials may be used to harvest energy in a small temperature window in the order of 10 K. We demonstrate that thermal energy can be harvested in a broad temperature range above 100 K. Significant improvement of performance is achieved by converting the change of magnetization to electricity through resonant excitation of actuator oscillations with large amplitudes and high frequency.

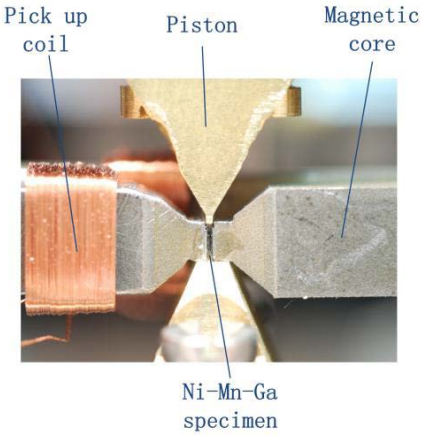

Fig. 1. Miniature energy harvesting device based on the magnetic shape memory effect [2].

1. V.A. Chernenko (Editor), *Advances in Shape Memory Materials: Magnetic Shape Memory Alloys* (Materials Science Forum) 2008.
2. M. Kohl, R. Yin, V. Pinneker, Y. Ezer and A. Sozinov, *Materials Science Forum* **738-739** 411 (2013).
3. M. Gültig, H. Ossmer, M. Ohtsuka, H. Miki, K. Tsuchiya, T. Takagi and M. Kohl, *Adv. Energy Mater*. 1400751 (2014) online (DOI: 10.1002/aenm.201400751).

GM-18 (Contributed Talk)

A Study of the Photovoltaic Properties of AZO:N/p-Si with an inserted ZnO or AZO layer

C.E. Benouis[1], I. Senouici-Zenaidi[1], Z. Mouffak[2], Y. S. OCAK[3,4], A. Tiburcio-Silver[5], M. Benhaliliba[1]

[1]*MaterialsTechnology Dept., Faculté de Physique, Université des Sciences et Technologie d'Oran, USTO-MB, BP1505 Oran, Algeria.*
[2]*Department of Electrical and Computer Engineering, California State UniversityFresno , CA, USA.*
[3]*Dicle University, Education Faculty, Science Dpt., 21280, Diarbakir, Turkey.*
[4]*Science and Technology Application and ResearchCenter (DUBTAM),Dicle University,Diyarbakır,Turkey.*
[5]*ITT- DIEE. Apdo. postal 20. Metepec 3, 52176 Estado de México, Mexico.*
Corresponding author: Z. Mouffak, email: zmouffak@csufresno.edu

In This work, we present heterojunctions made of Al-doped ZnO (AZO) that we additionally doped with Nitrogen (AZO:N), and deposited either directly on p-Si substrate or with an inserted layer of ZnO or AZO on top of p-Si. The films were deposited by DC sputtering under pressure and constant substrate temperature. Gold contacts were deposited by thermal evaporation. The effect of the insterted layer was investigated. The current-voltage characteristics were studied under dark and illumination. The AZO:N/pSi structure showed a good rectification of about 4e5, with an ideality factor of 1.63, and a barrier height of 0.99eV. A photobehavior was obtained with a photosensitivity ratio around 1e7 (Iph/ I dark). AZO:N/ZnO /pSi had a poor rectification, with an ideality factor far from 1, a barrier height of 0.46 eV, and a weak photosensitivity ratio.

The rectifing properties of Au/AZO:N/AZO/pSi were improved, with a coefficient of 4.73E3, an ideality factor of 4.86, a barrier height of 0.54 eV, and a photosensitivity of about 7.43. We conclude that while both Au/AZO:N/psi and Au/AZO:N/AZO/ psi show good rectification properties, and therefore could be used as diodes;

the Au/AZO:N/psi structure shows good properties as a photodiode.

GM-19 (Invited Talk)
Synthesis of clathrate single crystals by spark plasma sintering

Yongkwan Dong, George S. Nolas

Department of Physics, University of South Florida, Tampa, FL 33620, USA
web site:http://shell.cas.usf.edu/gnolas/

Inorganic clathrates based on group 14 elements have attracted attention due to their interesting structural and physical properties with nano-sized cages composed of group 14 elements. As a result, they are of interest for a variety of potential technological applications, including solid state energy conversion, photovoltaics, magnetocalorics, superconductivity, and as the anode for Li-ion batteries. Due to this scientific interest and technological importance an understanding of the fundamental structural and physical properties of inorganic clathrates is essential. In order to achieve this goal various synthetic techniques, such as soft chemical routes (chemical oxidation), kinetically controlled thermal decomposition, high-temperature high-pressure synthesis, and spark plasma sintering (SPS), have been employed to obtain stable or metastable compositions that are not accessible by conventional solid state reaction or single-crystal growth methods.[1] This talk will illustrate synthetic studies aiming at finding new clathrates by SPS, as a synthetic tool. Several new and known clathrates were synthesized with this technique. Our results indicate that SPS can be employed in topochemical ion exchange reactions, thus allowing for the rapid synthesis of single crystals of multinary intermetallic phases that cannot be accessible by traditional crystal growth techniques.

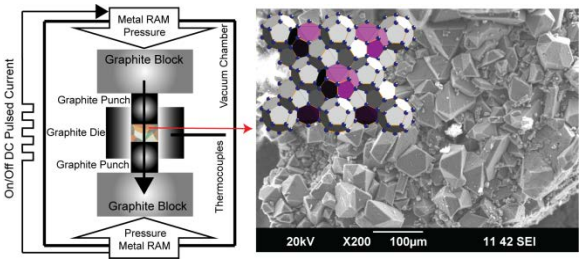

Fig1. Schematic diagram of the SPS approach (left). SEM image of single crystals grown by SPS together with the type-II crystal structure ($Rb_8Na_{16}Si_{136}$ crystals are shown) composed of Si_{28} (purple) and Si_{20} (gray) polyhedra encapsulating Rb and Na, respectively (right).

1. G. S. Nolas, *The physics and chemistry of inorganic clathrates* (Springer), 2014.

GM-20 (Invited Talk)
Synthesis of ZnO, In_2S_3, P3HT, ZnS and In_2O_3 nanomaterials

Najoua Kamoun Turki

Laboratory of condensed Matter physics,Faculty of Sciences of Tunis El Manar,Tunisia (2092).
Corresponding author . tel : +21698347470 ;
fax :+21671885073
E-mail Adress :n.najouakamoun@gmail.com

The development of transparent conductive electrode and optical window semicondictor nanomaterials are made by using simple low-cost techniques such as Chemical Bath deposition CBD, spin coating and spray pyrolysis. The objective of this conference is to present the synthesis and physical characterization of thin film semiconductors such as ZnO, In_2S_3, P3HT, ZnS and In_2O_3. Multi-scale characterization of these nanomaterials was made from measurements of reflection-transmission fluorimetry, atomic force microscopy, energy dispersive spectroscopy and XRD. From optical characterizations , one could deduce the optical band gap of these nanomaterials and their thicknesses. We could follow the variation of these optical parameters with the growth parameters of these different

materials and by doping with different elements. Local studies conducted could allow us to make a fairly accurate analysis of nanomaterials that are used as transparent conductive electrode or as optical window in solar cell devices.

The characterization carried out using complementary techniques can improve the performance of devices made from the nanomaterials, or even lead to new applications of nanocrystals constituent layers.

GM-21 (Contributed Talk)

Synthesis and characterization of manganese oxide particles and investigation of their catalytic activities for oxidation of benzyl alcohol in liquid phase

Muhammad Saeed[1], Mohammad Ilyas[2]

[1]*Department of Chemistry, Government College University Faisalabad Pakistan*
Email:pksaeed2003@yahoo.com

[2]*National Centre of Excellence in Physical Chemistry, University of Peshawar Pakistan*

Two types of manganese oxide were synthesized by mechano chemical process in solid phase by chemical reaction of manganese chloride and potassium permanganate at room temperature. The prepared catalysts were characterized by surface area and pore size, particle size, XRD, SEM, FTIR analyses and oxygen contents measurements. These oxides were used as catalysts for oxidation of benzyl alcohol in liquid phase. The catalytic activity of manganese oxide was studied by carrying out the oxidation of benzyl alcohol in liquid phase using n-octane as solvent over the temperature range of 323-373K and oxygen pressure of up to one atmosphere. Benzaldehyde and benzoic acid were identified as the reaction products. However, benzoic acid appeared in reaction mixture after complete conversion of benzyl alcohol to benzaldehyde. Typical batch reactor kinetic data were obtained and fitted to the Langmuir-Hinshelwood, Eley-Rideal and Mars-van Krevelene models of heterogeneously catalyzed reactions. The Langmuir-Hinshelwood model was found to give a better fit. However, the adsorption sites for benzyl alcohol were found to be homogeneous in nature and therefore, the adsorption of benzyl alcohol was taking place according to the Langmuir Adsorption Isotherm. The heat of adsorption for benzyl alcohol was determined as -18.14 $kJmol^{-1}$. The adsorption of oxygen followed the Temkin Adsorptin Isotherm, and therefore, the heat of adsorption of oxygen shows a linear decrease with increase in the surface coverage. The maximum heat of adsorption for oxygen at surface of catalyst was –31.12 $kJmol^{-1}$. The value of activation energy was found to be 71.18 $kJmol^{-1}$, which was apparently free from the influence of the heat of adsorption of both benzyl alcohol and oxygen.

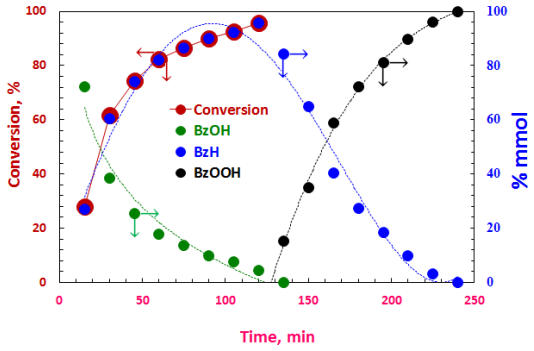

1. M. Saeed, M. Ilyas, Int.J. Chem. React. Engin., 2011, 9, A75
2. M. Saeed, M. Ilyas, Appl. Catal. B. Environ., 2013, 129, 247-254.
3. M. Saeed, M. Ilyas, Int. J. Chem. React. Engin., 2010, 8, A77
4. M. Saeed, M. Ilyas, M. Siddique, J. Chem. Soc. Pak., 2012, 34, 626-633.

GM-22 (Contributed Talk)

New Physical Mechanism of Diamond Growth in Low Pressure Linear Microwave Plasma

M. Varga, S. Potocky, O. Babchenko, M. Cada, T. Izak, Z. Remes, A. Kromka

Institute of Physics of the ASCR,v.v.i., Cukrovarnicka 10, Prague 6, 16253, Czech Republic
Email:varga@fzu.cz, web site: http://www.fzu.cz/en

Diamond is recognized as a promising semiconductor material with multifunctional features. Presently, there is an inherent demand on its growth over large areas (>100 cm^2) due to increased industrial interest. Here we investigate large area diamond growth by pulsed linear antenna microwave plasma at low pressures (<500 Pa). We show that decrease of pressure from 200 to 6 Pa results in an enlargement of diamond grains from nanoscale (<20 nm) to polycrystalline character. At the same time, the growth accelerated by factor 3x and film quality is improving [1]. Adding of CO_2 is needed to suppress re-nucleation process. Employing "extremely" high CO_2 concentration (80%) results in a formation of porous layer consisting of randomly oriented diamond nanowires. We conclude that growth conditions in linear plasma at low pressure are more sensitive to the gas composition and density of active species in the substrate vicinity as well as to microwave energy rather than to temperature of electrons (<2 eV). These observations were further successfully utilized in the carbon-carbon composite preparation, i.e. the direct overgrown or ingrown of carbon nanotubes net with the nanocrystalline diamond [2] and/or transformation of the polyvinyl alcohol nanofibre textile into a diamond [3]. The growth model supported by optical emission spectra of plasma and Langmuir probe measurements implies that the concentration of atomic hydrogen plays a crucial role in well-known hydrogen rich growth conditions and the gas pressure is the key process parameter controlling the growth regime [4]. Illustrative view of the plasma chemistry and diamond growth model is shown in figure 1.

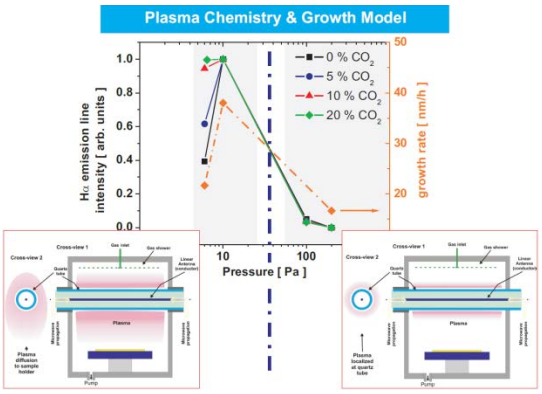

Fig. 1. Plasma chemistry and diamond growth model in linear antenna microwave plasma CVD system.

Acknowledgement:
This work was supported by the grant P108/12/G108. Work was carried out in the frame of LNSM infrastructure.

1. M. Varga, Z. Remes, O. Babchenko, A. Kromka, *Phys. Stat. Sol. B* **249** (12), 2635 (2012).
2. M. Varga, V. Vretenar, M. Kotlar, V. Skakalova, A. Kromka, *Appl. Surf. Sci.* **308**, 211 (2014).
3. M. Varga, S. Potocky, P. Tesarek, O Babchenko, et al., *Appl. Surf. Sci.* **312**, 220 (2014).
4. S. Potocky, M. Cada, O. Babchenko, T. Izak, et al., *Phys. Stat. Sol. B* **250** (12), 2723 (2013).

GM-23 (Contributed Talk)
Synthesis of Silica Nanoparticles with Controlled Size for Biological Applications

Huseyin Kizil[1], M. Balaban[2], L. Trabzon[3]

[1]*Department of Metallurgical and Materials Engineering, Istanbul Technical University, Istanbul 34469, Turkey*
Email: kizilh@itu.edu.tr

[2]*Department of Nanoscience & Nanoengineering, Istanbul Technical University, Istanbul, Turkey*

[3]*Department of Mechanical Engineering, Istanbul Technical University, Istanbul, Turkey*

Silica nanoparticles (NPs) have become promising alternative for a broad range of biological applications due to versatile silane chemistry for surface functionalization, excellent

biocompatibility, ease of large-scale synthesis and low cost production. They have attracted substantial interest because of their distinctive properties amenable for *in vivo* applications [1, 2], such as the site-specific delivery and intracellular controlled release of drugs, genes, and other therapeutic agents.

In this study, we present the effects of initial reagent concentrations and reaction temperature on the average size and size distribution of spherical silica NPs. In a reaction mixture of water-tetraethyl orthosilicate (TEOS)-ammonium hydroxide (NH_4OH) system was studied at a complete set of initial reagent concentrations (H_2O: 0.5-17.0 M, TEOS: 0.15-0.25 M, NH_4OH: 0.25-2.75 M) and at temperatures of 25-35°C. The NPs size was increased by increasing amounts of the catalyst (NH_4OH) and silica precursor (TEOS) and by decreasing the amount of water in the reaction mixtures. Monodispersed silica NPs with uniform diameters ranging from 80 nm to 500 nm were successfully prepared as seen in Figure 1.

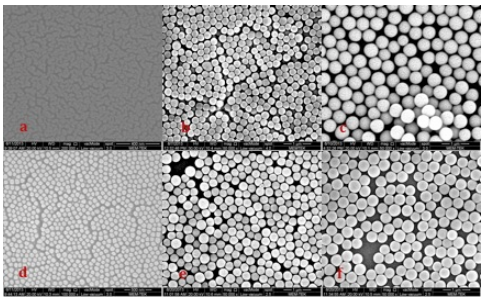

Fig. 1. NPs size at NH_4OH concentration (M) of a) 0.25, b) 1.25, c) 2.25 at 25ºC, and d) 0.75, e) 1.75, f) 2.75 at 35ºC

1. I.I. Slowing, J.L. Vivero-Escoto, C.W. Wu, V.S.Y. Lin, *Adv. Drug Deliv. Rev*. 60 1278 (2008).
2. C. Barbe, J. Bartlett, L.G. Kong, K. Finnie, H.Q. Lin, M. Larkin, S. Calleja, A. Bush, G. Calleja, *Adv. Mater.*16, 1959 (2004).

GM-24 (Contributed Talk)

Structural, electronic and optical properties of semiconductor nanostructures

A. Sanchez-Castillo[1] , J. M. Galicia-Hernández[2] , M. Lopez-Fuentes[3] , D. Garcia-Toral[3], Gregorio H. Cocoletzi[2]

[1]Universidad Autonoma del Estado de Hidalgo, Escuela Superior de Apan, Apan Hidalgo, Mexico
[2]Benemerita Universidad Autonoma de Puebla, Instituto de Fisica, Puebla, Mexico
[3]Benemerita Universidad Autonoma de Puebla, Facultad de Ingenieria Quimica, Puebla, Mexico

Semiconductor nanostructures are of current interest provided they are widely used in the nano-optoelectronic industry. In this presentation we will discuss structural, electronic and optical properties of two dimensional (2D) semiconductor structures. For our studies we consider CdSe which is a semiconductor suitable for solar cell fabrications therefore it is important to know the energy gap. The structural relaxation is done within the periodic density functional theory as implemented in PWscf code of the quantum espresso package. Calculations take into account the pseudopotential method in the local density approximation. For the 2D CdSe layer, two cases are explored; one is with dangling bonds and another with hydrogen saturated dangling bonds. Results indicate that hydrogenated system is the most stable structure. Using the relaxed 2D systems we calculate the energy gap applying the GW theory as developed in the Yambo project. The hydrogenated and non-hydrogenated structures exhibit larger energy gap than the bulk system. The dielectric constant for CdSe is determined using the time dependent density functional theory as implemented in the Yambo project.

This work has been partially supported by CONACYT Mexico.

GM-25 (Invited Talk)

Spin Dynamics of Skyrmionic Magnetic Bubbles and Domain Walls

Robert Reeve[1], B. Krüger[1], F. Büttner[1,2], C. Moutafis[3], M. Schneider[2], C. M. Günther[2], J. Geilhufe[4], C. von Korff Schmising[2], J. Mohanty[2], I. Makhfudz[5], O. Tchernyshyov[5], J.-S. Kim[1,6], M.-A. Mawass[1], A. Bisig[1], M. Foerster[1], T. Schulz[1], H. J. M. Swagten[6], S. Eisebitt[2,4], and M. Kläui[1]

[1]*Institut für Physik, Johannes Gutenberg-Universität Mainz, Staudinger Weg 7, 55128 Mainz, Germany Email:bkrueger@uni-mainz.de, web site: http://www.klaeui-lab.de/*

[2]*Institut für Optik und Atomare Physik, Technische Universität Berlin, Straße des 17. Juni 135, 10623 Berlin, Germany*

[3]*Swiss Light Source, Paul Scherrer Institut, 5232 Villigen PSI, Switzerland*

[4]*Helmholtz-Zentrum Berlin für Materialien und Energie GmbH, Hahn-Meitner-Platz 1, 14109 Berlin, Germany*

[5]*Department of Physics and Astronomy, Johns Hopkins University, Baltimore, Maryland 21218, USA*

[6]*Department of Applied Physics, Center for NanoMaterials, Eindhoven University of Technology, P.O. Box 513, 5600 MB Eindhoven, The Netherlands*

Magnetic devices can be inherently low power due to their intrinsic non-volatile nature. To make use of the spin structures for devices, they need to be nano-patterned to exhibit confined magnetic spin structures as used for sensing, logic and memory applications. In particular topological spin structures that emerge in such geometries possess a high stability and their dynamics resembles that of a composite quasi-particle. The dynamics of these structures is of key importance for magnetic memories and logic devices but also contains exciting physics and have received enormous scientific interest in recent years.

Examples of spin structures include the magnetic vortex state where the magnetization curls in-plane around a center region, in which the magnetization points out-of-plane and which has been suggested for memory devices [1]. Whereas its dynamics has been widely investigated [2,3], much less is known about the dynamics of the magnetic bubble, a counterpart of the vortex in a magnetic material with easy-axis perpendicular anisotropy. The magnetization in the bubble points out-of-plane. In the remaining part, the magnetization points in the opposite direction. These two domains are separated by a Bloch-type domain wall. Magnetic bubbles are skyrmions characterized by the spherical topology of their spin vector field that can be useful for memories [4].

Here, we study the GHz gyrotropic motion of a skyrmion spin structure, which has recently been found from micro-magnetic simulations [5]. Our analytical model [6] describes this motion in terms of two waves that travel along the domain wall that confines the bubble and the position of the bubble is then determined by the superposition of the two waves. This results in a finite momentum of the bubble quasi particle which does not exist for a magnetic vortex. Experimentally we observed this motion using pump-probe X-ray holography and report the first experimental observation of the GHz gyrotropic motion of a skyrmion. The trajectory of the skyrmion's position is accurately described by our quasi particle equation of motion [6]. From a fit we are able to deduce the inertial mass of the magnetic bubble and find it to be much larger than inertia found in any other magnetic system, which we attribute to the non-trivial topology [7].

Finally we also propose a new approach to shifting topological objects, such as in-plane domain walls using perpendicular field pulses [8]. We demonstrate that by engineering the pulses, synchronous displacement of multiple domain walls is efficiently possible [8], which could be a paradigm shift for low power magnetic memory.

1. S. Bohlens, et al., *Appl. Phys. Lett.* **93**, 142508 (2008).
2. B. Van Waeyenberge, et al., *Nature* **444**, 461 (2006).
3. B. Krüger, et al., *Phys. Rev. B* **76**, 224426 (2007).

4. A. Fert, et al., *Nature Nanotech.* **8**, 152 (2013).
5. C. Moutafis, et al., *Phys. Rev. B* **79**, 224429 (2009).
6. I. Makhfudz, et al., *Phys. Rev. Lett.* **109**, 217201 (2012).
7. F. Büttner, et al., *submitted.*
8. J.-S. Kim, et al., *Nature Comm.* **5**, 3429 (2014).

Session AP

ADVANCED PHOTONICS AND PLASMONICS FOR NANO-BIO APPLICATIONS

AP-01 (Invited Talk)
Tuning of the Surface Plasmon Resonance in the UV-IR Range for Biological Applications

Koichi Okamoto[1], and Kaoru Tamada[1]

[1]Institute for Materials Chemistry and Engineering, Kyushu University, Fukuoka, Japan
Email: okamoto@ms.ifoc.kyushu-u.ac.jp, web site: http://http://www.plasmonic.net/

Nano-structured interfaces between metallic and dielectric materials bring unique optical properties mainly by the surface plasmons (SPs). The SP resonance modifies emissions, absorptions or scatterings, and produce the complicated optical properties combined with other optical effects. For example, we could enhance the emission efficiencies of InGaN/GaN-based quantum wells (QWs) and the other various materials by using the metal nanograin structures. [1] The enhancement ratios depend on the metal grain sizes because the grains act as the nano-gratings. [2] This method should be useful to develop the higher efficiency light-emitting devices and solar cells. [3]

This highly enhanced light emissions should become also very useful and important tool for biosensing and bioimaging. Recently, various organic dyes and semiconductor nanocrystals are used as biomarkers in wider wavelength ranges. Therefore, flexible tuning of the SP resonance is very important for wider applications of the SP enhanced emission. For example, it is well known that the resonance spectra of the localized surface plasmon resonance (LSPR) can be tuned by controlling the size, shape, and distance of the metal nanoparticles. Two-dimensional metal nanosheet structures are also very promising for various applications, and we succeeded in more flexible and remarkable tuning of the resonance spectra by making the multilayered Ag nanosheet structures on metal substrates. [4]

Flexible tuning of the LSPR within the visible wavelength range was already achieved by using several metallic nanostructures. Next important challenge is extension of the SP resonance into UV or IR wavelength regions. To extend plasmonics tuning into deep UV regions, Al should be useful because the SP resonance frequency of Al is located at ~200nm. We fabricated the nanograin structures of Al and succeeded in 7-fold enhancements of deep UV (~250nm) light emissions from AlGaN/AlN-based QWs. [5] Further flexible tuning of the LSPR in the deep UV range should be feasible with Al nanoparticles, although it's difficult to fabricate. We obtained the LSPR spectra by the finite-difference time-domain (FDTD) simulations as shown in Fig. 1(b).

On the other hand, to extend plasmonics into IR wavelength region has been very difficult because the many kinds of metals have large dumping factors of the dielectric constants at the IR regions. We checked the optical properties of many metals and found that only a few metals have a potential to use for IR plasmonics. Fig. 1(b) shows the LSPR spectra of Ta nanoparticles calculated by the FDTD method. Clear peaks were obtained at the near-IR regions.

The methods presented here to tune the SP resonance over the UV-IR range should bring new possibilities of applications to plasmonics. We believe that our approach of device applications based on tunable plasmonics would lead to new class of several photonic and electronic technologies, and also several biological applications. Experiment verifications for the UV-IR tuning of plasmonics are now in progress.

1. K. Okamoto, I. Niki, A. Shvartser, Y. Narukawa, T. Mukai, A. Scherer, *Nat. Mater.* **3**, 601 (2004).
2. X.-Y. Xu, M. Funato, Y. Kawakami, K. Okamoto, and K. Tamada, *Opt. Exp.*, **21**, 3145 (2013).
3. *Advanced Photonic Sciences*, (chapter 8: Plasmonics for Green Technologies), InTech, 2012.
4. K. Okamoto, B. Lin, K. Imazu, A. Yoshida, K. Toma, M. Toma, K. Tamada, *Plasmonics*, **8**, 581 (2013).
5. A. Takada, T, Ohto, R. G. Banal, K. Okamoto, M. Funato, Y. Kawakami, *Meeting of JSAP* (2010).

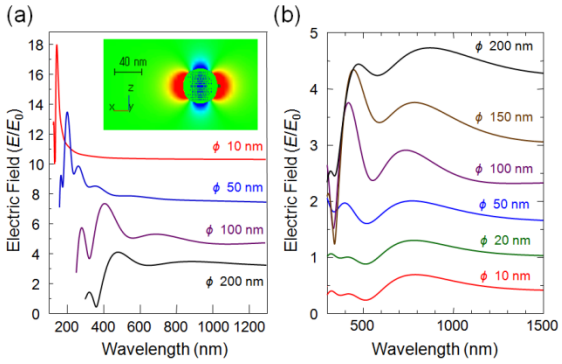

Fig. 1. FDTD simulations for LSPR of (a) Al and (b) Ta nanoparticles.

AP-02 (Invited Talk)
Quantum Dots and Upconverting Nanoparticles: Using Solid-Phase Platforms for Multiplexed Optical Sensing by Resonance Energy Transfer

Ulrich J. Krull, M. O. Noor, A.J. Tavares, F. Zhou

Department of Chemical and Physical Sciences, University of Toronto Mississauga, 3359 Mississauga Road North, Mississauga Ontario, L5L 1C6, Canada Email:ulrich.krull@utoronto.ca, web site: http://www.utm.utoronto.ca/cps/faculty-staff/krull-ulrich-j

Multiplexed solid-phase nucleic acid hybridization assays on paper-based or microfluidic platforms would be useful technology for rapid detection of genetic markers for pathogens and genetically-based disease. In the case of microfluidic platforms, quantum dots (QDs) can serve as energy donors in fluorescence resonance energy transfer (FRET) for transduction of nucleic acid hybridization, and are modified to carry oligonucleotide probes. [1] QD immobilization, activation, probe bioconjugation, passivation and target delivery were performed sequentially on microfluidic chips using electroosmotic and electrophoretic flow. Electrokinetic injection of oligonucleotide target was used to control volume and speed of delivery to the microfluidic channel. Hybridization and full signal development was complete within minutes for detection of fmol quantities of target oligonucleotides. The quantification of mixtures of targets was possible on the basis of interrogation of specific colors of QDs using spatial channel length coverage by target DNA, which correlated with the amount of target DNA injected into a channel. [2] The method was adapted to provide for the capability of detection of unlabeled target.

To simplify technology, the surface of paper was modified with imidazole groups for the assembly of a biorecognition interface comprised of immobilized green-emitting QDs (gQDs) and red-emitting QDs (rQDs) as FRET donors and two types of oligonucleotide probe sequences as biorecognition elements. Addition and subsequent hybridization of Cy3-labeled and Alexa Fluor 647 (A647) oligonucleotide targets provided the proximity for FRET sensitized emission from the acceptor dyes (Cy3 and A647). The gQD/Cy3 FRET pair served as an internal control, while the rQD/A647 FRET pair served to produce the analytical signal for quantitative transduction of nucleic acid hybridization. Single nucleotide polymorphism discrimination was possible by using a combination of ionic strength and formamide to control the stringency of nucleic acid hybridization. This bioassay could operate quantitatively based on either the intensity of emission, or on spatial length of zones where hybridization occurred, with detection of target oligonucleotides being achieved by use of an i-Pad camera at the zeptomole level.

To further advance the sensitivity of biosassays, a paper-based two-color oligonucleotide detection assay with tunable sensitivity has also been developed based on use of a single type of upconversion nanoparticle (UCNP) and luminescence resonance energy transfer (LRET). [3] Excitation was at 980 nm, thereby avoiding autofluorescnce and suppressing optical scatter. Water soluble UCNPs were designed to emit both green and red bands simultaneously by the upconversion process. Two different single stranded oligonucleotide probes were assembled on the UCNPs. Selective hybridization of two targets each with a different color dye as label provided the proximity for

LRET-sensitized emission from the dyes. It was possible to tune the detection limit and sensitivity for each probe by changing the relative ratio of the probes. The selectivity was sufficient such that single base pair mismatch discrimination was possible and target concentration could be quantitatively determined in undiluted serum.

1. M.O. Noor, E. Petryayeva, A.J. Tavares, U. Uddayasankar, W.R. Algar and U.J. Krull, *Coordination Chemistry Reviews* **263**, 25 (2014).
2. M.O. Noor, A.J. Tavares and U.J. Krull, *Analytica Chimica Acta* **788**, 148 (2013).
3. F. Zhou, M.O. Noor and U.J. Krull, *Analytical Chemistry* **86**, 2719 (2014).

AP-03 (Invited Talk)
Label-free multichannel biochip based on anomalous reflection of gold

Kotaro Kajikawa

Interdisciplinary Graduate School of Sience and Ingineering, Tokyo Institute of Technology, Yokohama, Japan
Email:kajikawa@ep.titech.ac.jp, web site: http://www.opt.ip.titech.ac.jp

Anomalous reflection of gold (AR) is a phenomenon that reflectance of gold surface is greatly modulated by existence of dielectric layer for blue or purple light. [1,2] This phenomenoon is due to the fact that the refractive index of gold has both metal and dielectric characters in these wavelengths 400-500 nm. Thus, AR can be applied to label-free optical biological sensors, like the surface plasmon resonance (SPR). Although the sensitivity is slightly lower than SPR sensors, the optical setup is simple and flexible (the detection can be made at normal incidence). In addition, spatial resolution is greater than the SPR sensors because AR is not a resonance phenomenon. Thanks to these merits, AR is one of the promising methods for label-free biosensing arrays.

Figure 1(a) shows AR microarray image, in which octadecanethiol (ODT) self-assembled monolayers (SAMs) are spotted. The ODT spots are 60 μm in diameter and the thickness is about 2.2nm. The number density of the spots is $10^2/mm^2$. As shown in the cross sectional plot (Figure 1(b)), the reflectivity contrast is about 2%, which can be easily detected.

Figure 2 shows the AR image for avidin detection. At spots A2, B1 and B3, anti-avidin is immobilized on the chip surface and BSA is immobilized at spots A1, A3 and B2, for control. This microarray is exposed to a sample of an avidin solution of 600 μg/mL. The change rate in the reflectivity is imaged. Clear difference in the reflectivity change at spots A2, B1 and B3 is observed, indicating successful detection of anti-avidin using the 60 μm diameter spots. Therefore, it is shown that AR is one of the promising methods for label-free biosensing arrays.

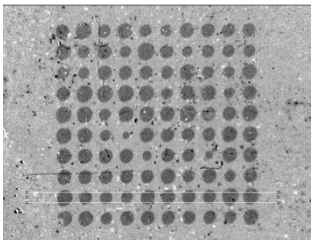

(a)

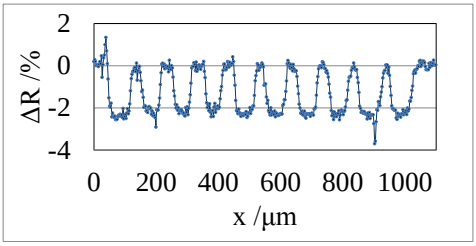

(b)

Fig. 1. (a) AR image of the array of ODT SAM spots; (b) Cross sectional image.

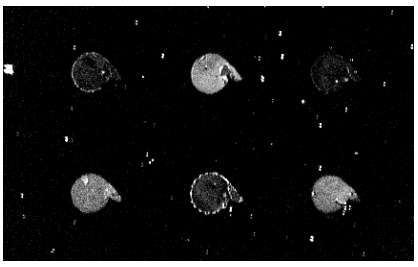

Fig. 2. Avidin detection with the AR microarray chip

1. M. Watanabe and K. Kajikawa, "An optical fiber biosensor based on anomalous reflection of gold", Sens. Actuators B (Chemical), **86**, 126-130 (2003).
2. S. Fukuba, R. Naraoka, K. Tsuboi and K. Kajikawa, "A new imaging method for gold-surface adsorbates based on anomalous reflection", Opt. Commun., **48**, 16, 3386-3391 (2009).

AP-04 (Invited Talk)
Control of Exciton Dynamics in a Single Colloidal Quantum Dot by Localized Surface Plasmon

Sadahiro Masuo[1], Keisuke Kanetaka[1], Ryota Sato[2], Toshiharu Teranishi[2]

[1]Department of Chemistry, Kwansei Gakuin University, Sanda, Hyogo, Japan
Email:masuo@kwansei.ac.jp, web site: http://sci-tech.ksc.kwansei.ac.jp/~masuo/

[2] Institute for Chemical Research, Kyoto University, Uji, Kyoto, Japan

One of the important exciton dynamics in semiconductor quantum dots (QD) is multiple exciton generation in a single QD. By utilizing the multiple excitons, the efficiency of the optoelectronic devices can be considerably increased. However, multiple excitons generate in a single QD, exciton annihilation process which is called the Auger recombination occurs. To utilize the multiple excitons, the Auger recombination has to be suppressed. On the other hand, if the Auger recombination efficiently occurs, a single QD can be used as a single-photon source which is an important photon source for the quantum information technologies. Therefore, it is important to control the exciton dynamics. We have investigated the emission behavior, particularly photon antibunching behavior, of a single QD interacted with metal nanostructures. As results, we have revealed that the Auger recombination process in the QD could be suppressed by the interaction with the metal nanostructure.[1-3] To reveal the mechanism of the exciton dynamics in more detail, the best way is the observation of the emission behavior with the coupling of a single QD with a single metal nanostructure with well-defined size and shape. In this work, AFM manipulation technique was employed to couple a single QD with a metal nanostructure, i.e., a single gold nanocube (AuCube) was approached to the single CdSe/ZnS QD using the AFM manipulation. The exciton dynamics of the single QD with the manipulation will be discussed.

Figures 1(a-d) show AFM images (a, c) and fluorescence images (b, d) observed simultaneously from a same area before (a, b) and after (c, d) the AFM manipulation of an AuCube. In Fig. 1(a), the AuCube marked by a square was pushed to a single QD marked by a circle. After the manipulation, the distance between the AuCube and the QD was shortened to 5 nm (center-to-center distance). In the fluorescence images, a slight change of the fluorescence intensity was observed. To understand the emission behavior, the time traces of the fluorescence intensity, fluorescence decay curves, fluorescence spectra, and photon antibunching of the single QD were measured before and after the manipulation. As results, the increase in the fluorescence intensity, the shortening of the decay curve, and the decrease in the probability of photon antibunching were observed after the manipulation. Furthermore, the modified emission behavior was changed to original emission behavior by separating the AuCube from the QD. Above results clearly indicated the exciton dynamics can be controlled by the coupling of AuCube with the single QD, i.e., the Auger recombination can be suppressed by the interaction with AuCube. We will discuss the mechanism in more detail.

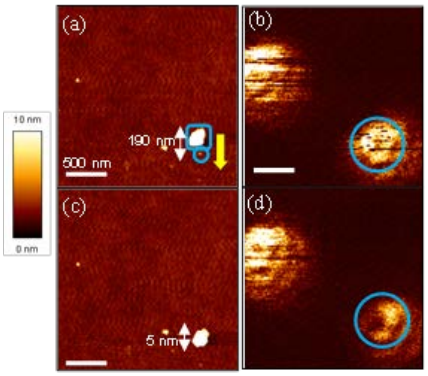

Fig. 1. AFM images (a, c) and fluorescence images (b, d) before (a, b) and after (c, d) AFM manipulation of an AuCube. A square and circles in the images indicate AuCube and QD, respectively.

1. S. Masuo, T. Tanaka, S. Machida, A. Itaya, *J. Photochem. Photobio. A*, **237**, 24 (2012).
2. H. Naiki, S. Masuo, A. Itaya, *J. Phys. Chem. C*, **115**, 23229 (2011).
3. S. Masuo, H. Naiki, S. Machida, A, Itaya, *Appl. Phys. Lett.*, **95**, 193106 (2009).

AP-05 (Invited Talk)
Assay on a tip – plasmonic fiber tip probe for intracellular protein detection

Qimin Quan[1]

[1]*Rowland Institute at Harvard University, Cambridge, MA, USA*
Email:quan@rowland.harvard.edu

Most of our knowledge in biology so far has been based on ensemble measurements on cells. However, a major challenge in biology is to understand how individual cells process information and respond to external stimuli. Traditional assays, such as enzyme-linked immunosorbent assay (ELISA) and western blot, lack the detection sensitivity and efficiency in sample preparation to achieve single cell capability. Fluorescent imaging is powerful technique for live cells, however, it is challenging for primary cells and clinical samples. We present the surface plasmon fiber-tip-probe (FTP) technique [1] and demonstrate detection of intracellular proteins in live cells dynamically.

3. W. Hong, F. Liang, D. Schaak, M. Loncar, and Q. Quan, Sci. Rep. **4**, 6179 (2014).

AP-06 (Invited Talk)
Highly Confined, Enhanced Surface Fluorescence Imaging with 2D Silver Nanoparticle Sheets

Kaoru Tamada[1], Eiji Usukura, Shuhei Shinohara, Daisuke Tanaka, Koichi Okamoto

[1]*Institute for Materials Chemistry and Engineering (IMCE), Kyushu University, Fukuoka, Japan*
Email:tamada@ms.ifoc.kyushu-u.ac.jp, web site: http://en.cm.kyushu-u.ac.jp/

A method of obtaining highly confined, enhanced surface fluorescence imaging is proposed using two-dimensional (2D) silver nanoparticle (AgMy) sheets [1]. This technique is based on the localized surface plasmon resonance (LSPR) excited homogeneously on a 2D silver nanoparticle sheet [2]. The AgMy sheets are fabricated at the air–water interface by self-assembly and transferred onto hydrophobic glass substrates. These sheets can enhance the fluorescence only when the excitation wavelength overlaps with the plasmon resonance wavelength. To confirm the validity of this technique, we performed the imaging of a single fluorescence bead with a total internal reflection fluorescent (TIRF) microscope. We confirmed that the AgMy sheet provides a 4-fold increase in fluorescence with a 160-nm spatial resolution at 30 msec/frame snapshot (Figure 1). The AgMy sheet will be a powerful tool for high sensitivity and high-resolution *real time* bio-imaging at nanointerfaces.

As the second topics, we propose the colormetric detection by use of multilayered 2D crystalline sheets [3]. The multilayered nanoparticle sheet fabricated by layer-by-layer deposition exhibits a unique color change on metal thin film, depending on the layer numbers [4, 5]. We demonstrated a high-sensitive detection of avidin-biotin interaction by use of this phenomenon. When AuNP was immobilized

on avidinized AgMy multilayers, the change of absorption spectra was more than the simple LSPR absorption of AuNP, but enlarged by their layered structures. Such homogeneous plasmonic nanosheets are quite valuable for a new design of plasmonic devices.

4. E. Usukura, S. Shinohara, K. Okamoto, J. Lim, K. Char, K. Tamada, *Appl. Phys. Lett.* **104**, 121906 (2014).
5. M. Toma, K. Toma, K. Michioka, Y. Ikezoe, D. Obara, K. Okamoto and K. Tamada, *Phys. Chem. Chem. Phys*. **13**, 7459-7466 (2011).
6. S. Shinohara, D. Tanaka, K. Okamoto, K. Tamada, in preparation.
7. K. Okamoto, B. Lin, K. Imazu, A. Yoshida, K. Toma, M. Toma, K. Tamada, *Plasmonics* **8**, 581-590 (2013).
8. A. Yoshida, K. Imazu, X. Li, K. Okamoto, K. Tamada, *Langmuir* **28**, 17153 (2012).

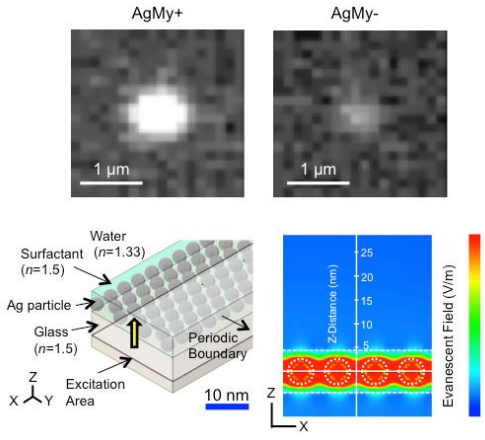

Fig. 1. LSPR-enhanced high resolution bio-imaging.

AP-07 (Invited Talk)
Short-Range Ordered Plasmonic Nanoholes and Nanopores for Sensing

Takumi Sannomiya

Department of Innovative and Engineered Materials, Tokyo Institute of Technology, Yokohama, Japan
Email: sannomiya.t.aa@m.titech.ac.jp, web site: http://www.iem.titech.ac.jp/~sannomiya/

An array of nanoholes created in a metallic film shows characteristic asymmetric optical resonances originating from the propagating film plasmon and polarization of each nanohole. This resonance sensitively shifts upon the refractive index change of the film surface as well as inside the hole[1]. Such plasmonic nanoholes can be applied to the molecular sensing such as biological substances and hazardous materials in the environment. Monitoring the surface chemical reaction in sub-nm range using the plasmonic sensing is also useful to analyze the surface corrosion or degradation at the very early stage.

We have been fabricating short-range ordered (SRO) nanohole arrays which can be readily created in a centimeter scale by colloidal lithography, without time-consuming and expensive lithographic facilities. The transmission minimum (or extinction maximum) of the optical spectrum of a SRO nanohole array occurs when the average spacing between the nanoholes matches the surface plasmon wavelength. The resonance peak width corresponds to the propagation length of the surface plasmon. Since the surface plasmon wavelength and propagation length can be calculated from the dispersion relation of the given multilayer system, it is possible to engineer the nanohole system so that the resonance is measurable in the visible/NIR range.[1]

In this presentation, various types chemical and bio-sensors based on SRO nanoholes as well as nanopores will be discussed.[2-5].

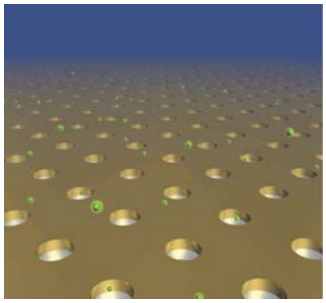

Fig. 1. Schematic illustration of nanohole arrays for sensing.[1]

1. T. Sannomiya, O. Scholder, K. Jefimovs, Ch. Hafner, A. B. Dahlin, *Small* **7**, 1653-1663 (2011).
2. A. B. Dahlin, T. Sannomiya, R. Zahn, G. A. Sotiriou, J. Vörös, *Nano Lett*. **1**, 1337-1343 (2011).
3. J. Junesch, T. Sannomiya, A. B. Dahlin, *ACS Nano* **6**, 10405-10415 (2012).
4. Y. Ikenoya, M. Susa, J. Shi, Y. Nakamura, A. B. Dahlin, T. Sannomiya, *J. Phys. Chem. C* **117**, 6373-6382 (2013).
5. J. Junesch, T. Sannomiya, *ACS Appl. Mater. Interfaces* **6**, 6322-6331 (2014).

Session SC
NANOMATERIALS FOR PHOTOCHEMICAL SOLAR CELLS

SC-01 (Invited Talk)
Radial Tandem Junction Thin Film Solar Cells Design for Optimal Light Harvesting and Balanced Photo-current Generation

Shengyi Qian[1], Jiawen Lu[1], Linwei YU[1,2], Jun Xu[1] and Yi Shi[1]

[1] *School of Electronics Science and Engineering, Nanjing University, 210093, Nanjing, China*
Email:yulinwei@nju.edu.cn
[2]*Laboratoire de Physique des Interfaces et Couches Minces, LPICM, UMR7647, CNRS, Ecole Polytechnique, Palaiseau, France*

Radial junction (RJ) solar cell has been proposed as a promising architecture to boost light harvesting in Si thin film solar cells. This strategy has been explored upon a matrix of self-assembled Si nanowires (SiNWs) fabricated upon glass substrate via a tin (Sn)-catalyzed vapor-liquid-solid (VLS) process [1, 2]. In this way, a low temperature (down to <300 ºC) fabrication of RJ a-Si:H thin film solar cells (without the need for ex-situ catalyst metal cleaning) has been demonstrated, showing a power conversion efficiency of 8.1% [3]. Finite element simulation of the light harvesting process realized within such a RJ thin film solar cell unit has also revealed interesting resonant-mode absorption enhancement and unique absorption profile in the cavity-like RJ cell [4].

In pursuit of higher performance and broader absorption spectrum, it will be interesting to explore a radial tandem junction (RTJ) thin film solar cell, with radially staking a-Si:H and nc-Si:H absorbers in the outer and inner *p-i-n* junctions, respectively. This will help to reduce aggressively the thickness of nc-Si:H layer, leading to a much shorter deposition time and a better photo-carrier collection. However, the RTJ thin film solar cell is indeed a quite sophisticated structure where the photo-currents generated within the a-Si:H and nc-Si:H layers have to be balanced.

In this work, we report a comprehensive modeling and simulation of the light propagation and absorption within the RTJ structure, by varying the length, separation and absorption layer thicknesses in the RTJ structure to maximize the effective absorption while keeping a balanced photo-current generation in the radial tandem structure. Our results indicate that a balanced and high photo-current density of more than 14 mA/cm^2 can be obtained, with an a-Si:H layer of only 75 nm thick and nc-Si layer of 120 nm, coated upon a matrix of 2 um long SiNWs spaced by 900 nm in periodicity. These results provide an instructive tool to assess the potential and develop optimal design for a new generation of RTJ Si-based thin film photovoltaics.

Reference:

1. Misra, S., et al., *Wetting Layer: The Key Player in Plasma-Assisted Silicon Nanowire Growth Mediated by Tin.* The Journal of Physical Chemistry C, 2013. **117**(34): p. 17786-17790.
2. Yu, L., et al., *Synthesis, morphology and compositional evolution of silicon nanowires directly grown on SnO2 substrates.* Nanotechnology, 2008. **19**(48): p. 485605.
3. Misra, S., et al., *High efficiency and stable hydrogenated amorphous silicon radial junction solar cells built on VLS-grown silicon nanowires.* Solar Energy Materials and Solar Cells, 2013. **118**(0): p. 90-95.
4. Yu, L., et al., *Understanding Light Harvesting in Radial Junction Amorphous Silicon Thin Film Solar Cells.* Sci. Rep., 2014. **4**: p. 4357.

SC-02 (Invited Talk)
Conducting Polymer-Dye Composites for Photoelectrochemical Solar Cells and Energy Storage

Arash Takshi[1]

[1]*Electrical Engineering Department, University of South Florida (USF), Tampa, FL, USA*
Email:atakshi@usf.edu, web site: http://eng.usf.edu/bio-organic-electronics/index.html

Given the sustainable, clean, and abundant nature of solar energy, studies on photovoltaic

devices for energy conversion to electric energy have been extensive. However, due to large variation of the solar energy availability in a day, energy storage is required in many applications when solar cells are used. Conventionally, the harvested energy is stored in an external device (i.e. batteries or supercapacitors) which adds substantially to the costs of solar energy systems, requires additional charging circuitry, and needs regular maintenance and replacement. The result is a relatively expensive and bulky system that is not ideal, particularly for portable, off-grid applications. Recently, we have found that a combination of a conducting polymer (PEDOT:PSS) and a porphyrin based dye molecule can be used as an electrode in a photoelectrochemical cell to generate electric charge from solar energy and store the charge in the device. The structure of the device is very similar to a supercapacitor, while the conducting polymer-dye composite film behaves likes a photoactive electrode. The device is able to generate up to 0.49 V under the open circuit conditions upon AM1.0 solar radiation. A charge stability (in dark) of more than 2 hrs has been achieved after charging the device with light for 20 min. The organic photoactive supercapacitor can deliver currents up to 0.12 mA/cm^2. The electrochemical study suggests a photoelectrochemical reaction at the composite film. Hence, the charge storage is likely due to the change in the polymer oxidation state.

SC-03 (Invited Talk)
The Solar Thermal Electrochemical Process (STEP) for the high solar efficiency production of ammonia, fuels, iron, cement and the removal of carbon dioxide from the atmosphere

Stuart Licht[1]

[1]*Department of Chemistry, George Washington University, Washington, DS, USA*
Email:slicht@gwu.edu, web site: http://home.gwu.edu/~slicht/

The solar thermal electrochemical process is capable of the production of societal staples with little or no carbon footprint, and can directly capture & convert carbon dioxide from the air that can be stored as useful graphite. In STEP the efficient formation of metals, fuels, cement, chlorine, and carbon capture is driven by solar thermal heated endothermic electrolyses of concentrated reactants occurring at voltage below that of the room temperature energy stored in the products.[1-9]

Steel (cathodes) and nickel (anodes) are the same robust electrodes for either hydrogen (in molten hydroxide) or CO production (in molten carbonate). As one example, CO_2 is reduced to either fuels, or storable carbon, at solar efficiency higher than the best photovoltaics. This is due to a synergy of efficient solar thermal absorption and electrochemical conversion at high temperature and reactant concentration. CO_2-free STEP iron production, from iron ore, occurs via Fe(III) in molten carbonate. Water is efficiently split to H_2 by molten hydroxide electrolysis, and chlorine, sodium and magnesium from molten chlorides. STEP cement uses a novel molten electrochemistry for the production of calcium oxide (lime from limestone).[1-9]

The solar electrochemical generation of societal staples and fuels decreases society's dependence on grid-based electricity. A pathway is provided for the STEP decrease of atmospheric carbon dioxide levels to pre-industrial age levels in 10 years.

Selected STEP references:

1. S. Licht, "STEP generation of energetic molecules: A solar chemical process to end anthropogenic global warming," *J. Phys. Chem.*, C, 113, 16283-16292 (2009).
2. S. Licht, B. Wang, S. Ghosh, H. Ayub, D. Jiang, J. Ganley, "A New Solar Carbon Capture Process: STEP Carbon Capture," *J. Phys. Chem. Lett.*, 1, 2363-2368, with online 2 page supplement (2010).
3. S. Licht, "Efficient Solar-Driven Synthesis, Carbon Capture, and Desalinization, STEP: Electrochemical Production of Fuels, Metals,

Bleach," *Advanced Materials*, *47*, 5592-5612 (2011).
4. S. Licht, H. Wu, C. Hettige, B. Wang, J. Lau, J. Asercion, J. Stuart, " STEP Cement: solar thermal electrochemical production of CaO without CO_2 emission " *Chem. Comm.*, **2012**, 48, 6019-6021, with online 20 page supplement (2012).
5. B. Wang, Y. Hu, H. Wu, S. Licht, "STEP Pollutant to Solar Hydrogen: Solar driven thermal electrochemical wastewater treatment with synergetic production of hydrogen," *Electrochemical Science Letters*, 2, H34-H36 (2013).
6. B. Cui, S. Licht, "Critical STEP advances for sustainable iron production," *Green Chemistry*, 15(4), 881-884, with 16 page online supplementary information (2013).
7. S. Licht, B. Cui, B. Wang, "STEP Carbon Capture: the barium advantage," *Journal of CO_2 Utilization*, 2, 58-63 (2013).
8. Y. Zhu, B. Wang, X. Liu, H. Wang, H. Wu and Stuart Licht, "STEP Organic Synthesis: An Efficient Solar, Electrochemical Process for the Synthesis of Benzoic Acid," ***Green Chemistry,*** 16 (2104).
9. S. Licht, B. Cui, B. Wang, F.-F. Li, J. Lau, and S. Lui,"Ammonia synthesis by N_2 and steam electrolysis in molten hydroxide suspensions of nanoscale Fe_2O_3," ***Science,*** **345**, 637-640, with 15 page online supplementary information (2014).

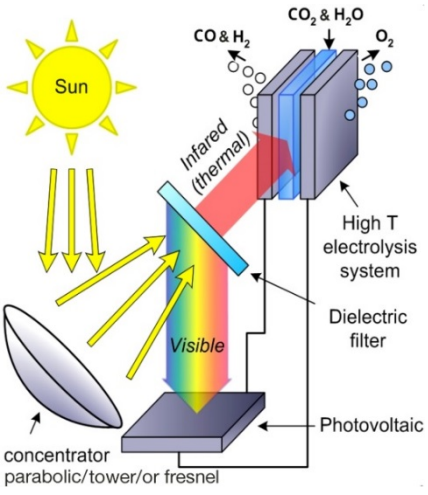

SC-04 (Invited Talk)
Synthesis of Nanostructured Titanium Dioxide for Energy Conversion

Eray S. Aydil[1], Bin Liu[2]

[1]*Department of Chemical Engineering and Materials Science, University of Minnesota, Minneapolis, MN 55455, USA*
Email:aydil@umn.edu, web site: http://research.cems.umn.edu/aydil/

[2]*School of Chemical and Biomedical Engineering, Nanyang Technological University, Singapore 637459*
Email:LIUBIN@ntu.edu.sg, web site:http://research.ntu.edu.sg/expertise/academicprofile/Pages/StaffProfile.aspx?ST_EMAILID=LIUBIN

Nanostructured titanium dioxide is important for many applications in energy conversion and storage. These applications range from their use in dye-sensitized solar cells to photocatalysis and lithium ion batteries. [1-8] In this talk, we will review our efforts in synthesis and structuring of titanium dioxide at multiple length scales, from nanometers to micrometers, to endow them with properties suitable for energy conversion and storage. Specifically, this talk will review (i) growth of oriented single-crystalline rutile TiO_2 nanorods on transparent conducting substrates for dye-sensitized solar cells, [1] (ii) synthesis of anatase TiO_2 films with reactive {001} facets, [2] (iii) synthesis of TiO_2-B/anatase core-shell heterojunction nanowires for photocatalysis [3] and (iv) synthesis and doping of high-surface-area mesoporous TiO_2 microspheres for visible light hydrogen production. [4] In the first of these four topics we will describe hydrothermal growth of oriented single-crystalline rutile TiO_2 nanorod films on transparent conductive fluorine-doped tin oxide (FTO) substrates. Changing the growth parameters varies the diameter, length and density of the nanorods. Since its first report [1], this method has been used for many applications and others have made improvements. In the second topic, we describe the growth of polycrystalline anatase films with high-reactivity {001} facets, again on transparent conductive fluorine-doped tin dioxide substrates. This

synthesis method relies on capping the high-energy {001} surfaces with hydrofluoric acid generated in situ through hydrolysis of TiF_4. The third topic is on strategies for segregating electrons and holes to different parts of a photocatalyst to take part in separate oxidation and reduction reactions. One way to achieve this is by building junctions into the catalyst that tend to separate the electron and the hole into two different regions of the catalyst. We synthesized TiO_2-B core and anatase shell core-shell nanowires to accomplish this and studied the effects of the surface coverage of the shell on the photocatalytic activity. In a model photocatalytic reaction, the maximum activity was obtained when the solution containing the reactants could contact both the anatase shell and TiO_2-B core. This was attributed to the effective electron-hole separation at the junction between the anatase and TiO_2-B phases. Finally, we synthesized anatase TiO_2 microspheres with nanopores and specific surface areas reaching as high as 500 m^2/g. The synthesis is based on solvothermal reaction of titanium isopropoxide with anhydrous acetone. The diameter of the microspheres and the nanopore diameters could be tuned from ~ 500 nm to 4 μm and from 3 to 11 nm, respectively. A controlled amount of carbon was incorporated into theses microspheres through post-synthesis low-temperature calcination. The resulting material absorbed visible light and had higher photocatalytic activity than undoped microspheres.

1. B. Liu and E. S. Aydil, *J. Am. Chem. Soc.* **131**, 3985-3990 (2009).
2. B. Liu and E. S. Aydil, *Chem. Commun.* **47**, 9507-9509 (2011).
3. B. Liu, A. Khare and E. S. Aydil, *ACS Appl. Mater. Interfaces* **3**, 4444-4450 (2011).
4. B. Liu, L. Liu, X-F. Lang, H.-Y. Wang, X. W. Lou and E. S. Aydil, *Energy Environ. Sci.* **7**, 2592-2597 (2014).
5. E. Enache-Pommer, B. Liu and E. S. Aydil, *Phys. Chem. Chem. Phys.* **11**, 9648-9652 (2009).
6. B. Liu, D. Deng, J. Y. Lee and E. S. Aydil, *J. Mater. Res.* **25**, 1588- 1594 (2010).
7. B. Liu and E. S. Aydil, Journal of Renewable and Sustainable Energy **3**, 043106 (2011).
8. B. Liu, A. Khare and E. S. Aydil, *Chem. Commun.* **45**, 8565-8567 (2012)

SC-05 (Invited Talk)
Intra- to Inter-Molecular Singlet Fission in Oligoenes

M. Tuan Trinh,* and Xiaoyang Zhu

Chemistry Department, Columbia University, New York, USA
**Email:mt2898@columbia.edu*

Singlet exciton fission is a spin allowed process in which the photo-excited singlet exciton splits into two triplet excitons. This process offers a great potential to increase efficiency of photovoltaic devices beyond conventional limits. Among the small number of singlet fission molecules discovered to date, two mechanisms have emerged: intra- or inter-molecular fission.[1,2] Here we show a combined intra- to inter-molecular singlet fission mechanism in the model system of diphenyl-dicyano-oligoene (DPDC). Excitation of DPDC to the first optically bright state leads to the ultrafast formation of an intra-molecular triplet pair, i.e., bi-exciton (BE). The bi-exciton decays in 40 ps in the solution phase, but in solid films can also split into two long-lived triplets ($2xT_1$) on adjacent molecules on the competitive time scale of 30 ps. The singlet fission yield depends on both energetics and inter-molecular coupling. These findings suggest a new design principle for efficient singlet fission: the independent tuning of singlet-BE coupling and BE→$2xT_1$ splitting from intra- and inter-molecular interactions, respectively.

Figure 1 shows the chemical structure of $DPDC_n$ oligoenes (n is number of double bonds in the oligoenes) used in this study (left) and the transient absorption spectra for $DPDC_7$ film (right). The initial excitation creates the optically bright S_2 singlet state and subsequently decays on ultrafast time scales into the "dark" BE and S_1 states. BE exciton can split into two individual long-lived triplets (T_1) in adjacent molecules.

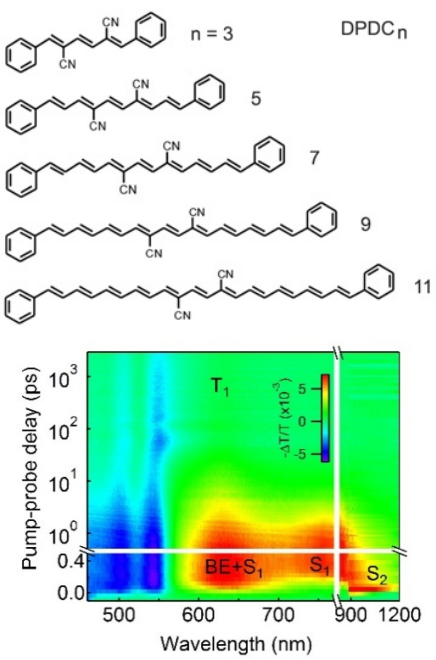

Fig. 1. Chemical structure of $DPDC_n$ oligoenes (left) and 2D pseudo-color (-ΔT/T) spectra as functions of probe wavelength and pump-probe delay time (right). The pump laser wavelength was 450 nm. The excited state absorption for BE, singlet S_1, and S_2 are indicated.

1. Smith, M. B. & Michl, J. *Chem. Rev.* **110**, 6891-6936 (2010).
2. Musser, A. J. et al. *J. Am. Chem. Soc.* **135**, 12747-12754 (2013).

SC-06 (Contributed Talk)
On the solar hydrogen production of α-Fe_2O_3 nanorings

Heberton Wender[1], Renato V. Gonçalves[2]

[1]*Physics Institute, Federal University of Mato Grosso do Sul (UFMS), Campo Grande-MS, Brazil. Email:hbtwender@gmail.com*

[2]*Department of Chemistry, São Paulo University (USP), São Paulo-SP, Brazil.*

The production of hydrogen from water using only a catalyst and solar energy, water photolysis, is one of the most challenging and promising outlets for the generation of clean and renewable energy. [1] Semiconductor photocatalysts for solar hydrogen production by water photolysis must employ stable, non-toxic, abundant and inexpensive visible-light absorbers capable of harvesting light photons with adequate potential to reduce water. Here, we prepared α-Fe_2O_3 nanorings (IONRs) with 37 nm mean inner diameter, 96 nm outer diameter and 72 nm height, as could be seen by FESEM in Figure 1. These IONRs produced hydrogen efficiently with an evolution rate of about 350 $\mu mols.h^{-1}.g^{-1}$. It showed that these IONRs meet the above requirements to reduce water, even with the inappropriate conduction band level reported in literature for hematite. [2] It is believed that bands position changed with nanostructuring process reaching values accessible for both O_2 and H_2 evolution. [3] In addition, by covering the NRs with $Co(OH)_2$ nanoparticles (NPs) of ~ 6 nm diameter (see HRTEM image of NP-coated IONRs, Figure 2), a H_2 evolution rate of 546 $\mu mols.h^{-1}.g^{-1}$ could be obtained, resulting in a 35% higher efficiency for H_2 generation. Both nanoparticle-coated and uncoated NRs displayed superior photocatalytic activity for hydrogen evolution when compared with TiO_2 nanoparticles, showing themselves to be promising materials for water-splitting using only solar light.

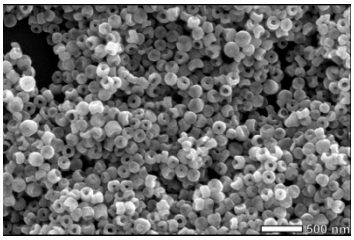

Fig. 1. FESEM image of the IONRs prepared by hydrothermal reaction.

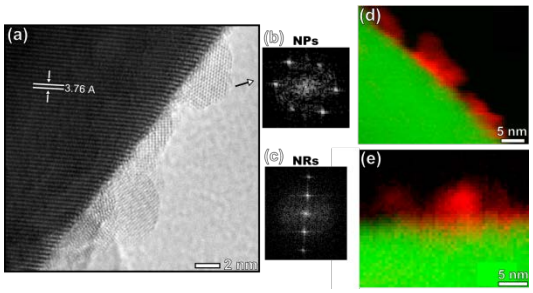

Fig. 2. HRTEM image of the as-prepared $Co(OH)_2$ NP-coated IONRs (a), FFT image of the NPs (b), and of the darker region corresponding to the IONRs (c), chemical mapping obtained by EELS wherein the green color corresponds to the NRs and the red color to the NPs before (d) and after annealing showing diffusion of Co to Fe.

1. H. Wender et al, *Nanoscale* **5**, 9310 (2013).
2. C. X. Kronawitter, et al, *Energy Environ. Sci.* **4**, 3889 (2011).
3. L. Vayssieres, et al, *Adv. Mater.* **17**, 2320 (2005).

SC-07 (Contributed Talk)
Discernment of Possible Organic Magnetic Field Effect Mechanisms Using Polymer Light-Emitting Electrochemical Cells

R. Geng, R. C. Subedi, S. Liang, T. D. Nguyen*

Department of Physics & Astronomy, University of Georgia, Athens, GA, USA
*Email:gengrg@uga.edu, *ngtho@uga.edu, web site: https://www.physast.uga.edu/research/nguyen/*

Organic magnetoresistance (OMAR) in organic light emitting diodes (OLEDs), an exciting research direction in organic spintronics, has been extensively studied for the last decade. [1] A relatively weak magnetic field can alter the conductivity and electroluminescence of the device up to 50% even at room temperature, promising for magnetically controlled optoelectronic device applications.[2] However, understanding about the effect is still limited due to the lack of fundamental experiments associated to the effect.

We report studies of OMAR effect in polymer light-emitting electrochemical cells (PLECs) using the 'super-yellow' poly-(phenylene vynilene), SY-PPV, polymer in vertical and planar device configurations to discern the existing OMAR mechanisms in OLEDs.[3,4] In particular, *we* investigate the mutual relationship between magnetoconductance (MC) and magnetoelectroluminescence (MEL) of the devices by studying the role of dissociated polarons from polaron pairs (PP) on the magnetic response. The dissociated polaron density is determined by the PP dissociation rate and the PP density. For the planar PLEC which possesses a small dissociation rate, we observed small and negative MC at all applied voltages regardless of the emission intensity, while MEL becomes positive when electroluminescence quantum efficiency increases. MC has a much narrower width than MEL, indicating that MC and MEL do not share a common origin. However, MC reverses and has the same width as MEL when the device is exposed to a threshold laser power. For the vertical PLEC, characterized by a large dissociation rate, MC and MEL were observed to be positive and have the same width. We discuss the results using the existing OMAR mechanism in OLEDs. We show that the PP model can explain the positive MEL and MC, while the negative MC can be explained by the bipolaron model. Finally, we present a possibility to complete an all-organic PLEC magnetic sensor by using an inkjet printer.

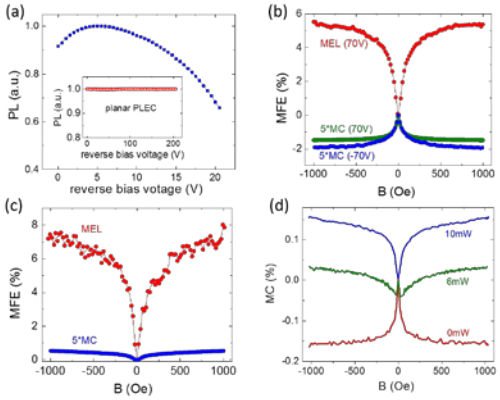

Fig. 1. shows (a) the PL quenching by the various applied voltages of the vertical PLEC under 450 nm laser illumination of 5mW intensity. The inset shows the PL quenching of the planar PLEC at the same illumination power. (b) MC and MEL of the planar PLEC at 70V and -50V after charging for 70 minutes. (c) MC and MEL of the vertical PLEC at 10V after

charging at 12V for 10 minutes. (d) The MC of the planar PLEC responses at 40V applied voltage at different laser illumination powers.

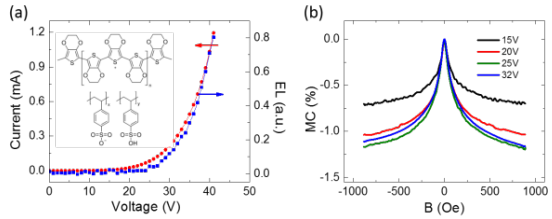

Fig. 2. shows the all-organic PLEC. (a) I-V and EL-V characteristics of vertical PEDOT:PSS/SY-PPV blend (200nm)/PEDOT:PSS PLEC. (b) The MC of the all-organic PLEC response at different applied voltages.

1. O. Mermer *et al.* Phys. Rev. B, 72, 205202 (2005).
2. T. D. Nguyen, *et al.* Phys. Rev. B 77, 235209 (2008).
3. R. Geng, *et al.* Spin 04, 1440010 (2014).
4. R. Geng, *et al.* Appl. Phys. Lett. 103, 243307 (2013).

SC-08 (Contributed Talk)
Thin Flexible Dye-Sensitized Solar Cell with SWCNT Cathode

V.O. Saik, N.N. Krechetova, M.R. Predtechensky

[1]OCSiAl Russia, Injenernaya Str., 24, Novosibirsk, 630090, Russian Federation
Email:saik.vo@ocsial.com, web site: http://ocsial.com/en/

We made DSSC with the SWCNT thin conductive film (TCF) used as the transparent cathode. The cathode is a substrate of a transparent polymeric material (PET) and a layer of carbon nanotubes (CNT) deposited on it. Tuball© SWCNTs made by OCSiAl were used. The anode consists of a titanium foil and a layer of semiconductor material nanoparticles (TiO_2), sensitized by a dye (Ruthenium N719). Iodide was used as electrolyte. The construction of the flexible DSSC is shown in Fig. 1.

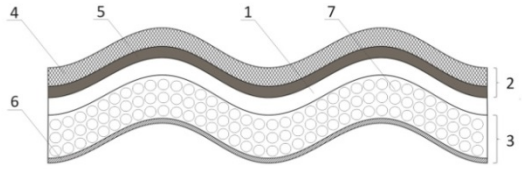

Fig. 1. The structure of the flexible solar cell: 1 – an electrolyte, 2 – a cathode, 3 – an anode, 4 – PET, 5 - CNT, 6 – a titanium foil, 7 - TiO_2 nanoparticles, sensitized by a dye.

The working principle of the proposed solar cell is based on the photoexcitation of dye molecules in layer 7 (see the figure). Light passes through cathode 2 and electrolyte 1 to layer 7. Light photons are absorbed by dye molecules thus transferring them into an excited state. Electrons from dye molecules are transferred to TiO_2 nanoparticles, and then they pass through layer 7 to metal foil 6.

A solar-to-electric energy conversion efficiency of 2% was obtained. This solar cell exhibits a prompt photocurrent response in the range of 0.4 – 0.5 mA/cm^2 and an open circuit voltage of about 600 mV. The number of factors affects the performance of the flexible DSSC. The most important is the transparency of the cathode together with the sheet resistance. There is well known the relationship between those two factors for the TCF [2]. We compared the dependences for the SWCNT Tuball and commercially available MWNT. The results are presented in Fig. 2. TCF made of SWCNT clearly exhibits superior performance in term of high transparency and low resistance and we hope to approach the values of T=90% and R_s=100 Ohm/sq. soon.

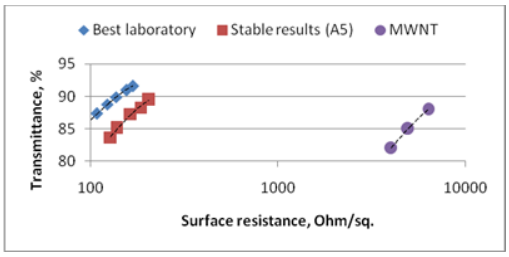

Fig. 2. The dependence of transmittance upon the resistance of the TCF made of SWCNT and MWNT on PET.

We are expecting the efficiency of our flexible DSSC to improve further in the near future.

References:

1. O. Kohle, M. Graetzel, A.F. Meyer and T.B. Meyer, *Advanced Materials* **9** (11), 904 (1997).
2. D. S. Hecht *et al.*, *Nanotechnology* **22**, 169501 (2011).

Session CG
CNTs, GRAPHENE AND 2D MATERIALS

CG-01 (Invited Talk)
One-Step Fabrication of Functionalized Graphene Materials via Submerged Liquid Plasma [SLP] in Solvent under Ambient Conditions

[*]Masahiro Yoshimura, J. Senthilnathan, K. SanjeevaRao
**Promotion Centre for Global Materials Research (PCGMR), Department of Material Science and Engineering, National Cheng Kung University, Tainan, Taiwan [*]yoshimur@mail.ncku.edu.tw*

Different forms of carbon prepared from diverse syntyetic routs are currently being used in various fields of research including energetical, environmental, electrical, chemical, and biomedical application. In general, carbon based materials like graphene, carbon nanotube, carbon nitride, diamond like carbon etc. are prepared from gaseous precursors such as CVD, PVD and ion-assisted sputtering techniques [1]. We believe that the large scale synthesis of nanostructured carbon should be free from using excess energy for firing, sintering, melting and expensive equipment. We, propose herewith "Submerged Liquid Plasma (SLP)" technique for direct formation of nanostructured carbon material and nitrogen polymers (NPs) at ambient conditions. The SLP process provides number of advantages which includes (a) simple reaction set up (b) reaction can be carried out at ambient conditions (c) periodic collection of samples gives clear information about the product (d) simple procedure and less operating cost. In the present study, we utilized SLP technique for the direct synthesis of NPs. Under SLP, organic compounds which have either unsaturated or high energy functional group (e.g. C=C, C=N and C≡N) form stable free radical monomer and initiate polymerization reaction.[1] The most significant differences are that the polymers produced by plasma process do not contain regular or repeating units and are enriched with radicalized functional groups. We have succeeded to prepare Nitrogen functionalized Graphene Nano sheets by these SLP in acetonitrile liquids.[2,3] We could confirm the functionalized Graphenes are electrochemically active. Then we are challenging to prepare the Nano-particle/Graphene hybrids by this SLP methods. Low temperature and/or Soft Processing of nanostructured carbon and NPs by SLP process will open up new possibilities for the development of functionalized/hybrid nanostructured carbon materials for various applications including Photovoltaic and Solar Cell areas.

References:

1. J. Senthilnathan, C. C. Weng, J. D. Liao, M. Yoshimura, *Sci. Rep*. **3**, 2414; DOI:10.1038/srep02414 (2013)
2. J. Senthilnathan, M.Yoshimura et al., J. Mater Chem A,(2014) **2,** 3332-3337, a Hot Paper 2014
3. J. Senthilnathan,K. SanjeevaRao, M. Yoshimura, et al ., Scientific Reports, **4**(2014), 04237 & 04395

CG-02 (Invited Talk)
Interfaces between transferred, CVD-grown graphene and MoS_2 probed with STM and ARPES

Horacio Coy Diaz[1], Jose Avila[2], Rafik Addou[1], Maria Carmen Asensio[2], Matthias Batzill[1]

[1]Department of Physics, University of South Florida, Tampa, FL 33620, USA
Email:mbatzill@usf.edu

[2]Synchrotron Soleil, Orme des Merisiers - Saint Aubin, BP 48 - 91192 - GIF SUR YVETTE Cedex, France

Heterostructures made of different van der Waals materials are of increasing interest because of potential applications in energy harvesting and combination of spin- and valley-tronics. However, the interface properties of these materials are not yet well characterized. One challenge for their characterization is the preparation of large-area high quality materials that enable employment of surface characterization techniques such as scanning

probe microscopy and photoemission spectroscopy. Here we demonstrate the transfer of CVD-grown graphene to bulk MoS_2 substrates and report the first STM and ARPES studies of such a system. As expected for weakly interacting materials STM studies only exhibit a very weak moire-superstructure and (nano) ARPES measurements show that the Dirac cone of graphene is maintained. However, (nano) ARPES also shows the formation of band-gaps in the pi-band of graphene where the out-of-plane molecular orbitals of MoS_2 intersect with the electronic-states of graphene, as shown in Fig.1. This modification of the electronic structure of graphene in the graphene/MoS_2 heterostructure is contrary to expectations of simple van-der Waals stacked materials. The high quality of the samples will enable further studies of the spin state of the graphene and MoS_2 substrate as well as enable preparation of other heterostructure materials and thus will give a detailed description of the interaction in these heterostructure systems.

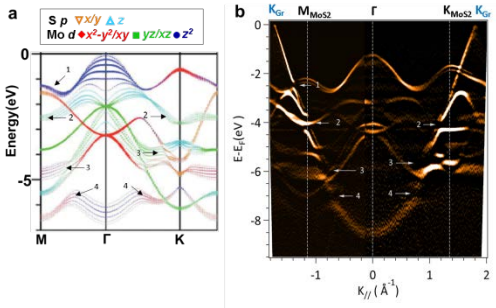

Fig. 1. (a) Calculated band structure of MoS_2 with the orbital character of the individual bands color coded. Data reproduced from: Han, S.W., Cha, G.-B., Frantzeskakis, E., Razado-Colambo, I., Avila, J., Park, Y.S., Kim, D., Hwang, J., Kang, J.S., Ryu, S., Yu, W.S., Hong, S.C., Asensio, M.C. Band-gap expansion in the surface-localized electronic structure of MoS_2 (0002). Phys. Rev. B 86, 115105 (2012). (b) 2nd derivative of E-k ARPES spectrum of graphene/MoS_2. The observed band gaps in the graphene π-band are labeled and their position with respect to the MoS_2 band structure are indicated in (a). This illustrates that the band-gaps in graphene open where there π-band overlaps in energy and momentum with MoS_2 states that exhibit out-of plane orbital character.

CG-03 (Invited Talk)

Silicene, germanene and stanene: Novel 2D honeycomb crystals from first principles

Friedhelm Bechstedt

Institut für Festkörpertheorie und –optik, Friedrich-Schiller-Universität Jena
Email:bech@ifto.physik.uni-jena.de, web site: http://www.ifto.uni-jena.de and http://www.ico.uni-jena.de

The discovery of graphene and the observation of its peculiar physical properties have caused an intense search for group-IV analogs such as silicene and germanene with a two-dimensional (2D) honeycomb symmetry [1]. Their realization is still a matter of controversy [2, 3]. This concerns their growth on substrates but also the transition from sp^2 to sp^3 bonding and the relation to Dirac cones. Chemical modifications such as the hydrogenation lead to novel 2D crystals like silicane or germanane with large gap openings and hence changed properties [4]. The group-IV sheet crystals may pave the way to a future nanotechnology, compatible with the Si-device technology, and be applied in novel optoelectronic and photovoltaic devices. Therefore, we have studied their properties from first principles:

(1) Stability and growth of silicene on various metallic and nonmetallic substrates are investigated within the density functional theory including van der Waals interaction. Monolayer and bilayers on Ag(111) [3, 6] and other substrates [5] are in the focus. Theoretical results are compared with STM and ARPES measurements.

(2) The infrared optical absorbance in silicene and germanene layers is shown to be independent of element, buckling and hybridization but is given by the Sommerfeld finestructure constant [7, 8]. Only spin-orbit interaction modifies the picture [9]. For higher photon energies drastic modifications due to interband van Hove singularities occur.

(3) The hydrogenation significantly changes the properties. The resulting silicane and germanane layers possess large gaps. Solving the Dyson and Bethe-Salpeter equations we study the

near band edge absorption spectra, in particular the bound excitons with huge binding energies [10].

(4) Spin-orbit interaction plays an important role for the gap opening and the topological properties of germanene and stanene.

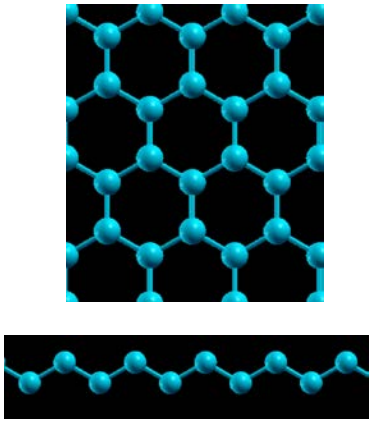

Fig. 1. Top and side view of a honeycomb crystal, e.g. silicene.

1. P. Vogt, P. De Padova, C. Quaresima, J. Avila, E. Frantzeskasis, M. C. Asensio, A. Resta, B. Ealet, and G. Le Lay, *Phys. Rev. Letters* **108**, 155501 (2012).
2. P. Gori, O. Pulci, F. Ronci, S. Colonna, and F. Bechstedt, *J. Applied Phys.* **114**, 113710 (2013).
3. P. Pflugradt, L. Matthes, and F. Bechstedt, *Phys. Rev. B* **89**, 035403 (2014); **89**, 205128 (2014).
4. E. Bianco, S. Butler, S. Jiang, O. D. Restrepo, W. Windl, and J. E. Goldberger, *ACS Nano* **7**, 4414-4421 (2013).
5. P. Pflugradt, L. Matthes, and F. Bechstedt, *Phys. Rev. B* **16**, 075004 (2014).
6. S. Kokott, L. Matthes, and F. Bechstedt, *Phys. Status Solidi RRL* **7**, 538-541 (2013); *J. Phys. CM* **26**, 185002 (2014).
7. F. Bechstedt, L. Matthes, P. Gori, and O. Pulci, *Appl. Phys. Letters* **100**, 261906 (2012).
8. L. Matthes, P. Gori, O. Pulci, and F. Bechstedt, *Phys. Rev. B* **87**, 035438 (2013).
9. L. Matthes, O. Pulci, and F. Bechstedt, *J. Phys.: Condens. Matter* **25**, 395305 (2013).
10. O. Pulci, P. Gori, M. Marsili, V. Garbuio, R. Del Sole, and F. Bechstedt, *EPL* **98**, 37004 (2012).

CG-04 (Invited Talk)
Bandgap control in graphene-molybdenum disulfide bilayer structures

Cristian V. Ciobanu

Department of Mechanical Engineering, Colorado School of Mines, Golden, CO 80401, USA
Email:cciobanu@mines.edu

Using density functional theory calculations with van der Waals corrections, we investigated how the interlayer orientation affects the structure and electronic properties of MoS2-graphene bilayer heterostructures. Changing the orientation of graphene with respect to MoS_2 strongly influences the type and the value of the electronic bandgap in MoS2, while not significantly altering the binding energy between the layers or the interlayer spacing. We show that the physical origin of this tunable bandgap arises from variations in the S--S interplanar distance (MoS2 thickness) with the interlayer orientation, variations which are caused by electron transfer away from Mo--S bonds.

CG-05 (Invited Talk)
Chemistry and electronic structure at graphene edges

Shintaro Fujii

Department of Chemistry, Tokyo Institute of Technology, Japan
Email:fujii.s.af@m.titech.ac.jp

The local electronic properties of graphene are crucially dependent on geometrical shape and chemistry of defect sites. According to current understanding, while the zigzag edge of graphene supports the localized π-state (edge state) on its boundary and gives rise to intra-valley scattering of extended electronic states, its armchair counterpart does not possess the edge state and leads to inter-valley scattering of charge carrier (Fig. 1). It is therefore appealing to tune electronic and magnetic properties of graphene-based nanostructures *via* changing geometrical shape of defects in graphene [*e.g.*, 1,2]. In a simple structural edge-defect model, each edge

site is passivated by a hydrogen atom to saturate the dangling bond and form mono-hydrogenated graphene edges. We prepared atomically well-defined hydrogenated graphene edges contained within nano-sized pits by atomic hydrogen etching of single-vacancies in the topmost graphene layer of graphite. To simulate scanning tunneling microscopy (STM) data, electronic calculations based on density functional theory (DFT) were performed. High-resolution STM characterizations and DFT simulations demonstrate that mono-hydrogenated zigzag edges are preferentially formed in the periphery of the nanoholes. In addition to the conventional mono-hydrogenated zigzag edge, we found a new type of zigzag edge, characterized by disappearance of the edge state and profound interference pattern in a form of electronic superlattice. To understand these two main features we have to take into account chemistry at zigzag edge. Systematic DFT simulations show that the edge state can be removed when every third zigzag-edge site is di-hydrogenated while two others remain mono-hydrogenated [3]. To further explore the effect of the edge chemistry on the electronic properties, oxidized graphene edges were prepared by electrochemical oxidation of graphitic surface. In sharp contrast to the conventional hydrogenated graphene edge in previous reports, newly found oxidized edges (*i.e.*, ketonated zigzag edge) with higher thermodynamic stability exhibited significantly modulated π-states near the Fermi level, which is characterized by (i) spatially extended π-state distribution and (ii) energy-dispersive character with quasi-band gap nature. This modulation can be understood by participation of the oxygen π-electron into graphene π-electron system and resultant change in the effective boundary condition of the π-electron network [4]. Although the number of researches investigating the chemistry of one-dimensional linear edges has increased in recent years, there is a considerable lack of the studies on the chemistry of point defects (*i.e.*, zero-dimensional vacancy-edges). The electronic properties of the hydrogenated single-vacancy-defects are subject to significant modulation in response to chemical details at the defect-edges. The defect-localized π-state at the fully mono-hydrogenated vacancy can be quenched by addition of a forth hydrogen atom at the defect-edge [5]. We provide experimental evidence of mechanical switching functionality of the edge-localized π-state at the oxidized point defects, which is induced by dynamic changes in the bonding configuration of the oxygen atoms. In addition to the number of foreign chemical species attached to the edge, their bonding configurations have in fact a strong impact on the electronic properties [6].

1. S. Fujii, M. Ziatdinov, M. Ohtsuka, K. Kusakabe, M. Kiguchi, T. Enoki, *Faraday Discussions* DOI: 10.1039/C4FD00073K, in press.
2. S. Fujii, T. Enoki, *Acc. Chem. Res.* **46**, 2202 (2013).
3. M. Ziatdinov, S. Fujii, K. Kusakabe, M. Kiguchi, T. Mori, T. Enoki, *Phys. Rev. B* **87**, 115427 (2013).
4. M. Ohtsuka, S. Fujii, M. Kiguchi and T. Enoki, *ACS Nano* **7**, 6868 (2013).
5. M. Ziatdinov, S. Fujii, K. Kusakabe, M. Kiguchi, T. Mori, T. Enoki, *Phys. Rev. B* **89**, 155405 (2014).
6. S. Fujii, T Enoki, *ACS Nano* 7, 11190 - 11199 (2013).

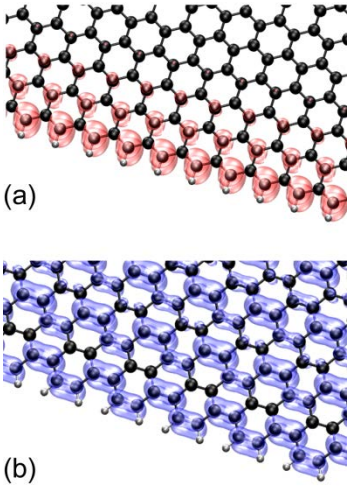

Fig. 1. DFT-simulated STM isosurface for zigzag (a) and armchair (b) edges (at -0.1 V).

CG-06 (Invited Talk)
Tailoring The Properties of Two Dimensional Molybdenum Disulfide

Saiful I. Khondaker[1], Muhammad R. Islam[2], Narae Kang[2], Udai Bhanu[2], Hari P. Paudel[2], Mikhail Erementchouk[2], Laurene Tetard[2], and Michael N. Leuenberger[2]

1.Nanoscience Technology Center and Department of Physics University of Central Florida, Orlando, Florida 32826, USA. Email: saiful@ucf.edu, website: http://physics.ucf.edu/~khondaker/
2.Nanoscience Technology Center and Department of Physics University of Central Florida, Orlando, Florida 32826, USA.

The ability to tailor the properties of a material is essential to optimize device functionality. Recently, attention has been focused to tailor the properties of two dimensional molybdenum disulfide (MoS_2), not only by controlling the number of layers but also by means of external controls. In this talk, I will present evidence that the electrical and optical propeties of monolayer and few layers MoS2 can be tuned by controlled exposure of the samples to oxygen plasma [1-2]. We find that the mobility, on-current and resistance of single layer and multilayered MoS_2 FET vary exponentially by up to four orders of magnitude with respect to the plasma exposure time. Photoluminescence (PL) study show a decrease of PL intensity leading a complete quenching. Raman studies conducted before and after plasma treatment show a significant decrease of intensity of MoS_2 peaks with the creation of new oxidation induced peak, while X-ray photoelectron spectroscopy (XPS) study show peaks associated with MoO_3 after plasma exposure. We suggest that during exposure to oxygen plasma, the energetic oxygen molecules interact with MoS_2 and create MoO_3 rich defect regions, which are insulating. MoO_3 defect regions acts as a tunnel barrier for the injected conduction electrons, giving rise to the exponential increase in resistivity as a function of plasma exposure time. Band structure calculation show that the PL quenching upon plasma exposure is due to the creation of MoO3 defect region which casues a direct to indirect badgap transition in monolayer MoS_2.

1. M. R. Islam, N. Kang, U. Bhanu, H. P. Paudel, M. Erementchouk, L. Tetard, M. N. Leuenberger, and S. I. Khondaker, Nanoscale **6**, 10033 (2014).
2. N. Kang, H. P. Paudel, M. N. Leuenberger, L. Tetard, and S. I. Khondaker, J. Phys. Chem. C **118**, 21258 (2014).

CG-07 (Invited Talk)
Band-to-band tunnel FETs in one and two-dimensional materials

Joachim Knoch[1]

[1]Institute of Semiconductor Electronics, RWTH Aachen University,Sommerfeldstrasse 24, 52056 Aachen Germany
Email:knoch@iht.rwth-aachen.de, web site: http://www.iht.rwth-aachen.de

In recent years, the power consumption of integrated circuits has become a major issue hindering a further increase of clock frequency and complexity of future ICs. The reason for this is predominantly the inability to decrease the supply voltage below approximately 1V without either severe performance degradation. This fact in turn is due to the fundamental working principle of conventional field-effect transistors that rely on the field-effect controlled modulation of current consisting of carriers injected from a thermally broadened Fermi distribution function. As a result, any conventional FET is bound to the so-clled 60mV/dec limit, meaning that at room temperature at least 60mV gate voltage change is needed in order to change the current by one order of magnitude.

Band-to-band tunnel FETs (TFETs) have recently attracted a great deal of interest since they potentially allows circumventing the 60mV/dec limit [1,2]. However, experimental devices to date exhibit a performance inferior compared to conventional FETs. Therefore, solutions are sought in order to realize substantial performance improvements and a number of performance boosters have been identified. One of the most effective one is an ultrathin channel layer [2,3,4,5], provided by e.g. 1D

nanostructures such as carbon nanotubes (CNTs) and 2D materials such as graphene and transition metal dichalcogenides (TMDs).

Here, the operating principles of TFETs will be discussed and experimental realizations as well as simulation results on TFETS realized in 1D and 2D materials will be presented. In particular, the role of the respective material properties and dimensionality will be elaborated on.

1. K.K. Bhuwalka, J. Schulze and I. Eisele, *Jpn. J. Appl. Phys.*, **43**, 4073 (2004).
2. J. Knoch, Tunnel FETs – Perspectives and Challenges, in Intelligent Integrated Systems, PanStanford, 2014.
3. K. Boucart and A. Ionescu, *IEEE Trans Electron Dev.*, **54**, 1725 (2007).
4. J. Appenzeller, Y.-M. Lin, J. Knoch, Z. Chen and Ph. Avouris, *IEEE Trans. Electron Dev.*, **52**, 2568 (2005).
5. J. Knoch and M. Müller, *IEEE Trans. Nanotechnol.*, 10.1109/TNANO.2014.2323436.

CG-08 (Invited Talk)
In Situ TEM Analysis of Catalyst-Assisted Growth of Multiwall Carbon Nanotubes and Nanofibers

Jean-Luc Maurice[1], D. Pribat[2], Z. He[1,3], G. Patriarche[4] and C. S. Cojocaru[1]

[1]*Laboratoire de Physique des Interfaces et Couches Minces, LPICM, UMR7647, CNRS, Ecole Polytechnique, Palaiseau, France Email:jean-luc.maurice@polytechnique.edu, web site: http://www.lpicm.polytechnique.fr/*

[2]*Department of Energy Science, Sungkyunkwan University, Suwon 440-746, Korea*

[3]*State Key Laboratory for Advanced Metals and Materials, University of Science and Technology Beijing, No. 30 Xueyuan Road, Haidian District, Beijing 100083, China*

[4]*Laboratoire de photonique et de nanostructures, LPN, UPR 20, CNRS, Marcoussis, France*

Direct-current Plasma Enhanced Chemical Vapor Deposition (dcPECVD) allows one to grow, at low temperature, vertically-oriented multiwall carbon nanotubes (MWCNTs) or nanofibers (CNFs), which can be organized in regular arrays, using lithography and precise positioning of the catalyst particles [1]. The vertically-oriented CNFs can provide electron emission in the 1 A/cm^2 range and can be used in turn in many devices from microwave tubes (i.e. travelling wave tubes) to portable X-ray generators.

In that low-temperature catalyst-assisted growth method, graphene layers continuously nucleate and grow at the surface of crystalline catalyst particles. The efficiency of electron emission depends notably on the electrical resistance of the nanotubes, which in turn depends on the microstructure produced by the nucleation and growth sequence. Here, we study the atomic mechanisms at work during these processes, by observing them *in situ* in the transmission electron microscope (TEM), in the case of iron-based catalysts. As in the seminal work of Helveg *et al.* on Ni catalysts [1], graphene layers appear at the surface of Fe-based particles by a mechanism of step flow, where the atomic layers of catalyst are ‘‘replaced’’ by graphene layers. Figure 1 shows the *in situ* growth of graphene layers at 550°C at the expense of an equivalent volume of a Fe_3C catalyst. Quite remarkably, catalyst facets systematically develop while this mechanism is at work [2]. We discuss the origin of faceting in terms of equilibrium particle shape and graphene layer nucleation.

The MWCNTs used in the present experiments were first obtained *ex situ* by dcPECVD. The *in situ* growth was performed with no gas, by using the carbon atoms already present in the samples.

Mastering the mechanisms of faceting and step bunching could open up the way to tailoring the structure of low temperature-grown MWCNTs, e.g. with highly parallel carbon walls and, ultimately, with controlled structure and chirality.

1. K.B.K. Teo *et al.*, *Appl. Phys. Lett.* **79**, 1534 (2001).

2. S. Helveg, *et al.*, *Nature* **427**, 426 (2004).
3. J.-L. Maurice, *et al.*, *Carbon*, to appear: http://dx.doi.org/ 10.1016/j.carbon.2014.07.047.

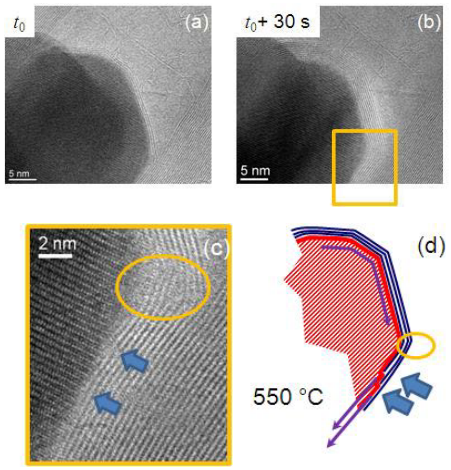

Fig. 1. HRTEM images of a CNF first obtained with iron carbide catalyst by dcPECVD at 650 °C. In (a) the CNF has been annealed in situ for t_0 = 4 min 10s at 550°C. In (b), after 30 additional seconds at 550°C, six graphene layers have developed at the expense of an equivalent volume of the carbide catalyst. (c) Enlargement of the yellow rectangle in (b) showing the surface steps that give birth to the graphene layers. (d) Schematic diagram showing the movement of the steps (purple arrows).

CG-09 (Invited Talk)
Atomically Thin Vertical Heterojunction Devices

Jing Guo[1]

[1]*Department of Electrical & Computer Engineering, University of Florida, Gainesville, FL, USA*
Email:guoj@ufl.edu, web site: http://www.guo.ece.ufl.edu

Two-dimensional (2D) layered dichalcogenide materials, which offer a bandgap that is absent in graphene, have attracted extensive research interest for potential electronic device applications[1]. Vertical tunneling field effect transistors (FETs), which uses graphene as the source and drain contacts, and sandwiched BN or 2D dichacolgenide layers as the tunneling barrier, have been experimentally fabricated and theoretically examined [2-3].

In this work, a vertical transistor based on a double gated, atomically thin heterojunction is theoretically examined [4]. It is shown that both p-type and n-type transistor operations can be conveniently achieved by using one of the two gates as the switching gate (Fig. 1). The transistor shows excellent saturation of output I-V characteristics due to drain-induced depletion and lack of tunneling barrier layers. The subthreshold slope could be below the thermionic limit due to band filtering as the switching mechanism (Fig. 2). The atomically thin vertical PN heterojunction can be electrostatically modulated from a type II heterojunction to a broken bandgap alignment, which is preferred for maximizing the on-current.

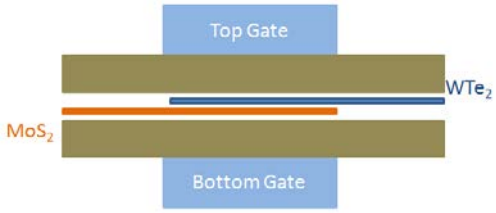

(a)

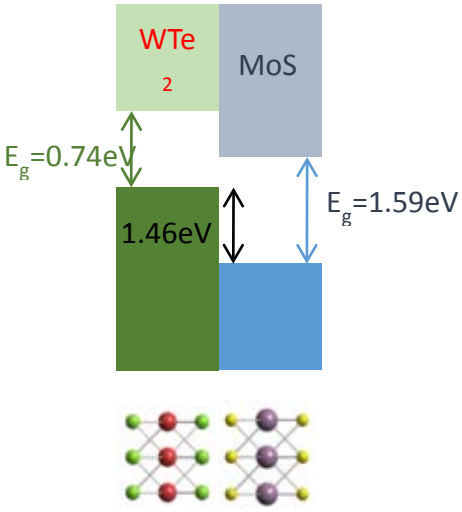

(b)

Fig. 1. (a) Modeled device structure. A double gated vertical monolayer WTe_2-MoS_2 heterojunction. The gate insulator has a thickness of t_{ox}=3nm and a dielectric constant of κ=20. The work function of both gates is assumed to be $\Phi = 4.3eV$. (b) The band alignment of a WTe_2-MoS_2 monolayer heterojunction in absence of gating.

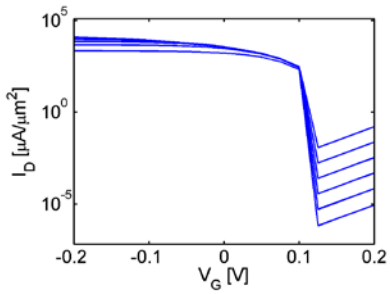

(a)

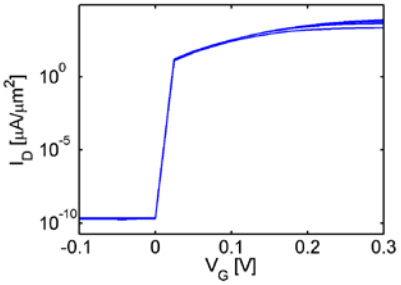

(b)

Fig. 2 (a) I_D vs. V_{TG} characteristics at different V_D (from -0.05V to -0.3V at -0.05V/step) when the top gate acts as the switching gate. The bottom gate voltage is fixed at $V_{BG} = 0.3V$. The transistor operates as a p-type FET, in which the source (MoS_2 layer) is grounded. (b) I_D vs. V_{BG} characteristics at different V_D (from 0.05V to 0.3V at 0.05V/step) when the bottom gate acts as the switching gate. The top gate voltage is fixed at $V_{TG} = -0.5V$. The transistor operates as an n-type FET, in which the source (WTe_2 layer) is grounded.

1. Q. H. Wang, et al, " *Nature Nanotechnology,* vol. 7, pp. 699-712, Nov 2012.
2. L. Britnell *et al.*, *Science,* vol. 335, pp. 947-950, Feb 24 2012.
3. C. Lee et al.," *Nature Nanotechnology*, 9, 676 (2014)
4. K. Lam, *Appl. Phys. Lett.*, 105, 013112 (2014).

CG-10 (Invited Talk)

Applications of Photon-electron interactions for advanced optoelectronics in 2D materials

Swastik Kar

Department of Physics, Northeastern University, Boston, MA, USA
Email:s.kar@neu.edu, web site: http://nuweb4.neu.edu/swastik/home.htm

The remarkable rise of graphene as a 2D functional material for a range of applications has paved the way for the discovery of a wide variety of other 2D, atomically thin, and layered materials with a broad range of electronic and optical properties. This, in turn, has led to exciting new directions of research in physics, chemistry, materials science, electrical and mechanical engineering. In this talk, some of our recent results in photonics, optoelectronics and nanomechanics using some of these atomically thin materials will be presented, focusing on the theme of structural and functional tunability of these materials. Specifically, the use of graphene for designing tunable photodetectors and ultrafast actuators with extremely high performances, effect of quantum confinement and tunable optical properties of bismuth selenide, and light emission and excitonic properties of molybdenum disulfide will be discussed. Finally, the idea of 2D alloys – materials with tunable compositions in a purely 2D lattice will be discussed. These materials and systems are just a small representative of the new field of 2D materials that can potentially revolutionize materials science in the next decade.

CG-11 (Contributed Talk)

Effective Thermal Properties and Interfacial Thermal Resistances of Multiphase Nanocomposites Containing Carbon Nanotubes and Inorganic Nanoparticles

Feng Gong[1], Dimitrios V. Papavassiliou[2], and Hai Minh Duong[1]*

[1]*Department of Mechanical Engineering, National University of Singapore, Singapore*
**mpedhm@nus.edu.sg*
[2]*School of Chemical, Biological and Materials Engineering, University of Oklahoma, USA*

A mesoscopic model was developed to investigate the effective thermal properties and interfacial thermal resistances of polymer nanocomposites containing carbon nanotubes (CNTs) and inorganic nanoparticles by the means of Off-Lattice Monte Carlo method. The developed model more accurately predicted the effective thermal conductivity (K_{eff}) of 3-phase nanocomposites than the Effective Medium Theories (EMTs) by taking into account the interfacial thermal resistance (R_{bd}) between any two phases and the synergistic effect of CNTs and nanoparticles. In the developed model, complex morphology of CNTs (CNT diameter and length, volume fraction, orientation and CNT bundle) and heat transfer mechanism at interfaces were quantified to study their effects on K_{eff} of the nanocomposites. Moreover, by fitting the simulated K_{eff} with the experimentally measured K_{eff}, interfacial thermal resistances of polymer-CNT and polymer-nanoparticle can be back-calculated, which are difficult to be determined by experiments. The simulation results showed that K_{eff} of multiphase nanocomposites increased when CNT fraction increased and when R_{bd} of polymer-nanofillers (CNTs and inorganic nanoparticles) decreased. CNT bundle exhibited different effects on K_{eff} of nanocomposites with different oriented CNTs. It decreased the K_{eff} in nanocomposites with random and parallel CNTs, whereas, increased the K_{eff} in those with perpendicular CNTs. The findings not only fill the gap to bridge the macroscopic Finite Element methods (FEMs) and the microscopic molecular dynamics (MD) approaches, but also suggest the way to fabricate multiphase nanocomposites with high thermal conductivity.

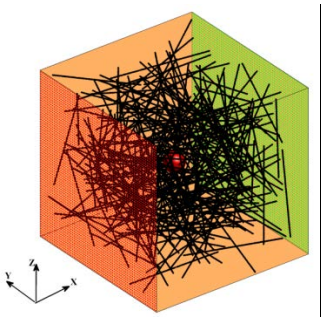

Fig. 1: Schematic plot of the computational model.

References:

[1] Feng Gong, Khoa Bui, Dimitrios V. Papavassiliou, Hai M. Duong. Carbon 78 (2014) 305-316.
[2] Gong F, Hongyan Z, Papavassiliou DV, Bui K, Lim C, Duong HM. Nanotechnology. 2014; 25(20):205101
[3] Feng Gong, D.V. Papavassiliou, Hai M. Duong. Numerical Heat Transfer Part A, 2014, 65, 1023-1043

CG-12 (Contributed Talk)

Graphene Oxide: Bacterial Stimulant or Antimicrobial Agent?

W. S. Kuo[1,2,*], J. Y. Wang[1]

[1]*Department of Biochemistry and Molecular Biology, National Cheng Kung University, Tainan 701, Taiwan*
Email:activesitess@gmail.com

[2]*Advanced Optoelectronic Technology Center, National Cheng Kung University, Tainan 701, Taiwan*

We examined whether graphene oxide sheets stimulate or inhibit bacterial growth. We found that it depended on whether the bacteria and graphene oxide materials (graphene oxide [GO], GO-polyoxyalkyleneamine [GO-POAA], and GO-chitosan) were incubated with a nutrient. Figure 1 shows Bacteria with or without GO, GO-POAA, and GO-chitosan characterized by TEM.

Graphene oxide not only stimulated bacterial growth and microbial proliferation for Gram-negative and Gram-positive bacteria, but also might have augmented surface attachment for both types of bacteria. Once an external barrier composed of graphene oxide-based materials had formed around a bacterial surface, it suppressed nutrients essential to microbial growth and simultaneously produced oxidative stress, which caused bacteria to die, even at high concentrations of biocompatible GO-POAA. Moreover, because graphene oxide may act as a biofilm, suppress the toxicity of low-dose chitosan. [1, 2]

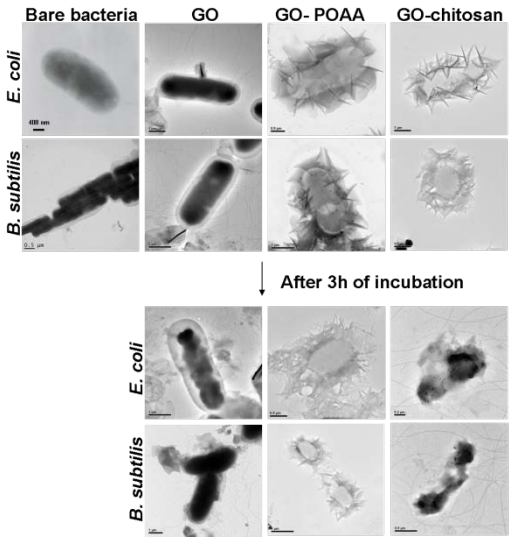

Fig. 1. Bacteria with or without GO, GO-POAA, and GO-chitosan characterized by TEM.

1. K. Hund-Rinke and M. Simon, *Environ. Sci. Pollut. Res.* **13**, 225 (2006).
2. I. Sondi and B. Salopek-Sondi, *J. Colloid. Interf. Sci.* **275**, 177 (2004).

CG-13 (Contributed Talk)

Carbon Nanospheres Synthesis using Palm Oil and Activated Carbons.

Arenst Andreas Arie, Hans Kristianto[1], Ratna Frida Susanti[1], Joong Kee Lee[2]

[1]*Department of Chemical Engineering, Parahyangan Catholic University,Bandung, Indonesia*
Email:arenst@unpar.ac.id

[2]*Battery Research Center, Korea Institute of Science and Technology, Seoul, Korea*

In the past few years, spherical carbon materials include carbon nanospheres (CNSs) have become interesting research subject due to their unique chemical and physical properties [1, 2]. CNSs are resulted from the pairing of pentagonal and heptagonal carbon rings which can enhance surface reactions, allowing CNSs as promising candidates for many emerging applications [1]. In general, we can classify the preparation of carbon spheres into two approaches such as direct (chemical vapor deposition, pyrolysis and hydrothermal treatment and templating techniques [3-6].

In this work, CNSs have been synthesized by the catalytic pyrolysis process using palm oil and activated carbons as the carbon source and Fe as the catalyst. Prior to the synthesis of CNSs, Fe-catalyst were prepared by both impregnation and urea deposition catalyst method. Products were characterized by Raman spectroscopy, X- Ray Diffraction (XRD), X-ray Photo Electron Spectroscopy (XPS) and High-Resolution (HR) TEM analysis. It was found that the presence of iron compound in the carbon product prepared by impregnation catalyst preparation method while lower amounts of iron were found in the carbon products synthesized by deposition method. HRTEM analysis revealed that the CNSs were poorly graphitized and showing a turbostratic structures. These results were confirmed by Raman reflected by intensity ratio between disorder and graphite like carbons (I_D/I_G).

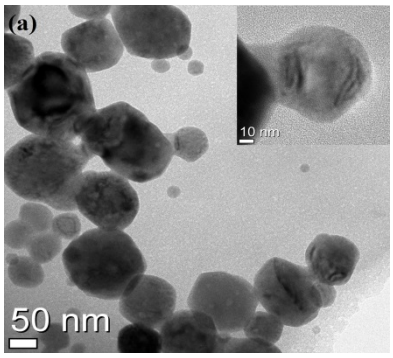

Fig. 1. TEM Image of CNSs prepared using palm oil and activated carbons

1. A.N. Marquez, R. Romero, A. Romero, J.L. Valverde, *J. Mater Chem*. 21, 1664-1672 (2011).
2. M. Li, Q. Wu, M. Wen, J. Shi, *Nanoscale Res Lett* 4, 1365-1370 (2009).
3. P. Serp, R. Feurer, p. Kalck, Y. Kihn, J. Faria, J. Figueiredo, *Carbon* 39, 621 (2001).
4. Y.Z. Jin et al., Carbon 43, 1944 (2005)
5. L. Qu, H. Zhang, J. Zhu, L. Dai, *Nanotechnology* 21, 305602-09 (2010).
6. A.N. Mohan and B. Manoj, *Int. J. Electrochem. Sci.*, 7 **9537** – 9549 (2012).

Session NP
NANOPHOTONICS AND PLASMONICS

NP-01 (Invited Talk)
Nonlinear Optical Imaging of Plasmonic Nanostructures at the Limits of Temporal Resolution and Spatial Precision

Kenneth L. Knappenberger, Jr.

Department of Chemistry and Biochemistry, Florida State University, Tallahassee, Florida, USA
Email:kknappenberger@fsu.edu, web site: http://www.chem.fsu.edu/~klk/KLK_group/

I will present recent spectroscopic advances for describing the time-dependent and frequency-resolved nonlinear optical and electronic properties of plasmonic nanoparticle assemblies. These properties for plasmonic nanostructures depend upon the exact arrangement of nanoparticles within a network, and therefore, require single-particle optical measurements to obtain insights into the structure-property interplay. I will describe the use of single-particle SHG imaging techniques developed in our lab that provide high spatial precision and femtosecond time resolution for examining plasmonic assemblies. The femtosecond time-resolution is achieved by employing a sequence of phase-locked laser pulses to examine the nanostructures. Phase-stabilized laser pulse replicas are generated collinearly, and used for nonlinear optical imaging by controlling the inter-pulse delay with attosecond precision, as shown in Figure1. The phase stability of the pulse replicas persists for several hours, which greatly exceeds the requirements for single-particle pump-probe measurements. Results obtained from femtosecond time-resolved imaging obtained from several different nanostructures will be presented. In addition, the spatial precision of these measurements will be discussed.

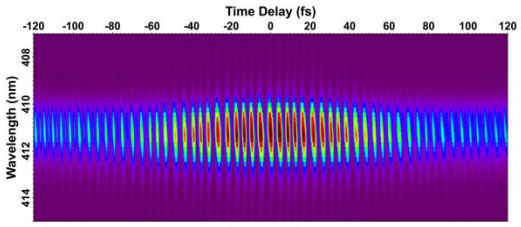

Fig. 1. Spectrally-resolved SHG-detected interferogram generated from pump-probe on a single plasmonic nanostructure.

NP-02 (Invited Talk)
Optically Launched Acoustic Phonon Modes Reveal Adhesion Strength to Substrate Supported Gold Nanodisks

Wei-Shun Chang[1], Fangfang Wen[1], Debadi Chakraborty[4], Man-Nung Su[1], Yue Zhang[2], Bo Shuang[1], Peter J. Nordlander[1,2,3], John E. Sader[4], Naomi J. Halas[1,2,3] and Stephan Link[1,2,3]

[1]Department of Chemistry, [2]Department of Physics, [3]Department of Electrical and Computer Engineering, Laboratory for Nanophotonics, Rice University, Houston, TX 77005, USA

[4]Department of Mathematics and Statistics, The University of Melbourne, Victoria 3010, Australia

Top-down lithography facilitates precise control over the physical dimensions of nano-objects. This control is critical for various applications utilizing the mechanical properties of nanomaterials. Unlike chemically prepared nanostructures that are deposited onto a substrate, lithographically fabricated nanostructures made of Au require an adhesion layer such as Ti or Cr between the Au and the substrate. Apart from a mostly practical standpoint, the binding strength and its variation with adhesion layer thickness are, however, not well understood. Here, we show how a non-invasive optical method, single particle ultrafast transient extinction spectroscopy, can be used to quantitatively probe the binding strength between Au nanodisks and a glass substrate by monitoring the frequencies of an impulsively launched acoustic phonon mode as a function of the Ti layer thickness as shown in

Figure 1(A). With increasing Ti thickness we observed an increase of the acoustic vibration frequency originating from the strength of the binding between the substrate and nanodisk. A clear transition from non-binding to strong binding was observed with increasing Ti thickness. A detailed FEM simulation with two extreme cases, free v.s. fixed surface model shown in Figure 1(B), further support the experimental results. Additionally, the breathing mode frequency of the nanodisks scaled linearly with the volume percent of Ti, suggesting that this could be a non-invasive optical method to determine the Ti content in Ti/Au bimetallic nanostructures. These results provide detailed understanding of the mechanical properties of lithographically fabricated structures.

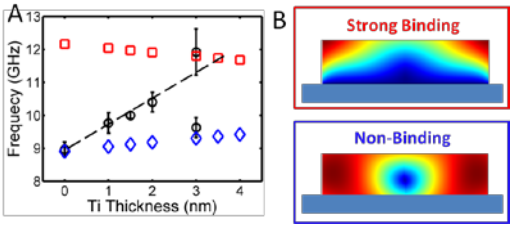

(A) Breathing mode frequencies of single Au nanodisk as a function of Ti thickness where the Au thickness is constant 35 nm. Black circles, blue diamonds and red squares represent the results from experiment, free surface and fixed surface models, respectively. (B) FEM simulations of the normalized displacement fields of the Au/Ti nanodisk using a fixed surface model (top) and a free surface model (bottom).

NP-03 (Invited Talk)

Investigation of optical nonlinearities in graphene and layered semiconductors by multiphoton imaging

Lasse Karvonen[1], A. Säynätjoki[1], S. Mehravar,[2] R. Norwood,[2] N. Peyghambarian,[1,2,3] H. Lipsanen,[1] K. Kieu,[2] and J. Riikonen[1]

[1]*Aalto University, Department of Micro and Nanosciences, Tietotie 3, FI-02150 Espoo, Finland*

[2]*University of Arizona, College of Optical Sciences, 1630 E University Blvd, Tucson, AZ 85721, USA*

[3]*University of Eastern Finland, Institute of Photonics, P.O. Box 111, FI-80101 Joensuu, Finland*

lasse.karvonen@aalto.fi

Due to the ever increasing demand for high speed data transfer, optical telecommunication is one of the key fields pursuing novel applications by exploiting second- and third-order optical nonlinearities. 2D nanomaterials have shown to be suitable materials for integration to silicon waveguides. Specifically, graphene was used to demonstrate waveguide-based modulators and detector devices [1, 2]. We have shown that graphene is a highly nonlinear material with the $\chi^{(3)}$ of ~$3*10^{-7}$ esu at the telecommunication wavelengths [3]. We have also observed multiphoton excitation fluorescence from graphene under the femtosecond laser excitation [3] (Fig. 1a shows RGB composite image generated from the fluorescence and THG signals from few-layer graphene flakes). However, in the guided-wave devices, the high absorption of graphene causes high propagation losses hindering its practical use. Therefore, the highly nonlinear layered semiconductors (with a band-gap) would be more suitable for real guided-wave applications.

We have studied the nonlinear optical properties of different layered semiconductors (including GaSe, WS_2, etc.) using multiphoton microscopy. Strong second- and third-harmonic generations were observed in few-layer gallium selenide flakes. The SHG and THG signals showed clear contrast between different numbers of GaSe layers. Figure 1b shows an RGB composite SHG-THG micrograph of the GaSe flake with different thicknesses. The red color in the RGB image represents the SHG signal, and the green color represents the THG signal. The areas that simultaneously show a high intensity for both SHG and THG appear yellow in the composite image. Even the fourth-harmonic generation signal was detected from a ~40 nm thick flake. Figure 1c and 1d show the optical and THG image of few-layer WS_2 flake. We will compare the nonlinear optical properties of graphene with other 2D layered materials, such as GaSe, WS_2, etc.. We discuss the generated nonlinear signal as the function of the number of

layers, the excitation power, and the excitation wavelength. In addition, we also discuss the spectral properties of the multiphoton excited luminescence.

[1] M. Liu *et al.*, *Nature* **474**, 64 (2011).
[2] X. Gan *et al.*, *Nature Photonics* **7**, 883-887 (2013).
[3] A. Säynätjoki *et al.*, *ACS Nano* **7**, 8441 (2013).
[4] L. Karvonen *et al.*, Nanocarbon Photonics and Optoelectronics 2014, Polvijärvi, Finland, July 28 - August 1 2014.

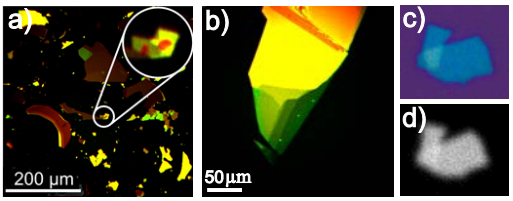

Fig. 1: a) RGB composite image generated from fluorescence (red) and THG (green) signals of few-layer graphene, b) RGB composite image generated from SHG (red) and THG (green) images of few-layer GaSe, c) optical image of few-layer WS_2 and d) THG image of few-layer WS_2.

NP-04 (Invited Talk)
Optical response of a single deposited metal nano-object

E. Pertreux, A. Lombardi, A. Crut, P. Maioli, N. Del Fatti and F. Vallée

FemtoNanoOptics Group, Institut Lumière Matière, Université Lyon 1 – CNRS, Villeurbanne - France
Email: fabrice.vallee@univ-lyon1.fr

Understanding and modeling the impact of size reduction on the optical properties of nano-objects is an intense field of research with both fundamental and technological motivations. With the advance of single nanoparticle optical spectroscopy methods, the optical response of a single nano-object can now be addressed and its morphology independently determined by characterization tools such as 2D or 3D transmission electron microscopy (TEM). It opens the way to precise comparison of the measured optical response, e.g., absorption or scattering, with the results of theoretical models. This is particularly interesting in the case of metal particles, whose absorption spectra show new resonances with their size reduction down to the nanoscale, the surface plasmon resonances (SPR). Their characteristics (frequency, spectral width and amplitude) are very sensitive to the particle size and shape, and to its environment, permitting to tune them for applications or to develop nano-sensors. Precise modeling of the impact of these different parameters on the particle optical response is thus of central interest, both from the fundamental point of view and for development of applications.

In this context we will describe investigation of different single nanoparticles deposited on a transparent or optically absorbing substrate, and analyze the influence of the latter on their optical absorption. Experiments are performed using the spatial modulation spectroscopy (SMS) method, which yields access to the absorption cross-section spectra and amplitude of a single nano-object with size down to a few nanometers [1]. In the case of silica-coated silver nanospheres or gold nanorods, isolation from the substrate provided by the silica shell largely reduces interaction with the substrate, and the optical response can be quantitatively reproduced using the core-shell particle morphology determined by TEM and the dielectric constants of the constituting materials [2]. This is no more the case for bare particles such as gold nanorods or bipyramids, whose SPR is strongly modified by the presence of the substrate and depends on the details of their interaction. This is ruled by the particle-substrate distance and particle orientation relative to the substrate, determined by TEM tomography. Similar impacts were observed in the case of the optical absorption of individual single-wall carbon nanotubes [3] and of the acoustic mode damping of a metal nanowire [4], by investigating the same nano-object either suspended over a trench or deposited on glass.

1. O. L. Muskens, P. Billaud, M. Broyer, N. Del Fatti, and F. Vallée, Phys. Rev. B**78**, 205410 (2008).
2. A. Lombardi, M. Loumaigne, A. Crut, P. Maioli, N. Del Fatti, F. Vallée, M. Spuch-Calvar, J. Burgin,

J. Majimel, and M. Tréguer-Delapierre, Langmuir **28**, 9027 (2012).
3. J. C. Blancon, M. Paillet, H. N. Tran, X. T. Than, S. Aberra Guebrou, A. Ayari, A. San Miguel, N-M.Phan, A.-A. Zahab, J.-L. Sauvajol, N. Del Fatti and F. Vallée, Nature Comm. **4**, 2542 (2013).
4. T. A. Major, A. Crut, B. Gao, S. Shang Lo, N. Del Fatti, F. Vallée, and G. V. Hartland, Phys Chem Chem Phys. **15**, 4169 (2013).

NP-05 (Invited Talk)
Taming the Blackbody: Thermal Radiation Spectrum Engineering with Plasmonic Semiconductor Nanowires

Michael A. Filler[1], Li-Wei Chou[1], Dmitriy S. Boyuk[1]

[1]School of Chemical & Biomolecular Engineering, Georgia Institute of Technology, Atlanta, GA, USA
Email: mfiller@gatech.edu, web site: http://fillergroup.gatech.edu

Nanoscale doped semiconductors are emerging as a diverse class of materials for engineering infrared localized surface plasmon resonances (LSPRs). Si's earth-abundance, low cost, and extensive processing know-how make it an excellent choice in this regard, particularly for applications requiring large quantities of material (e.g., coatings). This talk will overview our recent efforts to generate and characterize LSPRs in selectively doped Si nanowires. Resonant absorption (and emission) can be tuned between 5 and 20 μm by varying doped segment aspect ratio and carrier density [1,2]. Large absorption cross-sections, exceeding 10^{-10} cm^{-2} at room temperature, suggest that Si can compete with conventional, but more expensive infrared absorbers. Scattering simulations reveal the anisotropic dielectric environment inherent in the nanowire geometry and large permitivities of undoped semiconductors in the infrared underlie this behavior [3]. Complex absorption spectra are possible by encoding multiple, user-defined doped segments, each with distinct dimensions and/or dopant concentrations, along the length of individual nanowires. *Operando* infrared spectroscopy studies of nanowire growth also identify the need for novel surface species to control dopant profile.

1. L-W. Chou, N. Shin, S. V. Sivaram, M. A. Filler, *J. Am. Chem. Soc.* **134**, 16155 (2012).
2. L-W. Chou, M. A. Filler, *Angew. Chem. Int. Ed.* **51**, 8079 (2013).
3. L-W. Chou, R. D. Near, D. S. Boyuk, M. A. Filler, *J. Phys. Chem. C* **118**, 5494 (2013).

NP-06 (Invited Talk)
Glass nanowires for nonlinear optics and sensing: a top-down approach

R. Ismaeel, M.I.M. Abdul Khudus, M. Gouveia, T. Lee, M. Ding, P. Wang, G. Brambilla

[1]Optoelectronics Research Center, University of Southampton, Southampton, SO17 1BJ, UK
Email:gb2@soton.ac.uk, web site: http://www.orc.soton.ac.uk

Optical microfibers (OMs) are waveguides of diameters comparable to the wavelength of the light propagating in them. Fig.1 (a) shows a schematic of a typical microfiber: it consists of a region with thin waist connected to two conventional optical fibres by transition regions. Their sub-micron size, easy connectivity to conventional optical fibres and relatively high mechanical strength have made them ideal for a variety of applications including sensors, lasers and light sources(1). Moreover, their strong evanescent field, good light confinement and high nonlinearity have raised the interest in exploring the possibility to use these microfibers for cheap, compact optical devices.

The large majority of OM applications can be categorized in two groups according to the feature they exploit, namely strong light confinement and large evanescent field.

The first group of applications exploits the strong confinement to provide large optical nonlinearities. OMs have gained an increasing interest because, in addition to the high modal confinement and high nonlinearity, they also display a tailorable dispersion profile. When compared to microstructured fibers (which also

hold similar nonlinearities), OMs benefit from lower fabrication cost, easier manufacturing and negligible input/output coupling losses. Our recent work focused on OM nonlinearities in relation to supercontinuum (SC), third harmonic (THG) and second harmonic generation (SHG). Novel methods to increase the effective OM nonlinearities were proposed using resonators, in which the enhancement is raised by the circulation of the pump power at the resonant wavelength[(2)].

The second group of applications relies on the large evanescent field. As shown in fig. 1(a), in the minimum waist region light is not confined in the silica only, but it has a significant fraction of power propagating outside the fibre physical boundary. This has been exploited for sensors, plasmonic and optical components. Two examples of devices are shown in fig. 1 (b) and 1 (c), where a coupler and a plasmonic resonator are presented.

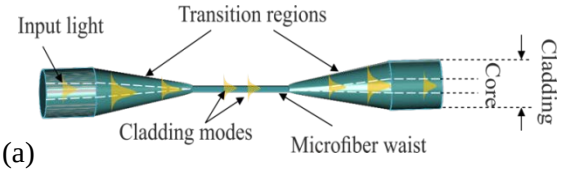

(a)

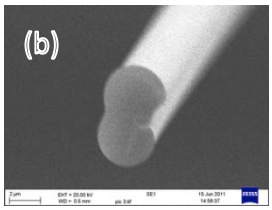

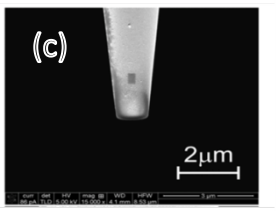

Fig. 1. (a) schematic of an optical microfiber. (b) SEM image of the coupler cross-section used for Bio-sensing applications. (c) Plasmonic slot nanoresonators embedded in a gold-coated microfiber tip.

OMs have found numerous applications in sensing because the large evanescent field surrounding the waist allows the propagating light to interact with the surrounding medium. The change in the surroundings is monitored by the change in the transmission of the device and sensitivities in excess of ~1000nm/RIU and detection limits smaller than 10^{-6} RIU were recorded. Sensors for temperature, current and biological molecules have also been demonstrated.

Plasmonics in OMs were investigated by coating them with a metal and exploiting the overlap of the evanescent field with the metal. Plasmonic slot nanoresonators embedded in a gold-coated microfiber tips (Fig. 1(c)) were demonstrated and showed strong localization in three dimensions and strong enhancement factor (7.24×10^3). The proposed geometry is suitable for wide range of applications, such as surface enhanced Raman scattering, optical filtering, bio sensing and spectroscopy [(3)].

1. R. Ismaeel, T. Lee, M. Ding, M. Belal, and G. Brambilla, "Optical microfiber passive components," Laser & Photonics Reviews 7, 350–384 (2013).
2. R. Ismaeel, T. Lee, M. Ding, N. G. R. Broderick, and G. Brambilla, "Nonlinear microfiber loop resonators for resonantly enhanced third harmonic generation," Opt. Lett. 37, 5121–5123 (2012).
3. M. Ding, P. Wang, and G. Brambilla, "A microfiber coupler tip thermometer," Opt. Express 20, 5402-5408 (2012).

NP-07 (Invited Talk)

Light emission from group-IV nanostructures in silicon

Søren Roesgaard Nielsen[1], Peter I. Gaiduk[2], Arne Nylandsted Larsen[1,3], John Lundsgaard Hansen[3], Peter Balling[1,3], Axel Svane[3], and Brian Julsgaard[3,*].

[1] Interdisciplinary Nanoscience Center (iNANO), Aarhus University, Gustav Wieds Vej 14, DK-8000 Aarhus C. [2]Belarusian State University, Minsk, Belarus.
[3]Department of Physics and Astronomy, Aarhus University, Ny Munkegade 120, DK-8000 Aarhus C.
[*]E-mail address: brianj@phys.au.dk.

Efficient light emission from silicon, or silicon compatible materials from group IV elements, remains a tough challenge from both a fundamental and an applied point of view. It is indeed desirable to combine electronic and

optical functionality in a monolithic setting, which requires light emission capabilities at energies below the band gap of silicon. The two elements, germanium and tin, or alloys thereof, present good candidates for such light emission and are thus interesting to study.

The present talk will be focused particularly on time-resolved fluorescence methods applied to such materials. It is described how these methods can help us separate and understand various physical processes behind the recombination of electron-hole pairs. Specifically, Auger recombination in Ge nano islands [1, 2] will be used as examples, and we also comment on more recent studies on silicon containing embedded tin nano-structures.

1. B. Julsgaard, P. Balling, J. Lundsgaard Hansen, A. Svane, and A. Nylandsted Larsen, *Appl. Phys. Lett.* **98**, 093101 (2011).
2. Brian Julsgaard, Peter Balling, John Lundsgaard Hansen, Axel Svane, and Arne Nylandsted Larsen, *Nanotechnology* **22**, 435401 (2011).

NP-08 (Invited Talk)
Bridging the Particle Size Gap for Nanoplasmonics and Nanocatalysis

Hui Wang[1]

[1] *Department of Chemistry and Biochemistry, University of South Carolina, Columbia, South Carolina 29208, United States*

Email:wang344@mailbox.sc.edu, web site: http://artsandsciences.sc.edu/chemgroup/wang/hui-wang-group-usc

Noble metal nanoparticles have been of tremendous interest because of their intriguing size- and shape-dependent plasmonic and catalytic properties. The combination of tunable plasmon resonances with superior catalytic activities on the same nanoparticle, however, has long been challenging because plasmonics and catalysis require nanoparticles in two drastically different size regimes. Tunable plasmons are a unique feature of sub-wavelength metal nanoparticles, whereas heterogeneous catalysis requires the use of sub-5 nm nanoparticles as the catalysts. My group has recently demonstrated that desired plasmonic and catalytic properties can be integrated on the same particle by controllably creating high-index facets on individual sub-wavelength metallic nanoparticles. The capabilities to both nanoengineer high-index facets and fine-tune the plasmon resonances through deliberate particle geometry control allow us to use these nanoparticles for a dual purpose: as substrates for plasmon-enhanced spectroscopies and efficient surface catalysts. Such dual functionality opens up unique opportunities for quantitative study of the intrinsic kinetics and mechanisms of surface-catalyzed reactions with unprecedented sensitivity and detail through time-resolved plasmon-enhanced spectroscopic measurements [1-5].

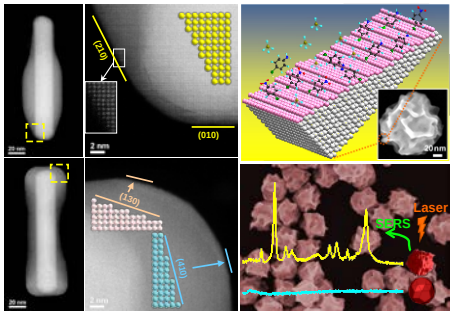

Fig. 1. Tunable plasmonic nanoparticles with catalytically active high-index facets.

1. Jing, H.; Zhang, Q. F.; Large, N.; Yu, C. M.; Blom, D. A.; Nordlander, P.; Wang, H., Tunable Plasmonic Nanoparticles with Catalytically Active High-Index Facets. ***Nano Lett.*** 2014, 14, 3674−3682.
2. Zhang, Q. F.; Large, N.; Nordlander, P.; Wang, H., Porous Au Nanoparticles with Tunable Plasmon Resonances and Intense Field Enhancements for Single-Particle SERS. ***J. Phys. Chem. Lett.*** 2014, 5 (2), 370-374.
3. Zhang, Q. F.; Blom, D. A.; Wang, H., Nanoporosity-Enhanced Catalysis on Subwavelength Au Nanoparticles: a Plasmon-Enhanced Spectroscopic Study. ***Chem. Mater.*** 2014, 26, DOI: 10.1021/cm502508d.
4. Zhang, Q. F.; Large, N.; Wang, H., Au Nanoparticles with Tipped Surface Structures as Substrates for Single-Particle SERS: Concave

Nanocubes, Nanotrisoctahedra, and Nanostars. 2014, manuscript submitted.
5. Zhang, Q. F.; Wang, H., Facet-Dependent Catalytic Activities of Au Nanoparticles Enclosed by High-Index Facets. 2014, manuscript submitted.

NP-09 (Invited Talk)
Spatiotemporal Near-Field Excitation Dynamics in Nanostructures

Katsuyuki Nobusada

Department of Theoretical and Computational Molecular Science, Institute for Molecular Science, Myodaiji, Okazaki, Aichi, JAPAN
Email: nobusada@ims.ac.jp, web site: http://raphael.ims.ac.jp

Optical response of molecules is undoubtedly essential for understanding their physicochemical properties. In conventional theoretical approaches to optical response of molecules, two conditions are usually assumed: (i) Wavelength of incident light is considered to be much longer than molecular size, i.e., dipole approximation. Thus, a target molecule is well approximated by a point dipole and the dipole feels a uniform electromagnetic field. (ii) Electric polarization in a molecule induced by incident-light excitation inevitably generates a new electromagnetic field, referred to as a “near filed”, according to Maxwell’s equations. However, such a self-consistent light-matter (LM) interaction between electron and electromagnetic field dynamics is ignored.

The near-filed confined in a nanometer-sized region induces characteristic physical and chemical phenomena: for example, (1) the near-filed strongly contributes to single molecule Raman imaging or surface enhanced Raman scattering, (2) light-energy conversion processes, such as photosynthesis, photocatalyst, and local plasmon polariton waveguide, are expected to easily occur with the aid of the near-filed excitation, (3) enegy-up-conversion, which is a very useful concept for developing quantum devices like quantum emitters or for generating new chemical fields, occurs through the near-field excitation. (4) chemical or bio sensors are realized when plasmon excitation occurs accompanying the near-filed excitation, and (5) quantum metamaterial might be realized by utilizing the near-filed excitation. To understand such LM interaction in a nanoscale region, we must develop a more general optical response theory, i.e., nano-optical response theory taking account of *nonuniform and self-consistent* LM interactions and a corresponding computational code suitable for large nanostructure systems.

We have developed a generalized theoretical description of full LM interactions with the aim of understanding the near-field excitation dynamics in nanostructures of more than ten-nanometers in size. Electron dynamics in a nanostructure interacting with an electromagnetic field is described by the time-dependent Kohn-Sham (TDKS) equation based on minimal coupling Hamiltonian with Coulomb gauge. On the other hand, electromagnetic field dynamics is represented by the microscopic Maxwell's equations. The nonuniform LM interaction is taken into account in the vector potential and self-consistent LM interaction is described by solving the electron and electromagnetic field coupled equations self-consistently. The coupled equations are solved numerically by using our developed computational program (GCEED*: Grid-based Coupled Electron and Electromagnetic field Dynamics*). Our computational approach is based on a finite-difference method in real-time and real-space. Since the approach employs very simple algorithms, it is very suitable for massively parallelized computations. We have achieved the parallelized calculations with more than 660,000 cores in the K computer (Kobe Riken), which is one of the worldwide leading supercomputers.

Our theory and its computational applications to nanostructures clearly illustrate that the full LM interactions induce unusual phenomena that are completely absent in usual optical response under the dipole approximation. Some computational demonstrations of near-field excitation dynamics will be presented.

This research was supported by Grant-in-Aid (No. 25288012) and by SPIRE and CMSI,

MEXT, Japan. The computed results have been mainly obtained by the K computer at RIKEN AICS (Proposal number hp120035 and hp140054). The computation was also partly performed at the Research Center for Computational Science, Okazaki, Japan.

1. T. Iwasa and K. Nobusada, *Phys. Rev. A* 80, 043409 (2009).
2. T. Iwasa and K. Nobusada, *Phys. Rev. A* 82, 043411 (2010).
3. M. Noda, T. Yasuike, K. Nobusada and M. Hayashi, *Chem. Phys. Lett.* **550**, 52 (2012).
4. T. Yasuike and K. Nobusada, Phys. *Chem. Chem. Phys.* **15**, 5424 (2013).
5. M. Noda, K. Ishimura, K. Nobusada, K. Yabana, and T. Boku, J. Comp. Phys. **265**, 145 (2014).

NP-10 (Invited Talk)
Enhanced light-matter interaction in graphene

Sanshui Xiao[1,2]

[1]*DTU Fotonik, Department of Photonics Engineering, Technical University of Denmark, 2800, Kgs. Lyngby, Denmark.*

[2]*Center for Nanostructured Graphene (CNG), Technical University of Denmark, DK-2800 Kgs. Lyngby, Denmark.*

mail:saxi@fotonik.dtu.dk, website: http://www.fotonik.dtu.dk/sem

Graphene has attracted lots of attention due to its remarkable electronic and optical properties, thus providing great promise in photonics and optoelectronics. However, the performance of these devices is generally limited by the relatively weak light-matter interaction in graphene. The combination of graphene with noble-metal nanostructures is currently being explored for strong light-graphene interaction. We introduce a novel hybrid graphene-metal system for studying light-matter interactions with gold-void nanostructures exhibiting resonances in the visible range [1]. The hybrid system is further explored for sensing of Rhodamine 6G molecules with respect to the strong surface-enhanced Raman scattering. The interaction between graphene plasmon (supported by nanodot and antidot arrays) and the substrate phonons [2] is also experimentally demonstrated and structural control is used to map out the hybridization of plasmons and phonons, where the graphene is structured by the nanosphere lithography with structural control down to the sub-100 nanometer regime, see Fig. 1.

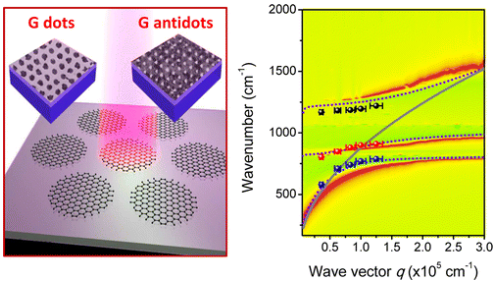

Fig. 1. Plasmon-phonon interaction in graphene nanostructures

References:

[1]. X. Zhu, W. Wang, W. Yan, M.B. Larsen, P. Bøggild, T. G. Pedersen, S. Xiao, J. Zi, and N. A. Mortensen, *Nano Lett.*, 14, 2907 (2014).
[2]. X. Zhu, L. Shi, M.S. Schmidt, A. Boisen, O. Hansen, J. Zi, S. Xiao, and N. A. Mortensen, *Nano Lett.* 13, 4690 (2013).

NP-11 (Invited Talk)
Light Management in Extremely Thin Photoelectrode Architectures

Isabell Thomann[1], Shah M. Bahauddin, Hossein Robatjazi, Chloe Doiron,

[1]*Electrical and Computer Engineering Department, Rice University, Houston, Texas, USA*
Email: isabell.thomann@rice.edu, web site: http://thomann.rice.edu/

Concepts from metamaterials, plasmonics and nanophotonics are expected to be highly beneficial for the design of future solar energy conversion devices. Here, I will describe how we use these concepts to design advanced photoelectrode architectures for two challenging photocatalytic reactions: water splitting and CO_2 reduction. We focus on the light management aspect in extremely thin absorber structures to

achieve broadband omnidirectional solar absorption while carefully choosing materials systems that allow for efficient charge separation and catalytic activity. Complementing these materials and device design efforts, we are developing an experimental characterization toolbox, including photoelectrochemical techniques and ultrafast spectroscopic techniques that will allow us to analyze the influence of distinct plasmon-induced effects on photocatalysis.

NP-12 (Invited Talk)
Surface-enhanced solar energy harvesting and conversion using plasmon active nanostructures

Shanlin Pan[1*], Zhichao Shan[1], Panikar Sathyaseelan Archana [1], Arunava Gupta[1, 2]

1. Department of Chemistry, The University of Alabama, Tuscaloosa, AL, USA, 35487-0336
*Email:*span1@bama.ua.edu, *web site: http://bama.ua.edu/~span1*

2. Department of Chemical and Biological Engineering, The University of Alabama, Tuscaloosa, AL, USA, 35487-0336

Solar energy can be harvested for producing chemical energy sources such as hydrogen *via* solar water splitting. Enormous progresses have been invested in the past several decades in identifying and optimizing photoactive catalytic materials for such solar energy conversion by tailoring their compositions and morphologies [1-3] since Fujishima and Honda's first experiment demonstrating direct water splitting using TiO_2 photoelectrode [4]. Plasmon antennas have been used as surface enhancement substrates to increase the light harvesting capability of a solar water splitting system. We will present a new nanostructured electrode of $Ti@TiO_2$ nanowires decorated with plasmonic active $Ag@Ag_2S$ core-shell nanoparticles for visible light driven photoelectrochemistry studies. The nanowires structure provides a high surface area for efficient light absorption and efficient charge collection from the plasmon active $Ag@Ag_2S$ NPs. The local field enhancement of Ag surface plasmon is found to be able to significantly increase the visible light response of the Ag_2S shell photocatalyst. The shell thickness and core size of the $Ag@Ag_2S$ core-shell structure can be controlled to achieve optimal photoelectrochemical performance. The optimal core-shell structure has been identified to show an ideal enhanced photoelectrochemical performance [5].

1. Walter, M. G.; Warren, E. L.; McKone, J. R.; Boettcher, S. W.; Mi, Q.X.; Santori, E. A.; Lewis, N. S. Chem. Rev. 110, 6446-6473 (2010).
2. Kudo, A.; Miseki, Y. Chem. Soc. Rev., 38, 253-278(2009).
3. Kisch, H. Angew. Chem. Int. Ed. 52, 812-847 (2013).
4. Fujishima A.; Honda, K. Nature, 238, 37-38, (1972).
5. J. Phys. Chem. B, DOI: 10.1021/jp504346k (2014)

NP-13 (Invited Talk)
Plasmonic Nanostructures for Sensing and Energy Applications

Kevin L. Shuford[1]

[1]Department of Chemistry and Biochemistry, Baylor University, One Bear Place #97348, Waco, TX 76798-7348, USA
Email: Kevin_Shuford@baylor.edu, web site: http://bearspace.baylor.edu/Kevin_Shuford/www

Noble metal nanostructures have loosely bound conduction electrons that collectively oscillate when excited by an electromagnetic field. These plasmon resonances reside in the visible and infrared portions of the electromagnetic spectrum for silver and gold. At the resonance frequencies, the nanoparticle is highly polarizable, and the oscillating charge density results in a strongly enhanced field near the surface. The large field enhancements and the ability to selectively tune the resonance wavelength via particle morphology makes plasmonic nanostructures ideal for many sensing and energy applications.

Herein, we present some of the more subtle aspects of how nanoparticles couple to light and each other, and how the nature of this coupling can affect the sensing properties of the system as a whole. As a first example, we investigate isolated disk-on-pillar structures, composed of a silicon pillar covered by thin layers of silica and silver, to understand the fundamental optical properties. Next, two-dimensional periodic arrays of these nano-elements are examined as a platform for surface-enhanced Raman spectroscopy (SERS) measurements. This system supports both localized surface plasmons and surface plasmon polaritons (see Fig. 1), whose interaction can be tuned to synergistically enhance the electric field resulting in larger SERS signals. Both of these examples highlight the importance of understanding the interplay between system components in plasmonic sensing applications.

Time permitting, an energy application of plasmonic nanostructures will be presented. In particular, we investigate a two-dimensional corrugated nanosurface for efficient light trapping in a photovoltaic cell. The design was chosen to minimize light polarization effects and generate robust optical properties for unpolarized sources. It consists of two, perpendicular gratings in the silver film that intersect to yield cross-shaped nano-elements. A thin, silicon film then covers all of this surface structure. An additional degree of freedom can be introduced into the design by interrupting the grid in both directions. We show that this extra spacing between the array elements can be used to tune the absorption properties of the nanosurface. We demonstrate how this two-dimensional configuration is more efficient than its one-dimensional counterpart in terms of the short circuit photocurrent density. We also briefly discuss possible extensions of this structure design, which can further enhance the solar cell performance.

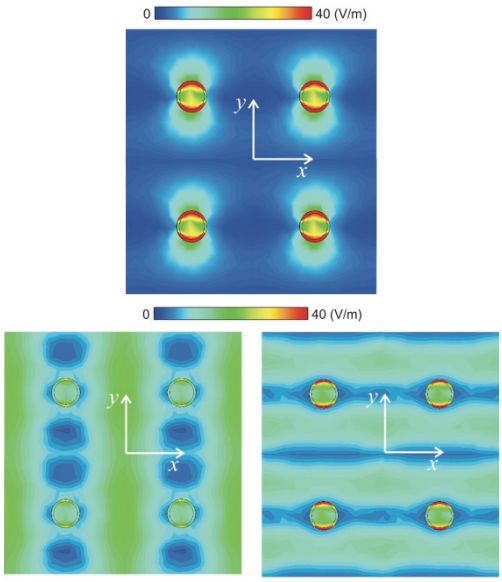

Fig. 1: Electric field intensity maps of localized surface plasmons (left) and two different surface plasmon polariton modes (center and right) supported by a pillar array nanostructure.

NP-14 (Invited Talk)
Resonance energy transfer and hot electron transfer from plasmonic metal to semiconductor: Applications in solar energy harvesting

Nianqiang Wu

Department of Mechanical & Aerospace Engineering, West Virginia University, P.O. Box 6106, Morgantown, WV 26506, USA

Email: nick.wu@mail.wvu.edu, web site: http:// www.statler.wvu.edu/~wu

Plasmonic photovoltaics, photocatalysts and photoelectrochemical cells have great potential in solar energy harvesting. This talk presents the underlying mechanism of plasmon-enhanced charge separation in semiconductors. In metal-semiconductor heterojunctions, the plasmonic energy can transfer from the metal to the semiconductor via two mechanisms: plasmon-induced resonance energy transfer (PIRET) and direct electron transfer (DET). In addition, this talk demonstrates the coupling of

plasmonic metal nanostructure with semiconductor for solar water splitting.

1. S. K. Cushing, J. Li, F. Meng, T. R. Senty, S. Suri, M. Zhi, M. Li, A. D. Bristow, N. Q. Wu, *Journal of the American Chemical Society*, **134**, 15033 (2012).
2. J. Li, S. K. Cushing, P. Zheng, F. Meng, D. Chu, N. Q. Wu, *Nature Communications*, **4**, 2651(2013).
3. J. Li, S. K. Cushing, P. Zheng, T. Senty, F. Meng, A. D. Bristow, A. Manivannan, N. Q. Wu, *Journal of the American Chemical Society*, **136**, 8438 (2014).

NP-15 (Invited Talk)
Boosting the Photocatalytic Efficiency of Semiconductor via Design of Charge-Transfer Hybrid Structures

Yujie Xiong[1,*], Jun Jiang,[1] Qun Zhang,[1] Xiaojun Wu[1]

[1]*School of Chemistry and Materials Science, University of Science and Technology of China, Hefei, Anhui, China*
Email: yjxiong@ustc.edu.cn, web site: http://staff.ustc.edu.cn/~yjxiong/

Photoexcited electrons should be efficiently separated from holes in semiconductors, allowing their delivery to specific regions for half-reactions in photocatalysis. In competition with charge transfer is electron and hole recombination, which has been a key process for limiting quantum efficiency in related applications. In order to suppress the recombination, an effective solution is formulation of Schottky junctions by integrating an electron-extracting agent with the semiconductor.[1,2]

In this presentation, I will demonstrate several different approaches to efficient electron-hole separation for CO_2 reduction and water splitting, respectively, by formulating Schottky barrier in semiconductor-based hybrid nanostructures. In the first approach, a semiconductor-metal-graphene design has been implemented to efficiently extract photoexcited electrons through the graphene nanosheets, separating electron-hole pairs (Figure 1).[3] Ultrafast spectroscopy characterizations exclusively demonstrate that the charge recombination occurring at interfacial defects can be substantially avoided, enabling superior efficiency in water splitting. The second approach is to utilize the capabilities of metal-organic frameworks (MOF) in capturing CO_2 and transferring electrons, leading to greatly improved activities of semiconductor in CO_2 reduction (Figure 2).[4] It is anticipated that this work opens a new window to rationally designing hybrid systems for photo-induced applications.

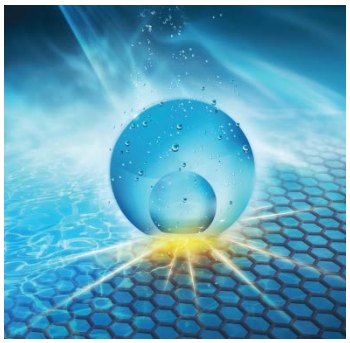

Fig. 1. Schematic illustrating the semiconductor-metal-graphene stack design.

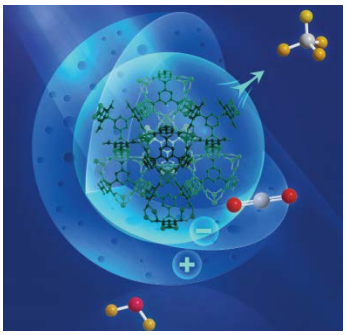

Fig. 2. Schematic illustrating the MOF-semiconductor core-shell structure.

1. L. Wang, J. Ge, A. Wang, M. Deng, X. Wang, S. Bai, R. Li, J. Jiang, Q. Zhang, Y. Luo and Y. Xiong, *Angew. Chem. Int. Ed.* **53**, 5107 (2014).
2. R. Long, K. Mao, M. Gong, S. Zhou, J. Hu, M. Zhi, Y. You, S. Bai, J. Jiang, Q. Zhang, X. Wu and Y. Xiong, *Angew. Chem. Int. Ed.* **53**, 3205 (2014).

3. S. Bai, J. Ge, L. Wang, M. Gong, M. Deng, Q. Kong, L. Song, J. Jiang, Q. Zhang, Y. Luo, Y. Xie and Y. Xiong, *Adv. Mater.* **26,** 5689 (2014).
4. R. Li, J. Hu, M. Deng, H. Wang, X. Wang, Y. Hu, H. L. Jiang, J. Jiang, Q. Zhang, Y. Xie and Y. Xiong, *Adv. Mater.* **26,** 4783 (2014).

NP-16 (Invited Talk)
From nanojets to threading plasmonic nanoparticle strings with light

Ventsislav K. Valev[1,2], Lars O. Herrmann[2], Christos Tserkezis[3], Jon S. Barnard[4], Oren A. Scherman[5], Javier Aizpurua[3], and Jeremy J. Baumberg[2]

[1] MultiPhoton NanoPhotonics, Department of Physics, University of Bath, UK
web site: http://www.valev.org; email: vkv23@bath.ac.uk
[2] NanoPhotonics Centre, Cavendish Laboratory, University of Cambridge, UK
[3] Donostia International Physics Center DIPC and Centro de Física de Materiales CSIC-UPV/EHU, Paseo Manuel de Lardizabal 5, Donostia-San Sebastián, 20018, Spain
[4] Department of Materials Science & Metallurgy, University of Cambridge, 27 Charles Babbage Road, Cambridge CB3 0FS, UK
[5] Melville Laboratory for Polymer Synthesis, Department of Chemistry, University of Cambridge, UK

Individual plasmonic nanoparticles (NPs) are the constitutive building elements for bottom-up assembled nano- and meta-materials. At the most fundamental level these nanomaterials consist of NP chains, in which single NPs are attached together with molecules. Here we demonstrate the next stage towards achieving continuous bottom-up assembled meta- and nanomaterials. We demonstrate that ultrafast laser pulses can produce a continuous metal thread bridging the chains, thereby allowing charge transfer[1]. The process is characterized by the appearance of a novel plasmon mode, exhibiting both chain- and rod-like features. Upon assembly, real-time monitoring of this plasmon mode enables highly precise control (±3 nm) over the width of the thread.

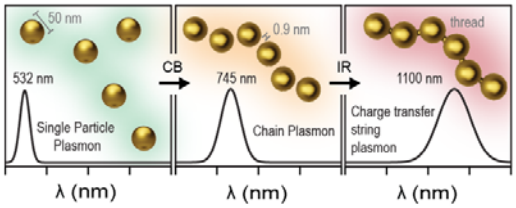

Fig. 1. Schematic nano-threading optical assembly.

Novel optical materials are finding increasing applications in transport, communications, healthcare and sensing. Just as light is used to characterize optical materials, light can also be used to build them. Ultrafast lasers have previously been used to shape continuous metal surfaces with diverse micro and nanostructures, such as ripples, needles, nanobumps, cavities and nanojets. Nanojets[2], promising for threading, are columns of liquid material, frozen in the process of surging from the metal surface in the direction opposite to that of the incoming laser pulse. However it is exceedingly difficult to align single nanostructures so that nanojets from opposite nanostructures would face each other. This limitation can be circumvented with surface plasmon resonances – the coherent oscillation of surface electrons. Plasmons enlarge even further the electric field of intense femtosecond pulses and localize it to sub-wavelength regions ('hotspots'). In dimers, or chains of plasmonic NPs, the plasmonic hotspots occur in the regions directly across the gap. It is consequently possible to form a continuous thread in such dimers or chains of nanoparticles, from first stage of nanoscale assembly[3].

In our work, assembly proceeds in water at an unprecedented large scale. Our results indicate that the width of the thread depends on the size of the nanoparticles, on the plasmon resonance wavelength of the chain modes, on the peak-to-peak laser power and on the number of nanoparticles in the chains, which can all be used to tune the optical properties of this novel type of material. Large-scale metamaterial manufacturing is thus in prospect

1. L.O. Herrmann *et al*, *Nat. Commun.* **5**, 4568 (2014).

2. V.K. Valev *et al*., *Adv. Mater.* **24**, OP29 (2012).
3. R. Taylor *et al*., *ACS Nano* **5**, 3878 (2011).

NP-17 (Invited Talk)

Surface plasmon sensors with high sensitivity and resolution to study electric-field induced changes in the refractive index of liquid crystals and modifications in the Kretschmann configuration system for SPR measurements on *not-easily-accessible* samples

Suresh C. Sharma[1,*], Kunal Tiwari[1], and Nader Hozhabri[2]

[1]*Department of Physics, University of Texas at Arlington, Arlington, TX 76019, USA*

[2]*Nanotechnology Research and Education Center, University of Texas at Arlington, Arlington, Texas 76019, USA*

[*]*Author to whom correspondence should be addresses: email, sharma@uta.edu*

Since the realization of the surface plasmon excitations (SPEs) in the 1950s[1,2], the subject matter continues to be of significant interest and has led to the development of sensors for biological, chemical, and physical applications.[3-6] In this presentation, we revisit the usefulness of the prism/single-metal, prism/bi-metal and prism/metal/dielectric/metal waveguide structures for improving the sensitivity and resolution of SPR sensors. Representative SPR curves are presented to assess sensors for monitoring electric-field induced changes in the refractive index of nematic liquid crystals. Among noteworthy results are: (a) high sensitivity to changes in the refractive index $\left(\partial\theta_{SPR}/\partial n\right)$, which is almost 28-times higher than the sensitivity of other known sensors, and (b) high resolution $\left(FWHM \text{ of the SPR curve} \leq 0.28 \text{ degrees}\right)$.[7,8] As expected, the metal/dielectric waveguide/metal sensor significantly modifies damping of surface plasmon polaritons propagating along the interface and evanescent fields beyond the outermost metal surface. We also discuss an important recent development in techniques; the utilization of a *fixed detector Kretschmann configuration optical system*, in which the sample and the detector remain fixed and the angular dependence of the SPR curves is examined *via* steering optics in the incident and reflected beams.[9] By eliminating the requirement for $\left(\theta, 2\theta\right)$ goniometer, this technique simplifies measurements on samples, which, for example, should be maintained under vacuum conditions. Selected examples of data, obtained by using the fixed detector Kretschmann configuration optical system, are presented.

[1]R. H. Ritchie, Phys Rev **106** (5), 874 (1957).
[2]H. Raether, Springer Tr Mod Phys **111**, 1 (1988).
[3]S. C. Hayden, L. A. Austin, R. D. Near, R. Ozturk, and M. A. El-Sayed, J Photoch Photobio A **269**, 34 (2013).
[4]O. Hugon, P. Benech, and H. Gagnaire, Sensor Actuat B-Chem **51** (1-3), 316 (1998).
[5]Y. K. Lee, K. S. Lee, W. M. Kim, and Y. S. Sohn, Plos One **9** (6) (2014).
[6]Y. Guo and M. Deutsch, Opt Lett **39** (13), 3860 (2014).
[7]K. Tiwari and S. C. Sharma, Sensor Actuat a-Phys **216**, 128 (2014).
[8]Kunal Tiwari, Suresh C. Sharma, and N. Hozhabri, ,submitted (2014).
[9]A. K. Singh and S. C. Sharma, Opt Laser Technol **56**, 256 (2014).

Session NS
NANOCARBON BASED SUPERCAPACITORS

NS-01 (Invited Talk)
Facile Preparation of Hierarchical Porous Carbon/graphene for Energy Storage

Yufeng Zhao[1], Faming Gao[1*]

[1] *Key Laboratory of Applied Chemistry, Department of Environmental and Chemical Engineering, Yanshan University, No. 438 Hebei Street, Qinhuangdao, 066004, P.R. China, Email: yufengzhao@ysu.edu.cn (Y. Zhao), fmgao@ysu.edu.cn(F. Gao)*

Carbon obtained from natural materials, which is generally renewable, inexpensive and environmentally benign, have attracted considerable interest in supercapacitor application. Their special features enable them to exhibit relatively high operating voltage, high specific capacitance, and even better stability when applied as supercapacitor electrode. In this work, we report the waste Artemia cyst shells as a novel carbon source. Through a very simple low-cost carbonization on the waste Artemia cyst shells, a hierarchical porous carbon (HPC) as well as hierarchical porous graphene (HPG) is produced. The combined hierarchical porous structure and oxygen rich properties make these materials exhibit excellent specific capacitance (369 F g^{-1}). An asymmetric supercapacitor is fabricated using MnO_2/GO as positive electrode and HPC as negative electrode material. The optimized asymmetric supercapacitor could be cycled reversibly in the high voltage range of 0-2V in Na_2SO_4 electrolyte, which exhibits maximum energy density of 46.7 W h kg^{-1} at a power density of 100 W kg^{-1} and remains 18.9 W h kg^{-1} at 2000 W kg^{-1}. Additionally, such device also shows superior long cycle life along with ~100% capacitance retention after 1000 cycles and ~93% after 4000 cycles.

Acknowledgement: Financial support from the NSFC (Grant 51202213), NSFHBP (Grant B2012203043), CPSF (Grant 2013M530889，2014T70230) and EYSFHP (Grant Y2012005) is acknowledged.

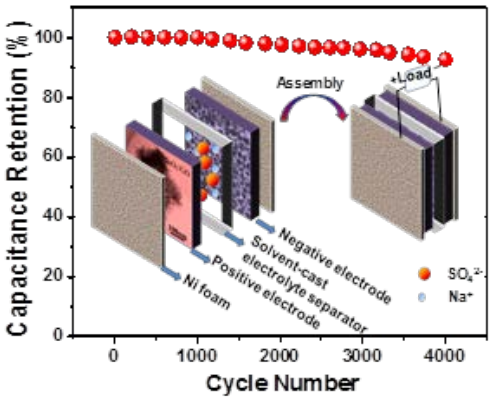

Fig1. Asymmetric Supercapacitor based on HPC and MnO_2/GO composites

NS-02 (Invited Talk)
Printed highly ordered carbon nanostructures for enhanced supercapacitor performance

Binh Duong,[1] Jayan Thomas[2]

[1]*Center for Polymers & Organic Solids, University of California, Santa Barbara, CA 93106, USA Email:bduong@chem.ucsb.edu*
[2]*NanoScience Technology Center, University of Central Florida, FL 32826, USA*

Compared to lithium ion batteries, supercapacitors (SCs) have attracted considerable attention because they can charge and discharge faster and have much longer lifetime. Carbon-based electrodes stand out among many other electrode materials for numerous advantages such as lightweight, high electrical conductivity, stable chemical and electrochemical properties at low cost [1] but a simple pathway to create high surface area carbon electrodes is still missing. Here, we present a facile method called spin-on nanoprint (SNAP) to print large area, well-ordered nanostructured carbon electrodes. To obtain a nanostructured electrode, we spin-coated PAN solution on a pre-fabricated silicon (Si) mold, followed by curing and removal of the mold as shown in Figure 1.

The simple casting and transferring steps involved in making the nanostructures reveal the potential to fabricate large area printed nanostructures by simply printing the structures side-by-side. The electrochemical results confirm that enhancement in surface area of the nanopatterns can improve the capacitance of the SC device by one to two orders of magnitude. These promising results indicate SNAP has great prospects in the fabrication of individual electrochemical devices as well as miniaturized integrated nanocomposite energy-storage systems.

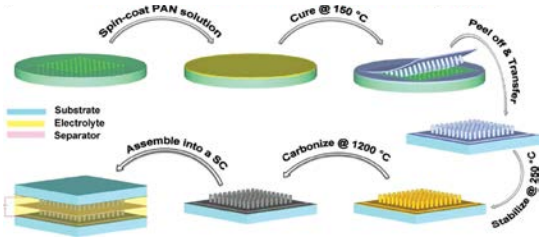

Fig. 1. Fabrication of carbon nanostructures by SNAP method.

1. H. Nishihara, T. Kyotani, *Adv. Mater.* **24,** 4473 (2012)

NS-03 (Contributed Talk)

Electrochemically Synthesized Polymer-Graphene Oxide Composite Films as Supercapacitor Materials

Pia Damlin[1], Milla Suominen[1], Suvi Lehtimäki[2], Sampo Tuukkanen[2], Donald Lupo[2], Carita Kvarnström[1]

[1]University of Turku, Turku University Centre for Materials and Surfaces (MATSURF), Laboratory of Materials Chemistry and Chemical Analysis, Vatselankatu 2, FIN-20014 Turku, Finland Email:pia.damlin@utu.fi

[2]Tampere University of Technology, Department of Electronics and Communication Engineering, Korkeakoulunkatu 3, P.O. Box 692, FI-33101, Tampere, Finland

Electrically conducting polymers (ECPs) exhibit high redox capacitance, making them interesting electrode materials for supercapacitor applications. To further improve the mechanical and electrical properties, ECPs have been fabricated as composites together with a wide variety of materials like metal nanoparticles and different carbon materials. Graphene oxide (GO) has become the most common starting material for graphene based applications as it can be produced in large quantities as well separated GO sheets. For many applications the reduction, using chemical or electrochemical methods or thermal annealing, of GO is desired in order to restore the graphitic structure.

In this work conducting polymer (CP) composite films of poly(3,4-ethylenedioxythiophene) (PEDOT) were electrochemically synthesized in the presence of different concentrations of graphene oxide (GO). Electropolymerization was performed in two solvent systems, using ionic liquids (1-butyl-3-methyl-imidazolium tetrafluoroborate ($BMIMBF_4$) and 1-hexyl-3-methyl-imidazolium tetrafluoroborate ($HMIMBF_4$)) and aqueous media. CP/reduced graphene oxide (CP/rGO) composite films were prepared by inducing electrochemical reduction of GO incorporated into the CP as the dopant. The electrochemical reduction method offers control of the reduction process under mild reaction conditions. Ionic liquids show a broad potential window thus allowing completeness of the reduction process. [1] A comparative study was performed for CP/rGO composite films to that of the pure polymer focusing on redox behavior and structural changes. As shown in Figure 1 the electroactivity of a PEDOT/rGO composite film increases considerably after the reduction process.

The composite films were also tested as electrode materials for supercapacitor applications. The device properties were determined from a galvanostatic discharge measurement according to an industrial standard. Supercapacitors were fabricated on flexible plastic electrode substrates evaporated with silver and further coated with a printable graphite ink as current collector. [2] The performances of bare CP, CP/GO and electrochemically reduced (CP/rGO) were studied and compared to a

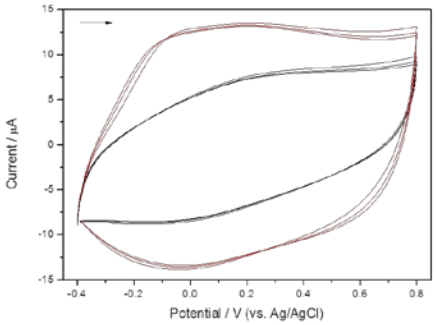

reference supercapacitor without the active layer. The supercapacitors were assembled in a symmetric configuration with a paper separator soaked in an aqueous NaCl electrolyte.

Fig. 1. CVs recorded for PEDOT/GO (black line) and for PEDOT/rGO (red line) in $BMIMBF_4$ after electrochemical reduction by cycling in the potential range -0.4 to -2.0 V (10 cycles).

1. J. Kauppila, P. Kunnas, P. Damlin, A. Viinikanoja and C. Kvarnström, *Electrochim. Acta* **89**, 84 (2013).
2. S. Lehtimäki, M. Li, J. Salomaa, J. Pörhönen, A. Kalanti, S. Tuukkanen, P. Heljo, K. Halonen and D. Lupo, *Electr. Power Energy Syst.* **58**, 42 (2014).

NS-04 (Invited Talk)

Application of Graphene Oxide • Ionic Liquid Gels for Supercapacitor electrodes

Hiroshi Hyodo[1], Itaru Honma[1]

[1]*Institute of Multidisciplinary Research for Advanced Materials, Tohoku University, 2-1-1 Katahira, Aoba-ku, Sendai, Japan*
Email: hyodo@tagen.tohoku.ac.jp

Graphene is a promising material for supercapacitor electrodes because of its superior electrical conductivity (2×10^5 cm^2/V s), high theoretical specific surface area (2630 m^2/g) and high chemical durability. However, the aggregation make it difficult to use its high specific surface area and the capacitance of usual graphene electrode is in the range of 100-200 F/g. [1] It is expected that bucky gel electrodes, which are synthesized by the grinding of graphene and ionic liquids (IL), show high specific surface area and high capacitance without aggregation since each graphene sheet is covered by IL in the form of bucky gel. [2] However, since we must dry the graphene before grinding with inducing the aggregation, we cannot fully use the high specific surface area of GO. Meanwhile, it is known that graphene oxide (GO), which is a precursor for graphene synthesis, shows high dispersibity in water. If we can gelate GO on high dispersion, capacitor with high capacitance would be realized. In this study, we developed the gelation process of GO with high dispersibility and investigated its capacitance properties.

Graphite oxides were synthesized by the modified Hummers method. GO dispersed in water or ethanol were obtained by the exfoliation of graphite oxides in water or ethanol by sonication. 1-ethyl-3-methylimidazolium tetrafluoroborate (EMI-BF_4) or 1-ethyl-3-methylimidazolium bis(trifluoromethylsulfonyl)amide (EMI-TFSA) was added in these suspensions. After the subsequent sonication, GO • IL gel was synthesized by the drying. The GO • IL gel electrode and the GO electrode were also prepared by the conventional grinding of dried GO powder and IL and by the mixture of dried GO powder and PTFE for comparison., respectively. Acetylene black (AB) were mixed in all samples. The electrochemical properties of the sample were measured with a standard three-electrode cell. Activated carbon, 0.5 M H_2SO_4 and the Ag/AgCl was used for counter electrode, electrolyte and reference electrode, respectively.

Fig. 1 shows the CV curves of a GO electrode and a GO • IL gel electrode synthesized by drying. The CV curve of a GO • IL gel electrode was almost the same as that of a GO electrode. The redox peaks near 0.35 V are due to the carbonyl group of GO and they were not observed when the electrolyte was ionic liquid. [3] Thus it was found that H^+ ions come into the hydrophobic IL based gel and contribute to the formation of electric double layer. Fig. 2 shows the capacitance of GO electrode and GO • IL gel electrodes synthesized by drying or grinding at different charging/discharging current densities.

The capacitance of GO • IL gel electrode synthesized by drying is higher than that of GO electrode and GO • IL gel electrode synthesized by grinding. It was found that high dispersibility of GO lead to high capacitance of GO • IL gel electrode

1. M. D. Stoller, *et. al*., *Nano Lett.* **8**, 3498 (2008).
2. X. Yang *et al*., *Science* **341**, 534 (2013).
3. Y. R. Nian *et al., J. Electrochem. Soc*. **149**, A1008 (2002).

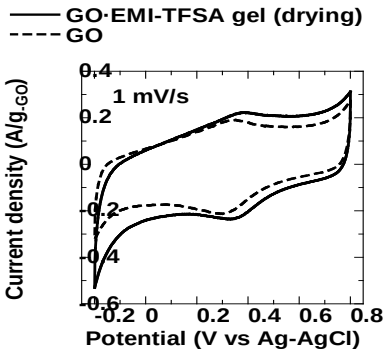

Fig. 1. Cyclic voltammograms of GO electrode and GO•IL gel electrode synthesized by drying. The weight ratio of GO and IL is 10:90.

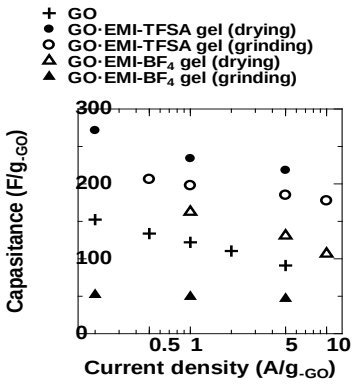

Fig. 2. Capacitance of GO electrode and GO•IL gel electrodes synthesized by drying or grinding at different charging/discharging current densities. The weight ratio of GO and IL is 10:90.

NS-05 (Invited Talk)
Graphene Materials Based Supercapacitors

Peng Chen

School of Chemical & Biomedical Engineering, Nanyang Technological University, Singapore

In the past years, graphene materials have been widely used to improve the performance of supercapacitors owing to their exceptional properties including high specific surface area, excellent electrical conductivity, ease to be functionalized or hybridized with other functional nanomaterials. We have demonstrated high-performance supercapacitors based on CVD-grown three-dimensional (3D) graphene foams hybridized with nanostructured metal oxides metal oxides (e.g., Co_3O_4) or polymers. Based on the amphiphilic graphene nanosheets, we have developed flexible planar micro-supercapacitors fabricated by layer-by-layer printing. More recently, we fabricated solid-state fiber-shaped symmetric or asymmetric supercapacitor by hybridizing graphene and transition metal dichalcogenide (TMD) nanosheets with long microfibers of carbon nanotubes. These fiber supercapacitors promise applications for woven or wearable electronics.

NS-06 (Contributed Talk)
Hybrid Composites of Porous carbon and Iron oxide for Supercapacitors – Morphological and Electrochemical Studies

Thanyalak Chaisuwan[1,2], Pattheera Hongsumreong[1], Uthen Thubsuang[1], Sujitra Wongkasemjit[1,2]

The Petroleum and Petrochemical College, Chulalongkorn University, Bangkok, Thailand
The Center of Excellence on Petrochemicals and Materials Technology
Email: thanyalak.c@hotmail.com

Porous polybenzoxazine was prepared through a sol-gel process before pyrolysis under nitrogen gas at high temperature, yielding nanoporous carbon. In order to improve an electrochemical performance of the electrodes,

nanoporous carbon was underwent the heat treatment at 300 ℃ in air to improve the wettability of the electrolyte on the surface of nanoporous carbon. . A specific capacitance of the heat–treated nanoporous carbon electrodes was 108 F/g obtained in 6M KOH at current density 5 mA/cm^2. In addition to the effect of the nanoporous carbon microstructure, the effect of iron oxide (Fe_3O_4) content (1, 3, and 5 wt.%) on the electrochemical properties of the composite electrodes was also investigated. Electrochemical characterization indicated that 3 wt.% Fe_3O_4–impregnated nanoporous carbon with heat treatment showed the highest specific capacitance (120 F/g) due to the pseudocapacitive properties of iron oxide. The electrochemical impedance spectroscopy and cyclic voltammetry were also confirmed this electrochemical behavior.

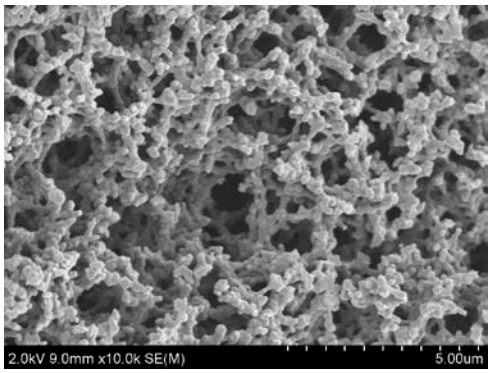

Fig. 1. SEM micrograph of polybenzoxazine-derived porous carbon after heat treatment at 300°C in air

Session RS
RESISTIVE SWITCHINGS OF OXIDES AND RELATED NANOCOMPOSITES/ HETEROSTRUCTURES

RS-01 (Keynote Talk)
p-n Characteristics and Switchings of LBMO/ZnO Hetero-junctions

Toshiki Mori[1], Kenta Inagaki[1], Kazuki Yamaji[1], Miyoshi Yokura[1,2], Hiroaki Nishikawa[3], Lakshmi Reddy[4], Reji Philip[5], Jayan Thomas[6], Yoshinobu Nakamura[7], Satoru Kaneko[8], Mikhail Belogolovskii[9], Tamio Endo[1]

[1]Mie University, Tsu, Mie, JAPAN (Email: endo@elec.mie-u.ac.jp). [2]APC Inc., Otsu, Shiga, JAPAN. [3]Kinki University, Kinokawa, Wakayama, JAPAN. [4]S.V.D College, Kadapa, INDIA. [5]Raman Research Institute, Bangalore, INDIA. [6]University of Central Florida, Orlando, Florida, USA. [7]University of Tokyo, Kashiwa, Chiba, JAPAN. [8]Kanagawa Industrial Technology Center, Ebina, Kanagawa, JAPAN. [9]Donetsk Institute for Physics and Engineering, Donetsk, UKRAINE

Resistive switchings are important for new memory devices called ReRAM. Many papers have been published on this subject, but here we report unique switching behaviors accompanied with rectification Current (*I*)-Voltage (*V*) characteristics.

Hetero p-n junctions of La(Ba)MnO_3/ZnO were fabricated on various substrates by ion beam sputtering at various substrate temperatures (*T*s) and oxygen partial pressures (*P*o). We measured *I*-*V* on these samples. Figure 1 shows *I*-*V* on LBMO/ZnO/Sapphire-substrate (*T*s=600℃, *P*o=1 mTorr for LBMO) for an electrode configuration-C. It shows a clear rectification (factor *F*r=11406) and a low- (*R*=2.1 MΩ) to high-resistance (13 MΩ) switching in forward bias. A reverse bias behavior is very stable. Figure 2 shows *I*-*V* for an electrode configuration-B, showing an opposite switching from high- (262 MΩ) to low-resistance (136 MΩ). The *F*r values are 3050 and 9242. A reverse behavior is very stable again. Figure 3 shows *I*-*V* on LBMO/ZnO/MgO-substrate annealed at 160℃. It shows a superior rectification behavior, *F*r=17039. It should be noted that the reverse current is unusually stable up to -106 V. Figure 4 shows *I*-*V* on LBMO/ZnO/Sapphire-substrate (*T*s=650℃, *P*o=1 mTorr) annealed at 160℃. For upward voltage sweep, it shows a stable current increase (14.5 kΩ) in V<1.77 V, then unstable current (small switchings) in V>1.77 V. During downward sweep, it shows the unstable current again, and a big switching occurs at 1.9 V. Then it shows extremely small *R* of 0.4 kΩ. Thus we could obtain huge rectifications. We are considering the mechanism of switchings in terms of percolation due to ferromagnetic-metallic grains in LBMO layer.

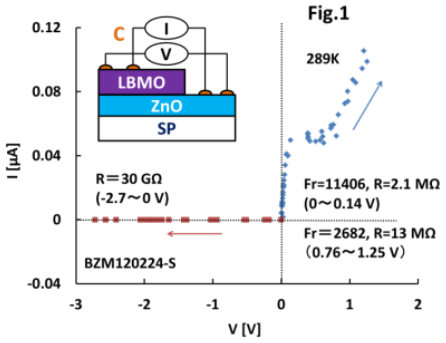

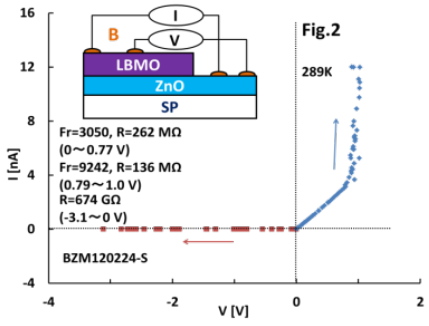

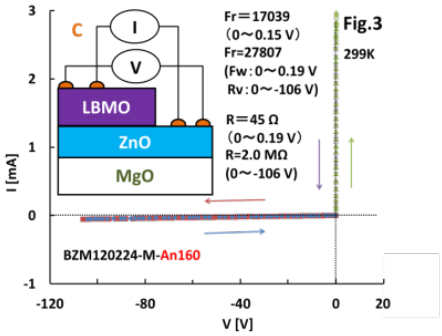

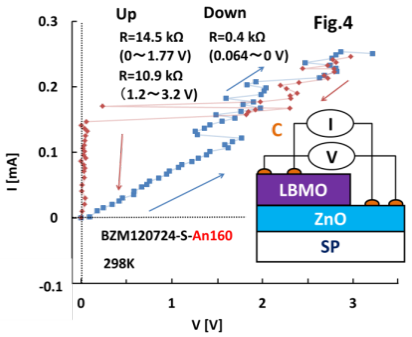

RS-02 (Invited Talk)
Ag/a-Si/c-Si Crossbar Switch: From Discovery to Commercialization

Yajie Dong[1]

[1] NanoScience Technology Center, University of Central Florida, Orlando, FL, USA
Email:yajie.dong@ucf.edu

I will present the discovery of unique rectified silver/amorphous silicon/crystalline silicon (Ag/a-Si/c-Si) crossbar resistive random access memory (RRAM) effect in c-Si/a-Si core/shell nanowires[1] and provide a comprehensive comparison between nanowire based[1] and planar silicon[2] based Ag/a-Si/c-Si RRAMs. The history of how this accidental nanowire based discovery solved a decades-long sneak current problem in RRAM field and eventually evolved into a game changing mainstream flash memory successor, Crossbar Memory[3], will be summarized.

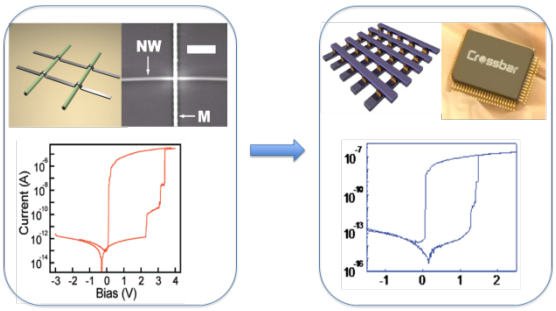

(a) (b)

Fig. 1. Ag/a-Si/c-Si Crossbar Switch: from the original discovery on nanowires (**a**, adapted from reference 1) to recent commercialization on planar Si platform (**b**, adapted from reference 3).

1. Y. Dong, G. Yu, M. McAlpine, W. Lu, C. M. Lieber, *Nano Lett.* **8**, 386-391 (2008).
2. S. Jo, and W. Lu, *Nano Lett.* **8**, 392-397 (2008).
3. https://www.crossbar-inc.com/

RS-03 (Invited Talk)
Electrical coupling of isolated cardiomyocyte clusters grown on aligned conductive nanofibrous meshes using electrospinning technique

Meng-Yi Bai[1], Chun-Wen Hsiao[2], and Hsing-Wen Sung[2]

[1]Graduate Institute of Biomedical Engineering, National Taiwan University of Science and Technology, Taipei,, Taiwan, ROC
Email:mybai@mail.ntust.edu.tw, web site: http://www-o.ntust.edu.tw/~MYBai/professor.html

[2] Department of Chemical Engineering, National Tsing Hua University, Hsinchu, Taiwan, ROC

Myocardial infarction is often associated with abnormalities in electrical function due to a massive loss of functioning cardiomyocytes. This work develops a mesh, consisting of aligned composite nanofibers of polyaniline (PANI) and poly(lactic-co-glycolic acid) (PLGA), as an electrically active scaffold for coordinating the beatings of the cultured cardiomyocytes synchronously. Following doping by HC1, the electrospun fibers could be transformed into a conductive form carrying positive charges, which

could then attract negatively charged adhesive proteins (i.e. fibronectin and laminin) and enhance cell adhesion.

In this work, test PANI/PLGA meshes were placed on a glass slide. Two silver wires were placed under two ends of the mesh with the direction perpendicular to the major axis of the fibers (Fig. 1). The product was subsequently covered by a glass well (1 cm × 1 cm inner well dimension) that acted as a sealant and prevented the wires from coming into direct contact with the medium. This assembly was tightly sealed with a silicone paste (Dow Corning Corp., Midland, MI, USA) and sterilized by exposure to UV light overnight [1].

The Dil-labeled cardiomyocytes were then seeded on test meshes; following culturing, trains of electrical pulses (1.25 Hz, 5 V/cm) were applied, which is characteristic of native myocardium [2]. The beating behaviors of the cardiomyocytes (before and after electrical stimulation) were then observed and recorded using a fluorescence microscope with a CCD camera. The video was recorded at 30 fps and in a resolution of 640 × 480 pixels. The images were digitized frame by frame with Image-Pro Plus software. Finally, the beating rate of the culture was analyzed by selecting and tracking a small area of the video frame sequence in a cell cluster where brightness clearly oscillated due to the cell beating.

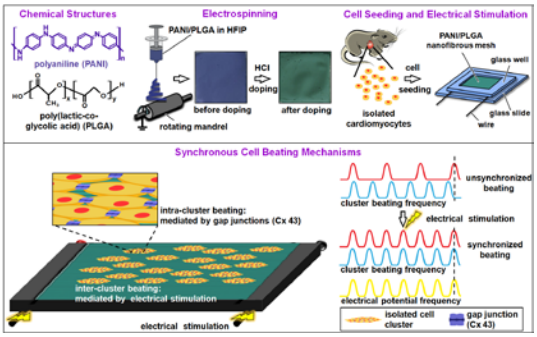

Fig. 1. Schematic diagrams displaying the processes for the fabrication of aligned conductive polyaniline (PANI)/ poly(lactic-co-glycolic acid) (PLGA) nanofibrous mesh, cell seeding, electrical stimulation and the mechanisms of the synchronous cell beatings.

1. J. Y. Lee, C. A. Bashur, A. S. Goldstein, C. E. Schmidt, Polypyrrole-coated electrospun PLGA nanofibers for neural tissue applications. Biomaterials 30, 4325 (2009).

2. M. Radisic, H. Park, H. Shing, T. Consi, F. J. Schoen, R. Langer, Functional assembly of engineered myocardium by electrical stimulation of cardiac myocytes cultured on scaffolds. Proc Natl Acad Sci USA, 101, 18129 (2004).

RS-04 (Invited Talk)
Making Oxide Nanocrystals via Green Chemistry: A Story of Cuprous Oxide

Chun-Hong Kuo[1], Michael H. Huang[2]

[1]*Institute of Chemistry, Academia Sinica, Nankang Taipei 11529, Taiwan*
Email:chunhong@gate.sinica.edu.tw, web site: http://chkuolab.chem.sinica.edu.tw/

[2]*Department of Chemistry, National Tsing Hua University, Hsinchu 30013, Taiwan*

Cuprous oxide (Cu_2O) is a *p*-type semiconductor with a direct band gap of 2.0 eV. It was initially interested for its photosensitive property in the 1920s and considerable work was done on Cu_2O characterization from 1930 to 1940. In the past decade, materials at nanoscale have attracted much attention and strategies for the synthesis of various Cu_2O nanocrystals were rapidly developed. Besides, several studies have also demonstrated the potential of Cu_2O for gas sensing, photodegradation of dye molecules, CO oxidation, photoactivated water splitting into H_2 and O_2, and as electrode material for lithium ion batteries. [1-3]

In this presentation, establishing a platform for studies on Cu_2O facet-dependent properties based on a protocol of green chemistry will be talked about. To build a green system, we avoided consuming huge energy, no heating and no irradiation at ambient, to aqueous synthesize Cu_2O nanocrystals with evolving shapes, hollow interior as cages and frames, enclosed Au cores directing surface structures. Apart from using water as the solvent, a kind of ionic capping agent named sodium dodecyl sulfate (SDS) and the

reducing agent called hydroxylamine were kept in various ratios in order to confine sizes and evolve shapes. [4-7] More importantly, an opportunity in studying the facet-dependent chemical and physical properties is available by such precise control on nanostructures. We not only *in-situ* observed the transformation from Cu_2O to Cu_2S via Kirkendall effect, but also measure the conductivity of a single Cu_2O nanocrystal in which we proved that resistance is facet-dependent. [8, 9] The figure below is a schematic summarization of Cu_2O nanostructures will be interpreted in this talk.

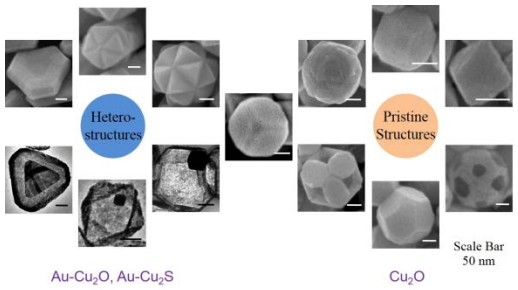

Fig. 1. The hetero- and pristine Cu_2O nanostructures can be achieved via green synthesis.

1. J. Zhang, J. Liu, Q. Peng, X. Wang, Y. Li, *Chem. Mater.* **18**, 867 (2006).
2. H. Xu, W. Wang,W. Zhu, *J. Phys. Chem. B* **110**, 13829 (2006).
3. M. Hara, T. Kondo, M. Komoda, S. Ikeda, K. Shinohara, A. Tanaka, J. N. Kondo, K. Domen, *Chem. Commun.* 357 (1998).
4. C.-H. Kuo, M. H. Huang, *J. Phys. Chem. C* **112,** 18355 (2008).
5. C.-H. Kuo, M. H. Huang, *J. Am. Chem. Soc.* **130,** 12815 (2008).
6. C.-H. Kuo, T.-E. Hua, M. H. Huang, *J. Am. Chem. Soc.* **131**, 17871 (2009).
7. W.-C. Huang, L.-M. Lyu, Y.-C. Yang, M. H. Huang *J. Am. Chem. Soc.* **134**, 1261 (2012).
8. C.-H., Kuo, Y.-T. Chu, Y.-F. Song, M. H. Huang, *Adv. Funct. Mater.* **21**, 792 (2011).
9. C.-H., Kuo, Y.-C. Yang, S. Gwo, M. H. Huang *J. Am. Chem. Soc.* **133**, 1052 (2011).

RS-05 (Keynote Talk)

Nonlinear Optical Absorption properties of LBMO/ZnO/LAO thin films

P. Sreekanth[1], H. Nishikawa[2], J. Thomas[3], T. Endo[4], R. Philip[1]

[1]*Ultrafast and Nonlinear Optics Lab, Light and Matter Physics Group, Raman Research Institute, Bangalore 560080, India*
[2] *Faculty of Biology-oriented Science and Technology, Kinki University, Kinokawa, Wakayama 649-6493, Japan*
[3] *NanoScience Technology Center, University of Central Florida, Orlando, FL 32826-3250, USA*
[4] *Electronic Materials Engineering Laboratory, Department of Electrical and Electronic Engineering, Mie University, Tsu 514-8507, Japan*
Email:reji@rri.res.in, web site: http://rri.res.in/~reji

$La(Ba)Mn_3$ (Perovskite manganite, LBMO) thin films frequently show phase separation consisting of ferromagnetic metallic grain and charge ordered insulating phases with decreasing temperature, which finds many applications. Here we present the nonlinear optical properties of LBMO/ZnO thin films prepared on $LaAlO_3$ substrates. Ion beam sputtering (IBS) was used to fabricate the films in the presence of oxygen. The films are characterized by XRD and AFM, and their I-V switching properties also have been investigated [1].

Nonlinear optical absorption studies were carried out using the open aperture Z-scan technique, employing 532 nm, 5 ns laser pulses obtained from a frequency doubled Nd:YAG laser. Fig. 1 shows the open aperture Z-scan curves (and the intensity dependent transmission calculated from the Z-scan curves) measured in LAO(001) and LBMO/ZnO/LAO thin films. The films show either saturable or reverse saturable absorption depending on the excitation pulse energy, indicating potential laser related applications such as Q-switching, mode-locking and optical power limiting.

1. A. Okada, K. Uehara, M. Yokura, M. Matsui, K. Inaba, S. Kobayashi, K. Endo, N. Iwata, S. Arisawa, J. Thomas, R. John, S.L. Reddy and T.Endo, Jap.J.Appl.Phys. **53**, 05FB10 (2014)

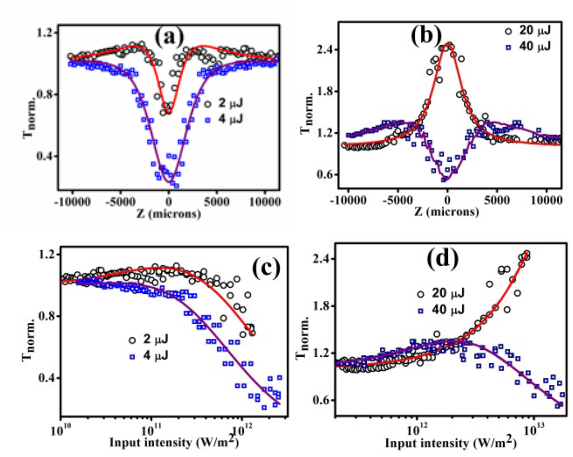

Fig. 1: Open aperture Z-scan curves (a and b) and the corresponding intensity dependent transmissions (c and d) measured in LAO(001) and LBMO/ZnO/LAO thin films respectively.

RS-06 (Invited Talk)
Improving Memory Performance of Cu/HfO_2/Pt Conducting-Bridge RAM by Solvent Substitution

Kentaro Kinoshita[1,2]

[1]*Department of Information and Electronics, Graduate School of Engineering, Tottori University, 4-101 Koyama-Minami, Tottori 680-8552, Japan*; *Email: kinoshita@ele.tottori-u.ac.jp*
[2]*Tottori University Electronic Display Research Center, 4-101 Koyama-Minami, Tottori 680-8552, Japan*

The research and development of resistive memories were advanced from the standpoint of circuit [1,2] and material technology [3]. However, the latter, for example, the selection of materials used for electrodes and memory layers and the control of their crystallinity seems not to be effective in controlling switching voltages and currents of conducting-bridge memory (CB-RAM), in which resistive switching (RS) effect is caused by the migration of metallic atoms that constitute an electrode. Under the circumstance, it was reported that both switching voltages and reset current were decreased by providing water to the HfO_2 memory layer in CB-RAM with a Cu/polycrystalline HfO_2 (poly-HfO_2)/Pt structure [3]. These results suggest that water absorbed in grain boundary due to capillary condensation causes the migration of Cu ions through electrochemical dissolution and diffusion. Therefore, we consider that the poly-HfO_2 layer should not be regarded as a diffusive medium for the migration of Cu ions as ever but should be regarded as a natural nano-porous body that absorbs water, where the pore corresponds to grain boundary.

In this paper, we propose the concept of a ‘pore-engineering’ as a method for controlling device performance, through (i) the kind and property of solvents, (ii) the shape and size of the pores, and (iii) the physical and chemical properties of the pore surface. In particular, the reduction of switching voltages and the stable switching operation that is robust against environmental change were achieved by providing ionic liquid (IL) to the polycrystalline HfO_2 memory layer of a Cu/HfO_2/Pt structure, evidencing the term (i).

Figs. 1(a)-1(c) respectively show cumulative probabilities of V_{form}, V_{set}, and V_{reset} for water-supplied (squares) and water-non-supplied (circles) Cu/HfO_2/Pt structures in the atmosphere. V_{form} and V_{set} are reduced by supplying water. However, resistive switching (RS) of water-supplied samples is unstable against environmental change, ex. temperature, voltage, and ambient pressure, due to the instability of the liquid phase of water. Fig. 2(a) shows *I-V* characteristics of a water-supplied sample in vacuum. The absence of RS effect can be attributed to the vaporization of water from the HfO_2 layer at low pressure. Therefore, stable solvent that can reduce switching voltages and can be replaced with water is necessary for the practical use of CB-RAM. The solid lines in Fig. 1 show cumulative probabilities of V_{form}, V_{set}, and V_{reset} for IL-supplied Cu/HfO_2/Pt structures, showing that switching voltages can be reduced by supplying IL as well as water. In addition, IL-supplied samples show stable RS even in vacuum due to low vapor pressure of IL, as shown in Fig. 2(b). Then, the cumulative probabilities (solid lines) were divided into two groups of $V_{form} \leq 3.0$ V (open triangles) and $V_{form} > 3.0$ V (solid triangles). V_{set} for $V_{form} \leq 3.0$ V shows excellent distribution property, suggesting that the

decomposition of IL by applying large V_{form} hinders effective reduction of switching voltages. Therefore, reducing V_{form} and expanding the potential window of IL are crucial in achieving further reduction of switching voltages. The high effectiveness of supplying solvents in improving memory characteristics strongly supports the validity of the pore-engineering.

[1] K. Kinoshita *et al*., APL **93**, 033506 (2008).

[2] S.-G. Koh *et al*., APL **104**, 083518 (2014).

[3] K. Tsunoda *et al*., Tech. Digest IEDM 2007, p.767.

[4] S. Hasegawa et al., ECS Transactions **50**, 61 (2013).

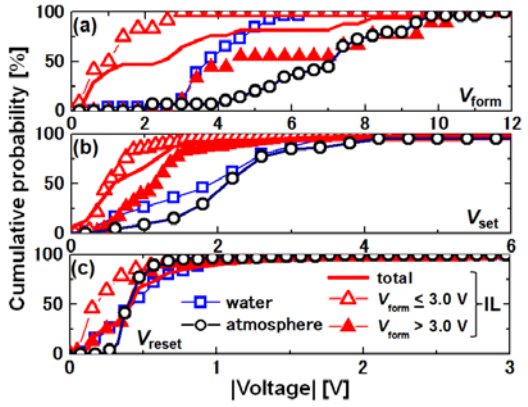

Fig. 1. Cumulative probabilities of (a) V_{form}, (b) V_{set}, and (c) V_{reset}.

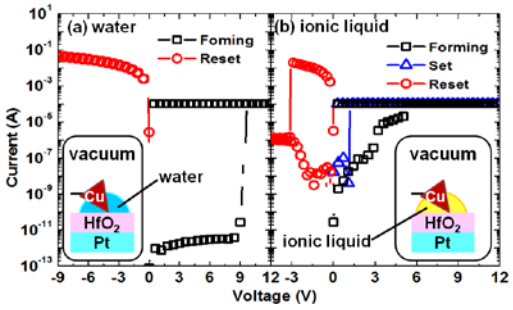

Fig. 2. *I-V* characteristics of (a) water-supplied and (b) IL-supplied samples in vacuum.

RS-07 (Contributed Talk)

The effect of changing electrode materials for the same resistive random access memory filament

Sang-Gyu Koh[1], Satoru Kishida[1, 2], and Kentaro Kinoshita[1, 2]

[1]*Department of Information and Electronics, Graduate School of Engineering, Tottori University, 4-101 Koyama-Minami, Tottori 680-8552, Japan*; *Email: kinoshita@ele.tottori-u.ac.jp*
[2]*Tottori University Electronic Display Research Center, 2-522-2 Koyama-Kita, Tottori 680-0941, Japan*

Nowadays, an idea that redox reaction caused by thermally activated migration of oxygen ions or vacancies is widely received as a resistive switching mechanism of resistive random access memory (ReRAM). However, there are still open issues that should be solved to prove the validity of the idea, such as, "where is oxygen reservoir, that is, an unbalance introduced into oxygen distribution by forming and set processes?" and "what is a role of electrodes in resistive switching effect?".

We have reported the method of preparing an extremely small ReRAM cell, which has the high robustness against the cantilever drift, by using an atomic force microscope (AFM) cantilever [1]. By depositing a transition metal oxide (TMO) film on the tip of a cantilever and by contacting the bottom electrode (BE) with the cantilever, a tiny ReRAM structure can be constructed at the contact area. Since the filament is formed in the TMO film and moves with the cantilever drift, this method has the high robustness against the cantilever drift compared with the conventional structure and enables one to perform a unique experiment to clarify a location of oxygen reservoir and a role of electrodes in resistive switching effect.

In this paper, we investigated the dependence of resistive switching characteristics on electrode materials for the same filament for the elucidation of a role of electrode on resistive switching effect.

A Pt film with a thickness of 20 nm was deposited on an AFM cantilever with a tip radius

of 50 nm (SI-DF3-R(100)) as the top electrode (TE), followed by the deposition of a NiO film with a thickness of 15 nm as a memory layer at room temperature using the DC magnetron sputtering method. Four kinds of BE were prepared by depositing Pt, Au, Ni, TiN film with a thickness of 100 nm on SiO_2/Si substrate, respectively. A TE/TMO/BE structure was formed by contacting a BE on a SiO_2/Si substrate with a Pt/NiO structure formed on the tip of the cantilever, as shown in Fig. 1(a). Current-voltage (*I-V*) measurement was performed in the contact mode of the AFM (Hitachi High-Technologies, E-sweep) using a source-measure unit (Keithley, 236). A bias voltage was applied to the BE, whereas the cantilever (that is, the TE) was grounded.

The effect of replacing BE for the same filament was investigated by preparing BE for set and four different BEs for reset as shown in Fig. 1(b). After confirming the successful resistive switching in air, we annealed the BEs at 300°C in a vacuum in order to desorb water from the BE surface. The desorption of water was confirmed from force curve measurement using AFM. Fig. 2 shows the resistive switching characteristics which were measured on different BE for each switching by applying positive bias to the BE. Here, set switching were performed on the same Pt, and reset switching were performed on Pt, Au, Ni or TiN. Pt and Ni are catalytic metals, which induce dissociative adsorption of oxygen molecules, whereas Au and TiN are non-catalytic metals. However, the occurrence of reset was confirmed in all the BEs. This result indicates that reset is caused by migration of oxygen ions inside the NiO film, suggesting that oxygen reservoir is NiO film itself.

[1] S. G. Koh *et al.*, Appl. Phys. Lett. 104, 083518 (2014).

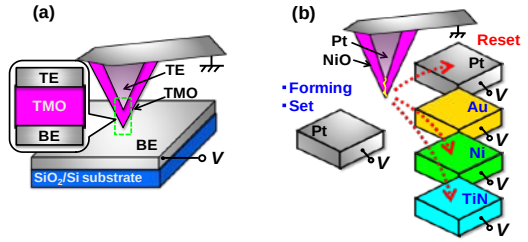

Fig. 1(a) Tiny ReRAM structure fabricated on the tip of a cantilever of an AFM. (b) Pt-BE for set and four kinds of BE (Pt, Au, Ni, TiN) for reset

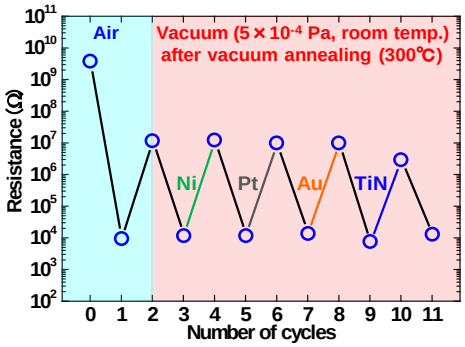

Fig. 2. Resistive switching characteristics which were measured on different BE for each switching by applying positive bias to the BE.

RS-08 (Invited Talk)
Advancing high resolution characterization for 2D materials

Laurene Tetard[1]

[1]*Nanoscience Technology Center, University of Central Florida, Orlando, FL, USA*
Email:Laurene.Tetard@ucf.edu, web site: http://www.nanoscience.ucf.edu/tetard/

The rapid ascendance of 2D materials, triggered by the first mechanical exfoliation of graphene and the subsequent discovery of the amazing properties of 2D single layers, urges for high spatial resolution characterization routes to study processes occurring at the 2D surface including those related to response to external controls or defect formation. Such capability would accelerate the ability to controllably tailor 2D materials electrical and optical properties.

We will discuss advances of submicron properties of 2D materials using a combination of Atomic Force Microscopy (AFM), Raman and photoluminescence spectroscopy. In particular, we will present evidence of optical properties variations of two types of single-layer MoS_2: one treated with oxygen plasma and the other decorated with Au nanoparticles. We showed that upon increasing plasma exposure time, the formation of defects forming in the MoS_2 layer could be monitored by photoluminescence (PL) and Raman spectroscopy mapping of the flake, with resolution close to 400 nm. The measurements revealed a transition from very high intensity to complete quenching [1, 2]. These changes were accompanied by gradual reduction and broadening of MoS_2 Raman modes, indicative of distortion of the MoS_2 lattice after oxygen bombardment. The studies were complemented by X-ray photoelectron spectroscopy of the treated MoS_2 flake and band structure calculations, which showed the formation of localized MoO_3 defects in the flake [1, 2]. In Au decorated 2D flakes, we will present evidence that PL quenching can be attributed to charge transfer (p doping) of MoS_2 [3]. Finally, we will discuss future outlooks on advanced nanoscale (below 100 nm) characterization for 2D materials assemblies.

1. Narae Kang, Hari P. Paudel, Michael N. Leuenberger, Laurene Tetard, and Saiful I. Khondaker. Photoluminescence Quenching in Single-Layer MoS_2 via Oxygen Plasma Treatment, Journal of Physical Chemistry C, 118 (36), 21258–21263, 2014.
2. Muhammad R. Islam, Narae Kang, Udai Bhanu, Hari P. Paudel, Mikhail Erementchouk, Laurene Tetard, Michael N. Leuenberger and Saiful I. Khondaker. Tuning the electrical property via defect engineering of single layer MoS2 by oxygen plasma, Nanoscale, 6, 10033-10039, 2014.
3. Udai Bhanu, Muhammad R. Islam, Laurene Tetard, Saiful I. Khondaker. Photoluminescence quenching in gold - MoS_2 hybrid nanoflakes, Scientific Reports 4, 5575, 2014.

Session NO
NANOSCALE OPTICS AND PHOTONICS

NO-01 (Invited Talk)
Ultrafast fiber lasers enabled by carbon nanotubes and their applications

K. Kieu[1], S. Mehravar[1], L. Karvonen[2], A. Saynatjoki[2],J. Riikonen[2], B. Norwood[1], N. Peyghambarian[1]

[1]University of Arizona, College of Optical Sciences, 1630 E University Blvd, Tucson, AZ 85721, USA Email:kkieu@optics.arizona.edu

[2]Aalto University, Department of Micro and Nanosciences, Tietotie 3, FI-02150 Espoo, Finland

Mode-locked lasers which generate femtosecond or picosecond pulses are important tools in modern scientific research and technological applications. These lasers are notorious for their high cost, bulkiness, and complexity in day-to-day operation. The discovery of carbon-based nano-materials (carbon nanotubes and graphene) as an effective saturable absorber (SA) for mode-locking may have changed the situation. It is now possible to build very compact, low cost, and reliable femtosecond fiber lasers working in a wide range of wavelengths with the use of this new SA technology. I will review the latest ultrafast fiber laser systems that we have developed using carbon nanotubes (CNT). The emphasis will be put not only on the excellent performance of the developed lasers but also on their commercialization path where long term operation and stability are crucial. A newly developed laser is only useful when it is successfully used in a real application. For that reason, I will also discuss the latest results that we have been able to achieve through the use of the laser systems that we have developed. In particular, I will discuss the application of these lasers in multiphoton microscopy of 2-dimensional layered materials (graphene, GaSe, MoS_2), photonic devices as well as biological tissues.

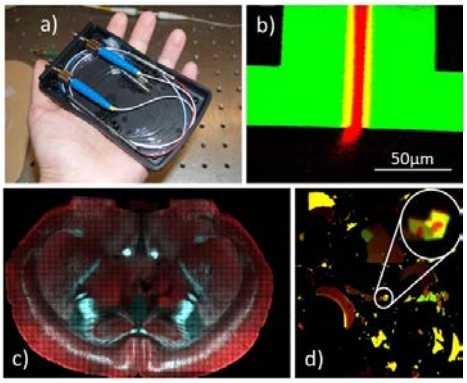

Fig. 1. a) A photograph of a compact mode-locked fiber laser with CNT SA; b) Second harmonic (red) and third harmonic (green) image of a polymer-based phase modulator; c) Multiphoton image of a mouse brain section; d) Multiphoton image of graphene flakes on a silicon substrate.

1. Christian W. Freudiger, Wenlong Yang, Gary R. Holtom, Nasser Peyghambarian, X. Sunney Xie, Khanh Q. Kieu, “Stimulated Raman microscopy with a robust fiber laser source,” *Nature Photonics* **8**,153–159 (2014)
2. K. Kieu, S. Mehravar, R. Gowda, R. A. Norwood, and N. Peyghambarian, "Label-free multi-photon imaging using a compact femtosecond fiber laser mode-locked by carbon nanotube saturable absorber," Biomed. Opt. Express **4**, 2187-2195 (2013)
3. A. Säynätjoki, L. Karvonen, J. Riikonen, W. Kim, S. Mehravar, R. Norwood, N. Peyghambarian, H. Lipsanen, and K. Kieu, “Rapid Large-Area Multiphoton Microscopy for Characterization of Graphene”, *ACS Nano* **2013** *7* (10), 8441-8446
4. K. Kieu, J. Jones and N. Peyghambarian, “Generation of Few-Cycle Pulses From an Amplified Carbon Nanotube Mode-Locked Fiber Laser System,” PTL, **22**, 1521-1523 (2010)
5. K. Kieu and M. Mansuripur, "Femtosecond laser pulse generation with a fiber taper embedded in carbon nanotube/polymer composite," Opt. Lett. **32**, 2242-2244 (2007)

NO-02 (Invited Talk)

Controlled coupling of nanoparticles to polymer-based photonic structures

Dam Thuy Trang Nguyen, Mai Trang Do, Qinggele Li, Isabelle Ledoux-Rak, and Ngoc Diep Lai

Laboratoire de Photonique Quantique et Moléculaire, UMR CNRS 8537, Institut D'Alembert, École Normale Supérieure de Cachan, 94235 Cachan cedex, France
Email: nlai@lpqm.ens-cachan.fr, web site: http://www.lpqm.ens-cachan.fr

In relation with the strong and fast development of sub-diffractive fabrication techniques, a great deal of interest has been devoted to suitable and inexpensive materials, which may form desired micro and nanostructures. Polymer materials offer unique opportunities since both top-down and bottom-up strategies can be pursued and combined towards the nanoscale. Besides, polymer materials can be functionalized with nonlinear optical or fluorescent materials. The ensemble can be optically structured in a flexible way to obtain a polymer-based photonic nanostructure ("host") containing active materials ("guest"). The engineered coupling between a guest (molecule, nanoparticle) and the host may provide an enhancement of the guest optical response, leading to attractive applications.

In this work, we first demonstrate a simple and robust fabrication technique, namely low one-photon absorption direct laser writing (LOPA DLW) [1, 2], which allows obtaining desired sub-micrometric 2D and 3D structures, equivalent to what realized by two-photon absorption technique. We then show that the LOPA DLW is very useful to embed a single active nanoparticle into various photonic structures containing at any desired position [3].

Figure 1(a) shows, as an example, various 2D photonic structures, fabricated by the LOPA-based DLW method. This technique requires only a very weak power, typically 2 mW, of a continuous laser at 532 nm. The smallest feature size of observed structure is about 150 nm. The pillar at center of each structure contains a single gold nanoparticle, as demonstrated in figures 1(b) and 1(c). The plasmonic/photonic coupling has been also characterized, showing a 5-fold enhancement in fluorescence extraction efficiency.

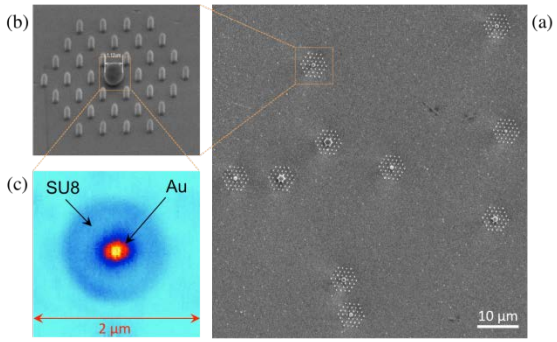

Fig. 1. (a) Scanning electron microscopy image of different SU8 photonic structures containing individual gold nanoparticles, fabricated by LOPA-based direct laser writing. (b) Zoom in a single structure. (c) Scanned fluorescence image of a polymeric microsphere containing a single gold nanoparticle at the center.

1. Q. Li, M. T. Do, et al., *A novel concept for three-dimensional optical addressing by ultralow one-photon absorption method*, Opt. Lett. **38**, 4640 (2013).
2. M. T. Do, T. T. N. Nguyen, et al., *Submicrometer 3D structures fabrication enabled by one-photon absorption direct laser writing*, Opt. Express **21**, 20964 (2013).
3. M. T. Do, D. T. T. Nguyen, et al., *Controlled coupling of a single nanoparticle in polymeric microstructure by LOPA direct laser writing*, submitted (2014).

NO-03 (Invited Talk)

Manipulating light with all-dielectric metasurfaces

Yuanmu Yang[1], Wenyi Wang[2], Parikshit Moitra[1], Ivan I. Kravchenko[3], Dayrl P. Briggs[3], Jason Valentine[4]

[1]*Interdisciplinary Materials Science Program, Vanderbilt University, Nashville, Tennessee 37212, USA*

[2]*Department of Electrical Engineering and Computer Science, Vanderbilt University, Nashville, Tennessee 37212, USA*
[3]*Center for Nanophase Materials Sciences, Oak Ridge National Laboratory, Oak Ridge, Tennessee 37831, USA*
[4]*Department of Mechanical Engineering, Vanderbilt University, Nashville, Tennessee 37212, USA*

Absorption loss continues to be one of the primary impediments to the application of plasmonic metamaterials and metasurfaces at optical frequencies. Dielectric metamaterials offer one potential solution to this issue by eliminating Ohmic loss, allowing the realization of highly transparent materials and, as with their plasmonic counterparts, manipulation of the unit cell structure of all-dielectric metasurfaces offers a means to engineer a wide variety of optical functionalities. In this talk, I will discuss our recent experimental efforts to demonstrate silicon-based reflect-array metasurfaces within the telecommunications band. The metasurface is shown to provide linear polarization conversion with a more than 98% conversion efficiency over a 200nm bandwidth. More importantly, by modulating the unit cell geometry, we also show that complete 2π phase coverage can be achieved with more than 93.6% average efficiency over a wavelength range from 1500 nm to 1600 nm. This freedom in phase manipulation is used to create an ultra-thin vortex beam generator at telecommunications frequencies.

The unit cell geometry of the metasurface is shown below in Fig. 1a. It consists of Si resonators placed above a silver ground plane. The resonators are designed such that the resonance along their short axis has a π phase shift with respect to the resonance along the long axis, resulting in linear polarization conversion over a 200 nm bandwidth (Fig. 1b). Furthermore, by controlling the dimension of the resonator, we can acquire full 2π phase control over the cross-polarized reflected light. This capability is demonstrated by employing the resonators with an azimuthally varied phase profile for generation of a vortex beam (Fig. 1c).

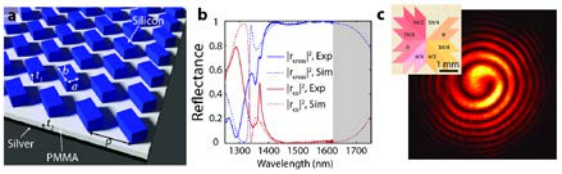

Fig. 1. (a) Schematic of Si-based metasurface. (b) Experimentally measured and simulated cross and co-polarized reflectance from the array. (c) Experimental image of vortex beam generated by the metasurface. The inset is an optical image of the array indicating how the phase is modulated across the sample.

NO-04 (Invited Talk)
Quantum States of Light in Metamaterials Require a New Effective-Medium Theory

Ehsan Amooghorban[1], N. Asger Mortensen[2,3], and Martijn Wubs[2,3]

[1] *Department of Physics, Faculty of Basic Sciences, Shahrekord University, P.O. Box 115, Shahrekord 88186-34141, Iran*
Email: Ehsan.Amooghorban@sci.sku.ac.ir, web site: http://www.sku.ac.ir/academic/members/Amooghorban/main.htm

[2] *Department of Photonics Engineering, Technical University of Denmark, DK-2800 Kongens Lyngby, Denmark Email: mwubs@fotonik.dtu.dk, web site: http://www.fotonik.dtu.dk/english/Research/Nanophotonics/SEM*

[3] *Center for Nanostructured Graphene (CNG), Technical University of Denmark, DK-2800 Kgs. Lyngby, Denmark Web site: http://www.cng.dtu.dk/*

Metamaterials have designed dielectric properties that often have no counterparts in nature. They are made out of unit cells much smaller than the optical wavelength, which allows their description as an effectively homogeneous medium, only characterized by their effective refractive index and geometry. Metamaterials are actively studied and hold the promise to manipulate and guide light in new ways.

Less well studied are the prospects of metamaterials in quantum optics. One of the key questions is then whether metamaterials allow the same effective description as for classical light

when for example a single photon passes through them. First reactions from colleagues to this question ranged between the two extremes that 1. obviously any effective-medium theory would break down for single photons, and 2. obviously the same effective-medium theories apply to a single photon as to classical light. This illustrates that the topic deserves attention, in our opinion both because of fundamental interest and because of possible applications of metamaterials in quantum optics.

A well-known difference between classical and quantum optics is that in quantum optics, loss and gain are inevitably connected with noise. So any effective theory of a metamaterial in quantum optics should be able to accurately predict the measurable effects of this quantum noise. More specifically, the question is whether the usual effective index accurately describes the quantum-noise properties of the metamaterial. We recently found [1] this to be the case for passive metamaterials, but not in the field of active plasmonics, where metamaterials are driven out of equilibrium, for example to compensate losses in one constituent of the metamaterial unit cell by amplification in another. Nevertheless we also found that effective-medium descriptions are still quite well possible in active plasmonics, when introducing a single additional effective parameter that measures how much loss is compensated by how much gain [1].

Very recently we found how our quantum optical effective-medium (QOEM) theory for one-dimensional light propagation can be generalized to three-dimensions [2], and how the loss-compensation parameter depends on the angle of incidence and polarization. Our calculations of intensities and balanced homodyne detection of the output states of light illustrate that the additional effective-medium parameter in our QOEM theory is both necessary and sufficient.

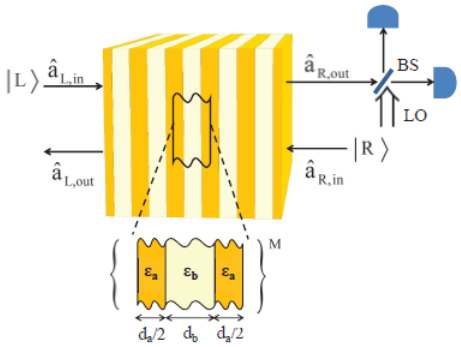

Fig1. Quantum states of light entering and leaving an archtetypical multilayer metamaterial. From Ref. [1].

1. E. Amooghorban, N. A. Mortensen, and M. Wubs, Phys. Rev. Lett. **110**, 153602 (2013).
2. E. Amooghorban *et al.*, to be submitted (2014).

NO-05 (Invited Talk)
Structured Light-Matter Interactions at the Nanoscale

Xiaobo Yin

Materials Science and Engineering
Mechanical Engineering
University of Colorado Boulder, CO 80309
Email:Xiaobo.yin@colorado.edu, web site:
https://sites.google.com/site/xblab2000/

The rapid development of nanoscale science and technology not only permits explorations of advanced scientific ideas and observations of unprecedented phenomena, but also offers practical solutions to the world's most serious issues such as energy and pollution crises, health and food safety concerns, as well as military and homeland security needs. Exploiting and enhancing the originally weak light-matter interactions, we will be able to devise better imaging and manufacturing tools, to catalyze more efficient photochemical reactions, to sense and to diagnose contaminants at single molecule levels.

This talk will be focusing on how judiciously designed nanostructures and materials can tailor and eventually control the light-matter interactions at the deep-sub-wavelength scale. I will illustrate these design

principles by using specific examples. In particular, I will elaborate the strategies to harvest substantial amount of energy-efficient emissions from a sub-wavelength laser cavity and to achieve close-to-unit utilization of light, providing coherent sources at the nanoscale. These nanolasers can perform much brighter and faster when quantum engineering is employed and show great potential in ultra-trace chemical sensing. More interestingly, introducing uniquely structured quantum materials such as monoatomic layer transition metal dichalcogenides, the light-matter interaction at the nanoscale senses the atomic structural and topological symmetries that are embedded in the system, revealing the fascinating physics and redefining the applications based on these unique physical processes. I will discuss some of the preliminary assessments of the observed valley physics and illustrate the structure and function relationship in these impactful materials that have been widely utilized in both mechanical systems and energy sciences.

NO-06 (Invited Talk)

Rainbow trapping effect: Broadband light trapping and splitting in hyperbolic metafilm patterns

Qiaoqiang Gan*

Electrical Engineering Department, University at Buffalo, The State University of New York, Buffalo, USA

Email:qqgan@buffalo.edu, web site: http://sites.google.com/site/qqganlab/research

Perfect absorbers are important optical components required by a variety of applications [1]. While there is great interest in achieving highly absorptive materials exhibiting large broadband absorption using optically thick, micro-structured materials [2,3], it is still challenging to realize ultra-compact subwavelength absorber for on-chip optical/thermal energy applications. In this presentation, we will discuss the “rainbow” trapping effect, an enhanced light-matter interaction mechanism, in patterned hyperbolic meta-film with engineered and freely tunable absorption band [4,5]. These on-chip absorbers can easily be integrated with other on-chip electronic/optoelectronic devices, which is promising to create new regimes of optical/thermal physics and applications.

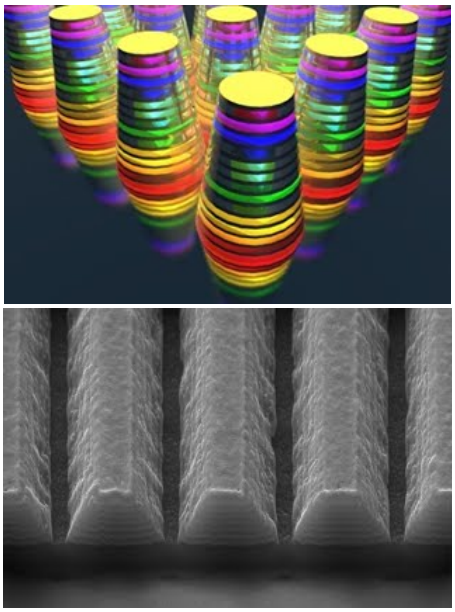

1. Watts, C. M., Liu, X. & Padilla, W. J. Metamaterial electromagnetic wave absorbers. Adv. Mater. **24**, OP98–OP120 (2012).
2. Aydin, K., Ferry, V. E., Briggs, R. M. & Atwater, H. A. Broadband polarization independent resonant light absorption using ultrathin plasmonic super absorbers. Nature Commun. 2, 517 (2011).
3. Sondergaard, T. et al. Plasmonic black gold by adiabatic nanofocusing and absorption of light in ultra-sharp convex grooves. Nature Commun. 3, 969 (2012).
4. H. Hu, D. Ji, X. Zeng, K. Liu, Q. Gan, Rainbow Trapping in Hyperbolic Metamaterial Waveguide, Scientific Reports **3**: 1249 (2013).
5. D. Ji, H. Song , X. Zeng , H. Hu , K. Liu , N. Zhang, Q. Gan, Broadband absorption engineering of hyperbolic metafilm patterns, Scientific Reports **4**: 4498(2014)

NO-07 (Invited Talk)
Superradiant thermal emission and light absorption

Zongfu Yu

Department of Electrical and Computer Engineering, University of Wisconsin – Madison, WI 53706

Email:zyu54@wisc.edu

Discovered by Dicke six decades ago, superradiance effect shows that N emitters when placed together emit light with an intensity N^2 times stronger than a single emitter. As an analog of quantum emitters, optical resonances offer the same physics to create superradiance effects. Moreover, the characteristics of optical resonances can be engineered with greater flexibility, allowing us to study superradiance in a broader regime. Here, we will show that superradiance can lead to coherent suppression of absorption as well as thermal emission.

NO-08 (Invited Talk)
Slow-Light Spectroscopic Devices On Chips

Zhimin Shi[1], Andreas C. Liapis[2], Boshen Gao[2], and R. W. Boyd[2,3]

[1] *Department of Physics, University of South Florida, Tampa, Florida 33620 USA*

Email:zhiminshi@usf.edu

[2] *The Institute of Optics, University of Rochester, Rochester, New York 14627 USA*

[3] *Department of Physics and School of Information Technology and Engineering, University of Ottawa, Ottawa, K1N 6N5 Canada*

Interferometric spectrometers refer to a large family of instrument that extract the spectral information of a given optical field through optical interference. Integrated spectrometers with high spectral sensitivity are becoming more and more desired in applications such as metrology, optical sensing, quantum information processing, biomedical engineering, etc.

In this work, we study the use of photonic crystal (PhC) structures for on-chip spectroscopic applications. In specific, we study three types of PhC spectroscopic devices, including the use of slow-light PhC line-defect waveguides to construct on-chip slow-light interferometric spectrometers, cascaded PhC cavities spectrometers, and a PhC super-prism spectrometer.

We show that the loss-limited spectral resolution of a slow-light grating-based spectrometer scales as the loss–group-index ratio of the waveguide array. We further show that one can achieve a spectral resolution of a few GHz using currently available slow-light photonic crystal waveguides while greatly shrinking the on-chip footprint of the spectrometer.

Secondly, we demonstrate that an array of high-Q photonic crystal cavities can be used as a compact high-resolution on-chip spectrometer. We show the use of such a device to distinguish two gas species, C_2H_2 and HCN, by scanning through their absorption lines.

Lastly, we show that an optimum PhC superprism structure for practical spectroscopic applications should have large angular group dispersion over a large bandwidth, i.e., a flat-top dispersion profile. We demonstrate the advantage of such a new design consideration by optimizing the geometry of a two-dimensional parallelogram-lattice PhC superprism structure to construct a flat-band spectrometer.

Poster Session – Group I
CARBON-BASED MATERIALS AND TECHNOLOGIES, CATALYTIC MATERIALS, POLYMER COMPOSITES

PC-01:
Microstructure and surface properties of carbon nanostructured materials obtained by chlorination reaction of $Zr(C_5H_5)_2Cl_2$

D.J. Araujo-Pérez[1], P. Gonzalez-García[1], M.E. Poisot-Vázquez[2], L. García-González[1].

[1]*Centro de Investigación en Micro y Nanotecnología, Universidad Veracruzana, Boca del Río, Veracruz, México.*
Email presenting autor: iq.daraujo88@gmail.com
Web site: http://www.uv.mx/veracruz/microna/
[2]*Instituto de Química Aplicada, Universidad del Papaloapan, San Juan Bautista Tuxtepec, Oaxaca, México*

Microporous Carbons are the primary materials used to produce electrodes for electrochemical double layer capacitors (EDLC). Nanostructured carbons have large specific surface area (SSA) and narrow porosity, necessary for enhancing the capacitance. In addition they are available in a wide variety of commercial forms. This diversity of surface properties and shapes are the most attractive properties of carbon. By adjusting these features, it is possible to tune the electrochemical performance of the materials and to adapt them to various kinds of electrolytic media and system configurations. [1]

In this work, carbon materials were obtained by the chlorination of bis(cyclopentadienyl)Zirconium IV dichloride $Zr(C_5H_5)Cl_2$ at 900°C, varying the reaction time at 30, 60, 90 and 120 min. The microstructure of the obtained carbons were studied by X-ray diffraction and Raman spectroscopy and the textural properties were studies by nitrogen adsorption and desorption at 77K. In Figure 1 X-ray diffraction patterns show that the obtained carbons are mainly disordered consisting of relatively small graphitic domains. The lattice parameters L_a and L_c were calculated and analyzed, from this values we can observe that the particles consist from 4 to 5 graphene layers stacked along the c direction and the length of the graphene sheets varies between 2.3 and 2.9 nm. These data were compared to the First order Raman Spectra where Disordered induced band (D-band at 1350cm^{-1}) and graphitic band (G-band at 1580cm^{-1}) were observed as shown in Figure 1. The adsorption/desorption isotherms, also displayed in Figure 1, showed a small decrease on the amount adsorbed as the reaction time increases, then, the SSA varies from 633 to 754 m^2/g; while the average pore diameters vary from 0.6 to 0.8 nm, ideal for high performance EDLC.

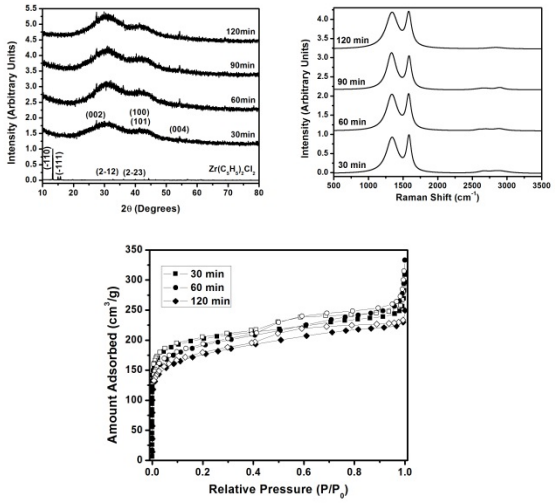

Fig1. Left, X-ray Difractogram of the precursor, and the samples obtained at 30, 60, 90 and 120. Right, Raman Spectra of the carbon samples at different reaction times. Bottom, Adsorption/desorption isotherms of the samples.

1. F. Béguin and V. Presser, *Advanced Materials* ***26***, 2219 (2014).

PC-02:
Nanoporous Carbon for the Applications in Supercapacitor and Batteries

Areeya Ninlerd, Thanyalak Chaisuwan, Sujitra Wongkasemjit, and Bussarin Ksapabutr

The Petroleum and Petrochemical College, Chulalongkorn University, Bangkok 10330, Thailand
Email: Aninlerd@gmail.com

Electrochemical capacitors or supercapacitors are new kind of energy storage devices which have high efficiency and outstanding properties such as high power density and long life cycle. In order to reach high capacitance, choosing the electrode material is very important. Porous carbon is a great candidate because of its excellent properties such as high surface area, easy to process, flexibility of morphology design. Polybenzoxazine prepared via a sol-gel method was used as a carbon precursor and morphology of polybenzoxazine precursor was shown in figure 1. Cetyltrimethyl ammonium bromide (CTEB) was used as a soft template so as to increase amount of mesopores. In order to enhance the capacitance by faradic redox reaction, metal oxide (1, 3, and 5 wt.%) was incorporated into the electrodes. The electrochemical properties of electrodes were investigated by the electrochemical impedance spectroscopy, cyclic voltammetry, and galvanostatic charge/discharge.

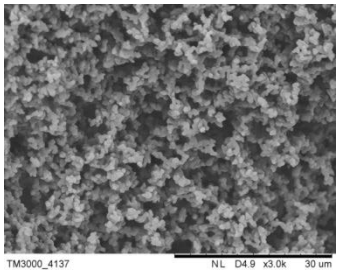

Fig. 1. Morphology of resulting porous polybenzoxazine precursors

PC-03:
Facile synthesis of morphologically controlled nanoporous carbon using a soft-templating method for supercapacitors

Pornpichaya Thawepornpuriphong, Sujitra Wongkasemjit and Thanyalak Chaisuwan

The Petroleum and Petrochemical College and the Center of Excellence on Petrochemical and Materials Technology, Chulalongkorn University, Bangkok 10330, Thailand
Email: Pornpichaya.t@gmail.com

Porous materials have been extensively studied and used in various applications especially in electrode materials for energy storage devices. The template synthesis has been used for the preparation of carbon material with controlled pore size and pore distribution via through approaches; hard-templating and soft-templating. However, the hard-templating method still has some drawbacks which are multi-step requirement and high cost. Hence, we reported a facile soft-templating method to design pore formation and size by adding surfactant to overcome the drawbacks of the hard-templating method. Polybenzoxazine, an additional-cure phenolic resins providing excellent properties over conventional novolac and resole types of phenolic resin, was used as precursor to synthesize organo gel and triblock co-polymer, Pluronic P123, was used as a template. The morphology of carbon particles could be designed by varying concentrations of polybenzoxazine and P123. The results from SEM show that the spherical-connected nanoparticles can be obtained when the concentration of polybenzoxazine was set at 20 wt. % and concentration of P127 was set at 3-12 wt. % as shown in Fig.1. The spherical-connected mesoporous carbon allows electrolytes to pass through the electrodes better, resulting in higher capacitance.

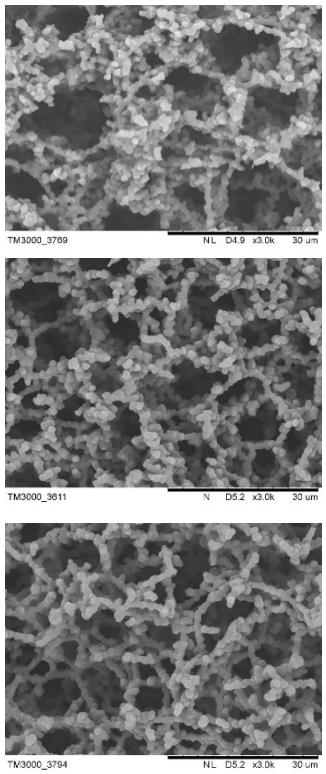

Fig. 1. SEM micrographs of porous carbon derived from polybenzoxazine: (a) 20 wt. % polybenzoxazine and 3 wt. % P123 in DMF; (b) 20 wt. % polybenzoxazine and 8 wt. % P123 in DMF; (c) 20 wt. % polybenzoxazine and 12 wt. % P123 in DMF.

PC-04:
Novel CO_2 storage by using hierarchical N-rich Nanoporous carbon via facile templates synthesis as an adsorbent

Nanthawut Chokaksornsan, Bussarin Ksapabutr, Sujitra Wongkasemjit and Thanyalak Chaisuwan

The Petroleum and Petrochemical College and the Center of Excellence on Petrochemical and Materials Technology, Chulalongkorn University, Bangkok 10330, Thailand
Email: chokaksornsan33@hotmail.com

Nanoporouscarbon material has been prepared by pyrolysis polybenzoxazine precursor in inert atmosphere which can be successfully synthesized by bisphenol A, formaldehyde and aliphatic diamine via sol-gel process. The morphology of carbon particle could be designed by varying the ratio of cetyltrimethylammonium bromide (CTAB) and silica templates. In this study, the effect of varying pyrolysis temperatures to obtain nitrogen-rich nanoporous carbon and exhibited good CO_2 adsorption performance with high nitrogen content and high surface areas is investigated. In addition, AS1-MP was used to determine the surface area of the resulting nanoporous carbon. The elemental composition on the surface of nanoporous carbon analyzed by x-ray diffraction spectroscopy and x-ray photoelectron spectroscopy.

PC-05:
Theoretical Study of Hydrogen Adsorption and Diffusion in Spillover Process on Microporous Carbon

K. Suzuki[1], M. Tachikawa[2], M. Kayanuma[1], Yoshihisa Oko[1], U. Nagashima*[1], H. Nishihara[3], and T. Kyotani[3]

[1]Research Institute for Computational Sciences, National Institute of Advanced Industrial Science and Technology, Ibaraki, Japan.
e-mail: u.nagashima@aist.go.jp

[2]Graduate School of Nonobioscience, Yokohama City University, Yokohama, Japan
e-mail: tachi@yokohama-cu.ac.jp

[3]Institute of Multidisciplinary Research for Advanced Materials, Tohoku University, Sendai, Japan

Using density functional theory (DFT) and path integral molecular dynamics (PIMD) simulation, we investigated the hydrogen distribution on microporous carbon such as zeolite templated carbon (ZTC) [1, 2].

Evaluation of chemisorption energies of a hydrogen atom on four graphene-like fragments with different curvature (Fig. 1) showed that hydrogen atoms adsorb strongly at the edge site and convex surface. We also showed that hydrogen chemisorption at edge sites enhances the adsorption energy at the inner site. To reveal the mechanism of hydrogen diffusion on a carbon surface in the spillover process with DFT,

transition states of two types were examined: hydrogen moving along the C–C bond keeping a weak C–H bond, and hydrogen dissociation from the carbon surface. The results suggest that the latter path is more likely to occur than the former path in flat surface and the situation might be modified by introducing curvature. These results suggest that efficiency of hydrogen spillover on carbon-based hydrogen storage materials will be enhanced by controlling the structure of the carbon surfaces [3].

In the PIMD simulation nuclei are treated as quantum mechanical particle, and one can take account of quantum and thermal fluctuations for molecular vibrational and rotational degree of freedom. Five kinds of carbons inside of buckybowl $C_{36}H_{12}$ were selected from innermost to edge as the adsorption site for additional hydrogen atom [4]. We have found that hydrogen atom at 100 K adsorbed on each carbon, while stable hydrogen adsorption sites are gradually decreasing as temperature becomes higher. This is because the additional hydrogen atom at high temperature is easy to go over the potential barrier between one to other carbon by thermal and nuclear quantum effects. Our PIMD results are in consistent with the corresponding experimental observations [5].

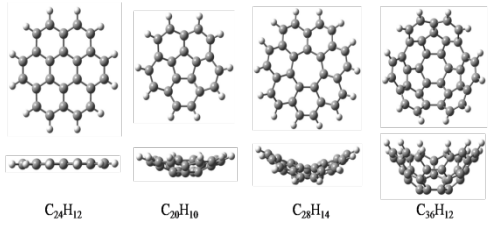

Fig. 1. Front and side views of molecular structures of $C_{24}H_{12}$ (coronene, [6]circlene), $C_{20}H_{10}$ (corannulene, [5]circlene), $C_{28}H_{10}$ (pleiadannulene, [7]circlene), and $C_{36}H_{12}$ (triacenaphthotriphenylene).

References

[1] H. Nishihara, P.-X. Hou, L.-X. Li, M. Ito, M. Uchiyama, T. Kaburagi, A. Ikura, J. Katamura, T. Kawarada, K. Mizuuchi, T. Kyotani, J. Phys. Chem. C, **113**, (2009), 3189-3196.

[2] H. Nishihara, Q.-H. Yang, P.-X. Hou, M. Unno, S. Yamauchi, R. Saito, J.I. Paredes, A. Martínez-Alonso, J.M.D. Tascón, Y. Sato, M. Terauchi, T. Kyotani, Carbon, **47**, (2009), 1220-1230.

[3] M. Kayanuma, U. Nagashima, H. Nishihara, T. Kyotanani, and H. Ogawa, Chem. Phys. Lett., **495**, (2010), 251-255.

[4] K. Suzuki, M. Kayanuma, M. Tachikawa, H. Ogawa, H. Nishihara, T. Kyotani, and U. Nagashima, J. Alloys and Compounds, **509**, (2011) S868-S871, K. Suzuki, M. Tachikawa, H. Ogawa, S. Ittisanronnachai, H. Nishihara, T. Kyotani, and U. Nagashima, Theor. Chem. Acc. **130**, (2011), 1039-1042.

[5] H. Nishihara, S. Ittisanronnachai, H. Itoi, L. Li, K. Suzuki, U. Nagashima, H. Ogawa, T. Kyotani, and M. Ito, J. Phys. Chem. C, (2014) DIO: JCA10.0.1465.

PC-06:
Applications of Fe_3O_4@Ag nanoparticles above graphite

Anh D. Phan[1,2] and N. A. Viet[2]

[1]*Department of Physics, University of Illinois, 1110 West Green St, Urbana, Illinois 61801, USA*
Email:anhphan2@illinois.edu

[2]*Institute of Physics, Vietnam Academy of Science and Technology, 10 Dao Tan, Ba Dinh, Hanoi 10000, Vietnam*

We theoretically study absorption properties of Fe_3O_4@Ag nanoparticles on graphite substrates based on the Mie theory. There are two maxima at around 380 nm and near-infrared regime in the absorption spectrum of the nanoparticle. In the absence of substrate, the second optical peak induced by excitations in Fe_3O_4 dramatically changes both the magnitude of absorption cross section and the peak position when the sizes of the core and shell are varied. These results can be exploited to design photothermal agents with high efficiency for cancer treatment. Graphite substrate has strong influence on the plasmonic resonance in near-infrared regime. This finding suggests that it is possible to use the nanoshell to detect the surface roughness of graphite substrate and use graphite

to enhance ability of the nanoparticles for killing cancer cells.

PC-07:
Electronic effects in nanoparticle silver catalysts

Nigora Turaeva, M. L. Preuss

Biology Department, Webster University, Webster Groves, MO, USA
Email:nigoraturaeva82@webster.edu

There are basically two fundamental principles in nanoparticles which lead to their size-dependent properties: significant fraction of atoms at the surface and quantum confinement. While the former exhibits smoothly scalable dependence but the latter can result in smooth behavior as well as discontinuous one due to completion of shells in systems with delocalized electrons [1].

In this work the theoretical model describing size-dependent catalytic activity of silver nanoparticles regarding to the CO oxidation reaction has been proposed. We consider the following mechanism of this reaction. The surface of catalyst contains chemo-absorbed oxygen atoms, which in their ionic-radical forms represent adsorption centers for CO molecules. Then at adsorption of CO molecules ionic-radicals of CO_2^- are formed as intermediates, which after neutralization are desorbed as CO_2 molecules. Thus this reaction occurs in two stages: acceptor stage, when adsorbed oxygen is accepted electron from silver nanoparticles and donor stage, when ion-radicals of CO_2^- is neutralized returning electron to catalyst. Basing on the size dependence of ionization energy in the frame of classical droplet model and two stage electronic theory of the CO oxidation reaction [2] it has been demonstrated a non-monotonic behavior of reaction rate with respect to the size of silver nanoparticles (fig.1), which is qualitatively in agreement with the experiments.

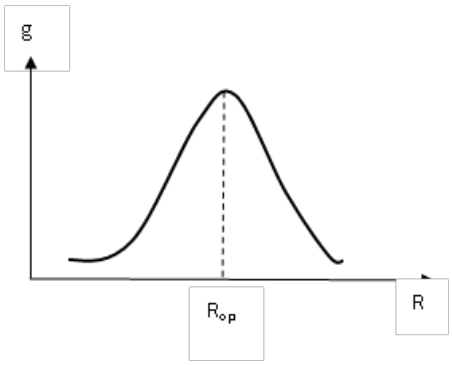

Fig. 1 Reaction rate as a size function.

1. E. Roduner, *Chem. Soc. Rev.*, **35**, 583 (2006).
2. T. Volkenstein, The electron theory of catalysis on semiconductors (McMillan, New York), (1963).

PC-08:
Unexpected catalytic performance of Ni/SiO_2 nanoparticles prepared by magnetron sputtering deposition for reverse water gas shift reaction

Renato V. Gonçalves[1], Liane M. Rossi[1]

[1]*Institute of Chemistry - University of São Paulo, São Paulo, SP, Brazil*
Email:rsvg12@iq.usp.br

Problems associated with the exhaust gases emissions of carbon dioxide (CO_2) from fossil fuels used in industry and vehicles have attracted much attention due to the strong environment impacts, especially in urban areas where they are causing serious effects on climate changes due to the ‘‘greenhouse effect’’ and human health.[1] The conversion of CO_2 to CO is highly desirable due to the potential use of synthesis gas (H_2 and CO) in the manufacture of various products in different industrial processes. The reverse water–gas shift reaction (RWGS) is one of the available methods for production of CO. The active compounds most commonly used in RWGS are platinum group metals (Pt, Pd, and Rh) and copper-based catalysts which are highly active, selectivity and stable at high temperatures (>800 °C). However, a serious disadvantage of this kind

of catalysts is their very high cost and limited availability. Very few studies have been reported the RWGS with the Ni-based catalysts for conversion of CO_2 to CO. Usually, Ni-based catalysts favors CH_4 formation instead of CO.[2] Here we prepared very small Ni(0) nanoparticles (NPs) supported onto SiO_2 nanopowder by magnetron sputtering deposition method and investigated how the local structure and surface species (in situ XPS and XAFS) were affected during an unexpected catalytic performance for conversion of CO_2 to CO in RWGS. The magnetron sputtering deposition method was specially adapted for deposition of Ni NPs onto powder SiO_2 substrates, as previously reported.[3-5] The morphology and size of the sputtering deposited Ni NPs catalyst was examined by TEM. Figures 1 revealed spherical NPs with a mean diameter of ~2 nm. The catalytic properties of the Ni/SiO_2 NPs prepared by magnetron sputtering were, for the first time, investigated for conversion of CO_2 to CO and results showed that active, selectivity and stability of Ni/SiO_2 catalyst could be a promising system for CO_2 hydrogenation. In situ and ex situ XAS and XPS investigations of structure-activity relationships of the catalyst were performed to evaluate the catalyst properties and abilities for carbon dioxide dissociation.

1. R. Prasad and P. Singh, Catalysis Reviews-Science and Engineering **54**, 224-279 (2012).
3. D. Baudouin, U. Rodemerck, F. Krumeich, A. d. Mallmann, K. C. Szeto, H. Ménard, L. Veyre, J.-P. Candy, 2. P. B. Webb, C. Thieuleux and C. Copéret, J. Catal. **297**, 27-34 (2013).
4. R. V. Gonçalves, R. Wojcieszak, P. M. Uberman, D. Eberhardt, E. Teixeira-Neto, S. R. Teixeira and L. M. Rossi, Catal. Commun. **48**, 50-54 (2014).
5. L. Luza, A. Gual, D. Eberhardt, S. R. Teixeira, S. S. X. Chiaro and J. Dupont, ChemCatChem **5**, 2471-2478 (2013).
6. R. Bussamara, D. Eberhardt, A. F. Feil, P. Migowski, H. Wender, D. P. de Moraes, G. Machado, R. M. Papaleo, S. R. Teixeira and J. Dupont, Chem. Commun. **49**, 1273-1275 (2013).

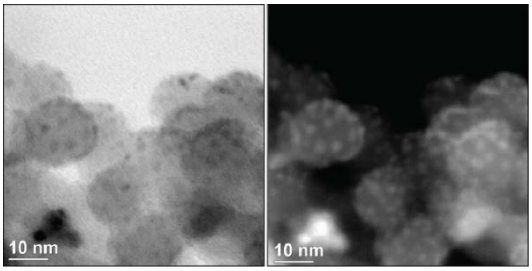

Fig. 1. TEM image of Ni NPs sputtering deposited on the SiO_2 support.

PC-09:
Preparation of dewetting surface showing low contact angle hysteresis toward control of water droplet behavior

D. Yashima, T. Ishizaki

Department of Materials Science and Engineering, Faculty of Engineering, Shibaura Institute of Technology, Japan
Email:ishizaki@shibaura-it.ac.jp

Development of surface treatment technology for control of water droplet behavior is essential for various applications such as μ-TAS, automobile, ship, and so on, because the technology holds the promise for considerably reducing energy consumption in their industries. Superhydrophobic surface with a water contact angle of more than 150° is known as a surface to repel extremely water. The superhydrophobicity is created by two factors, i.e., low surface energy and nanostructure. In general, the nanostructure is easily damaged by physical contact, resulting in the decrease in the water contact angle. Thus, it is required to create a novel surface that can control wetting behavior of water droplet after physical contact. Hydrophobic surface with a low contact angle hysteresis is considered to be an alternative surface to respond to the request, because the surface can control wetting behavior of water droplet. In addition, the surface does not have nanostructure, so it is hardly affected by the physical damage. Thus, it is very important to develop a technology for creating hydrophobic surface with a low contact angle hysteresis. In this

study, we aimed to prepare dewetting surface showing a low contact angle hysteresis by a simple and easy process.

A glass or Si wafer was used as substrate. The substrates were ultrasonically cleaned in acetone, ethanol, and, ultrapure water. UV/O_3 cleaning was performed on the cleaned substrate for 30 min at atmospheric pressure. Smart surface showing low contact angle hysteresis was prepared on the cleaned glass substrate from a 1,3,5,7-Tetramethylcyclotetrasiloxane by a vapor phase method at 333 to 443 K for 6 to 72 h. The cleaned substrate and the raw material were placed in a Teflon vessel. The vessel was maintained at 333 to 443 K in an electric oven for 6 to 72 h. Static and dynamic contact angles of the samples were estimated using a contact angle meter. The topographic images of the samples were acquired using AFM.

Fig 1 shows the advancing and receding contact angles of the samples fabricated at 353 and 443 K. The averaged advancing contact angles of the samples at 353 and 443 K for 24 h were approximately 100 and 160°, respectively, indicating that the sample at 443 K showed superhydrophobicity. The advancing and receding contact angles of the samples at 353 K increased with an increase in the treatment time. The contact angle hysteresis of the samples were approximately kept constant at 20°. In case of the samples at 443 K, the contact angle hysteresis decreased with an increase in the treatment time and became less than 10° when the treatment time was more than 12 h. The topographic images of the samples fabricated at 353 and 443 K showed that minute granular structures were observed on the sample surface at 353 K. Nodular structures could be observed on the sample at 443 K. The average root mean square roughness (R_{rms}) values of the samples at 353 and 443 K were estimated to be 3.58 and 165.20 nm, respectively. The increase in R_{rms} of the sample surface contributed to the improvement of the water contact angle.

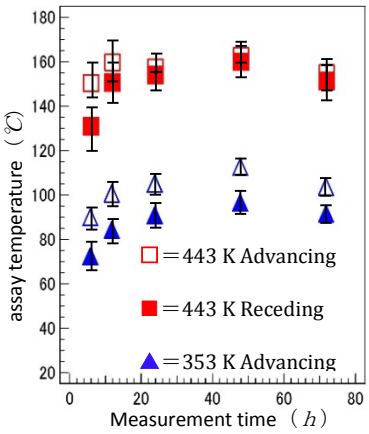

Fig. 1. Dynamic contact angle of samples at 353 and 443 K.

Acknowledgement

This work was partly supported by Grant-in-Aid for Young Scientists (A) (No. 25709061) from Japan Society for the Promotion of Science.

Poster Session – Group II

SMART SENSOR MATERIALS, SOFT MAGNETIC MATERIALS, OPTICAL PROPERTIES

PS-01:
High Frequency Giant Magnetoimpedance Effect of amorphous microwires

Valentina Zhukova[1,2], Mihail Ipatov[1,2], Ahmed Talaat[1,2], Juan M. Blanco[2] and Arcady Zhukov[1,2,3]

[1]*Dpto. de Fís. Mater., UPV/EHU San Sebastián 20018, Spain*
[2]*Dpto. de Física Aplicada, EUPDS, UPV/EHU, 20018, San Sebastian, Spain*
[3]*IKERBASQUE, Basque Foundation for Science, 48011 Bilbao, Spain*

Studies of amorphous glass coated ferromagnetic microwires (typically of 1-30 μm in diameter) have attracted growing attention in the last few years owing to their outstanding soft magnetic properties and Giant Magnetoimpedance, GMI, effect [1,2]. The aforementioned GMI effect usually observed in soft magnetic materials phenomenologically consists of the change of the AC impedance, *Z* when submitted to an external magnetic field, *H*. The GMI effect was well interpreted in terms of the classical skin effect in a magnetic conductor assuming the dependence of the penetration depth of the *ac* current flowing through the magnetically soft conductor on the *dc* applied magnetic field [2,3]. The extremely high sensitivity of the GMI effect to even low magnetic field attracted great interest in the field of applied magnetism basically for applications for low magnetic field detection.

Depending on the frequency *f* of the driving AC current *I*ac flowing through the sample and considering comparison of the skin depth with the radius or half thickness of the sample, few different GMI regimes might be considered. In low frequency range (usually1-10 kHz) when the skin depth is larger than the radius or half thickness of the sample (weak skin effect) the changes of impedance are due to a circular magnetization process exclusively. At higher frequencies (from 10-100 kHz to 1 GHz) the GMI originates basically from variations of the magnetic penetration depth due to strong changes of the effective magnetic permeability caused by a DC magnetic field. It is widely believed that the magnetization rotation contribute to changes of the circular permeability in a whole frequencies range and consequently to the skin effect. But for frequencies above 10 – 100 MHz the domain walls are strongly damped. Finally at GHz frequencies the GMI peaks are shifted to higher fields where sample is magnetically saturated. At this frequency range strong changes of the sample's impedance have been attributed to the ferromagnetic resonance (FMR)[4].

Recently major attention is focused on high frequencies (GHz range) GMI applications owing to the development of thin magnetically soft materials and recent tendency in miniaturization of magnetic field sensors [1,2]. Therefore, the purpose of this paper is to study the GMI effect in thin amorphous magnetically soft microwires suitable for miniaturized GMI based magnetic field sensors paying attention to the high frequency GMI effect.

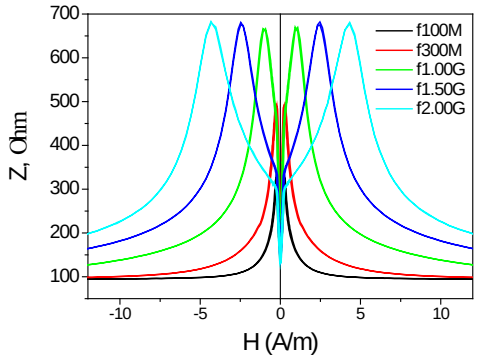

Fig.1. Z(H) dependences of $Co_{67.71}Fe_{4.28}Ni_{1.57}Si_{11.24}B_{12.4}Mo_{1.25}C_{1.55}$ microwires measured at different frequencies

We measured magnetic field, H, dependence of real part, Z_1 of the longitudinal wire impedance Z_{zz} ($Z_{zz} = Z_1+iZ_2$), up to 4 GHz in various Co-rich microwires. General features of these dependences is that the magnetic field of

maximum shifts to the higher field region increasing the *f*. High enough magnetic field sensitivity, i.e. GMI effect till GHz- range frequencies has been observed. On the other hand, from the point of view of applications GMI ratio, $\Delta Z/Z$, defined as:$\Delta Z/Z = [Z(H) - Z(H_{max})] / Z(H_{max})$ is relevant. In most studied Co-rich microwires the optimum frequency for achievement of the highest GMI ratio is about 100- 300 MHz.

In summary, we studied GMI effect of amorphous Co-Fe rich microwires and reveal that they present GMI effect at GHz frequencies. Features of high frequency GMI effect can be described using FMR-like approximation. Hysteresis loops and magnetic field dependences of GMI effect are affected by microwires magnetic anisotropy. Magnetic properties and GMI effect can be tailored controlling magnetoelastic anisotropy of Co-rich microwires.

1. M. Vazquez, H. Chiriac, A. Zhukov, L. Panina, and T. Uchiyama, *Phys. Status Solidi A*, 208, 493 (2011)
2. M.-H. Phan, H.-X. Peng, Prog.Mater. Science vol. 53, 323 (2008)
3. L.V. Panina and K. Mohri, Appl. Phys. Lett. 65, 1189 (1994)
4. D. Ménard, M. Britel, P. Ciureanu, and A. Yelon, *J. Appl. Phys.*, 84, 2805, (1998)

PS-02:
Radiation Hardness of Candidate Luminescent Sensor Materials

Stephen Williams, Colin McRae, Ross Fontenot, and William Hollerman

Physics Department, University of Louisiana at Lafayette, Lafayette, LA, USA
Email:hollerman@louisiana.edu

Research has shown that triboluminescent materials show promise for use as the active element in impact sensors. A so-called 'smart' structure with embedded material could be capable of determining whether a particle had struck, and record the relative intensity of its impact. In order to use such materials in space, we need to understand the radiation susceptibility of the material [1]. The term "half brightness fluence" was coined as a consistent figure of merit to evaluate the effectiveness of a material to emit fluorescence as a function of radiation exposure [2]. It is defined as the amount of light that reduces the fluorescence efficiency to one half of its original value [2]. The space environment contains a variety of ionizing radiations, including protons of all energies [3-5]. As a rule, it is necessary to test material response to the action of the same type of ionizing radiation existing in the space environment. This poster will summarize research that has been completed to measure the proton half brightness fluence for selected luminescent materials.

[1] W.A. Hollerman, "Investigation of Proton Induced Fluorescence From Yttrium and Gadolinium Compounds", Ph.D. Dissertation, Alabama A&M University, 1996, Unpublished.
[2] J.B. Birks and F.A. Black, "Deterioration of Anthracene Under α Particle Bombardment", Proc. of the Phys. Soc. (Lond.), vol. A64, pp. 874-875, 1951.
[3] N.A. Schwadron, L. Townsend, K. Kozarev, M.A. Dayeh, F. Cucinotta, M. Desai, M. Golightly, D. Hassler, R. Hatcher, M.-Y. Kim, A. Posner, M. PourArsalan, H.E. Spence, R.K. Squier, Sp. Weather 8 (2010) S00E02.
[4] F.A. Cucinotta, W. Schimmerling, J.W. Wilson, L.E. Peterson, G.D. Badhwar, P.B. Saganti, J.F. Dicello, Radiat. Res. 156 (2001) 682–688.
[5] N.A. Schwadron, M. Owens, N.U. Crooker, Astrophys. Sp. Sci. Trans. 4 (2008) 19–26.

PS-03:
Using Luminescent Materials to Detect Space Radiation

Jacque Meche, Lewis Baltz, Ross Fontenot, and William Hollerman

Physics Department, University of Louisiana at Lafayette, Lafayette, LA, USA
Email:hollerman@louisiana.edu

Space radiation poses a significant challenge to human and robotic exploration missions to the Moon, Mars, and beyond. As we consider long duration missions, the risk from radiation

exposure increases. Protons with energies of about 30 MeV can penetrate spacesuits and spacecraft walls [1–3]. High energy radiation (>100 MeV), can produce secondary penetrating particles such as neutrons and nuclear fragments inside the shielding material. Selecting the "wrong" kind of shielding material can actually increase the radiation hazard. The extensive use of radiation has led to the development of radiation dosimetry. There is no current technique that is capable of real-time radiation detection. Luckily in 2013, the authors discovered that adding uranium to europium tetrakis dibenzoylmethide triethylammonium (EuD_4TEA) temporarily increased the luminescence [4]. However, the radiation emitted from the depleted uranium slowly caused the luminescence to decrease over the course of a year. While this showed that uranium is a useless additive, it indicated that EuD_4TEA would be useful as an active element for a real time radiation sensor. As such, in 2014 the authors began to investigate the effects of radiation on the luminescence of EuD_4TEA. This poster will show the results of this ground breaking results.

[1] N.A. Schwadron, L. Townsend, K. Kozarev, M.A. Dayeh, F. Cucinotta, M. Desai, M. Golightly, D. Hassler, R. Hatcher, M.-Y. Kim, A. Posner, M. PourArsalan, H.E. Spence, R.K. Squier, Sp. Weather 8 (2010) S00E02.

[2] F.A. Cucinotta, W. Schimmerling, J.W. Wilson, L.E. Peterson, G.D. Badhwar, P.B. Saganti, J.F. Dicello, Radiat. Res. 156 (2001) 682–688.

[3] N.A. Schwadron, M. Owens, N.U. Crooker, Astrophys. Sp. Sci. Trans. 4 (2008) 19–26.

[4] R.S. Fontenot, W.A. Hollerman, K.N. Bhat, M.D. Aggarwal, J. Lumin. 134 (2013) 477–482.

PS-04:

High frequency magneto-resistance effects of Co-rich soft ferromagnetic ribbons and microwires

Dao Son Lam[1,2], J. Devkota[1], N. T. Huong[2], H. Srikanth[1], and M. H. Phan[1]

[1]*Department of Physics, University of South Florida, Tampa, FL 33620, USA*

Email: daosonlamln@gmail.com

[2]*Department of Physics, Hanoi National University, 334 Nguyen Trai, Hanoi, Vietnam*

Soft ferromagnetic materials are widely used for applications in high-frequency transformers, magnetic sensors, and biomedical engineering [1]. The discovery of the so-called giant magneto-impedance (GMI) effect in these materials make them very promising for high-performance magnetic sensor application [2]. The GMI effect refers to a large change in the AC impedance of a ferromagnetic conductor subject to an applied DC magnetic field. While most research was focused on exploiting the GMI effect in the low and moderate frequency range 100 kHz – 10 MHz, little work has dealt with the high frequency GMI behavior (100 MHz – 1 GHz) where the ferromagnetic resonance may occur and become responsible for the observed effect.

In this work we have investigated the magnetic field dependence of the AC resistance (the real component of the AC impedance) of Co-rich soft ferromagnetic ribbons and microwires in the frequency range 100 MHz – 1 GHz. Amorphous ribbons of the composition $Co_{65}Fe_4Ni_2Si_{15}B_{14}$ and amorphous microwires of the composition $Co_{68.2}Fe_{4.3}B_{15}Si_{12.5}$ were prepared by the rapid quenching and melt-extraction methods, respectively. Both types of sample were annealed at 100, 200, 300, 400, and 500 ^oC for 15 minutes, in order to release residual stresses and hence improve the magnetic softness without degrading the good mechanical property of the amorphous material. We have observed that for the ribbon samples, annealing improved the AC magneto-resistance (MR) effect in the annealed ribbons relative to its as-quenched amorphous counterpart. The MR ratio reached a

maximum (300% at f = 800 MHz) for the ribbon annealed at 100 ^{o}C, and it decreased as the annealing temperature was increased. For the annealed microwire samples, however, the MR ratios were found to be smaller than that of the as-quenched amorphous microwire in the investigated frequency range. The MR ratio decreased with increasing the annealing temperature. These results are attributed to considerable modifications in the magnetic domain structure and magnetic softness due to annealing. Our studies show the possibility of improving the MR effect and field sensitivity of Co-rich soft ferromagnetic materials for high-frequency sensor applications.

1. M.E. McHenry, M.A. Willard, D.E. Laughlin, *Progress in Mater Science* **44**, 291 (1999).
2. M. H. Phan and H. X. Peng, *Progress in Materials Science* **53**, 323 (2008).

Supports:

Research at USF was supported by the Florida Cluster for Advanced Smart Sensor Technologies (FCASST) and by USAMRMC through grant numbers W81XWH-07-1-0708 and W81XWH1020101/3349. Research at HUS was supported by the National Foundation for Science and Technology Development of Vietnam through Grant number 103.02-2012.69.

PS-05:
Excellent magnetocaloric properties of Gd-based amorphous microwires for active magnetic refrigeration in the liquid nitrogen temperature range

Hongxian Shen[1], Dawei Xing[1], Jingshun Liu[2], Manh-Huong Phan[3], Huan Wang[1], Dongming Chen[1], Yanfen Liu[1], Jianfei Sun[1],

[1] School of Materials Science and Engineering, Harbin Institute of Technology, Harbin 150001, People's Republic of China
Email:hitshenhongxian@163.com (Hongxian Shen); jfsun_hit@263.net (Jianfei Sun)

[2] School of Materials Science and Engineering, Inner Mongolia University of Technology, Hohhot 010051, People's Republic of China

[3] Department of Physics, University of South Florida, Tampa, Florida 33620, USA

Rapidly quenched microwires with the nominal composition of $Gd_{50}Al_{30}Co_{20}$ were fabricated by the melt-extraction method, and their structural and magnetic properties were systematically studied. The as-extracted wire shows a representative characteristic of amorphous phase, with its Curie temperature (T_C) of around 86 K. The H/M ratio as a function of temperature obeys the Curie-Weiss law above T_C and the slopes of Arrott plots exhibit positive values around T_C, both of which consistently indicate the nature of a second-order magnetic transition (SOMT) for the wires [1, 2]. Interestingly, these metallic glass microwires exhibit a large and reversible magnetocaloric effect (MCE) around T_C. The isothermal magnetic entropy change ($-\Delta S_m$) reaches a large value of 10.1 $J \cdot kg^{-1} \cdot K^{-1}$, with the refrigerant capacity (RC) and relatively cooling power (RCP) being 672 $J \cdot kg^{-1}$ and 861 $J \cdot kg^{-1}$ for a field change of 5 T, respectively. Their excellent magnetic and magnetocaloric properties make the Gd-based metallic glass microwires ideal for active magnetic refrigeration for liquid nitrogen liquefaction.

Figure 1 shows a three-dimensional (3D) plot of $-\Delta S_m(H, T)$for the melt-extracted $Gd_{50}Al_{30}Co_{20}$ microwires in the temperature range of 25-195 K for varying applied magnetic fields up to 5 T.

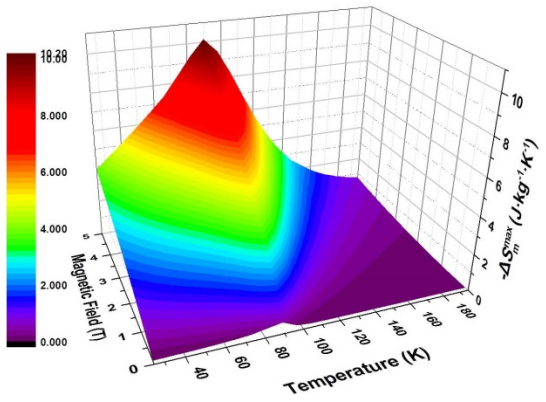

Fig1. Magnetic field and temperature dependence of the magnetic entropy change ($-\Delta S_m$) of the melt-extracted $Gd_{50}Al_{30}Co_{20}$ metallic glass microwires.

1. Z.Y. Xu, X. Hui, E.R. Wang, J. Chang, G.L. Chen, *Journal of Alloys and Compounds*, **504**, S146(2010).
2. H. Shen, H. Wang, J. Liu, D. Xing, F. Qin, F. Cao, D. Chen, Y. Liu, J. Sun, *Journal of Alloys and Compounds*, **603**, 167(2014).

PS-06:

A novel biosensor based on magneto-impedance technology and functionalized magnetic nanoparticles for sensitive detection of cancer cells and biomolecules

J. Devkota, P. Mukherjee, H. Srikanth, and M. H. Phan

Department of Physics, University of South Florida, Tampa, FL 33620, USA

Email: devkotaj@mail.usf.edu

Biosensors based on functionalized magnetic nanoparticles are very promising for early detection of cancer cells and biomolecules [1]. However, developing a simple and cost-effective magnetic biosensor for quick, reliable, and sensitive detection of cancer cells and molecules is a challenging task. Recently, a novel class of biosensors based on the magneto-impedance (MI) effect of soft ferromagnetic ribbons has been developed to fulfil the increasing requirements in biomedical diagnosis [1-4]. Improving their sensitivity for detection of low concentrations of cancer cells and biomolecules in biological systems is of current focus.

Here, we report our recent efforts on improving the detection sensitivity of MI based biosensors and their implementation for sensitive detection of cancer cells and biomolecules tagged to functionalized magnetic nanoparticles. As a first approach, we have demonstrated that the detection sensitivity of a MI sensor can be improved by at least four times when the magneto-reactance (MX) effect, the change in the imaginary component of the impedance, is exploited for biodetection [5]. The detection sensitivity of the biosensor was further improved by patterning nanoholes arrays on the sensing surface of the ribbon [3]. The MX based biosensor was used to detect and quantify the amount of Curcumin (an anticancer drug) tagged to Alginate/Fe_3O_4 superparamagnetic nanoparticles, showing a linear response at low concentrations with a maximum detection sensitivity of about ~ 30%, which is the highest value ever reported [2,4]. This biosensor was also implemented to probe Luis lung carcinoma (LLC) cancer cells that have taken up MnO nanoparticles. Since these functionalized magnetic nanoparticles are widely used as contrast agents for MRI of various cells, our studies show that a MX-based sensor can be used as a quick and simple pre-detection technique before MRI.

[1] J. B. Haun, T.-J. Yoon, H. Lee, and R. Weissleder, Wiley Interdisciplinary Reviews: Nanomedicine and Nanobiotechnology **2**, 291 (2010).

[2] J. Devkota, T. Mai, K. Stojak, P. Ha, H. Pham, X. Nguyen, P. Mukherjee, H. Srikanth, and M. Phan, Sensors and Actuators B: Chemical **190**, 715 (2014).

[3] J. Devkota, A. Ruiz, P. Mukherjee, H. Srikanth, and M.-H. Phan, Magnetics, IEEE Transactions on **49**, 4060 (2013).

[4] J. Devkota, J. Wingo, T. Mai, X. Nguyen, N. Huong, P. Mukherjee, H. Srikanth, and M. Phan, J Appl Phys **115**, 17B503 (2014).

[5] J. Devkota, C. Wang, A. Ruiz, S. Mohapatra, P. Mukherjee, H. Srikanth, and M. Phan, J Appl Phys **113**, 104701 (2013).

Supports:

This research was supported by the Florida Cluster for Advanced Smart Sensor Technologies (FCASST) and by USAMRMC through grant numbers W81XWH-07-1-0708 and W81XWH1020101/3349.

PS-07:
Tunable magnetocaloric response in high-speed melt-spun La-Ce-Fe-Si ribbons

X.L. Hou [1,2,*], Y.Xue [1,2], C.Y. Liu [1,2], Q.Q. Lu [1,2], M. H. Phan [3]

[1]Laboratory for Microstructures of Shanghai University, Shanghai University ,Shanghai, China Email: flybird1656@163.com

[2]School of Materials Science and Engineering, Shanghai University, Shanghai, China

[3]Department of Physics, University of South Florida, Tampa, USA

Magnetic refrigeration based on the magnetocaloric effect (MCE) is a promising alternative to the conventional gas compression refrigeration, owing to its higher cooling efficiency, environmental friendliness, and compactness. The majority of research in this field is to seek materials that exhibit large MCE over a wide temperature range, with manufacturing flexibility, and are cost-effective. Among existing magnetocaloric materials, the cubic $NaZn_{13}$-type $La(Fe,Si)_{13}$ alloys have attracted particular attention due to their giant MCE and cheap raw materials [1,2].

In this work, we have carried out a systematic investigation of structure and magnetocaloric effect of La-Ce-Fe-Si compounds prepared by melt spinning with a speed of 55 m/s and subsequent annealing at 1273 K for different time periods of 10-60 min. Among the samples investigated, the ribbon annealed for 20 min was found to exhibit the largest magnetic entropy change of about 33.8 J/kg·K at the Curie temperature (T_C=182 K) for a magnetic field change of 1.5 T. When the annealing time was greater than 20 min, the amount of the $NaZn_{13}$-type phase (hereinafter: 1:13 phase) remained stable as confirmed by XRD patterns and analysis. However, the Curie temperature (T_c) of the material increased and maximum magnetic entropy change ($|\Delta S_{M,Max}|$) decrease with increasing the annealing time. Scanning Electron Microscope (SEM) images and Energy Dispersive Spectrometer (EDS) revealed that LaCe easily gathered together at grain boundaries during rapid solidification. In the process of heat treatment, LaCe located at the grain boundaries was easy to be oxidized and became the $(LaCe)_2O_3$ phase in the ribbon surface. This $(LaCe)_2O_3$ phase is not conducive to improve the MCE of La-Ce-Fe-Si compounds. The SEM and the values of $|\Delta S_{M,Max}|$ together revealed that the big grain size will not benefit the magnetocaloric response. Interestingly, there was only a small difference of about 3 J/kg K between the values of $|\Delta S_{M,Max}|$ measured for magnetic field changes of 1.5 T and 5 T in the ribbon annealed at 1273 K for 20 min. Compared to La-Fe-Si compounds, when Ce content was 0.2 to replace La and annealing at 1273 K for 60 min, the values of $|\Delta S_{M,Max}|$ for La-Ce-Fe-Si ribbons increased from 13.79 J/kg·K (LaFeSi) to 32.8 J/kg·K for a magnetic field of 1.5 T and the Curie temperature T_C of the ribbons decreased slightly. It is very effective to tune MEC of LaFeSi by adding Ce, which is of practical importance for advanced magnetic refrigeration.

1. X. B. Liu, X. D. Liu, Z. Altounian, G. H. Tu, J. Alloys Compd., 397, 120(2005).
2. Hirosawa, S., Tomizawa, H.; Bekki, K. IEEE Trans. Magn, 42, 3608-3610(2006)

PS-08:
Design and fabrication of interdigital nanocapacitors coated with Hafnium for biological sensing

Gabriel Gonzalez[1,2], Samuel Kolosovas[2] and Fco. Javier Gonzalez[2]

[1]Catedras Conacyt, Universidad Autonoma de San Luis Potosi, San Luis Potosi, Mexico Email:gabriel.gonzalez@uaslp.mx

[2]Coordinacion para la Investigacion y Aplicacion de la Ciencia y Tecnologia, Universidad Autonoma de San Luis Potosi, San Luis Potosi, Mexico

The use of interdigital nanocapacitors for the development of biological sensors has been receiving a lot of interest in the last years. The principle of detection is based on the change of the impedance of the nanocapacitor. The impedance of the sensor is a function of the substrate thickness and the geometry of the electrodes. The performance of the interdigital nanocapacitors depends on the sensor design.

We fabricated Nickel interdigital capacitors on top of a Silicon substrate. The capacitance of the interdigital capacitor has been optimized by coating the electrodes with a 60 nm layer of Hafnium. Several authors have proposed analytical models to calculate the capacitance for the interdigital capacitors [1]. We compare the analytical solution and the electromagnetic simulations using COMSOL with experimental measurements. Our results show that the design of interdigital capacitors using a Finite Element Method software such as COMSOL is a powerfull modelling tool for the design and electrical characterization of this biological sensors.

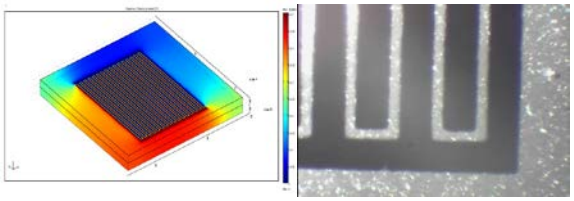

Fig. 1. Numerical Simulation with Comsol and Fabrication of the interdigital nanocapacitor.

3. Igreja, R., Dias, C.J., Sensors Actuators A 112, 291-301.

PS-09:

Modified Solvothermal Synthesis of Cobalt Ferrites ($CoFe_2O_4$) Nanoparticles and Their Optical Studies

Abdullah G. Al-Sehemi[a,b,c] and Abul Kalam[a]

[a] *Department of Chemistry, Faculty of Science, King Khalid University, Abha 61413, P.O. Box 9004, KSA.*
[b] *Unit of Science and technology, Faculty of Science, King Khalid University, Abha 61413, P.O. Box 9004, Saudi Arabia.*
[c] *Center of Excellence for Advanced Materials Research, King Khalid University, Abha 61413, P.O. Box 9004, Saudi Arabia.*
Email:agmasq@gmail.com

We synthesized nanocrystalline cobalt ferrites ($CoFe_2O_4$) through modified Solvothermal method by using sodium hydroxide as a precipitating agent and polysaccharides and used for degradation of methylene blue. The samples were labeled as MST-a (blank), MST-b (cellulose) and MST-c (starch), respectively, where the molar ratios of Co : Fe was 1:2. The synthesized nanocrystalline cobalt ferrites were characterized by X-ray diffraction (XRD), transmission electron microscopy (TEM), high resolution transmission electron microscopy (HRTEM) and Fourier transform infrared spectroscopy (FTIR) techniques. The optical band gap (Eg) of nanocrystalline cobalt ferrites were determines by ultraviolet visible spectroscopy (UV-vis) technique at room temperature. The effect of precipitating agent, starch and cellulose were investigated. Results exhibit that MST-b showed the best catalytic performance for the degradation of methylene blue. The degradation efficiency increased with initial pH decreasing in the pH range of 5–9. By means of the above mentioned investigations, it is found that the using of cellulose decrease the crystallite size but starch increases the crystallite size of cobalt ferrites therefore, band gap increases with cellulose. We hope that the procedure mentioned can be suitable for the high–grade synthesis of $CoFe_2O_4$ nanoparticles and may have potential applications in waste water treatment, electrode, sensors, catalysts etc.

The objective of this work is to compare the structure, size and optical properties of $CoFe_2O_4$ nanoparticles obtained by modified Solvothermal method.

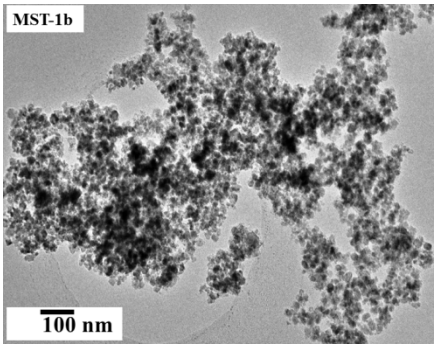

Fig. 1. The TEM image of MST-b.

PS-10:
Structural, optical and electrical studies on Eu-doped ZnO thin films for optoelectronic devices

Olfa Kamoun, A. Boukhachem and M. Amlouk

Unité de physique des dispositifs à semi-conducteurs, Faculté des Sciences de Tunis, Université de Tunis El-Manar 2092, Tunisia.

Europium-doped zincl oxide (ZnO:Eu) thin films have been prepared by the spray pyrolysis technique on glass substrates at 460°C using $Zn(CH3COO)_2.2H_2O$ and $EuCl_3 \cdot 6H_2O$ (ACROS pure more than 99.0%) as precursor. X-ray analysis shows that ZnO:Eu thin films crystallize in hexagonal structure with a preferred orientation of the crystallites along (002) direction. Optical measurements show that the band gap energies of the films vary with europium concentration. The effect of the europium incorporation of in ZnO matrix on the disorder is studied in terms of energy Urbach. PL measurements confirmed the effect of doping europium. The characteristic peak of ZnO shows a shift to larger energy than the PL spectrum shows the appearance of other peaks related to energy levels in the forbidden band.

This work aims at providing new optoelectronic devices based on Eu doped ZnO thin films especially in photocatalysis since recently studies reveled that the rare earth-doped ZnO products exhibited excellent photocatalytic degradation of organic molecules compared with the pure ZnO and commercial TiO_2 under visible light irradiation [1].

1. Jin.Chung Sin and Sze-Mun Lam, Ceramics International 40 (2014) 5431-5440

PS-11:
First principles simulation of phonon confinement effects in Ge [111] nanowires

A. Trejo[1], A. Miranda[2], L. A. Pérez-Lopez[2], M. Cruz-Irisson[1,2]

[1]*ESIME Culhuacan, Instituto Politécnico Nacional, Av. Santa Ana 1000, Mexico D. F., México*
Email:atrejob0800@alumno.ipn.mx

[2]*Instituto de Física, Universidad Nacional Autónoma de México, Apartado Postal 20-364, México D. F., México*

Recently, Germanium has gained a renewed interest in the electronics field due to its improved characteristics compared with silicon, such as a higher charge carrier mobility of 1900 and 3900 cm2/(Vs) respectively for holes and electrons in crystalline Ge (c-Ge), compared with 450 and 1400 cm2/(Vs) in crystalline Si (c-Si). Germanium nanostructures such as nanowires (GeNWs) have attracted attention in the photovoltaic field as substrate material in solar cells, as well as in other applications like as an anode in Li-ion batteries, as a fabric material and as field effect transistors. There has been plenty of theoretical and experimental investigations about GeNWs, however the analysis of the vibrational properties of this material are scarce [1].The analysis of the vibrational properties of the GeNWs could give a hindsight of their thermal properties as well as other properties such as surface roughness and infrared and Raman spectrum. In this work a study of the vibrational properties of [111] oriented GeNWs is developed through the first principles density

functional perturbation theory using the generalized gradient approximation and norm conserving pseudopotentials. The nanowires were modelled by removing atoms outside a circumference on the [111] direction according to the supercell scheme [1, 2], where three diameters were chosen to observe the effect of phonon confinement on the vibrational properties of the GeNWs. All surface dangling bonds were saturated with H atoms. Results show that there is a shift of the highest frequency optical modes of Ge towards lower frequencies compared to bulk Ge due to phonon confinement, however such shift is masked by the inclusion of H bending modes near the highest bulk Ge optical mode frequencies. The surface H atoms also create two extra region of bands pertaining their bending and stretching motion which, according to the partial phonon DOS analysis have minimal contribution of the Ge atoms. These results could be useful for the characterization of this nanowires especially for spectroscopy techniques such as Raman and IR.

Acknowledgments: Thiss work was supported by Instituto Politécnico Nacional project grants: SIP-IPN 2014-1640 and 2014-1641

2. A. Trejo, L. Lopez-Palacios and M. Cruz-Irisson, *Physica B,* (In press, 2014) DOI:10.1016/j.physb.2014.05.005.
3. A. Trejo and M. Cruz-Irisson, *Molecules,* **18**(4), 4776-4785 (2013).

PS-12:
Magnetic deposition of aligned silver nanowire transparent electrodes

Oleksandr Trotsenko[1], Alexander Tokarev, Sergiy Minko

[1]Nanostructured Materials Laboratory, University of Georgia, Athens, GA, 30602, USA
Email:otrotsen@uga.edu

Transparent conductors that combine properties of low resistance and high transparency find many applications in modern technology. Depending on the application, sheet resistance can range from 10 Ω/sq to 10^6 Ω/sq, and usually the transparency needs to be higher than 90%. Transparent conductors made of silver nanowire networks possess unique and superior mechanical, optoelectronic and chemical stability properties comparing to widely used indium tin oxide coatings. Optimizing conductivity to transparency ratio is a central challenge in the fabrication silver nanowire transparent electrodes. Traditional scalable and cost-efficient deposition methods are based on a random deposition of the building blocks where the coating formation is complicated by aggregation, precipitation and capillary forces that induce misalignment of the nanoscale particulates, which in turn compromises coating performance. In contrast to random deposition methods, field assisted or field directed assembly methods provide ample opportunities for the alignment of the building blocks immediately prior to and at the moment of deposition. During these time and length scales, the forces exerted from the field can align nanowires and compete with colloidal forces in the system. Recently, methods of magnetophoretic self-assembly have been receiving attentions. Magnetic deposition has been used at the laboratory scale to create superhydrophobic structures, aligned carbon nanotubes composites and magnetically controllable photonic crystals. We developed a novel method for deposition of silver nanowires on a transparent substrate using magnetite nanoparticles as deposition carrier. Proposed method of the magnetic field assisted deposition of silver nanowires provides substantial improvement of quality of transparent conductors due to the alignment of the nanowires in magnetic field and formation of highly-aligned multilayer networks of silver nanowires (Fig1). The method is simple, scalable and insensitive to solvents and allows fabrication of transparent electrodes with a lower amount of materials.

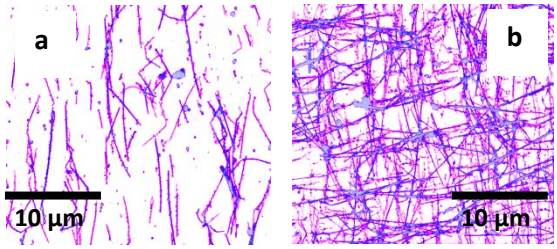

Fig. 1. AFM topography images of magnetically deposited silver nanowires aligned in one and two directions

Poster Session – Group III
ENERGY-RELATED MATERIALS AND APPLICATIONS, BIOMEDICAL MATERIALS AND APPLICATIONS

PE-01:
Development of Graphene Based Materials for Energy Conversion

Nanda Gopal Sahoo[1,2], James T. McLeskey, Jr[2]

[1]*Department of Chemistry, Kumaun University, Nainital, Uttarakhand, India*
Email:ngsahoo@yahoo.co.in,

[2]*Department of Mechanical and Nuclear Engineering, Virginia Commonwealth University, Richmond, USA*

Meeting the world's energy needs is one of the Grand Engineering Challenges for the twenty-first century. Today's energy crisis is one of the most serious issues facing humankind because of rapidly growing energy usage and the depletion of conventional sources. Recent scientific work on energy conversion devices such as solar cells and fuel cells has achieved some promising milestones. Graphene—a single or few layers of two-dimensional (2D) sp^2 -bonded carbon sheets—has attracted a great deal of interest because of its unique structure and exceptional physical properties, such as high electrical and thermal conductivities, mechanical flexibility, charge transport mobility, high specific surface area, good chemical stability, and optical transparency. We have synthesized graphene oxide (GO) using modified Hummer's and electrochemical methods from natural graphite powder. The properties of the GO samples have been characterized by using optical microscopy, field emission scanning electron microscopy (FESEM), transmission electron microscopy (TEM), X-ray photoelectron spectroscopy (XPS), Raman spectroscopy, etc. It has been found that the GO synthesized by the modified Hummer's method existed as micron-sized platelets, and the GO sheets had a thickness of about 1-2 nm with very sharp edges and flat surfaces. In contrast, GO synthesized from electrochemical methods was thicker (~3-9 nm). We have synthesized nitrogen-doped graphene (NG) by thermal annealing of GO with melamine, urea and NH_3 as nitrogen sources. The nitrogen-doping not only increases the electrical conductivity of graphene, but also improves the graphene–metal binding and chemically active sites for catalytic reactions. We have also prepared 2D graphene and 1D carbon nanotube hybrid nanomaterials. These materials can be applied in the field of energy conversion devices such as solar cells and fuel cells.

Acknowledgement: Authors acknowledge the financial supports from BASE Fellowship, Indo-US Science & Technology Forum, India.

PE-02:
Anisotropic thermoelectric generator made from semimetal microwire

L. A. Konopko[1,2], A. A. Nikolaeva[1,2], T. E. Huber[3], A. K. Tsurkan[1]

[1]*D.Ghitu Institute of Electronic Engineering and Nanotechnologies, ASM, Chisinau MD-2028, Moldova*
Email:l.konopko@nano.asm.md

[2]*International Laboratory of High Magnetic Fields and Low Temperatures, Wroclaw 53-421, Poland*

[3]*Howard University, 500 College St. N.W., Washington, DC 20059, USA*

In the thermoelectric-anisotropic media there is transverse to the temperature gradient electric field. At room temperature we have investigated the transverse thermopower in thin single-crystal Bi and Bi-Sn microwires for the purpose of using them in anisotropic thermoelectric generator. The single-crystal microwires in the diameter range 2 - 15 μm were prepared by the high frequency liquid phase casting in a glass capillary using an improved Ulitovsky technique; they were cylindrical single-crystals with (10$\underline{1}$1) orientation along the wire axis. In this orientation, the wire axis makes an angle of 19.5° with the bisector axis C_1 in the bisector-trigonal plane. It was found that in temperature range of 200 – 300 K doping of

bismuth wires with tin increases the thermopower anisotropy in comparison with Bi by a factor of 2 – 3. The experimental model of the anisotropic thermoelectric generator (ATG) was created from long Bi-0.05 at% Sn microwire in a glass coating (long microwire was coiled into a flat spiral so that at any point of the spiral axis C_3 and microwire axis lying in a plane perpendicular to the flat spiral). The voltage E that arises on the ATG outputs is equal to

$$E = S_{12}\Delta T\frac{a}{b} = (S_{\parallel} - S_{\perp})\sin\theta\cos\theta\ \Delta T\frac{a}{b} = (S_{\parallel} - S_{\perp})\sin 2\theta\ \Delta T\frac{a}{2b}$$

were ($S_{||}$ - $S_{\perp}$) - anisotropy of thermopower, θ - inclination angle of the crystallographic axes C_3, ΔT - transverse temperature gradient, a – length of the sample, b - thickness of the specimen. For the single crystal microwire with a core diameter d = 2 μm, outer diameter D= 20 μm and a length of 8 m ATG can generate voltage E=1 V at a transverse temperature gradient (perpendicular to the flat spiral) of 5 K. [1]

Figure 1 shows schematic of the anisotropic thermoelectric generator made of long Bi-Sn microwire in a glass coating (long microwire coiled into a flat spiral so that the plane containing the axis C_3 was directed along the gradient T). The developed ATG module can be used in many other heat harvesting applications such as rapid nonselective IR detector and gradient heat flux sensor (GHFS) with a characteristic time above 10^{-3} s. GHFS is used for the direct measurement of heat fluxes to a flat plate in pulsed hypersonic gas flow.

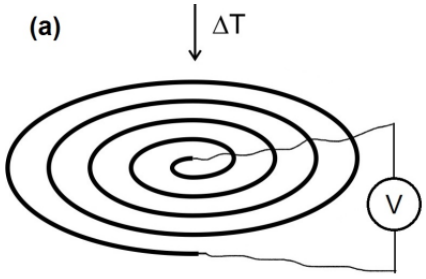

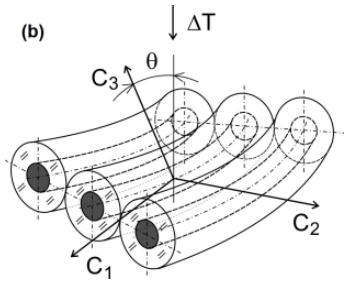

Fig. 1. (a) Schematic of the anisotropic thermoelectric generator made of long Bi-Sn microwire in a glass coating; (b) Schematic drawing of a small piece of flat spiral.

This work was supported by ASM grant 13.820.05.12/BF, and US National Science Foundation PREM.

4. L. Konopko, T. Huber, A. Nikolaeva, *AIP Conf. Proc.* **1449**, 287 (2012)

PE-03:
Electrochemical behaviour of a new transparent conductive oxide(TCO) layer-less cell structure

Ho-Gyeong Yun[1, *], Myeong Kim[1, 2], In-Hwan Lee[2] and In-Kyu You[1]

[1]*Electronics and Telecommunications Research Institute (ETRI), Daejeon, 305-700, Republic of KOREA*
Email: yunhg@etri.re.kr, web site: http://www.etri.re.kr

[2] *Chonbuk National University, Jeonju 561-756, Republic of Korea*

Dye-sensitized solar cells (DSSCs) have been widely studied since their introduction by O′Regan and Grätzel.[1] Efforts have been mainly paid for the increasing conversion efficiency, resulting in a conversion efficiency of 12.3%.[2] However, the cost of the fluorine doped tin oxide(FTO)-glass, is evaluated to be about a half of the module fabrication cost.[3] As a matter of course, if the cost can be decreased, the application of the DSSC will be increased. Several type TCO-less DSSCs such as DSSCs with a metal substrate and a monolithic structure,

have been suggested in order to decrease the fabrication cost. However, almost all of them have weaknesses including complex fabrication process, low conversion efficiencies,[3] using high cost metal mesh instead of TCO-glass,[4] and so on.

In this study, in addition to the previous TCO-less DSSC,[5] we present the newest TCO-less DSSC. The cell is comprised with a metal foil and a honey-cob like holes patterned stainless steel foil. By virtue of these two metal foils, the newest DSSC doesn't require any TCO-glass. Furthermore, the electrochemical analysis, including electrochemical impedance spectra, open circuit voltage decay measurement and intensity modulated photocurrent spectroscopy, exhibit the reasonable behaviour of the proposed cell, resulting in the conversion efficiency of 6.04%.

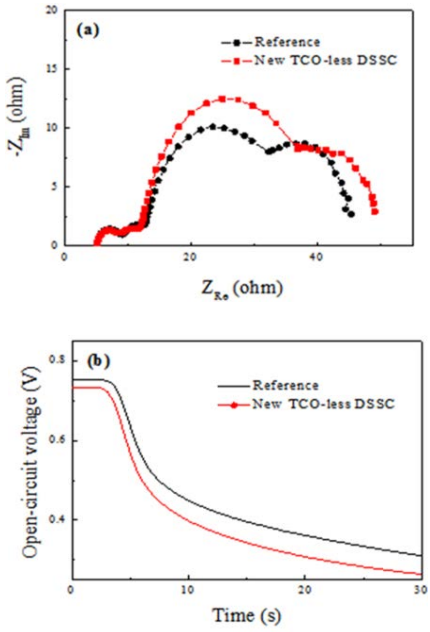

Fig. 1(a) EIS spectra (b) Voc decay measurement for the reference and the proposed New TCO-less DSSC

1. B. O'Regan and M. Grätzel, *Nature*, 1991, **353**, 737.
2. Yella et al., Science 334 (2011) 629.
3. J. M. Kroon et al., Prog. Photovoltaics, 2007, 15,
4. Y. Yoshida et al., Appl. Phys. Lett., 2009, 94, 093301.
5. H. –G. Yun et al., Phys. Chem. Chem. Phys., 2012, 14, 6448

PE-04:
Fabrication and evaluation of Al paste with Bi_2O_3- B_2O_3-ZnO glass frit for screen-printed energy devices

Bit-Na Kim, Ho-Gyeong Yun, Yong-Suk Yang, In-Kyu You *

Information & Communications Core Technology Research Lab., Electronics and Telecommunications Research Institute (ETRI), Daejeon, Republic of Korea
**Email : ikyou@etri.re.kr, web site: www.etri.re.kr*

Recently, the printing technique has been developed in the various energy field such as supercapacitor and solar cell by virtue of its suitability for large-area/mass production and low cost fabrication. [1] Conventional Al paste contains Pb-based glasses. However, the solar cell industry has been moving towards environment-friendly materials, especially Pb-free Al pastes.

In this study, we studied Al back conductor paste with the glass composition of Bi_2O_3-B_2O_3-ZnO system in a screen-printed solar cell. The glass compositions were optimized by changing the ratio of ZnO and B_2O_3 in the glass-forming range. The conductor paste was fabricated on a Si substrate with a screen printing and a heat treatment. The effects of glass frit on the electrical resistance of the Al electrode and on the cell performance were investigated.

Figure 1 shows the plot of efficiency and sheet resistance versus ZnO to B_2O_3 ratio. As the ratio of ZnO to B_2O_3 in the Al back conductor paste increased, the glass transition temperature and sheet resistance decreased but the efficiency increased. The surface morphology of Al conductor and BSF (Back Surface Field) were characterized using scanning electron microscope (SEM), its total conversion efficiency by solar simulator and sheet resistance by 4-point-probe. [2]

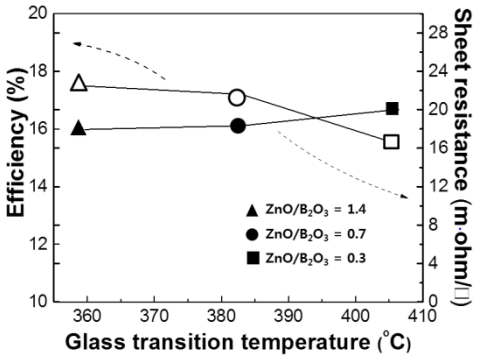

Fig1. Effect of glass frit transition temperature on the solar cell efficiency and electrical sheet resistance.

1. Ac Arias, JD MacKenzie, I McCulloch, J Rivnay and A Salleo, *Chem. Rev.* **110**, 3-24 (2010).
2. Kim S, Sridharan S, Khadikar C, Shaikh A, Proceedings of the IEEE 31St Photovoltaic Specialists Conference and Exhibition. 1100-1102 (2005)

PE-05:
Initial Studies on Nanocrystalline Silver Sulfide Films

Pooja P. Magar[1], Habib M.Pathan[2]

Advanced Physics Laboratory, Department of Physics,
University of Pune, Pune - 411 007, Maharashtra, India
Email:pooja.p.magar@gmail.com

Dye, quantum dot or semiconductor sensitized solar cells are promising alternatives to the traditional, silicon solar cells. In the present investigation, silver sulfide was prepared using successive ionic layer adsorption and reaction (SILAR), Figure 1 (a) to (d) [1].

Silver sulfide was characterized for their structural, surface morphological and optical properties by means of X-ray diffraction, scanning electron microscopy and optical absorption measurement techniques. X-ray diffraction shows the formation of silver sulfide however energy dispersive spectroscopy (EDS) analysis shows films are sulphur rich. XRD study reveals that formed material is amorphous for low deposition time. The optical absorption studies showed that the band gap of silver sulfide films increased from 1.8 to 2.2eV with the increase in time (number of cycles) and decreases thereafter. This silver sulfide will be used for the sensitization of metal oxides to form the semiconductor sensitized solar cells.

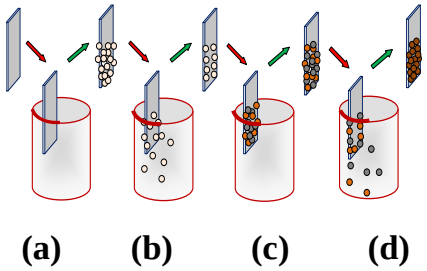

Fig. 1: The scheme of SILAR method for the deposition of Ag_2S films

1. H. M. Pathan and C. D. Lokhande, *Bull. Mater. Sci.*, 27 (2004) 85–111.

PE-06:
Development of Bioprocess Technology for Jet Fuel Production from Photosynthetic Cells

Ganapathy Sivakumar

Arkansas Biosciences Institute and College of Agriculture and Technology, Arkansas State University, Jonesboro, AR 72401, USA
Email: sivakumar@libero.it

Petroleum-based fuels will be in higher demand or depleted for future generations; alternative or substitute liquid fuels need to be developed for transportation. *Stichococcus bacillaris* strain siva2011 (figure 1) is a green microalga which has an efficient photosynthetic mechanism and is rich in jet fuel range carbon substrates such as fatty acids/triacylglycerols [1-2]. *S. bacillaris* strain siva2011-based jet fuel can provide carbon neutrality which could positively impact air transportation. The conversion of *S. bacillaris* strain siva2011-based jet fuel is mainly from triacylglycerols to an alkane which is a chemical process that can produce high-value aviation fuel. However, the scale-up of *S.*

bacillaris strain siva2011-based fuel is not yet established due to the lack of: 1) cost-effective efficient bioprocess technology for biomass or jet fuel substrate production; and 2) cost-effective conversion of jet fuel. I will present the bioprocess engineering data of *S. bacillaris* strain siva2011 cells for jet fuel substrate production. In the long-term this bioprocess technology could reduce the atmospheric CO_2 and improve bioeconomic development in the clean energy sector.

Fig. 1. Biomass production of *Stichococcus bacillaris* strain siva2011 in 5L bioreactors (working volume 4L each)

1. G. Sivakumar, K. Jeong, J. O. Lay, *Biotechnology for Biofuels*, **7**: 62 (2014).
2. G. Sivakumar, K. Jeong, J. O. Lay, *Microbial Cell Factories*, **13**: 79 (2014).

PE-07
Iron oxide nanoparticles with controlled morphology for advanced hyperthermia

Z. Nemati, H. Khurshid, J. Alonso, M.H. Phan, and H. Srikanth

Department of Physics, University of South Florida, Tampa, FL 33620

Magnetic nanoparticles (MNPs) are interesting for a wide range of applications. In biomedicine, they have been exploited for use in drug delivery, magnetic resonance imaging, and magnetic hyperthermia. While magnetic hyperthermia, using MNPs to convert electromagnetic energy into heat to destroy the cancer cells, represents a novel cancer treatment technique, a poor heating conversion efficiency of the existing MNPs restricts its practical use. Different strategies have been proposed to overcome this limitation, mainly by tuning the size, saturation magnetization and effective anisotropy of the MNPs.

Here we report a magnetic hyperthermia study on Fe_3O_4 MNPs, where the effective anisotropy was tuned by varying particle morphology from the spherical to octopod shape. The Fe_3O_4 MNPs were synthesized using a thermal decomposition method. Transmission electron microscopy (TEM) and high-resolution TEM images show high crystalline monodisperse nanoparticles. X-ray diffraction patterns confirm the presence of Fe_3O_4 phase. Hyperthermia experiments indicate that the nano-octopods possess a higher SAR as compared to their spherical counterpart. Our findings provide an effective approach to improve the SAR of MNPs by manipulating the shape anisotropy of the nanoparticles.

Support: Research was supported by USAMRMC through grant numbers W81XWH-07-1-0708 and W81XWH1020101/3349.

PE-08
Mechanical Properties of Nanocomposite Polymers for Tissue Regeneration

Bailey Barnes[1], Shawn Bourdo[2], Alex Biris[3]

[1]*Department of Systems Engineering, University of Arkansas at Little Rock, Little Rock, Arkansas, USA*
Email: bkbarnes@ualr.edu
[2]*Department of Applied Science, University of Arkansas at Little Rock, Little Rock, Arkansas, USA*
[3]*Department of Systems Engineering, University of Arkansas at Little Rock, Little Rock, Arkansas, USA*

Current tissue regenerative scaffolds are constructed of metals, ceramics, bio-compatible polymers and composites [1] that have been shown to be fine catalyst for cell proliferation. However the properties, in specific mechanical properties, of these materials as compared to their host tissue have not been studied up to our

knowledge. In order to improve host stability as well as the tissue around the damaged region, it would be advantageous to create scaffolds with properties closely resembling the healthy tissue. Hydromed, a hydrophobic urethane, with hydroxyapatite nanoparticles has the possibility to perform similarly to mammalian bone. 15% wt/vol Hydromed films were synthesized with various hydroxyapatite nanoparticles concentrations ranging from 0-20% wt/wt. Using tensile testing, DSC, TGA, and XRD; the composite films' properties were compared. Figure 1 shows the stress-strain data for six nanoparticle concentrations. While the stress parameters remain relatively constant, the strain decreases as concentrations increase. Further exploration of these films will lead to a better understanding of the ways in which nanoparticles play a role in material properties. In the future, these composites should be able to closely resemble the properties of mammalian bone as well as promote successful cell proliferation and tissue growth.

1. Cheung, H., K. Lau, T. Lu, and D. Hui. "A Critical Review On Polymer-based Bio-engineered Materials For Scaffold Development." *Composites Part B: Engineering* (2006): 291-300.

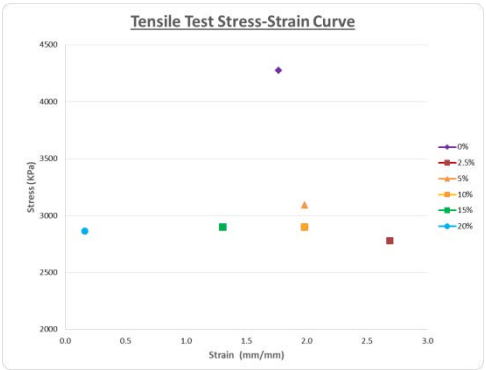

Fig 1. Tensile test curve for varying nanoparticle concentrations

PE-09

Ceramic-metal bionanocomposites for improved performance of medical implants

J. F. Bartolomé

Instituto de Ciencia de Materiales de Madrid (ICMM), Consejo Superior de Investigaciones Científicas (CSIC), Madrid, Spain
Email:jbartolo@icmm.csic.es, web site: http://www.icmm.csic.es

The most obvious advantage of cermets is that they can favorably combine the often dissimilar properties of ceramic and metal components in one material. Because of the many possible combinations of components this field is very creative, since it provides the opportunity to invent an almost unlimited set of new materials with a large spectrum of properties and with multifunctionallity. For instance, these new materials can be used in biomedical field for a new generation of reliable and longer lasting implants with biointegration (osteoinduction, osteoconduction and osseointegration), antibacterial activity, high mechanical properties (fatigue resistance, hardness, wear resistance), mechanical compatibility, etc. Multifunctionality within a material can be integrated on several dimensional scales with increasing interconnectivity between phases and engineering difficulty as the scale decreases. This possibility clearly reveals the power of nanocomposite materials to generate complex multifunctional structures that are hierarchically organized at the nano-, micro-, and meso-levels to meet the overall system goals. Our group has recently succeeded in the development by conventional powder processing of a new macro-micro-nano biocermet with high mechanical behavior, similar to the one of natural bone [1-5]. In this new generation of zirconia-alumina-/Nb-Ta nanocomposite, biomultifunctional synergism (biointegration, biomechanical, biocompatibility) with mechanisms operating at different scales is achieved.

6. A. Smirnov, A., J. F. Bartolomé, *Ceramics International* **40**, 1829 (2014).
7. A. Smirnov, C. F. Gutiérrez-González, J. F. Bartolomé, *Journal of the American Ceramic Society* **96**,1709 (2013).

8. A. Smirnov, A., J. F. Bartolomé, *Journal of the European Ceramic Society* **32**, 3899 (2012).
9. T. Rodriguez-Suarez, J. F. Bartolomé, J. S. Moya, *Journal of the European Ceramic Society* **32**, 3887 (2012).
10. J. F. Bartolomé, C. F. Gutiérrez-González, R. Torrecillas, *Composites Science and Technology* **68**, 1392 (2008).

PE-10
Stability and instability of lipid multilayer drug screening microarrays

Nicholas Vafai[1], Steven Lenhert[1,2]

[1]*Biological Science Department, Florida State University, Tallahassee, FL, USA*
Email: nvafai@bio.fsu.edu

[2]*Integrative Nanoscience Institute, Florida State University, Tallahassee, FL, USA*

Surface supported lipid multilayer arrays are a promising new type of nanostructured interface with potential applications in drug screening(1) and biosensing,(2) both of which require integrating many different materials for high throughput processes.(3) These applications depend on a balance between stability and instability of the supramolecuar structures in aqueous solution. For instance, lipid gratings for a sensor depend on the structures to remain static and not degrade upon immersion, yet must be instable enough to change shape upon analyte binding.(4) Similarly, in applications in cell-based drug delivery, the structures must be stable enough to be immersed in water, yet instable enough to be taken up by adherent cells.(5) We have observed four mechanisms by which lipid multilayer patterns can be disrupted seen in Figure 1, including: 1. patterns of multilayers dissolving at the water contact line; 2. shearing forces that separate patterns during immersion; 3. lipid spreading and wetting underwater; and 4. leakage of drugs as a function of hydrophobicity. Here, we present methods used to quantify stability and instability at the various stages, which is necessary information for diagnostic biosensing and high throughput screening applications.

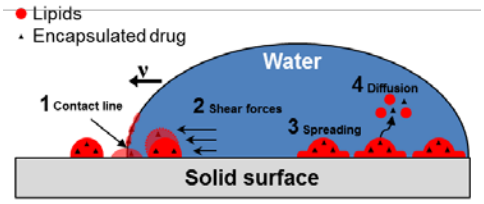

Fig. 1. Schematic of the use of lipid multilayer microarrays highlighting steps where stability is required.

1. Kusi-Appiah AE, Vafai N, Cranfill PJ, Davidson MW, & Lenhert S (2012) Lipid multilayer microarrays for in vitro liposomal drug delivery and screening. *Biomaterials* 33(16):4187-4194.
2. Anrather D, Smetazko M, Saba M, Alguel Y, & Schalkhammer T (2004) Supported membrane nanodevices. *Journal of Nanoscience and Nanotechnology* 4(1-2):1-2.
3. Lowry TW, *et al.* (2014) Materials Integration by Nanointaglio. *Advanced Materials Interfaces* 1(4):1300127.
4. Lenhert S, *et al.* (2010) Lipid multilayer gratings. *Nature Nanotechnology* 5(4):275-279.
5. Yamazaki V, *et al.* (2005) Cell membrane array fabrication and assay technology. *Bmc Biotechnology* 5.

PE-11
Impedance Analysis of Solvent Substitution Effect on Resistive Switching Property of HfO_2-CB-RAM

Masato Yoshihara[1], Satoru Kishida[1, 2], and Kentaro Kinoshita[1, 2]

[1]*Department of Information and Electronics, Graduate School of Engineering, Tottori University, 4-101 Koyama-Minami, Tottori 680-8552, Japan*; *Email: kinoshita@ele.tottori-u.ac.jp*
[2]*Tottori University Electronic Display Research Center, 4-101 Koyama-Minami, Tottori 680-8552, Japan*

11. The establishment of a method to control resistive switching (RS) property is required for conducting-bridge memory (CB-RAM) to be put into practical use. We have reported that switching voltages and current were reduced by supplying water to the HfO_2 memory of CB-RAM with Cu/polycrystalline HfO_2 (poly-

HfO_2)/Pt structures [1]. This result suggests that formation and rupture of the conductive bridge of CB-RAM are caused by electrochemical diffusion mediated by water. In this paper, we investigated the solvent type dependence of RS property of Cu/poly-HfO_2/Pt CB-RAM by impedance method.

12. A poly-HfO_2 layer with the thickness of 25 nm was deposited on a Pt (100 nm)/Ti (20 nm)/SiO_2 (100 nm)/Si (650 μm) substrate in the mixed gas of Ar and O_2 (Ar : O_2 = 3.8 : 1.5 Pa) by using an RF reactive sputtering method. The total gas pressure, RF power and substrate temperature were maintained at 5.3 Pa, 100 W and 300 °C, respectively. By contacting the surface of the HfO_2 film with a Cu-probe which tip radius is 15 μm, a Cu-probe/poly-HfO_2/Pt (Cu/HfO_2/Pt) structure is composed at the contact area. A voltage was applied to the Cu-probe with the Pt-electrode grounded. The effect of providing solvents to the HfO_2 layer on *I-V* characteristics and AC impedance, $Z(\omega)$, for the frequency, ω, range of 10 Hz - 100 kHz were measured by dropping a small amount of ultrapure water, methanol, and xylene on the HfO_2 surface and contacting the HfO_2 surface with the Cu-probe through the droplet.

13. Fig. 1 shows *I-V* characteristics for water- (squares), methanol- (triangles), and xylene- (circles) supplied Cu/HfO_2/Pt structures. The magnitude relation of both V_{form} and initial resistance for respective solvents is in the order of water < methanol < no solvent < xylene, where polarity π* of water, methanol, and xylene are 1.14, 0.58, and 0.48, respectively. Therefore, V_{form} becomes smaller with decreasing solvent polarity and is suggested to be controllable by selecting a solvent with appropriate polarity. Fig. 2 shows $Z(\omega)$s for water- (square), methanol- (triangle), xylene- (circle) supplied samples. Straight line whose tilt angle with respect to the real axis is 45° was observed in low ω region. This line is known as Warburg impedance, and the transition from the straight line to the semicircular region by increasing ω means that the rate of reaction changes from diffusion-controlled to charge-transfer-controlled. Charge transfer resistance, R_{ct}, double layer capacitance, C_{dl}, and σ were estimated by fitting the $Z(\omega)$ to the equivalent circuit model shown in the inset of Fig. 2. Here, σ is constant given by $\sigma = RT/2^{1/2}n^2F^2AD^{1/2}c^*$, where R is the ideal gas constant, T is the absolute temperature, n is the number of electrons transfer, F is Faraday's constant ,and A is electrode area. σ becomes smaller with increasing c^* and/or D. R_{ct}, C_{dl} and σ were estimated to be 280 kΩ, 3.98 pF, 1.49×10^6 $\Omega sec^{-1/2}cm^2$ for the water-supplied sample, whereas 0.70 kΩ, 1.74 pF, $2.38\times10^6\Omega sec^{-1/2}cm^2$ for the methanol-supplied sample. On the other hand, $|Z(\omega)|$ of the xylene-supplied sample was too high to be measured. Our results showed that the elution and the diffusion of Cu ions are enhanced by increasing a solvent polarity, supporting the RS model basing on the electrochemical diffusion of Cu ions.

[1] S. Hasegawa et al., ECS Transactions **50**, 61 (2013).

[2] J. Macdonald, Impedance Spectroscopy, Wiley, New York, 23(1987).

PE-12

Particle size and morphology dependent magnetic properties of *o*-$EuMnO_3$ and *h*-$YbMnO_3$ nanoparticles

Raja Das[1,2,3] and Pankaj Poddar[1,2]

[1]Physical and Materials Chemistry Division, CSIR-National Chemical Laboratory, Dr Homi Bhabha Road, Pune 411 008, India
[2]Academy of Scientific and Innovative Research (AcSIR), Anusandhan Bhawan, 2 Rafi Marg, New Delhi 110001, India
[3]Department of Physics, University of South Florida, Tampa, FL 33620, USA
Email:rajadas@usf.edu

Multiferroics are rare because the criteria for existence of electric and magnetic ordering are uncorrelated. Nano size effects on both magnetic and ferroelectric property are subject of recent studies due to their potential applications. There are very few reports on the size and morphology dependent multiferroic property of rare-earth manganites, due to challenges associated with the synthetic chemistry, as high

temperature calcination is required to form these phases. Nanoparticles of *h*-$YbMnO_3$ and *o*-$EuMnO_3$ were synthesized using modified hydrothermal method. [1,2] By using ionic chemistry without the use of surfactant or template we demonstrated control synthesis of one and two dimensional nanoparticles of $YbMnO_3$. Nanoparticles of *o*-$EuMnO_3$ showed reduction in the width of thermal hysteresis between field cooling and heating magnetisation curve as compare to bulk phase. Isothermal magnetization showed large exchange bias below ICAFM to c*A*AFM transition temperature.

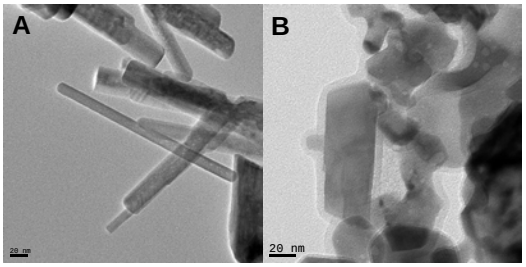

Figure: TEM images of *h*-$YbMnO_3$ A) nanorods, and B) nanoplates. Scale bar 20 nm.

1. Raja Das and Pankaj Poddar *RSC Adv.* **4**, 10614 (2014).
2. Raja Das and Pankaj Poddar *J. Phys. Chem. C* **118**, 13268 (2014).

Author Index